amU
Aix Marseille Université

NNT : 2024AIXM0001

THÈSE DE DOCTORAT

Soutenue à AMU — Aix-Marseille Université
le 10 décembre 2024 par

Victoria JOPPIN

Développement d'outils d'analyse biomécanique in vivo de la paroi abdominale saine, herniée, réparée

---

Development of in vivo biomechanical analysis tools for healthy, herniated and repaired abdominal wall

Discipline

Sciences du Mouvement Humain

École doctorale

ED 463 Sciences du Mouvement Humain

Laboratoire/Partenaires de recherche

Université Gustave Eiffel
Laboratoire de Biomécanique Appliquée (LBA)
Centre de Résonance Magnétique Biologique et Médicale (CRMBM)

Composition du jury

Aline BEL-BRUNON — Présidente du jury et Rapporteure
Directrice de recherche, LBMC, Lyon, France

Benoît ROMAIN — Rapporteur
PU-PH, Hôpitaux Universitaires de Strasbourg, France

Izabela LUBOWIECKA — Examinateur
MCU, Faculté de Technologie de Gdańsk, Pologne

Baptiste PIERRAT — Examinateur
Ingénieur de recherche, Sainbiose, Saint-Etienne, France

Thierry BEGE — Co-directeur de thèse
MCU-PH, Assistance publique - Hôpitaux de Marseille, France

David BENDAHAN — Co-encadrant de thèse
Directeur de recherche CNRS, CRMBM, Marseille, France

Catherine MASSON — Directrice de thèse
Directrice de recherche, LBA, Marseille, France

LABORATOIRE DE BIOMÉCANIQUE APPLIQUÉE
Sous la co-tutelle de : AIX-MARSEILLE UNIVERSITÉ UNIVERSITÉ GUSTAVE EIFFEL

CRMBM-CEMEREM UMR 7339

Université Gustave Eiffel

Affidavit

I undersigned, Victoria Joppin, hereby declare that the work presented in this manuscript is my own work, carried out under the scientific supervision of David Bendahan, Thierry Bège and Catherine Masson, in accordance with the principles of honesty, integrity and responsibility inherent to the research mission. The research work and the writing of this manuscript have been carried out in compliance with both the french national charter for Research Integrity and AMU charter on the fight against plagiarism.

This work has not been submited previously either in this country or in another country in the same or in a similar version to any other examination body.

Marseille, December 10th 2024

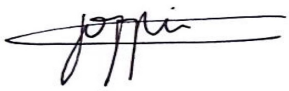

This work is licensed under Creative Commons Attribution-NonCommercial-NoDerivatives 4.0 International Public License

List of publications and conference participation

List of publications and/or patents produced as part of the thesis project:

1. V. Joppin, A. Jourdan, D. Bendahan, A. Soucasse, M. Guye, C. Masson, and T. Bege, "Towards a better understanding of abdominal wall biomechanics: in vivo relationship between dynamic intra-abdominal pressure and magnetic resonance imaging measurements," Clinical Biomechanics, Nov. 2024. Post-print version available free of charge on HAL. Publisher's version online

2. V. Joppin, N. Belton, M. Hostin, M. Bellemare, A. Lawlor, K. Curran, T. Bege, C. Masson, D. Bendahan, "Automatic muscle segmentation on healthy abdominal MRI using nnUNet" presented at the Medical Imaging with Deep Learning, Apr. 2024 Online

3. N. Belton, V. Joppin, A. Lawlor, K. Curran, C. Masson, T. Bege, D. Bendahan, "DyABD: A Dataset and Technique for Synthetically Generating Dynamic Abdominal MRIs with Dual Class and Anatomically Conditioned Diffusion Models" presented at the Medical Imaging with Deep Learning, Apr. 2024 Online

4. P. Gueroult, V. Joppin, K. Chaumoitre, M. Di Bisceglie, C. Masson, and T. Bege, "Linea alba 3D morphometric variability by CT scan exploration," Hernia, Apr. 2024. Post-print version available free of charge on HAL. Publisher's version online

5. V. Joppin, C. Masson, and T. Bege, "Chapitre 2 - Biomécanique de la paroi abdominale," in Chirurgie Pariétale, G. Passot and Y. Renard, Eds., Paris: Elsevier Masson, 2023 Online

List of datasets published as part of the thesis project:

1. N. Belton *et al.*, "niamhbelton/DyABD." Jul. 10, 2024 Online.

2. V. Joppin *et al.*, "Abdominal in vivo metrics derived from axial dynamic MRI of healthy participants." Recherche Data Gouv, Jan. 24, 2024 Online

3. V. Joppin *et al.*, "In vivo intra-abdominal pressure of healthy participants." Recherche Data Gouv, Jan. 24, 2024 Online

Participation in conferences during the thesis period:

1. V. Joppin, N. Belton, M. Hostin, M. Bellemare, A. Lawlor, K. Curran, T. Bege, C. Masson, D. Bendahan, "Automatic muscle segmentation on healthy abdominal MRI using nnUNet", poster – Medical Imaging with Deep Learning (MIDL), Paris, France, July 2-5, 2024

2. N. Belton, V. Joppin, A. Lawlor, K. Curran, C. Masson, T. Bege, D. Bendahan, "DyABD: A Dataset and Technique for Synthetically Generating Dynamic Abdominal MRIs with Dual Class and Anatomically Conditioned Diffusion Models", poster – Medical Imaging with Deep Learning (MIDL), Paris, France, July 2-5, 2024

3. V. Joppin, D. Bendahan, T. Bege, C. Masson, "Assessment of human abdominal wall stress through cylindrical approximation during in vivo exercises", oral presentation – European Society of Biomechanics (ESB), Edinburg, Scotland, July 1-3, 2024

4. V. Joppin, T. Bege, C. Masson, D. Bendahan, "Dynamic MRI in vivo investigation of abdominal hernia repair during standardized exercises", oral presentation – International Society for Magnetic Resonance in Medicine (ISMRM), Singapore, May 4-9, 2024

5. V. Joppin, C. Masson, T. Bege, "New tools for biomechanical characterisation of the abdominal wall", oral presentation – Mecabio Research group, Lyon, France,

Nov 29- Dec 1, 2023

6. V. Joppin, T. Bege, C. Masson, D. Bendahan, “Dynamic MRI investigation for abdominal wall hernia repair”, oral presentation – Imaging in Neuromuscular Disease Conference (Myo-MRI), Berlin, Germany, Nov 5-7, 2023

7. V. Joppin, T. Bege, D. Bendahan, C. Masson, “Dynamic MRI investigation for abdominal wall hernia repair: preliminary study”, poster – French society of biomechanics (SB), Grenoble, France, Oct 25-27, 2023

8. V. Joppin, C. Masson, T. Bege, “Dynamic imaging: a new tool for exploring abdominal wall function ”, oral presentation – French society of parietal surgery (MESH), Paris, France, June 16, 2023

9. T. Bege, V. Joppin, C. Masson, “Quantitative evaluation of the abdominal wall mechanical behaviour by a new connected abdominal binder: a preliminary study”, oral presentation – European Hernia Society (EHS), Barcelona, Spain, May 3-5, 2023

10. V. Joppin, T. Bege, D. Bendahan, C. Masson, “A better understanding of abdominal wall behaviour in vivo using dynamic MRI and pressure measurements”, oral presentation – Computer Methods in Biomechanics and Biomedical Engineering (CMBBE), Paris, France, May 3-5, 2023

11. V. Joppin, A. Jourdan, C. Masson, T. Bege, D. Bendahan, “Multi-parametric characterisation of the abdomen based on semi-automatic registration of dynamic MRI images ”, oral presentation - Meeting researcher - industrial Carnot STAR , Marseille, France, March 17, 2023

12. V. Joppin, C. Masson, T. Bege, “Biomechanics of the pathological anterior wall”, oral presentation – French society of parietal surgery (MESH), Paris, France, Dec 3rd, 2021

Participation in summer schools during the thesis period:

1. Deep learning for Medical Imaging school (Lyon, April 2023)

Résumé et mots clés

Cette thèse de doctorat vise à améliorer la compréhension de la biomécanique de la paroi abdominale et à développer des outils pour son évaluation dans des contextes de paroi saine, herniée et réparée. Ce projet combine des mesures basées sur l'IRM dynamique, de la modélisation biomécanique, et des outils basés sur de l'IA pour fournir une approche complète de l'analyse de la mécanique de la paroi abdominale, avec un accent particulier sur l'amélioration des résultats cliniques de chirurgie de hernies.

L'introduction définit les notions anatomiques et de biomécanique de la paroi abdominale, en soulignant son rôle fonctionnel et sa physiopathologie. Le chapitre développe l'état de l'art des études portant la paroi abdominale, ainsi que les modalités d'imagerie actuelles et leurs limites. Ce chapitre souligne la nécessité d'améliorer les stratégies thérapeutiques, et définit les différents objectifs et la structure de ce projet doctoral.

Dans le chapitre 1, la relation entre la pression intra-abdominale (PIA) et le mouvement de la paroi abdominale est étudiée à l'aide de l'IRM dynamique, sur une cohorte de sujets sains. Cette analyse souligne des éléments de compréhension sur le comportement de la paroi abdominale au cours de différentes activités physiologiques (par exemple, la respiration, la toux, la manœuvre de Valsalva), fournissant la base d'une analyse plus poussée axée sur la répartition des contraintes dans la paroi abdominale.

Sur cette base, le chapitre 2 développe un modèle cylindrique pour estimer la contrainte mécanique sur la paroi abdominale en se basant sur les données utilisées dans le chapitre précédent. Cette approche permet d'identifier les régions abdominales à forte contrainte, en particulier le long de la ligne médiane, où des structures telles que la ligne blanche jouent un rôle majeur.

Le chapitre 3 développe ces résultats en proposant une analyse anatomique 3D complète de la ligne blanche. Cette étude montre que la largeur, la courbure et la forme de la ligne blanche varient en fonction des caractéristiques démographiques (âge, indice de masse corporelle, sexe), ce qui est essentiel pour comprendre et traiter des

pathologies telles que les hernies abdominales.
Compte tenu des limites de la segmentation manuelle rencontrées dans le chapitre précédent, le chapitre 4 présente des outils basés sur de l'IA pour automatiser davantage l'analyse de la paroi abdominale. Le chapitre 4.1 utilise le réseau nnUNet pour automatiser la segmentation des muscles de la paroi abdominale. Le chapitre 4.2 explore également l'utilisation de modèles pour générer des IRM synthétiques, afin de faire face au défi de la rareté des données et du post-traitement parfois chronophage et laborieux.
Ensuite, à la lumière des connaissances et des outils développés dans les chapitres précédents, le chapitre 5 se concentre sur une cohorte de patients ayant subi une chirurgie de hernie ventrale. Ce chapitre explore via des acquisitions IRM dynamique dans les plans axial et sagittal la façon dont les aspects anatomiques et fonctionnels de la paroi abdominale changent avant et après l'opération.
Enfin, le chapitre 6 démontre le potentiel de combiner des techniques d'imagerie, de la modélisation biomécanique et des outils d'intelligence artificielle pour mieux comprendre et traiter les pathologies de la paroi abdominale. L'extension de ces méthodes à des populations de patients plus larges et plus diversifiées, ainsi que l'exploration de la manière dont les résultats peuvent améliorer la planification chirurgicale personnalisée et le suivi postopératoire, sont des axes de recherches futures. Également, l'accessibilité de l'IRM au niveau mondial et les campagnes préventives telles que la lutte contre l'obésité et le sevrage du tabac pourraient contribuer à réduire le risque de formation et de récurrence des hernies.

Mots clés

Paroi abdominale ; Biomécanique ; Imagerie dynamique par résonance magnétique ; IRM ; Pression intra-abdominale ; Comportement mécanique ; Contrainte ; Loi de Laplace ; Biomécanique ; In vivo ; Linea alba ; Tomodensitométrie ; Anatomie ; Imagerie médicale ; Segmentation ; Réseau neuronal ; Synthèse d'images ; Chirurgie de hernie ; Résultats chirurgicaux ; Imagerie 2D+t

Abstract and keywords

This doctoral thesis aims to enhance the understanding of the biomechanics of the abdominal wall and develop tools for its evaluation in healthy, herniated, and post-operative conditions. This project integrates dynamic MRI-based measurements, biomechanical modelling, and AI-driven tools to provide a comprehensive approach to analysing abdominal wall mechanics, with a particular focus on improving clinical outcomes in hernia surgery.

The introduction provides an overview to the anatomical and biomechanical context of the abdominal wall, outlining its functional role and pathophysiology. The chapter develops the state-of-art of abdominal wall studies, as well as the current imaging modalities and their limitations. This chapter emphasises the need for improved diagnostic and therapeutic strategies, and set the different objectives and structure of this doctoral project.

In chapter 1, the relationship between intra-abdominal pressure (IAP) and abdominal wall motion is investigated using dynamic MRI in a cohort of healthy subjects. This analysis reveals important insights into how the abdominal wall behaves during different physiological activities (e.g., breathing, coughing, Valsalva maneuver), providing the basis for further analysis focusing on the distribution of stresses across the abdominal wall.

Building on this, chapter 2 develops a cylindrical model to approximate the mechanical stress on the abdominal wall based on the data used in chapter 1. The model helps identify regions of high stress, particularly along the midline, where structures like the linea alba play a crucial stabilising role.

The chapter 3 expands on these findings by providing a comprehensive 3D anatomical analysis of the linea alba. This study highlights how the width, curvature, and shape of the linea alba vary across patient demographics (age, body mass index, gender), which is critical for understanding and treating conditions like hernia formation.

Recognising the limitations of manual segmentation from the previous studies, chap-

ter 4 introduces AI-based tools to further automate abdominal wall analysis. Specifically, chapter 4.1 used the nnUNet architecture to automate the segmentation of abdominal wall muscles in MRI. The chapter 4.2 also explores the use of generative models to create synthetic MRI data, addressing the challenge of data scarcity and time-consuming post-processing.
Finally, in light of the knowledge and tools developed in the previous chapters, chapter 5 focuses on a cohort of patients undergoing ventral hernia surgery. This chapter explores with dynamic MRI acquisitions in both axial and sagittal planes how the anatomic and functional aspects of the abdominal wall change before and after surgery.
In conclusion, chapter 6 demonstrates the potential of combining advanced imaging techniques, biomechanical modelling, and AI tools to better understand and treat abdominal wall pathologies. Future research should focus on expanding these methods to larger, more diverse patient populations and exploring how the findings can improve personalised surgical planning and post-operative monitoring. Additionally, addressing global access to MRI and promoting preventive measures like obesity reduction and smoking cessation could help mitigate the risk of hernia formation and recurrence.

Keywords

Abdominal wall; Biomechanics; Dynamic magnetic resonance imaging; MRI; Intra-abdominal pressure; Mechanical behaviour; Stress; Laplace law; Biomechanics; In vivo; Linea alba; CT scan; Anatomy; Medical imaging; Segmentation; Neural network; Image Synthesis; Hernia surgery; Surgical outcomes; 2D+t imaging

Remerciements

Cette thèse représente l'aboutissement de trois années de recherche au sein du LBA et du CRMBM à Marseille, et je tiens à exprimer ma profonde reconnaissance à toutes les personnes présentes au long de ce parcours.
Je remercie d'abord mon équipe encadrante: Catherine, Thierry et David. Merci pour votre implication dans ce travail, vos conseils, votre confiance et votre bonne humeur qui m'ont permis de m'épanouir dans cette thèse. Merci plus largement à ceux avec qui j'ai eu l'opportunité de collaborer sur ce projet: Arthur, Andréa, Pierre, Juline, Clément, Hoai-Anne et Timothée.
Je souhaite remercier les membres du jury: Izabela Lubowiecka, Baptiste Pierrat, Benoît Romain et enfin Aline Bel-Brunon. Merci Aline et Benoît d'avoir pris le temps de rapporter ce manuscrit, et merci à vous quatre d'avoir évaluer la qualité de ce travail, en l'enrichissant de vos remarques et points de vue respectifs.
Merci à l'ED 463 Sciences du Mouvement Humain de m'avoir accueilli au sein de leur structure et à l'Université Gustave Eiffel d'avoir financé ce projet doctoral.
Merci aux équipes du CRMBM/CEMEREM et de l'imagerie de l'hôpital Nord pour avoir rendu ce travail commun possible et de m'avoir initié au monde fascinant de l'IRM.
Merci aux pôles chargés de l'éthique et de l'ouverture de la science d'Aix-Marseille Université et de l'Université Gustave Eiffel de m'avoir accompagné dans ce long mais beau processus.
Mes remerciements vont aussi à l'ensemble des membres du LBA pour m'avoir accueilli et fait profiter de leur bonne humeur et de nombreux moments d'échange et de convivialité.
À mes collègues doctorants et amis, merci pour votre appui, les discussions enrichissantes, les moments de partage et de détente qui m'ont permis de passer 3 belles années à Marseille.
Je tiens également à remercier mes proches, en particulier mes amis, Lucas et ma famille, d'être à mes côtés.

Contents

Affidavit 2

List of publications and conference participation 3

Résumé et mots clés 6

Abstract and keywords 8

Remerciements 10

Contents 11

List of Figures 17

List of Tables 19

Glossary of Definitions 20

Nomenclature 22

List of Acronyms 24

Introduction 27

Introduction to biomechanics research 29

Structure and role of the abdominal wall 30

Abdominal cavity 30

Anatomy 33

Function of the abdominal wall 38

Key points 39

General mechanical concepts 40

Overview of biomechanical quantities 40

Methods of biomechanical characterisation 43

Functional mechanics of abdominal wall tissues . . . 47
Function of the aponeuroses . . . 47
Role of intra-abdominal pressure . . . 50
Influence of muscles . . . 52
Abdominal compliance assessment . . . 53
Inter-individual variability . . . 54
Pathophysiology of hernia formation . . . 56
Definition of an abdominal hernia . . . 56
Etiology of abdominal hernia . . . 58
Mechanism of hernia formation . . . 60
Impact of a hernia on the mechanical behaviour . . . 62
Surgical restoration of the abdominal wall . . . 65
Impact of repair on the mechanical behaviour . . . 66
Surgical repair . . . 68
Recurrence factors . . . 71
Imaging of abdominal wall . . . 77
Brief definitions of imaging techniques . . . 77
Current imaging techniques and limitations . . . 79
Benefits of MRI in abdominal wall study . . . 80
Image post-processing . . . 81
Conclusion . . . 83
Objectives of the doctoral project . . . 84

1. Towards a better understanding of abdominal wall biomechanics: in vivo relationship between dynamic intra-abdominal pressure and magnetic resonance imaging measurements 88

1.1. Introduction . . . 91
1.2. Methods . . . 93
1.2.1. Participants . . . 93
1.2.2. Protocol . . . 94
1.2.3. Data processing . . . 94
1.2.4. Correlation intra-abdominal pressure - abdominal wall motion 98
1.3. Results . . . 99
1.3.1. Intra-abdominal pressure and MRI time-dependent changes . . 99

1.3.2. Relationship between intra-abdominal pressure and visceral area 101
1.3.3. Relationship between intra-abdominal pressure and displacement 103
1.4. Discussion . . . 105
1.5. Conclusion . . . 108

2. Stress approximation of in vivo human abdominal wall during breathing 109
2.1. Introduction . . . 111
2.2. Material and methods . . . 113
2.2.1. Cohort and participant protocol . . . 113
2.2.2. MRI data processing . . . 113
2.2.3. Analytical stress computation . . . 114
2.2.4. Young modulus approximation . . . 117
2.3. Results . . . 117
2.3.1. Cylinder geometry . . . 117
2.3.2. Cylinder stress . . . 118
2.3.3. Cylinder elastic moduli . . . 120
2.4. Discussion . . . 121
2.5. Conclusion . . . 125

3. Linea alba 3D morphometric variability by CT scan exploration 127
3.1. Introduction . . . 129
3.2. Materials and Methods . . . 131
3.2.1. Cohort's selection . . . 131
3.2.2. CT scans . . . 131
3.2.3. Output metrics from CT scans . . . 132
3.2.4. Statistical analysis . . . 134
3.3. Results . . . 135
3.3.1. Demographic data . . . 135
3.3.2. Linea alba measurements . . . 135
3.3.3. Influence of age . . . 139
3.3.4. Influence of gender . . . 139
3.3.5. Influence of BMI . . . 140
3.3.6. Correlations . . . 141

3.4. Discussion . . . 142
3.4.1. Limitations . . . 145
3.5. Conclusion . . . 146

4. AI applications in abdominal MRI 148

4.1 Automatic muscle segmentation on healthy abdominal MRI using nnUNet 149

4.1.1 Introduction . . . 151
4.1.2 Material and methods . . . 153
4.1.2.1 Dataset . . . 153
4.1.2.2 Neural network . . . 154
4.1.2.3 Assessment of segmentation quality . . . 154
4.1.3 Results . . . 155
4.1.4 Discussion and conclusion . . . 155

4.2 Dynamic MRI generation for abdominal wall analysis 156

4.2.1 Introduction . . . 158
4.2.2 Methods . . . 159
4.2.3 Results . . . 160
4.2.4 Discussion . . . 162
4.2.5 Conclusion . . . 163

5. Assessing the effects of hernia repair on abdominal wall biomechanics using dynamic MRI 164

5.1. Introduction . . . 167
5.2. Methods . . . 169
5.2.1. Participants . . . 169
5.2.2. MRI protocol . . . 169
5.2.3. Data processing . . . 170
5.3. Results . . . 177
5.3.1. Cohort description . . . 177
5.3.2. MRI parameters . . . 179
5.3.3. Principal component analysis . . . 180
5.3.4. Axial displacement of lateral muscles and rectus abdominis . . . 181

5.3.5. Shape of lateral muscles and rectus abdominis 184
5.3.6. Sagittal displacement of linea alba 186
5.3.7. Inter-recti distance and hernia defect angle 187
5.3.8. Hernia sac and ratio 189
5.3.9. Visceral area 190
5.3.10. Total abdomen area 190
5.4. Discussion 191
5.5. Conclusion 195
5.6. Appendix 196
5.6.1. Segmentation of MRI 196
5.6.2. Registration of axial MRI 196
5.6.3. Registration of sagittal MRI 197
5.6.4. Influence of sex assigned at birth 198
5.6.5. Principal component analysis 198

6. Discussion **202**
6.1. Contribution of the findings 203
6.1.1. Intra-abdominal pressure and abdominal wall motion 203
6.1.2. Cylindrical model for abdominal wall stress approximation . . . 203
6.1.3. Anatomical variability of the linea alba 204
6.1.4. AI for MRI segmentation and synthetic data generation 204
6.1.5. Post-operative changes and MRI analysis 205
6.2. Clinical significance 205
6.3. Limitations and perspectives 206
6.3.1. Imaging limitations 206
6.3.2. Simplifying assumptions 208
6.3.3. AI model generalisability 208
6.3.4. Sample size generalisability 209

Bibliography **214**

Appendix **251**

A. Appendix: Ethic committee approval **252**

B. Appendix: README file of dataset "Abdominal in vivo metrics derived from axial dynamic MRI of healthy participants" 257

C. Appendix: README file of dataset "In vivo intra-abdominal pressure of healthy participants" 264

List of Figures

1. Anatomical planes . . . 31
2. Body cavities . . . 32
3. Organ in the abdominal cavity . . . 33
4. Abdominal muscles . . . 35
5. Cross-sectional view of the abdomen . . . 36
6. Abdominal wall stress elements . . . 41
7. Abdominal compliance . . . 43
8. *Ex vivo* experimental tests . . . 44
9. *In vivo* experimental tests . . . 45
10. Numerical model of a healthy abdominal model . . . 46
11. Abdominal wall muscle thickness on MRI . . . 50
12. Abdominal cavity . . . 53
13. Abdominal morphometry . . . 55
14. Abdominal hernia . . . 56
15. Common hernia locations . . . 57
16. Risk factor for incisional hernia . . . 60
17. Schematic stress-strain curve . . . 61
18. Numerical model of healthy, herniated and repaired abdominal wall . . . 67
19. Experimental model of abdominal wall . . . 68
20. Wound suturing techniques . . . 72
21. Numerical model peak stress at mesh wall interface . . . 73
22. Post-operative herniation time . . . 76
23. Abdominal wall imaging modalities . . . 78

1.1. Segmentation of abdominal MRI . . . 94
1.2. Metrics derived from MRI . . . 95
1.3. Averaging process of exercises repetitions . . . 97
1.4. Evolution of pressure and abdominal wall motion . . . 100

1.5. Pressure as a function of visceral area 103

2.1. Abdominal cylinders design 115
2.2. Abdominal cylinders radius-to-thickness ratio 116
2.3. Abdominal cylinders radii and thicknesses 118
2.4. Abdominal cylinders circumferential stress 119

3.1. Linea alba measurements 133
3.2. Linea alba width according to age, gender, and BMI groups 136
3.3. Linea alba of the most representative patient 137
3.4. Graphical representation of Pearson's correlation coefficient r 142

4.1.1 Abdominal metrics 154
4.1.2 Dice similarity coefficient (DSC) and Hausdorff distance results depending on the label 155

4.2.1 Diffusion process 161

5.1. Sagittal and axial planes selection for dynamic MRI acquisition 170
5.2. Segmentation masks on axial pre-operative MRI 172
5.3. Muscle displacement of a pre-operative patient performing a Valsalva maneuver 173
5.4. Segmentation masks on sagittal pre-operative MRI 174
5.5. Pre and post-operative sagittal MRI during Valsalva contraction 175
5.6. Pre-operative and post-operative muscle displacement on axial MRI . 183
5.7. Pre-operative and post-operative linea alba displacement on sagittal MRI 187
5.8. Hernia defect angle before and after surgery 189
5.9. Visceral area before and after hernia surgery 190
5.10. PCA done on pre-operative and post-operative morphometric data . . 199
5.11. PCA done on pre-operative and post-operative axial maximum values 200
5.12. PCA done on pre-operative and post-operative sagittal maximum values 201

B.1. Illustration of abdominal muscles segmented 258
B.2. Illustration of radial distances and abdominal muscle barycenters . . . 259
B.3. Illustration of abdominal muscles length 259
B.4. Illustration of visceral area 260

List of Tables

1. Stiffness of abdominal wall components 49

1.1. Maximum values in pressure and abdominal wall motion 101
1.2. Pearson correlation coefficients between pressure and visceral area . . 102
1.3. Pearson correlation coefficients between pressure and muscle displacement 104

2.1. Abdominal cylinders stress and elastic moduli 120

3.1. Demographic data and linea alba measurements 138
3.2. Influence of age on linea alba measurements 139
3.3. Influence of gender on linea alba measurements 140
3.4. Influence of BMI on linea alba measurements 141

4.2.1 Results of synthesised MRI 161

5.1. Morphometric data of the patients 178
5.2. MRI parameters 180
5.3. Pre-operative and post-operative muscle strains 185
5.4. Pre-operative and post-operative inter-recti distance 188
5.5. Percentage of manually segmented slices 196

Glossary of Definitions

axial plane

Plane dividing the upper (superior) and lower (inferior) parts of the body. This term is commonly used in radiology and cross-sectional imaging

circumferential direction

Refers to the circumference or perimeter of a structure, parallel to the abdominal wall surface, along the transverse plane

coronal plane

Plane dividing the anterior (front) and posterior (back) parts of the body

cranio-caudal direction

Refers to the up-down direction along the vertical axis of the body (from head-to-toe), equivalent to the superior-inferior direction, parallel to the sagittal plane

longitudinal direction

Refers to the lengthwise direction of a structure, which, for the abdomen, often aligns with the cranio-caudal direction

sagittal plane

Plane dividing the left and right parts of the body

transverse direction

Refers to the left-right direction along the horizontal axis, parallel to the transverse plane

transverse plane

Refers to the same as axial plane in this context, divides the upper (superior) and lower (inferior) parts of the body. This term is commonly used in anatomy and biomechanics.

Nomenclature

C

Abdominal compliance ($mL/mmHg$)

C_{ab}

Pseudo abdominal compliance ($cm^2/mmHg$)

E

Young modulus or elastic modulus, $E = \sigma/\varepsilon$ (Pa)

ε

Strain (-)

ε_r

Radial strain (-)

$\varepsilon_{rupture}$

Strain at rupture (-)

ε_θ

Circumferential strain (-)

F

Force (N)

F_r

Radial force (N)

F_θ

Circumferential force (N)

λ

Stretch $\lambda = (\Delta l + l_0) / l_0$ (-)

l

Tissue length (m)

l_0

Tissue length at rest (m)

Δl

Elongation $\Delta l = l - l_0$ (m)

p

p-value

r

Pearson correlation coefficient (-)

S

Surface (m^2)

σ

Stress (Pa)

$\sigma_{elastic}$

Elastic limit (Pa)

σ_r

Radial stress (Pa)

$\sigma_{rupture}$

Ultimate tensile strength (Pa)

σ_θ

Circumferential stress (Pa)

List of Acronyms

CNN

Convolutional neural network

CT

Computed tomography

CV

Coefficient of variation

DDPM

Denoising diffusion probabilistic model

DSC

Dice similarity coefficient

EHS

European hernia society

EMG

Electromyography

EO

External oblique

FE

Finite element

IAP

Intra-abdominal pressure

IAV

Intra-abdominal volume

IO

Internal oblique

IPOM

Intra-peritoneal onlay mesh

IRD

Inter-rectus distance

LM

Lateral muscles

MPR

Multiplanar reconstruction

MRI

Magnetic resonance imaging

MSE

Mean squared error

nnUNet

No-new-Net

RA

Rectus abdominis

SSIM

Structural similarity index measure

TA

Transversus abdominis

UTS

Ultimate tensile strength

Introduction

Table of contents

Introduction to biomechanics research 29
Structure and role of the abdominal wall 30
Abdominal cavity 30
Anatomy 33
Musculo-aponeurotic complex 33
Abdominal muscles 34
Abdominal connective tissue 36
Function of the abdominal wall 38
Key points 39
General mechanical concepts 40
Overview of biomechanical quantities 40
Methods of biomechanical characterisation 43
Functional mechanics of abdominal wall tissues 47
Function of the aponeuroses 47
Anisotropy 47
Stiffness 48
Thickness 49
Role of intra-abdominal pressure 50
Influence of muscles 52
Abdominal compliance assessment 53
Inter-individual variability 54
Pathophysiology of hernia formation 56
Definition of an abdominal hernia 56
Etiology of abdominal hernia 58
Mechanism of hernia formation 60

Impact of a hernia on the mechanical behaviour 62
Surgical restoration of the abdominal wall 65
Impact of repair on the mechanical behaviour 66
Surgical repair 68
Mechanical contribution of a prosthetic implant 68
Mechanical properties of implants 69
Impact of hernia defect size on repair 70
Influence of repair on intra-abdominal pressure 70
Recurrence factors 71
Influence of patient parameters 71
Influence of surgical technique 71
Influence of abdominal wall loading 75
Early signs of recurrence 75
Imaging of abdominal wall 77
Brief definitions of imaging techniques 77
Current imaging techniques and limitations 79
Benefits of MRI in abdominal wall study 80
Image post-processing 81
Conclusion 83
Objectives of the doctoral project 84

Preface

This introductory chapter aims to lay the terminological foundations and introduce the notions that will be used throughout this manuscript. This chapter presents a literature review on the main concepts of this doctoral project. The first part describes the anatomy and function of the abdominal wall, as well as the problems associated with this tissue and which provide the context for this PhD. This is followed by a more in-depth description of the concepts inherent in the study of the abdominal wall, supported by literature reviews. The next section deals with abdominal hernias, and the one after that with their management.

Introduction to biomechanics research

Biomechanics is a broad and interdisciplinary field that combines the principles of mechanics with biological systems. It is focused on understanding the forces and movements generated and experienced by living organisms. The field spans many scales, from cellular-level mechanics to the behaviour of the whole human body, encompassing areas such as tissue mechanics, muscle dynamics, bone mechanics, cardiovascular function, and movement science.

Biomechanics provides valuable insights for various fields, including medicine, rehabilitation, sports science, and bioengineering. By studying the mechanics of biological systems, researchers can understand how tissues and organs respond to mechanical stresses, how movement patterns emerge, and how these systems fail under certain conditions (e.g., injury, disease). This knowledge is crucial for designing prosthetics, improving surgical techniques, enhancing athletic performance, and developing new treatments for musculoskeletal disorders.
The human musculoskeletal system is often a primary focus in biomechanics research. Researchers investigate how muscles, tendons, ligaments, and bones work together to produce movement and support bodily functions.

During this doctoral project, a particular area of focus is the abdominal wall, which plays a critical role in maintaining core stability, posture, and respiratory function. The alarming rates of hernia occurrence and recurrence underline the lack of knowledge and understanding of the abdominal wall behaviour. The mechanisms underlying the formation and recurrence of hernias remain poorly understood. Presently, surgeons have a paucity of quantitative data at their disposal to inform their decision-making regarding abdominal wall repair. A deeper comprehension of the mechanical behaviour of the abdominal wall is crucial for enhancing the diagnosis, treatment, and prevention of hernias. This can facilitate the development of personalized solutions that are tailored to the specific abdominal wall characteristics of the individual patient at each stage of the surgical process, including the preoperative, perioperative, and postoperative phases.

Structure and role of the abdominal wall

Abdominal cavity

In the field of biomechanics, anatomical planes and directions are frequently used to describe the body, as shown in Figure 1. The **sagittal** plane serves to differentiate between the left and right portions of the body. The **coronal** plane divides the body into anterior (front) and posterior (back) sections. Finally, the **transverse** plane, also called **axial** plane, divides the body into upper (superior) and lower (inferior) sections. Several directions along these anatomical planes will be used in this manuscript. The **cranio-caudal** direction, equivalent to the **longitudinal** or superior-inferior direction, refers to the up-down, lengthwise direction of a structure. For the abdomen study, the longitudinal direction aligns the vertical axis of the body (from head-to-toe), parallel to the sagittal plane. The transverse direction refers to the left-right direction along the horizontal axis, parallel to the transverse plane. The **circumferential** direction refers to forces or movements that act around the circumference or perimeter of a structure, parallel to the transverse plane.

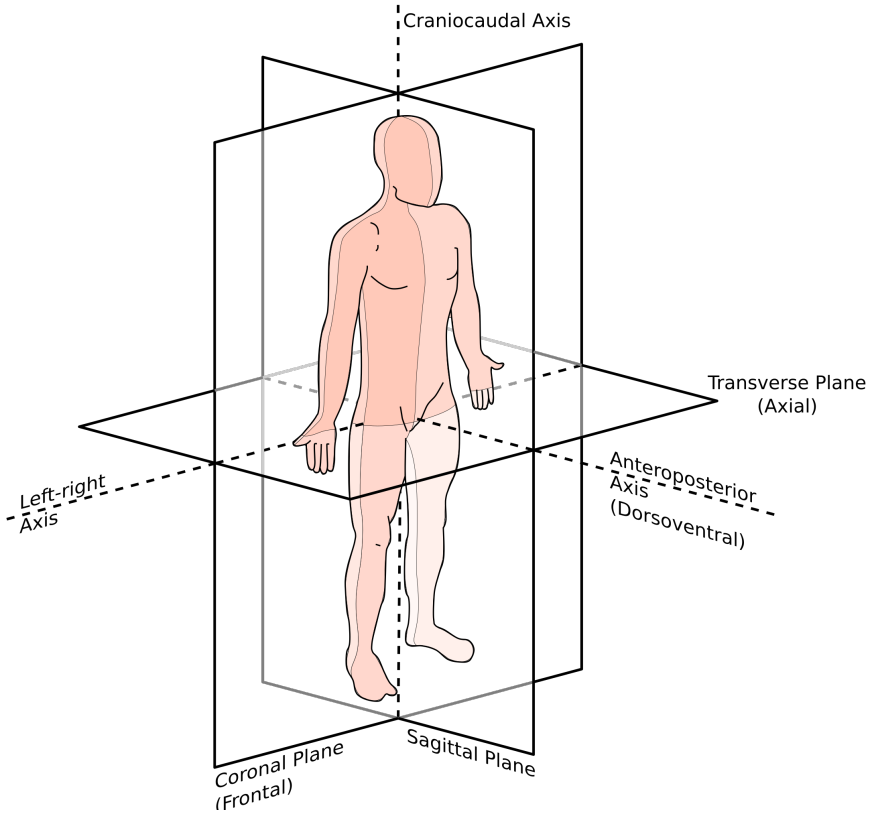

Figure 1.: Anatomical planes. Figure from Wikimedia Commons images (Edoarado 2011)

The abdominal wall surrounds the abdominal cavity or abdominal compartment, which can be approximated as a closed, roughly cylindrical volume, as represented in Figure 2. The abdominal cavity is a large space within the torso that contains the majority of the digestive organs and is part of the abdominopelvic cavity. As shown in Figure 2, the abdominal cavity is separated from the thoracic cavity by the diaphragm (superiorly), the pelvic cavity (inferiorly), and the abdominal wall (anteriorly and laterally). Posteriorly, the abdominal cavity is bound by the spine and muscles of the back.

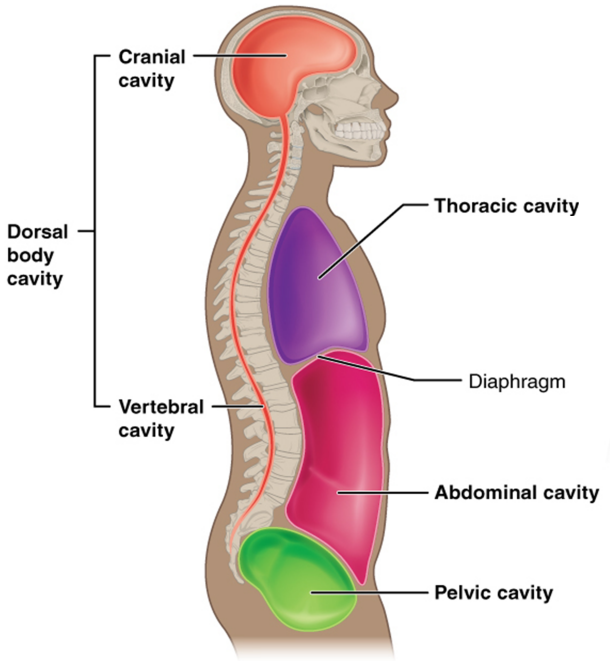

Figure 2.: The different body cavities. Figure adapted from Wikimedia Commons images (OpenStax 2013)

The abdominal cavity contains many vital organs and structures as schematised in Figure 3, including the stomach, liver, gallbladder, small intestine, large intestine (comprising the colon, rectum and anus), pancreas (located behind the stomach), spleen, and kidneys. The majority of the digestive process occurs within the abdominal cavity, where food is broken down, nutrients are absorbed, and waste is excreted.

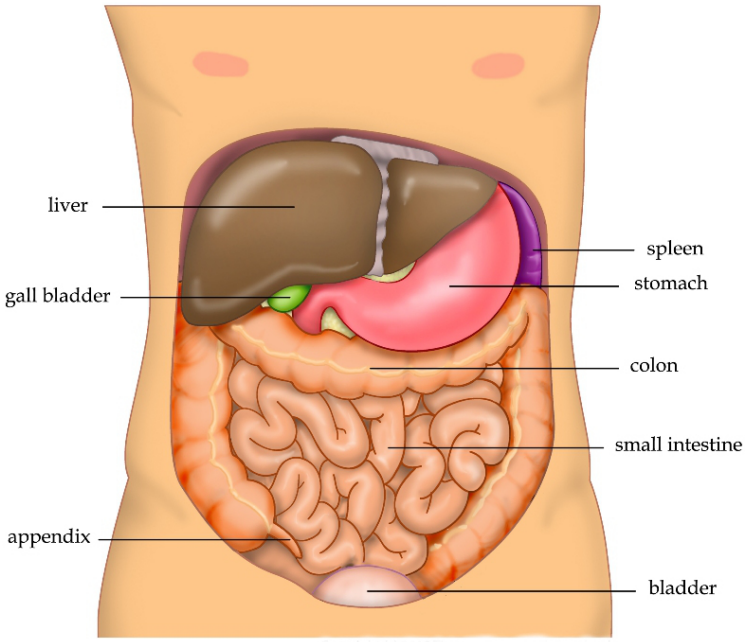

Figure 3.: Organs located in the abdominal cavity. Figure from Wikimedia Commons images (Tvanbr 2010)

Anatomy

Musculo-aponeurotic complex

The musculo-aponeurotic complex of the abdominal wall refers to the structure formed by the muscles and the aponeuroses (fibrous sheaths) that cover and support the abdominal cavity. This complex provides both mechanical stability and flexibility to the abdominal region. The musculo-aponeurotic complex primarily consists of the abdominal muscles and the aponeuroses, which contribute to a range of movements, including flexion, rotation, and stabilization of the trunk. Aponeuroses encircle the muscles and function as a continuation of the muscle tendons, extending outward to form robust, supportive layers. The musculo-aponeurotic complex is also central in surgical considerations, particularly in hernia repairs and abdominal wall reconstruction, where understanding the balance between muscle function and aponeurotic support is key.

Abdominal muscles

The antero-posterior wall, commonly referred to as the abdominal wall is a complex, multi-layered structure that plays a vital role in protecting internal organs and maintaining the mechanical integrity of the abdominal cavity. The abdominal wall is composed of three layers: skin, superficial fascia, and muscles, with the deep fascia, fat, and peritoneum situated below. These structures are schematised in Figure 4.

Each muscle of the abdominal wall has a specific role. The lateral part of the abdominal wall contains three main muscles, each of which contributes to distinct functional capabilities, including movement, stability, and pressure regulation. These muscles are arranged from superficial to deep layers. The most superficial muscle is the external oblique, running diagonally from the lower ribs towards the midline. The internal oblique is located beneath the external oblique, with its fibers oriented perpendicular to the external oblique. This muscle facilitates trunk rotation and lateral flexion. The transversus abdominis is the deepest muscle layer, running horizontally across the abdomen. This muscle is essential for stabilizing the trunk and compressing the abdominal contents. The rectus abdominis is primarily responsible for trunk flexion and stabilization.

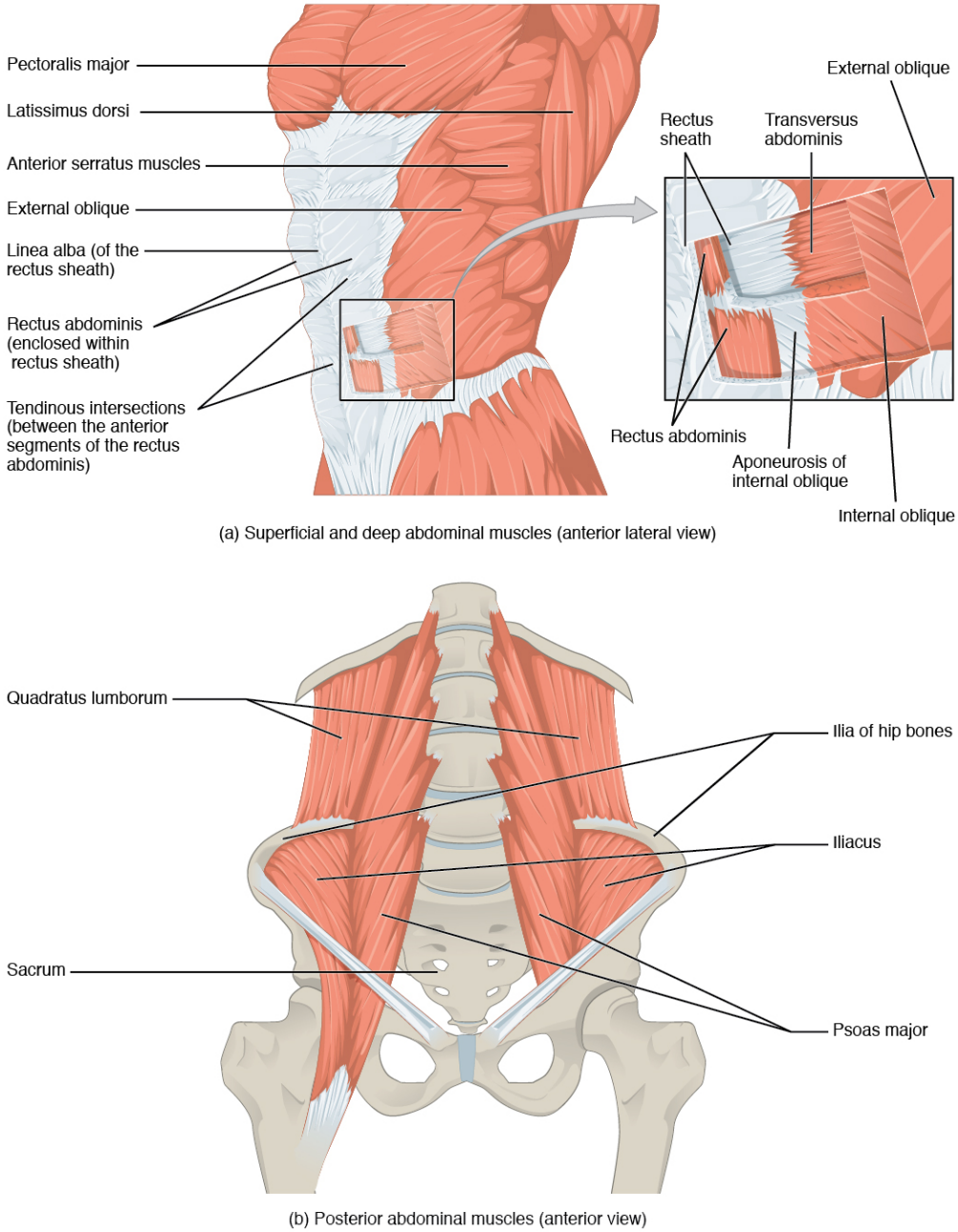

Figure 4.: Abdominal muscles. Figure from Wikimedia Commons images (OpenStax 2016)

In the context of this study, the posterior wall of the abdominal cavity (comprising the spine, dorsal muscles, and ribs), as schematised in Figure 4, exhibits minimal displacements and can thus be considered rigid in comparison to the more flexible and deformable upper wall (diaphragm) and anterolateral wall (musculo-aponeurotic complex).

Additionally, the ribs and costal cartilages contribute to the structure of the upper abdominal wall. The lower ribs serve as attachment sites for both the external and internal oblique muscles, while the diaphragm originates from the lower ribs and attaches to the central tendon. This structural relationship ensures coordinated movement between the abdominal wall and the thoracic cage during activities such as breathing and coughing.

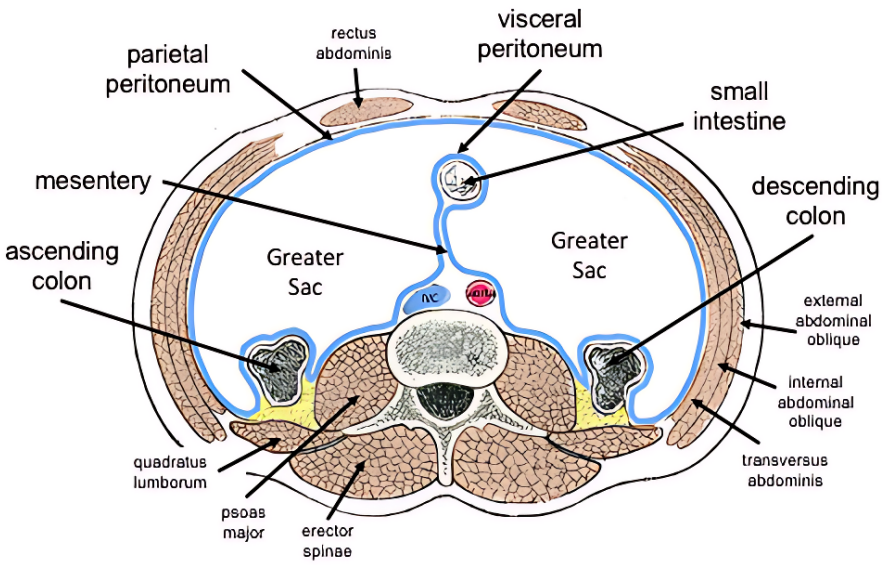

Figure 5.: Cross-sectional view of the abdomen. Figure from Wikimedia Commons images (PhD 2019)

Abdominal connective tissue

Connective tissue, one of the four basic tissue types in the body (along with epithelial, muscular, and nervous tissue), provides structural support, cushions organs, and stores fat in adipose tissue (Cherkas et al. 2023).

Fascia is a connective tissue sheet that surrounds muscles, vessels, and nerves. It is primarily composed of collagen, serving to protect, bind, and compartmentalize body parts. It transmits mechanical forces, maintains tissue integrity, and reduces friction. Fascia is classified according to its location (Bordoni et al. 2024; Gatt et al. 2024). Superficial fascia is located beneath the skin and serves to store fat and facilitate skin movement. Deep fascia, on the other hand, surrounds muscles, bones, and organs and plays a crucial role in force transmission and preventing friction during movement. Notable fascial structures within the abdominal wall include the

superficial Camper's fascia (fatty) and Scarpa's fascia (membranous), as well as the deeper fascia transversalis. It is situated along the internal surface of the abdominal wall and lies between the transversus abdominis muscle and the peritoneum. Visceral fascia provides support and stabilization for internal organs.

An aponeurosis is a type of dense fibrous connective tissue that functions as a broad, flat tendon-like structure, enabling the transmission of muscle force across extensive areas, such as the abdomen or palm hand. In contrast to fascia, which serves to separate and protect, the aponeurosis connects muscles to bones or other muscles, thereby distributing tension over wide surfaces. Together, the fascia and aponeurosis play a vital role in the structure and function of the abdominal wall.

The linea alba is a fibrous band that runs vertically in the midline of the abdomen, extending from the xiphoid process of the sternum to the pubic symphysis. It serves to connect the left and right sides of the abdominal muscles' aponeuroses. The linea alba is formed by the fusion of the aponeuroses of the right and left external oblique, internal oblique, and transversus abdominis muscles. It serves as an attachment point for the rectus abdominis and plays a role in stabilizing the abdominal wall. Additionally, it provides a site of attachment for muscles and supports the anterior abdominal wall.

The rectus sheath is an aponeurosis that encases the rectus abdominis muscle. It is formed by the fusion of the aponeuroses of the external oblique, internal oblique, and transversus abdominis muscles. The rectus sheath protects the abdominal organs and helps the transmission of mechanical forces generated by the abdominal muscles, thereby providing protection for the underlying viscera.

The peritoneum is a serous membrane that lines the abdominal cavity and covers the majority of abdominal organs. The peritoneum is composed of two distinct layers: the parietal peritoneum, which lines the inner surface of the abdominal wall, and the visceral peritoneum, which encircles the organs themselves. The space between these two layers is designated the peritoneal cavity. It contains a minimal quantity of fluid to reduce friction between organs during movement.

The thoracolumbar fascia is a deep connective tissue that covers the posterior ab-

dominal wall and provides attachment points for the internal oblique and transversus abdominis muscles.

Function of the abdominal wall

The abdominal wall serves a number of key functions, including first posture and movement. The muscles of the abdominal wall are essential for maintaining an upright posture and stabilizing the spine. The coordinated action of the external and internal obliques, transversus abdominis, and rectus abdominis primarily drives movements such as twisting, bending, and flexing the trunk. The abdominal wall serves as a physical barrier, protecting the internal organs from external injury.

Additionally, the abdominal wall plays a vital role in maintaining and regulating the intra-abdominal pressure (IAP), which is essential for supporting the abdominal viscera (stomach, intestines, liver, etc.) and preventing herniation under normal physiological conditions. The abdominal wall is capable of undergoing passive deformation in response to the pressure exerted by abdominal contents, such as during inspiration. Furthermore, the abdominal wall can deform actively by contracting the abdominal muscles, which increases IAP. This pressure is necessary for a number of bodily functions, including urination, defecation, vomiting, coughing, and childbirth. In instances where a high degree of stability is necessary, such as during weightlifting, the abdominal muscles contract to form a rigid cylinder around the internal organs. This cylinder provides support for the vertebral column, thereby preventing excessive spinal motion and reducing the risk of injury to the lower back.

During breathing, the abdominal wall functions in conjunction with the diaphragm to facilitate the expulsion of air from the lungs. During inspiration, the diaphragm contracts, resulting in an expansion of the thoracic cavity (Figure 2) and an increase in IAP. The abdominal muscles, particularly the transversus abdominis, play a key role in forceful exhalation, as seen during coughing.

The abdominal wall plays a role in maintaining the positioning and function of the pelvic organs. The abdominal muscles prevent the descent of the pelvic organs, particularly in conditions of increased IAP, such as during pregnancy.

Key points

The abdominal wall is a dynamic and multifunctional structure. Its complex anatomy, composed of layers of muscles, fascia, and connective tissue, plays an integral role in stabilizing the spine and protecting the internal organs. An understanding of the biomechanics and anatomy of the abdominal wall is of critical importance in fields such as surgery, physical therapy, and sports medicine, where injuries or surgical interventions may result in the disruption of normal function.

The next part of this chapter introduces the mechanical concepts that will subsequently be used to describe the mechanical behaviour of the abdominal wall. A state-of-the-art review of the current knowledge on the mechanical behaviour of healthy, herniated, and repaired abdominal walls will then be presented, followed by a focus on abdominal wall imaging and a conclusion that will summarise the key concepts addressed.

General mechanical concepts

Overview of biomechanical quantities

The biomechanics of the abdominal wall depends on the mechanical properties of the various tissues that compose it. Evaluating the mechanical loads applied to the abdominal wall, combined with the study of the abdominal wall's response to these loads, helps define its mechanical behaviour. A commonly used representation of a material's mechanical behaviour is the stress-strain curve. Stress (σ), measured in units of pressure (Pa), represents the forces that particles within a medium exert on each other per unit of surface area (Equation 0.1, ("Stress (Mechanics)" 2024)). As represented in Figure 6, the force F (measured in Newtons) exerted within the abdominal tissues is multidirectional. It has a circumferential component F_θ, which is parallel to the abdominal wall surface, and a radial component F_r, perpendicular to the abdominal wall. There is also a sagittal component acting mainly on the pelvic floor and diaphragm, which will not be discussed here.

These forces are linked to mechanical loads on the abdominal wall, primarily arising from IAP and muscle activation (Novak et al. 2021). The surfaces (measured in m^2 or its subunits) where the stresses are evaluated are those on which these forces are applied. The circumferential force F_θ acts on the cross-sectional area S (m^2) of the abdominal wall (two examples of sections are shown in light and dark green in Figure 6), while the radial force F_r acts on the inner surface of the abdominal wall. The stress within the tissues resulting from these forces is defined by Equation 0.1 below. In the abdominal cavity, the circumferential stress σ_θ is greater than the radial stress σ_r.

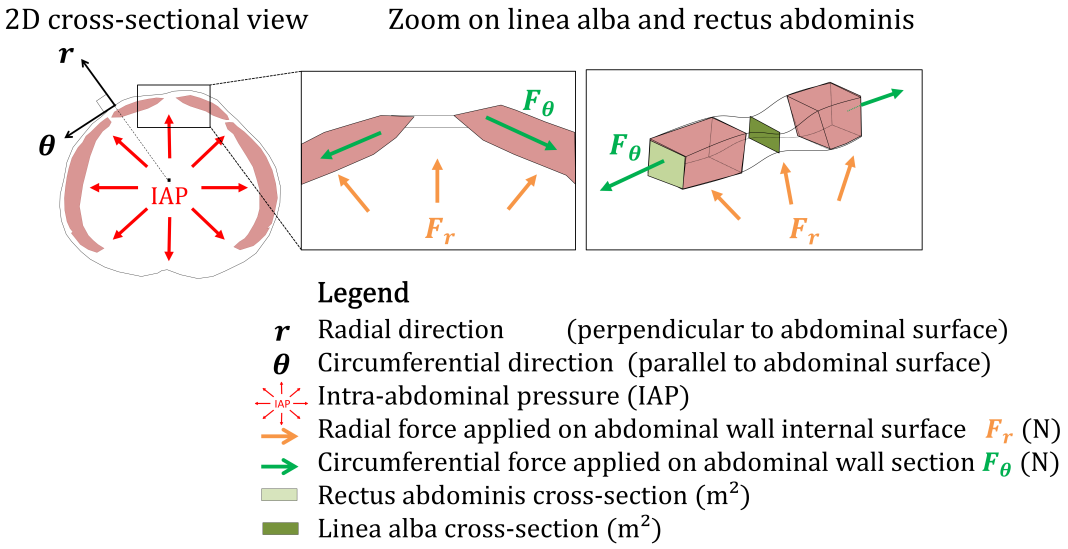

Figure 6.: Scheme defining the different elements of stress within the abdominal wall. Figure inspired from Joppin *et al.* (V. Joppin et al. 2023)

$$\sigma = \frac{F}{S} (Pa = \frac{N}{m^2}) \tag{0.1}$$

When a tissue is subjected to forces, it undergoes deformation. Deformation is a broad term that refers to the change in shape or size of a material due to applied forces (tensile, compressive, shear, etc.). It can include elongation, compression, bending, and twisting. A material can deform in one or more directions. Elongation relates to the change in tissue dimension in one direction, $\Delta l = l - l_0$ (m). Strain is a dimensionless measure of deformation in a given direction, representing the relative elongation of a material. Denoted by ε, strain is the ratio of elongation in that direction, relative to its initial length l_0 (m) (Equation 0.2). The length l_0 generally corresponds to the tissue's resting state. Elongation and strain are equals to zero when the tissue is at rest. Another metric reflecting tissue deformation is the stretch, defined as $\lambda = \frac{l_0 + \Delta l}{l_0}$, and is equals to one when tissue is at rest.

$$\varepsilon = \frac{l - l_0}{l_0} \tag{0.2}$$

The mechanical properties of the abdominal wall can be deduced from measuring the stress applied to the tissue and the resulting strain. The tissue's tensile strength, noted $\sigma_{rupture}$, is a mechanical property defined as the maximum stress the tissue can with-

stand before rupture. This parameter is critical for understanding hernia formation. A key mechanical property in studying abdominal wall behaviour is elasticity, evaluated by the elastic modulus (or Young's modulus), denoted E (Pa). The elastic modulus is defined as the ratio between stress and strain (Equation 0.3). It should be noted that there are not necessarily correlations between the different mechanical properties of a material.

$$E = \frac{\sigma}{\varepsilon}(Pa) \tag{0.3}$$

The elastic modulus quantifies the ability of the abdominal wall to deform under stress. A material with greater elasticity, i.e., lower stiffness, will have a lower elastic modulus. For the same strain, a highly elastic abdominal wall will experience less stress than a less elastic one.

Sometimes, the concept of compliance is used to describe a material's elasticity. Compliance, denoted C, is inversely proportional to the elastic modulus, and its unit is Pa^{-1}. Thus, a more elastic material will have higher compliance. Often used in biomechanics, compliance has several variants adapted to the study of biological tissues. For instance, vascular compliance measures the ease with which a blood vessel expands under internal pressure (Hunt et al. 2002). In the case of the abdominal wall, abdominal compliance, denoted C, quantifies the abdomen's ability to expand (IAV variation) in response to IAP changes (Kirkpatrick et al. 2013), which can be measured, for example, during laparoscopic insufflation. For the same IAP variation, a more compliant (i.e., more elastic) abdominal wall will exhibit a larger IAV change (Figure 7). Abdominal compliance is defined as the ratio between the change in IAV and the change in IAP ($mL/mmHg$) (Equation 0.4). The average compliance of an abdominal wall ranges between 250 and 450 $mL/mmHg$ (Malbrain, De Laet, et al. 2014).

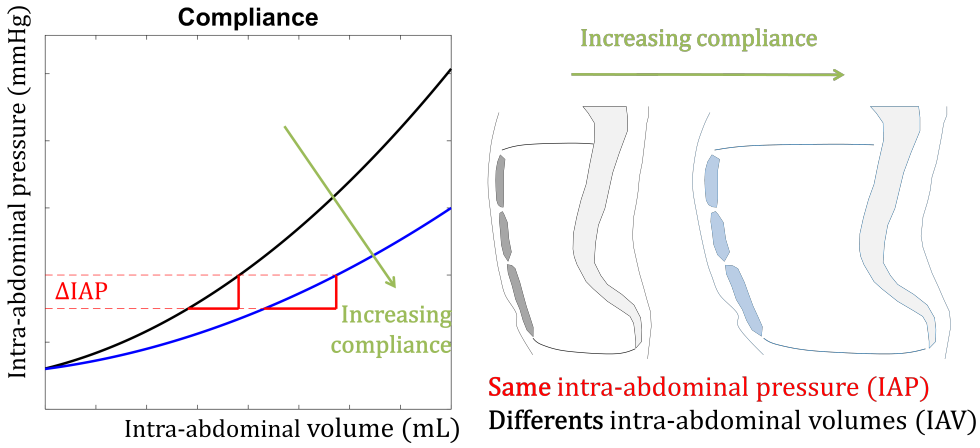

Figure 7.: Scheme of compliance of two different abdominal walls
Legend: **Blue** curve represents an abdominal wall more compliant than the **black** curve.
For a same intra-abdominal pressure variation (ΔIAP), the most compliant abdominal wall will have a higher variation of intra-abdominal volume (ΔIAV)
Figure inspired from Malbrain *et al.* (Malbrain, De Laet, et al. 2014) and Joppin *et al.* (V. Joppin et al. 2023)

$$C = \frac{\Delta IAV}{\Delta IAP}\left(\frac{mL}{mmHg}\right) \tag{0.4}$$

Identifying and measuring these properties helps to characterise the abdominal wall mechanically, offering potential insights for preventing and improving the repair.

Methods of biomechanical characterisation

Biomechanical characterisation of tissues can be conducted on animal or human models, employing either *ex vivo* mechanical tests on tissue samples or *in vivo* techniques. The most common *ex vivo* tests include tensile/compression, swelling, and indentation experiments (illustrated in Figure 8). These tests facilitate the study of the abdominal wall under different loading conditions, i.e., various mechanical stresses, and at multiple scales, from isolated components such as aponeurotic sheaths or muscles to the entire wall structure.

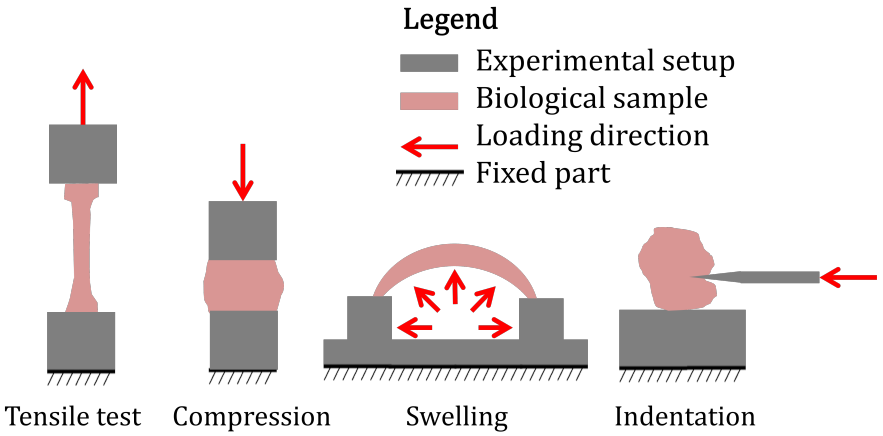

Figure 8.: Scheme of different mechanical *ex vivo* experimental tests. Figure adapted from Joppin *et al.* (V. Joppin et al. 2023)

In vivo tests allow for a more accurate replication of the physiological state, both passive and active, such as during muscle contraction. Imaging techniques like ultrasound, X-ray, computed tomography (CT), or MRI can measure the deformation of the abdominal wall, from its outer surface to deeper tissues. Additionally, measurements of IAP and muscle activation provide an evaluation of the mechanical stresses, complementing the biomechanical study. These techniques are depicted in Figure 9.

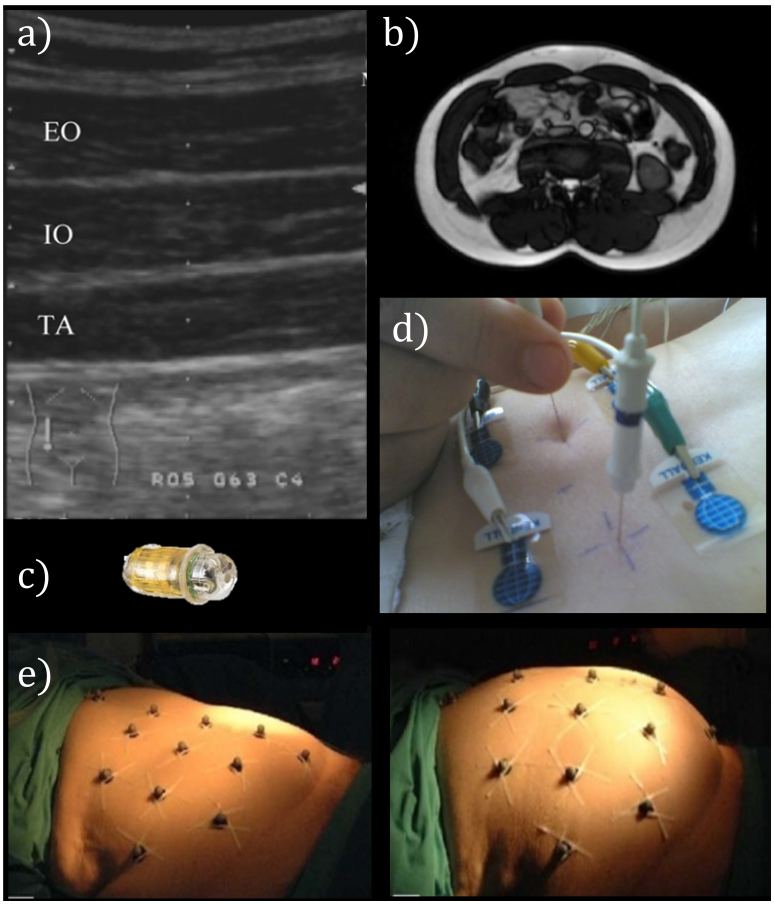

Figure 9.: Different *in vivo* experimental tests
Legend: **a)** Ultrasound from John *et al.* (John et al. 2007), with visible internal and external obliques (IO, EO) and transversus abdominis (TA)
b) Cross-sectional abdominal MRI
c) SmartPill^{TM}
d) EMG sensor image from Wikimedia Commons (Kychot 2009)
e) Image correlation of abdomen (left: at rest, right: insufflated) (Song et al. 2006)

In addition to experimental studies, numerical simulation is used to replicate the behaviour of the abdominal wall, as shown in Figure 10. It enables access to parameters that may be challenging to measure experimentally and allows for evaluating the impact of specific variables (e.g., changes in the thickness or rigidity of an aponeurosis). These simulations rely on numerical models that are developed and validated based on experimental data and simplified assumptions that facilitate the mathematical formulation of the problem.

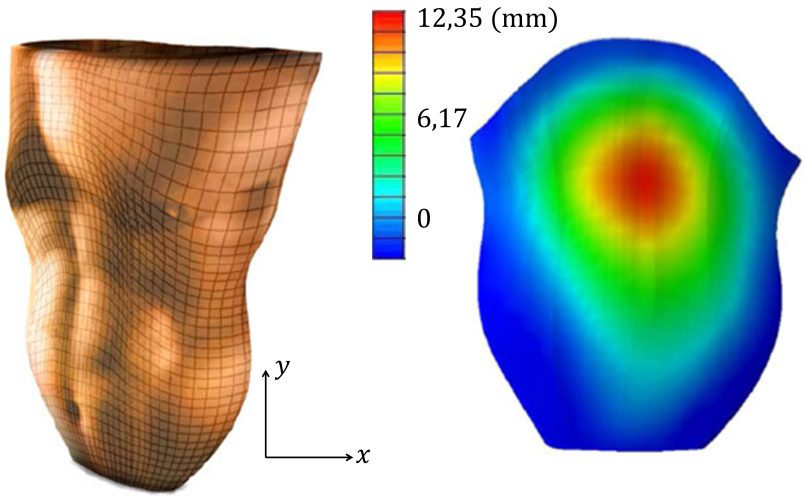

3D geometrical model

Displacement along z-axis (mm), standing position loading

Figure 10.: Numerical model of a healthy abdominal model, from Hernandez *et al.*, 2013 (Hernández-Gascón et al. 2013)

Key points

Stress and strain are the fundamental concepts in the biomechanical study of the abdominal wall. Within the abdominal cavity, stress is predominantly circumferential.

Functional mechanics of abdominal wall tissues

The abdominal wall is a heterogeneous, multi-layered structure. The mechanical behaviour of the entire wall differs from that of its individual components (Hernández et al. 2011) and is influenced by the architectural configuration of all its elements.

Function of the aponeuroses

Abdominal wall hernias occur due to a rupture in the aponeurosis within a region of constitutional or acquired weakness. The most common site for these hernias is the linea alba (Nguyen et al. 2014), an aponeurotic structure that separates the rectus abdominis muscles along the midline of the abdomen, as illustrated in Figure 14. Studying the mechanical properties of healthy abdominal wall tissues provides insights into the frequent occurrence of hernias along this midline.

Anisotropy

Ex vivo mechanical tests have demonstrated that both the aponeuroses and the abdominal wall as a whole are stiffer and therefore deform less in the circumferential direction compared to the cranio-caudal direction (Hernández et al. 2011; Hollinsky et al. 2007; Tran, Mitton, et al. 2014; Astruc et al. 2018; Gräβel et al. 2005; Förstemann et al. 2011; Gerard M. Cooney et al. 2016; Levillain et al. 2016; Junge, Klinge, et al. 2001; Podwojewski et al. 2014; Śmietański, Bury, et al. 2012; Song et al. 2006; Martins et al. 2012; Kirilova et al. 2011; Anurov et al. 2012; Mathew Lyons et al. 2014). This is illustrated by the higher elastic moduli on Table 1. At the level of the umbilicus, the midline deforms twice as much in the cranio-caudal direction as in the circumferential direction (Czesław Szymczak et al. 2011). This difference in mechanical properties depending on the loading direction is known as anisotropy. Locally, this can be explained by the structure of the aponeuroses, which are composed of fibrous connective tissue with multiple layers of interwoven collagen fibers, predominantly oriented circumferentially (Gräβel et al. 2005; Förstemann et al. 2011; Axer et al. 2001b).

Beyond the anisotropic mechanical properties of the abdominal wall, the differences observed between the circumferential and cranio-caudal directions of the abdominal wall can be attributed not only to its anisotropic mechanical properties but also to boundary conditions, which refer to how the abdominal wall interacts with the rest of

the body. This can be demonstrated through *in vivo* or *ex vivo* tests on the entire torso (Czesław Szymczak et al. 2011; Śmietański, Bury, et al. 2012; Song et al. 2006; Le Ruyet et al. 2020; Lubowiecka et al. 2022). At the scale of the whole abdominal wall, when IAP increases, the abdomen transitions from a cylindrical shape to an oval dome, with the abdominal wall bulging more in the sagittal direction (Song et al. 2006). In this direction, the rectus abdominis muscles attach to the xiphoid process of the sternum and the 5th, 6th, and 7th ribs, which move due to the intercostal muscles (e.g., during inhalation). In contrast, the posterior portions of the lateral muscles are attached to the dorsal area, which is almost immobile when the IAP increases.

Stiffness

On one hand, the linea alba is the most rigid (i.e., the least elastic) and the most resistant to rupture among the components of the abdominal wall (Hollinsky et al. 2007; Tran, Mitton, et al. 2014), playing a crucial mechanical role in the structural response. Thus, under equal strain, the most rigid structure will experience the highest stress according to Equation 0.3. Table 1 presents the elastic moduli of different abdominal wall components according to the considered anatomical direction, illustrating the significant variation in stiffness among tissues. The higher the elastic modulus (E), the stiffer the component. Table 1 also illustrates the highly anisotropic behaviour of abdominal wall tissues.

	Young modulus E (MPa)	
Component / Anatomical plane	Circumferential	Cranio-caudal
Linea alba (Astruc et al. 2018)	4.8	1.2
Anterior rectus sheath aponeurosis (Astruc et al. 2018)	11	1.2
Posterior rectus sheath aponeurosis (Astruc et al. 2018)	15	0.82
Fascia transversalis (Deeken and Lake 2017)	3	1.5
Rectus abdominis muscle (Cardoso 2012)	-	0.5
Lateral muscles (composite*) (Cardoso 2012)	1	-
Abdominal skin (Yang et al. 2018)	0.0095	
Subcutaneous fat (Comley et al. 2010)	0.001	
Peritoneum (Ge et al. 2020)	0.002	
***In vivo* full abdominal wall** (Song et al. 2006)	0.042	0.022

Table 1.: Young modulus E (or elastic modulus) describing the stiffness of different abdominal wall components according to the considered direction (see Figure 5) *The lateral muscles are a grouping of the internal and external obliques and the transversus abdominis

Thickness

On the other hand, the linea alba is the thinnest region of the abdominal wall, as depicted in Figure 5 and visible in MRI images (Figure 9 and Figure 11). The cross-sectional area of the rectus abdominis, where force is applied (due to IAP and muscle activation), is larger than that of the linea alba. Given equal applied force, the linea alba will experience higher stress, as stress is inversely proportional to the cross-sectional area over which the force is applied (Equation 0.1). Furthermore, the central region of the linea alba undergoes the greatest displacement and strain (Jourdan, Rapacchi,

et al. 2022; Czesław Szymczak et al. 2011; Silvia Todros, de Cesare, Pianigiani, et al. 2019).

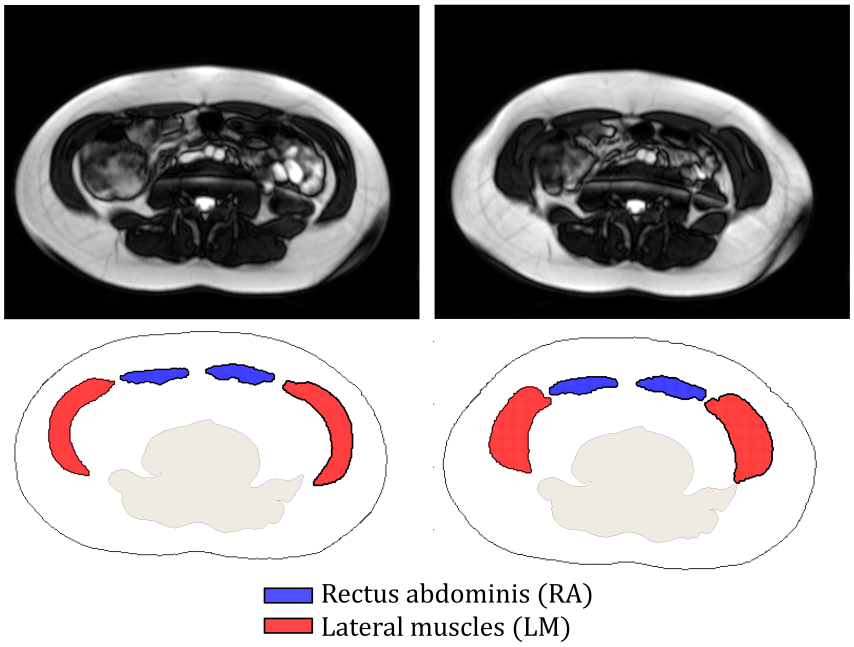

Figure 11.: Thickening of lateral muscles (LM) visible at MRI during contraction of a healthy volunteer. MRI images (top) and delineated abdominal wall muscles (bottom)

Role of intra-abdominal pressure

The walls of the abdominal cavity maintain the position of internal organs by exerting a compressive force on them, resulting in a pressure known as intra-abdominal pressure (IAP), which exists throughout the abdominal cavity (Malbrain, M. L. Cheatham, et al. 2006). Variations in IAP are generally considered uniform across the abdominal cavity (Malbrain, M. L. Cheatham, et al. 2006).

Monitoring and controlling IAP is of critical clinical importance in abdominal wall surgery, as IAP represents the main force acting on the abdominal wall. The IAP has long been studied for clinical concerns in the management of patients with abdominal hypertension (IAP > 12 mmHg) which represent 50% of the patients in intensive care unit (Malbrain, Chiumello, et al. 2004) and the possibly resulting abdominal compartment syndrome (M. Schein et al. 1995; Schein et al. 1998; Roberts et al. 2016; Malbrain, Chiumello, et al. 2004; Malbrain and M. Cheatham 2011). IAP serves as a valuable indicator of the mechanical stresses applied to the abdominal wall (Konerding et al.

2011; Novak et al. 2021). Understanding IAP and its clinical implications is essential for the management of abdominal wall hernias, but also for various medical conditions such as abdominal trauma, respiratory disorders and cardiovascular disease.

Kotidis *et al.* (Kotidis et al. 2011) studied the histological impact of intra-abdominal hypertension on rectus abdominis muscle of rabbit species. A prolongated high level of IAP increase the level of type I fibers. These muscle fibers, also known as slow-twitch fibers, are designed for endurance and sustained activities, efficient at using oxygen to produce energy over long periods, but they contract more slowly and with less force compared to fast-twitch (type II) fibers. Type I fibers are ideal for activities like maintaining posture and low-intensity exercises, where stamina is more important than strength. This may suggest that the rectus abdominis muscle is adapting to chronic stress by shifting towards a more endurance-oriented composition. This shift could have several implications, such as a weakening of the overall strength of the abdominal muscles, making the abdominal wall less able to resist high pressures.

At rest, in the supine position, IAP is close to atmospheric pressure (Cobb et al. 2005), meaning the organs are held in place within the abdomen without being compressed. In reality, IAP is not exactly equal to atmospheric pressure, as the internal organs always bear some weight, either the weight of the abdominal wall in the supine position or the weight of the organs above in the standing position. Studying IAP in relation to various activities helps identify high-risk situations. The Valsalva maneuver, coughing, or jumping cause the most significant spikes in IAP, which may contribute to hernia formation. Beyond muscle activation, the speed of the movement, and thus the rate of loading on the abdominal wall—affects tissue elasticity (Ben Abdelounis et al. 2013). The faster the movement, the stiffer the tissues become, resulting in higher stress for a given strain (Ben Abdelounis et al. 2013). Activities that involve rapid muscle activation produce the highest rates of pressure increase, i.e. the IAP rise per unit time, in $mmHg/s$ (Soucasse, Jourdan, Edin, J. F. Gillion, et al. 2022).

Most devices for measuring IAP are invasive and carry a risk of infection. The gold standard for IAP measurement is intra-vesical pressure monitoring (Kron et al. 1984; Iberti et al. 1989; Fusco et al. 2001), especially for tracking abdominal compartment syndrome. Reliable IAP measurements can also be obtained via intra-gastric (Turnbull et al. 2007; Wise et al. 2017), intra-rectal (Shafik et al. 1997), intra-vaginal (Y. Hsu et al. 2012), or even through the vena cava (Lacey et al. 1987; Gudmundsson et al.

2002), though these methods cause discomfort and present risks that limit their use in abdominal wall surgery.

Less invasive methods for indirectly measuring IAP are being developed (Tayebi et al. 2021), including strain gauges, ultrasound, and image correlation techniques. Measurements using ingested capsules (McCaffrey et al. 2008; Saad et al. 2011; Liao et al. 2020) allow for continuous IAP assessment in daily life (Soucasse, Jourdan, Edin, J. F. Gillion, et al. 2022).

Influence of muscles

In vivo tests allow for the analysis of the influence of muscle contraction on the behaviour of the abdominal wall. During passive activities, such as inhalation, the diaphragm contracts and acts like a piston (Figure 12), compressing the abdominal cavity and thereby increasing IAP (Wilson 1933). In response, the abdominal muscles deform passively, meaning no electrical activity is detected (Jourdan, Rapacchi, et al. 2022; Campbell et al. 1953; Hodges, Cresswell, et al. 2001).

The contraction of abdominal muscles during activities such as the Valsalva maneuver, coughing, or forced expiration exerts additional tension on the aponeuroses (Hernández et al. 2011; Mathew Lyons et al. 2014). The Valsalva maneuver involves attempting to exhale after a deep breath while keeping the airways closed (Talasz et al. 2011), simulating several everyday activities like defecation, inflating a balloon, or playing the saxophone (Srivastav et al. 2022). During this maneuver, the abdominal muscles and pelvic floor contract, increasing IAP by compressing the viscera (Cobb et al. 2005). The IAV decreases, and the diaphragm is pushed upward (Talasz et al. 2011).

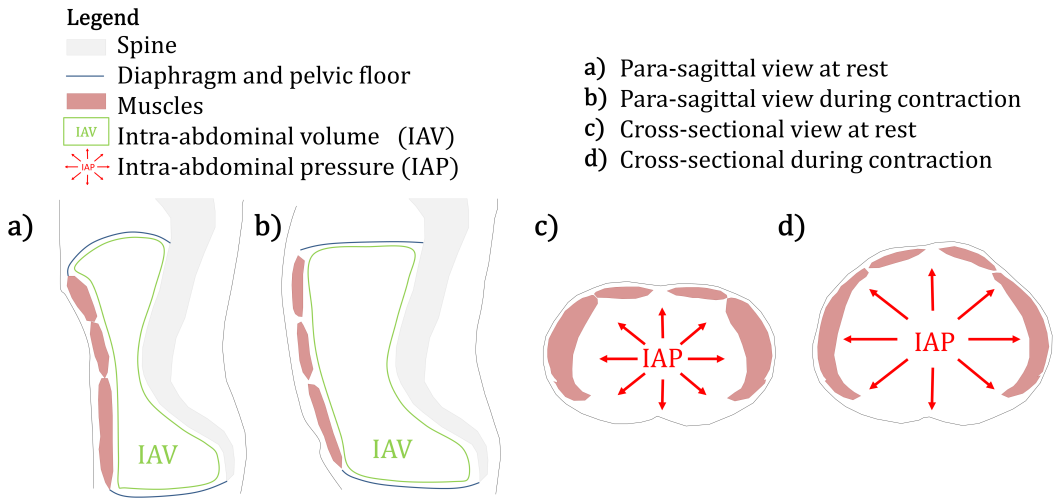

Figure 12.: Scheme of abdominal cavity based on healthy volunteer's magnetic resonance image (MRI). Figure inspired from Joppin *et al.* (V. Joppin et al. 2023)

During these exercises involving contraction, the primary muscles involved are the lateral muscles (Figure 11) (Jourdan, Rapacchi, et al. 2022; Cardoso 2012). The contraction of the lateral muscles reduces the circumference of the abdomen, leading to a narrowing of the waist in the left-right axis and a thickening in the anteroposterior axis (Jourdan, Rapacchi, et al. 2022; Silvia Todros, de Cesare, Pianigiani, et al. 2019; Silvia Todros, de Cesare, Concheri, et al. 2020).

The transversus abdominis, often referred to as the «core» muscle, is composed mainly of circumferential fibers and is the key muscle responsible for generating force and increasing IAP (Axer et al. 2001b; Misuri et al. 1997). The thickness of the transversus abdominis correlates with its length, both in passive states and during muscle activation (Jourdan, Rapacchi, et al. 2022). Well-developed abdominal muscles lead to significant increases in IAP (Misuri et al. 1997; Jourdan 2021).

Abdominal compliance assessment

The assessment of abdominal wall compliance (Equation 0.4) has primarily been studied during laparoscopic procedures by evaluating the relationship between the flow and pressure of insufflated CO_2, complemented by studies of abdominal surface displacement (Song et al. 2006; Le Ruyet et al. 2020). Beyond a certain threshold, the displacement of the abdominal wall in a passive state is no longer proportional to the increase in IAP (Malbrain, De Laet, et al. 2014). In the initial phase, small increases in

IAP lead to large displacements, followed by a phase where further IAP increases result in limited displacement (Song et al. 2006; Le Ruyet et al. 2020; McDougall et al. 1994; Ott 2019). This can be explained by the hyperelastic behaviour of biological tissues, which means their stiffness increases with strain. For instance, during laparoscopy insufflation (increasing IAP from 0 to 12 mmHg), 90% of the working abdominal volume is achieved with only 4 mmHg of pressure (Song et al. 2006). These observations may have clinical implications. In laparoscopic surgery, the concept of «low-impact laparoscopy» (de'Angelis et al. 2018) seeks to determine the lowest possible working pressure for each patient, minimising the impact of pneumoperitoneum on the body (Malbrain, M. L. Cheatham, et al. 2006; Becker et al. 2017; Casati et al. 1997; Kamine et al. 2014).

Inter-individual variability

Morphometric parameters such as muscle and aponeurosis thickness, or IAV capacity influence how stresses are distributed across the abdominal wall. There is no clear correlation between gender, BMI, age, and the mechanical properties of the abdominal wall (Hollinsky et al. 2007; Martins et al. 2012; Rath, Attali, et al. 1996; Rath, J. Zhang, et al. 1997; van Ramshorst et al. 2011).

However, these parameters do affect IAP and the geometry of the abdominal cavity (Jourdan, Soucasse, et al. 2020). An increase in BMI is associated with a decrease in the thickness of the internal and external oblique muscles and a thickening of the transversus abdominis muscle (Jourdan, Soucasse, et al. 2020), which must support the increased visceral mass and, consequently, the rise in IAP (Cobb et al. 2005; Sanchez et al. 2001). Males tend to have higher muscle mass and visceral fat than females (Jourdan, Soucasse, et al. 2020) (Figure 13). With age, visceral fat mass increases, while the abdominal muscles (except for the transversus abdominis muscle) and aponeuroses lengthen (Jourdan, Soucasse, et al. 2020). The effects of these morphometric variations on hernia risk remain poorly understood.

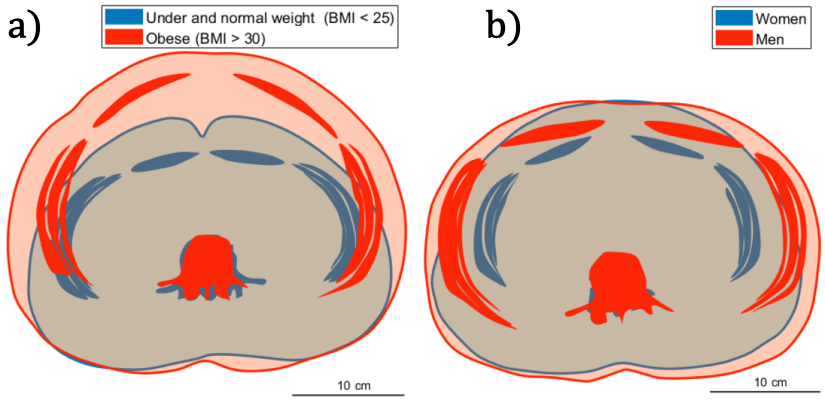

Figure 13.: Typical abdominal wall morphologies established from CT scans as a function of **a)** BMI **b)** gender
Figure from Jourdan *et al.* (Jourdan, Soucasse, et al. 2020)

Key points

- The linea alba is the stiffest and thinnest structure of the abdominal wall, where stress will be maximal.
- The abdominal wall deforms twice as much in the cranio-caudal direction compared to the circumferential direction. In the circumferential direction, strains are more pronounced in the lateral muscles than in the rectus abdominis.
- Forces acting on the abdominal wall arise from muscle activation and intra-abdominal pressure (IAP).
- There is significant variability (in terms of pressure, strain, and mechanical properties) among measurement methods and between individuals.

Pathophysiology of hernia formation

Definition of an abdominal hernia

Despite its robust design, the abdominal wall is vulnerable to pathologies such as hernias, where defects in the musculo-aponeurotic layers allow the protrusion of abdominal contents. The herniated organ or tissue is situated within a protruding pouch of peritoneum called the hernia sac (Joachim Conze et al. 2001), as illustrated in Figure 14. Hernias can lead to painful symptoms and reduced quality of life (O. A. Smith et al. 2022).

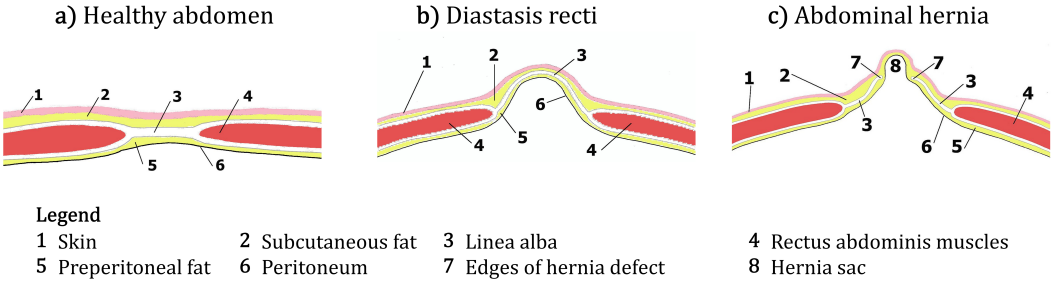

Figure 14.: **Legend**: **a)** healthy, **b)** diastasis and **c)** herniated abdominal wall zoomed on midline zone. Figure adapted from Wikimedia Commons images (Fedenko 2018b; Fedenko 2018a; Fedenko 2018c)

There are two types of hernia, which differ in their origin and causes (Leonard F. Kroese, Jean-Francois Gillion, et al. 2018; Verstoep et al. 2021): primary and incisional hernias. Primary hernias occur spontaneously, often due to inherent weaknesses in the abdominal wall. They are not related to prior surgical procedures. Incisional hernias form at the site of a previous surgical incision. After surgery, surgical site complications can happen leading the abdominal wall may not heal properly, leaving a weak spot in the tissue (Romain et al. 2020; Parker et al. 2021). This allows internal tissues or organs to protrude through the weakened area. Incisional hernias are common after abdominal surgery (Romain et al. 2020) and can occur months (Burger et al. 2005) or even years after the initial surgery (Bhardwaj et al. 2024; Fink et al. 2014).

Hernias have different locations, as shown in Figure 15. Ventral hernias occur through the front (anterior) abdominal wall. This category includes the umbilical hernia, occurring near the navel (umbilicus). It is often congenital but can develop later in

life due to increased intra-abdominal pressure (e.g., pregnancy (Al-Khan et al. 2011), obesity (Sanchez et al. 2001)). Epigastric hernia occurs between the navel and lower part of the ribcage. It is typically small and involves fatty tissue pushing through the abdominal wall. Incisional hernia develops at the site of a previous surgical incision, where the abdominal wall has become weakened. This is more common in people who have undergone multiple abdominal surgeries.

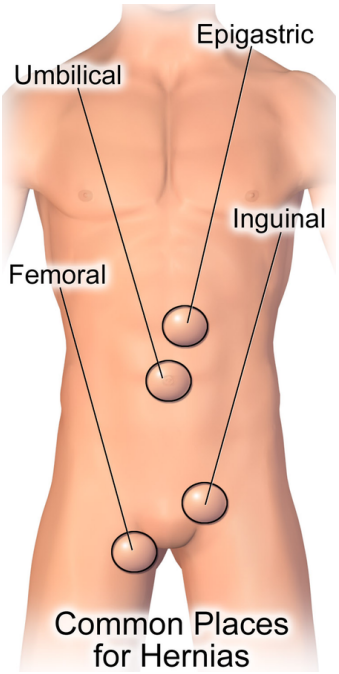

Figure 15.: Common hernia locations. Figure from Wikimedia Commons images (BruceBlaus 2017)

Other types of hernia can occur, including hiatal hernia, when abdominal contents push through a defect in the diaphragm, the muscle that separates the chest cavity from the abdominal cavity. Spigelian hernia occurs along the edge of the rectus abdominis muscle, through a weakened area in the spigelian fascia, which lies between the muscle and the lateral obliques. Femoral hernias occur when tissue pushes through a weak spot in the femoral canal, located just below the inguinal ligament, which carries the femoral artery to the thigh. A parastomal hernia forms around a stoma, which is an artificial opening made during surgery for waste elimination (e.g., colostomy, ileostomy). Inguinal hernias are located in the lower abdominal wall, specifically in the inguinal canal, in the groin area. Inguinal hernias are indeed the most common type of hernia, accounting for around 66 to 83% of all hernias (Ira M. Rutkow et al.

1993; Ira M Rutkow 2003; Qin et al. 2021). Around 25% of men and 2% of women will experience an inguinal hernia at some point in their lives (Primatesta et al. 1996). They are more common in men due to the presence of the spermatic cord in this region. Umbilical and incisional hernias follow as the second most common, with other types like epigastric, femoral, and hiatal hernias being less prevalent (Ira M Rutkow 2003). Although inguinal hernias are predominant, this study will be focusing on abdominal (ventral) hernias. Incisional hernias, which occur at the site of previous surgeries, tend to have higher recurrence rates. In fact, recurrence after ventral hernia repair can range up to 40-70% within a 5-year follow up (Bhardwaj et al. 2024), whereas inguinal hernia surgeries generally have a lower recurrence rate of around reaching 11% recurrence rate over 10-year follow up (Junge, Rosch, et al. 2006).

With the aim of improving the understanding, treatment, and prevention of hernias in Europe, the European Hernia Society (EHS, (*EHS History – EHS* 2024)) was founded in 1979. This organisation provides guidelines, research, and a platform for collaboration among surgeons, researchers, and healthcare professionals focused on hernia repair and management. By developing classifications, grading systems, and treatment protocols, the EHS plays a role in standardising hernia treatment globally (Muysoms, S. A. Antoniou, et al. 2015). The EHS classification system (Muysoms, Miserez, et al. 2009) for hernias is widely recognised and used to categorise hernias based on location, size, and characteristics. This system allows for a standardised approach, helping surgeons plan the most appropriate repair strategies and facilitating consistent research and data collection across studies (Leonard F. Kroese, Kleinrensink, et al. 2018).

Etiology of abdominal hernia

Several factors contribute to hernia etiology, including age-related changes, mechanical stress and overload, and comorbidities that affect tissue integrity such as predisposing anatomical or iatrogenic weaknesses. Clinical studies focusing on risk factors highlight the influence of morphometric, behavioural, or biological parameters. Some of them are reported in Figure 16.

Increased body mass index (BMI) is a well-documented risk factor for hernia, individuals with a BMI over 30 have a significantly higher incidence of both primary and recurrent hernias (Owei et al. 2017; Gignoux et al. 2021; Frommer et al. 2024; Bhardwaj

et al. 2024; van Silfhout et al. 2021). Elevated abdominal fat increases intra-abdominal pressure (Sanchez et al. 2001), which in turn, places chronic mechanical stress on the abdominal wall. Increase BMI is also associated with increased wound complications (Tastaldi et al. 2019).

Age-related changes in tissue composition contribute to weakened fascia and muscle function (Jourdan, Soucasse, et al. 2020; García Moriana et al. 2023). Older adults, particularly those over the age of 50, are at higher risk for developing abdominal wall hernias (Frederik Helgstrand et al. 2013; Le Huu Nho et al. 2012) due to decreased tissue elasticity and slower healing rates following surgery or injury (Holt et al. 1992; Goswami et al. 2022).

Activities involving heavy lifting increase intra-abdominal pressure, leading to repetitive strain on the abdominal muscles. This strain, especially when combined with an existing weakness in the abdominal wall, can result in hernia formation, especially inguinal hernias (Jha et al. 2020).

Pregnancy stretches the abdominal wall, potentially leading to diastasis recti (separation of the rectus abdominis muscles). Although this condition is different from a hernia, it can weaken the central fascia, predisposing individuals to hernia formation later in life. The linea alba width increased with both age and BMI (Gueroult et al. 2024) Pregnancy also increases intra-abdominal pressure (Al-Khan et al. 2011).

Smoking, chronic obstructive pulmonary disease and diabetes are also a well-known risk factors of developing a hernia (Sørensen et al. 2005; Gignoux et al. 2021; Parker et al. 2021). It also appears that heredity and collagen properties may affect hernia recurrence (Franz 2006; Jansen et al. 2004; Nadia A. Henriksen et al. 2015).

Incisional hernias are a frequent complication of abdominal surgeries (Romain et al. 2020). Surgical procedures that involve large incisions can weaken the abdominal wall, especially if postoperative healing is poor or infection occurs. Acute mechanical events, such as trauma or surgery, can also compromise the structural integrity of the abdominal wall. Surgical incisions can weaken the fascia, and improper healing processes might predispose the region to develop incisional hernias.

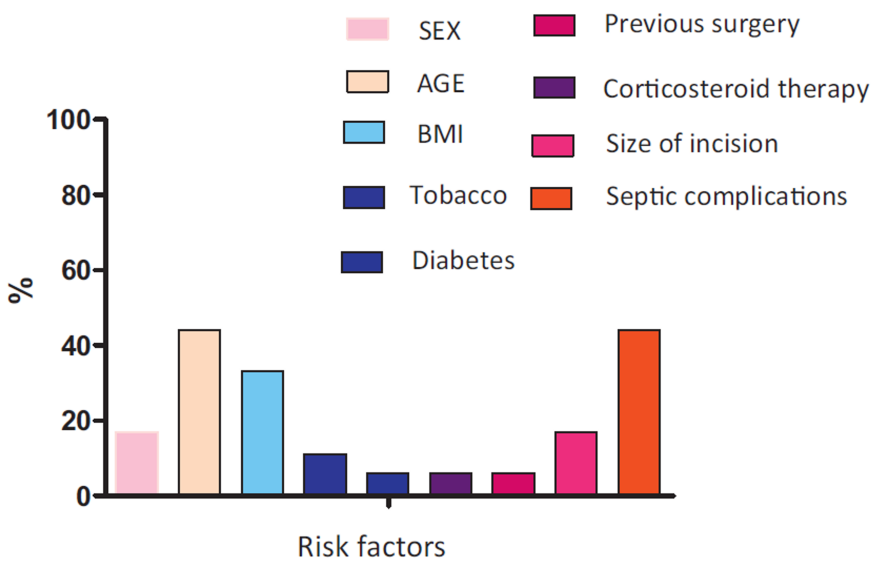

Figure 16.: Percentage of each independent risk factor for incisional hernia. Figure from Le Huu Nho *et al.* study (Le Huu Nho et al. 2012)

Mechanism of hernia formation

This section aims to illustrate that a hernia can result from a mechanical conflict. It is important to note that this diagram is intended to illustrate the mechanical concepts of stress and strain applied to the biomechanical study of the abdominal wall. However, this scheme is highly simplified by limiting this explanation to linear elasticity and does not take into account the wide range of complex mechanical behaviours beyond simple linear elasticity. In reality, the abdominal wall exhibits large deformations with non-linear stress-strain relationships, viscoelasticity with stress relaxation behaviour, anisotropy, hysteresis during cyclic loading or active contractile behaviour.
The stages of hernia formation are illustrated schematically in Figure 17. During physical activities, increased IAP leads to deformation and stress in the tissues. Under normal conditions, the abdominal wall responds elastically, i.e. in a completely reversible way, returning to its original state once the stress is removed. This is represented by the green section of the stress-strain curve in Figure 17.

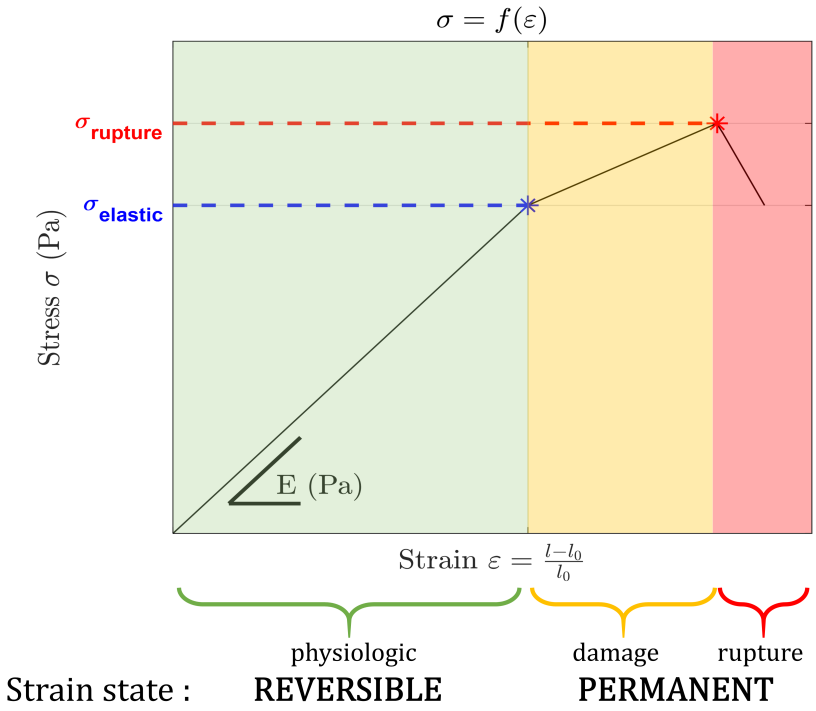

Figure 17.: Schematic stress-strain curve illustrating the main stages in hernia formation
Legend: Elastic and undamaged zone delimited by the elastic limit $\sigma_{elastic}$
Microstructural irreversible damage (e.g. diastasis in Figure 14-b) delimited by the tensile strength $\sigma_{rupture}$
Macrostructural irreversible damage (e.g. hernia in Figure 14-c)
Figure inspired from Joppin *et al.* (V. Joppin et al. 2023)

Beyond a certain stress threshold, known as the elastic limit or yield strength, denoted $\sigma_{elastic}$, tissues begin to undergo irreversible damage, represented by the yellow region of Figure 17. Microstructural injury appears first, marking the beginning of the domain where deformations are no longer fully reversible.

The tissue's tensile strength (or ultimate tensile strength, UTS) $\sigma_{rupture}$ is indicated on the curve, and the corresponding strain at this stress level is noted $\varepsilon_{rupture}$. At this point, the entire wall ruptures, resulting in a hernia, represented by the red region of Figure 17.

These mechanical phenomena are typically assessed qualitatively in clinical practice during the diagnosis of a hernia when the surgeon observes the deformation of the

abdominal wall induced by a cough, or during the surgical repair, when evaluating the force required to bring the hernia defect edges together.
Mechanical properties such as the elastic modulus (or Young modulus, E), elastic limit $\sigma_{elastic}$, and tensile strength $\sigma_{rupture}$ define each individual's unique «mechanical profile». The increased risk of hernia in patients with aortic aneurysms, who often have collagen dysfunction, highlights the importance of accounting for individual tissue properties (G. A. Antoniou et al. 2011). A hernia alters the mechanical properties of the abdominal wall, influencing the stability or progressive enlargement of the hernia orifice and sac volume.

Another mechanism for hernia formation, less studied in the literature, is fatigue rupture (DuBay, Xue Wang, et al. 2006). Fatigue rupture refers to the progressive damage and loss of tissue integrity when exposed to cyclic (repeated) stresses. This means that the multi-layered abdominal wall eventually loses its ability to withstand loads without experiencing permanent strain or rupture. Damage can occur suddenly, even if the applied stresses are lower than the tissue's tensile strength $\sigma_{rupture}$. Sustained increases in intra-abdominal pressure; from obesity, pregnancy, chronic coughing, straining during defecation, or heavy lifting; lead to progressive tissue fatigue.

Impact of a hernia on the mechanical behaviour

The mechanical behaviour of an abdominal wall with a rupture in the musculo-aponeurotic complex differs from that of a healthy or repaired wall. A hernia, whether natura, such as the umbilicus or groin, or iatrogenic such as a post-surgical scar, introduces a geometric discontinuity (hole) in the abdominal wall, which represents an area of fragility where stress is concentrated (Simón-Allué, Ortillés, et al. 2018). This explains the frequent occurrence of hernias at the umbilicus or near surgical scars and the progressive widening of the hernia orifice.

An abdominal wall with a hernia exhibits greater displacement than a healthy or repaired wall (Podwojewski et al. 2014; Silvia Todros, Paola Pachera, et al. 2018), the rupture of the musculo-aponeurotic complex allowing increased mobility of the abdominal wall. The presence of a hernia also increases the overall elasticity of the abdominal wall, causing it to deform more (Silvia Todros, Paola Pachera, et al. 2018; Podwojewski et al. 2013; Kallinowski et al. 2021), even though the oblique muscles

experience fiber stiffening and atrophy (DuBay, Choi, et al. 2007). The lateral portion of the abdominal wall shortens (DuBay, Choi, et al. 2007), which tends to widen the aponeurotic orifice leading to particularly high stress on the linea alba.

The strength of the abdominal muscles (rectus abdominis, external oblique, internal oblique) is markedly diminished in patients with incisional hernia in comparison to healthy controls, as determined by surface electromyography (Roy et al. 2023). Various studies using isokinetic dynamometer (Strigård et al. 2016; García Moriana et al. 2023) and strain gauge (Sánchez Arteaga et al. 2024) showed a negative correlation between abdominal wall muscle strength and hernia defect width.

During laparoscopic insufflation or voluntary muscle contraction by the patient, the size of the hernia orifice and the volume of the hernia sac significantly increase (Bellio et al. 2019; Jaffe et al. 2005; Qandeel et al. 2016). In the studies of Jaffe *et al.* (Jaffe et al. 2005) and Bellio *et al.* (Bellio et al. 2019), CT scan was used to quantify different abdominal metrics at two key times: at rest and during the Valsalva maneuver. Jaffe *et al.* quantified on 2D axial CT scan a significant increase in antero-posterior diameter of the abdomen, the antero-posterior diameter of hernia sac and width (left-right direction) of fascial defect during Valsalva maneuver compared to at rest. Additionally, half of the hernias became more visible with the Valsalva maneuver. Bellio *et al.* measured a 23% increase in cross-sectional hernia orifice area during Valsalva straining, and an 83% increase in hernia sac volume. These changes depend on the mechanical properties of the patient's abdominal wall, with substantial inter-individual variability.

Finally, the occurrence of a hernia reduces IAP, patients with hernia generally have lower IAP compared to healthy individuals, both at rest and during physical activity (Shafik et al. 1997).

Key points

- The mechanical conflict between the abdominal wall's ability to deform and the forces applied (related to internal organs and muscle activation) influences hernia formation and growth.
- Abdominal hernias occur mainly at geometric discontinuities (e.g., umbilicus or

scars). Once a hernia forms, stress concentrates on the hernia orifice, promoting its enlargement.

- A hernia increases the mobility and thus the elasticity of the abdominal wall.

Surgical restoration of the abdominal wall

The management of an abdominal hernia involves several key steps to ensure optimal patient outcomes. The process begins with an initial evaluation by a surgeon to assess the size and location of the hernia and the patient's overall health. This evaluation may include a detailed medical history and physical examination. Depending on the clinical findings, imaging studies such as ultrasound or CT scans may be ordered to better delineate the characteristics of the hernia. Based on this, the surgeon will discuss the most appropriate surgical options with the patient, taking into account factors such as the type of hernia, patient comorbidities and risk factors. The European Hernia Society provides guidelines to support evidence-based approaches to hernia management (Bittner et al. 2019; N A Henriksen et al. 2020). After surgery, patients can be advised to wear an abdominal binder to support the abdominal wall, reduce surgical site infections and postoperative pain (Graziani e Sousa et al. 2024). Regular follow-up visits are scheduled to monitor the patient's recovery, assess for complications, and provide guidance on resuming normal activities. The frequency and duration of follow-up depends on individual patient factors and the complexity of the hernia repair.
The mechanical concepts are still not sufficiently integrated into current therapeutic strategies. Yet, their incorporation could offer significant improvements in abdominal hernia surgery. The surgery consists in closing the musculo-aponeurotic neck, and can be done either by laparotomy or laparoscopy. Laparotomy is an open surgical procedure where a large incision is made in the abdominal wall to directly access internal organs. Laparoscopic surgery, in contrast, is a minimally invasive surgical technique in which small incisions are made to insert a camera (laparoscope) and surgical instruments, allowing surgeons to operate inside the abdomen without large incisions. In order to have a sufficient visibility and room to maneuver surgical instruments, it is necessary to lift the abdominal wall away from the organs. This is called pneumoperitoneum and involves insufflating gas, typically carbon dioxide (CO_2), into the abdominal cavity during laparoscopic surgery.

Although surgical procedures are constantly being challenged, such as less invasive surgery technique like laparoscopy (Luján et al. 2004; Barbaros et al. 2007; Le Huu Nho et al. 2012) or the use of mesh implants when closing the hernia defect (Schumpelick

et al. 1996; Anthony et al. 2000), hernia surgery is still associated with a high recurrence rate, reaching up to 30% within two years (Jean-François Gillion et al. 2019; Romain et al. 2020).

Impact of repair on the mechanical behaviour

The mechanical properties of a repaired abdominal wall differ significantly from those of a healthy one. In general, a repaired abdominal wall tends to be more rigid (DuBay, Xue Wang, et al. 2006; Le Ruyet et al. 2020), with stiffness increasing by as much as 58% (Silvia Todros, Paola Pachera, et al. 2018). This increased stiffness is often associated with postoperative discomfort and pain for the patient (Welty et al. 2001). Additionally, the repaired abdominal wall exhibits lower resistance to rupture (DuBay, Choi, et al. 2007) and reduced mobility compared to a healthy wall (Junge, Klinge, et al. 2001; Silvia Todros, Paola Pachera, et al. 2018; He et al. 2020). Figure 18, based on Todros *et al.* (Silvia Todros, Paola Pachera, et al. 2018) numerical study, illustrates the comparative displacement of abdominal wall models subjected to coughing effort, showing the largest displacement for the herniated wall, followed by the healthy wall, and finally, the repaired abdominal wall which exhibits the lowest displacement.

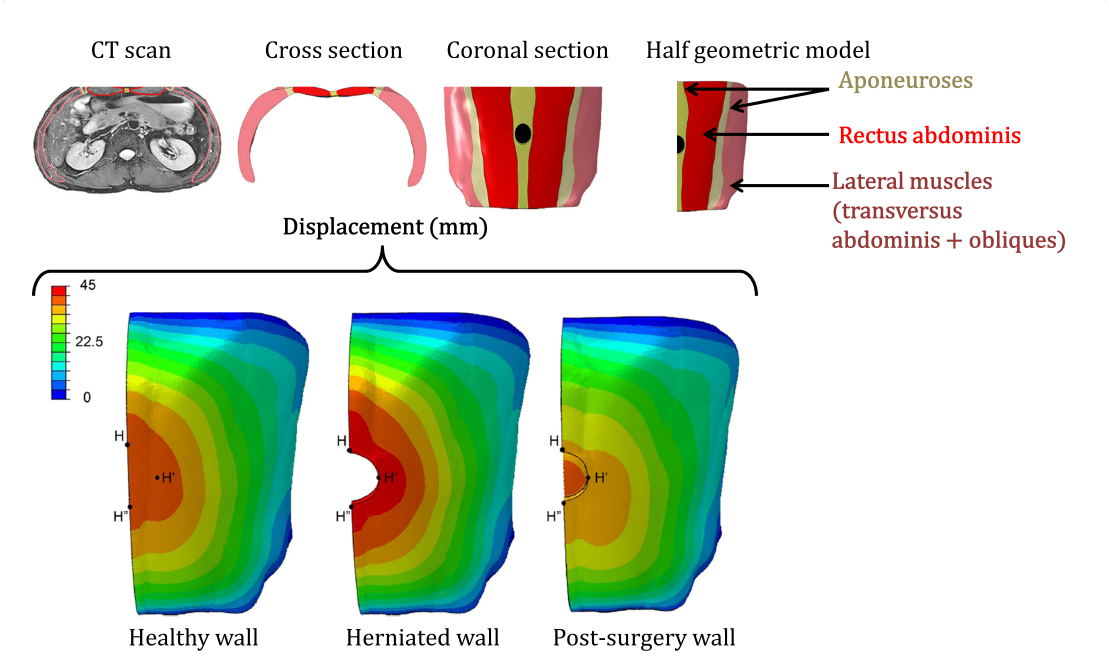

Figure 18.: Displacements obtained during coughing loading of a numerical model of a healthy, herniated and repaired abdominal walls from Todros *et al.* (Silvia Todros, Paola Pachera, et al. 2018)

Mechanical behaviour of the repaired abdominal wall is evaluated through both experimental (Joris J. Harlaar et al. 2009; L. F. Kroese, J. J. Harlaar, et al. 2017; Lyons et al. 2015) and numerical studies (Silvia Todros, Paola Pachera, et al. 2018; He et al. 2020; Guérin et al. 2013; Simón-Allué, B. Hernández-Gascón, et al. 2016; Simón-Allué, Ortillés, et al. 2018; Agnieszka Tomaszewska et al. 2018). These studies aid in understanding the observed clinical differences and help optimise surgical repair strategies, guiding the surgeon in the choice of suture and implant. For instance, the «Abdoman» experimental model (Figure 19) was developed to simulate various surgical closure techniques, such as elastic sutures, on synthetic, porcine, and human walls, replicating dynamic muscle contraction and IAP phenomena (L. F. Kroese, J. J. Harlaar, et al. 2017).

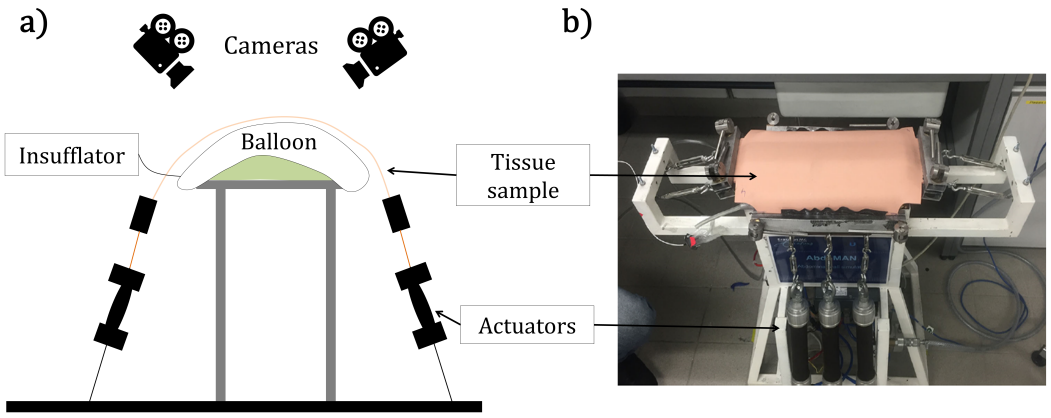

Figure 19.: «Abdoman», an experimental model of abdominal wall from Kroese *et al.*, 2017 (L. F. Kroese, J. J. Harlaar, et al. 2017)
Legend: **a)** Scheme of the setup **b)** Experimental setup

On the functional aspect of the abdominal wall repair, Criss *et al.* showed through isokinetic and isometric measurements of the rectus muscle that hernia repair with linea alba restoration improved abdominal wall functionality (Criss et al. 2014). Another study showed that training the abdominal muscles before the surgery had a significant impact on strengthening the abdominal muscles after repair of a ventral hernia (Ahmed et al. 2018).

Changes in abdominal wall morphometry induced by hernia surgery were investigated on CT scans (Lisiecki et al. 2015), showing a decrease of the cross-sectional anterior-posterior distance, area and circumference of the abdomen after the surgery.

Surgical repair

Mechanical contribution of a prosthetic implant

Hernia repair is typically conducted through suturing the aponeurotic defect, which is often reinforced with a prosthetic implant. The use of an implant (also called mesh) is recommended for all repairs of incisional hernias (i.e., recurrent hernia at a scar site) with an orifice larger than 2 cm (Liang et al. 2017). Implants are also being considered for prophylactic use in primary closure to prevent incisional hernias. Implants partially restore the mechanical properties of the herniated abdominal wall by reducing the excess mobility induced by the hernia and therefore the level of strain (Junge, Klinge,

et al. 2001; Podwojewski et al. 2014; Kallinowski et al. 2021; B. Hernández-Gascón et al. 2011). Compared to suturing alone, using an implant limits the stiffening of the repaired abdominal wall (DuBay, Xue Wang, et al. 2006) by slowing down the deposition of type III collagen at the scar site. Although a repaired abdominal wall with a mesh has greater mobility than without, it remains less resistant to rupture (DuBay, Xue Wang, et al. 2006). Surgical decisions, such as implant positioning (intraperitoneal or retromuscular in most cases), mesh overlap and fixation methods, also influence the mechanical behaviour of the repaired abdominal wall.

Mechanical properties of implants

Various mechanical tests are used to characterise implants (Deeken, Abdo, et al. 2011; Deeken and Lake 2017). Many manufacturing parameters, such as material and structure (pore size, fiber diameter, weaving), influence their mechanical characteristics and, consequently, the behaviour of the repaired abdominal wall (C. Brown et al. 2010; J. Conze et al. 1999; S. Todros et al. 2017).

The key mechanical properties that should guide the surgeon in selecting an implant are the elastic modulus (E), the tensile strength (σ_{rupture}), and the corresponding strain at rupture ($\varepsilon_{\text{rupture}}$) (C. Brown et al. 2010; J. Conze et al. 1999). Ideally, manufacturers should provide the mechanical characteristics of the implants, and surgeons should assess the elasticity of the patient's abdominal wall preoperatively. An implant with elasticity similar to that of the biological abdominal wall is most suitable for successful repair, as a large disparity in elasticity between the implant and the abdominal wall leads to stress concentrations at the wall-implant interface (Junge, Klinge, et al. 2001; Anurov et al. 2012; B. Hernández-Gascón et al. 2011; C. Szymczak et al. 2010; A. Tomaszewska et al. 2013). Physiological movements of the abdomen induce displacement and deformation of the abdominal wall, and an implant with much higher rigidity than the abdominal wall will generate high stresses (Equation 0.3) (DuBay, Xue Wang, et al. 2006; Hernández-Gascón et al. 2013; Simón-Allué, B. Hernández-Gascón, et al. 2016; Simón-Allué, Ortillés, et al. 2018).

An overly rigid implant excessively restricts mobility and increases the sensation of a foreign body. The overall stiffness of the repaired abdominal wall also increases with the size of the implant (Le Ruyet et al. 2020). Conversely, an overly elastic implant

presents a higher risk of rupture (Blázquez Hernando et al. 2015), as soft materials (with low elastic modulus) are generally less resistant to rupture. Insufficient implant stiffness, leading to excessive deformation, can result in complications when IAP increases, especially in large incisional hernia repairs, referred to as bulging (DuBay, Xue Wang, et al. 2006; Guérin et al. 2013; Simón-Allué, B. Hernández-Gascón, et al. 2016; Blázquez Hernando et al. 2015; E. B. Deerenberg et al. 2016).

An implant with slight anisotropy is more suitable because it better matches the mechanical properties of the abdominal wall, which is also anisotropic. These implants are particularly useful for large abdominal defects where the anisotropic behaviour is more pronounced (Simón-Allué, B. Hernández-Gascón, et al. 2016).

Impact of hernia defect size on repair

The size of the hernia defect is an important parameter because it allows classification of the hernia according to the EHS classification (Muysoms, Miserez, et al. 2009) and will influence the choice of implant for repair. However, it has been shown that the defect size is not correlated with the force required to close the hernia orifice, highlighting the importance of considering the mechanical properties of each patient's abdominal wall (Hope et al. 2018). On the other hand, for a given patient with specific mechanical properties, experimental and numerical studies show that the defect size plays an important role in the stress and displacement of the repaired abdominal wall (Guérin et al. 2013; Simón-Allué, B. Hernández-Gascón, et al. 2016; Hernández-Gascón et al. 2013). Intraoperative estimation of the force needed to close the aponeurotic defect is difficult; the value measured during surgery with a dynamometer is not correlated with the surgeon's estimation, underscoring the need for surgical decisions to be supported by objective measurements (Hope et al. 2018).

Influence of repair on intra-abdominal pressure

The closure of an incisional hernia defect using an implant increases the IAP by approximately 2.7 mmHg (Angelici et al. 2016). For more complex hernias (those with a defect larger than 10 cm and a significant hernia sac), the increase in IAP can reach up to 4 mmHg (Espinosa-de-los-Monteros et al. 2022). These values are important to consider in the context of preventing intra-abdominal hypertension, which is

defined as a sustained IAP above 12 mmHg while in a supine position (Malbrain, M. L. Cheatham, et al. 2006). The surgical technique known as component separation is used in abdominal wall reconstruction to treat large hernias by mobilising and separating the muscle layers of the abdominal wall, allowing for the closure of large defects without excessive tension, and is typically employed when primary closure is not possible due to the size of the hernia or previous surgical complications.

Recurrence factors

Incisional hernias following laparotomy, laparoscopy, or hernia repair are both frequent and poorly understood events.

Influence of patient parameters

As of now, no clinical studies have established a link between compliance and either postoperative pain or the risk of incisional hernia.

Recent studies from patient registries have not found a statistical correlation between defect size and the risk of recurrence (DuBay, Xue Wang, et al. 2006; Jolissaint et al. 2020; Luijendijk et al. 2000; Poruk et al. 2016; Wormer et al. 2013). However, mechanical studies suggest that for patients with equal mechanical properties, increased defect size leads to higher stresses (Guérin et al. 2013). From a mechanical standpoint, these two seemingly contradictory findings suggest that while defect size plays a role in recurrence risk, other factors, such as abdominal wall elasticity, are more significant.

Influence of surgical technique

Beyond patient-specific parameters, inappropriate surgical decisions, such as the choice of suture technique or implant type, appear to contribute to early repair failure (Burger et al. 2005; J. J. Harlaar et al. 2017). The technique of using interrupted sutures, sometimes supplemented with full-thickness sutures (including the whole thickness of the wall, from skin to peritoneum), has been largely abandoned due to its association with a higher risk of incisional hernias (Diener et al. 2010).

Clinical studies have demonstrated that the «small bites» closure technique, as illustrated in Figure 20 inspired from Meijer *et al.* (Meijer et al. 2016), with closely spaced stitches and small bites of tissue (thickness of tissue trapped in the suture),

combined with a fine suture thread, results in the lowest recurrence risk (Jenkins 1976; Millbourn et al. 2009; Varshney et al. 1999). These clinical findings are supported by mechanical studies comparing different closure techniques (Joris J. Harlaar et al. 2009; G. M. Cooney et al. 2018; Eva B. Deerenberg et al. 2015). Additional studies have varied both the stitch spacing and bite size, demonstrating that the lowest strains and highest rupture forces are achieved with a small stitch spacing (5 mm) and a large tissue bite (16 mm) (G. M. Cooney et al. 2018). This combination reduces the risk of ischemia and scar opening, as a smaller stitch spacing allows for more suture points, which increases the contact area between the suture and the abdominal wall. Thus, the total tension is distributed over a larger number of individual points, reducing the recurrence rate (Millbourn et al. 2009; Eva B. Deerenberg et al. 2015). A larger tissue bite better distributes the tension along the suture line (Joris J. Harlaar et al. 2009; Jenkins 1976; Varshney et al. 1999; G. M. Cooney et al. 2018), which also aligns with the preference for a large overlap between the implant and abdominal wall (Kallinowski et al. 2021) to reduce abdominal wall deformation (Le Ruyet et al. 2020).

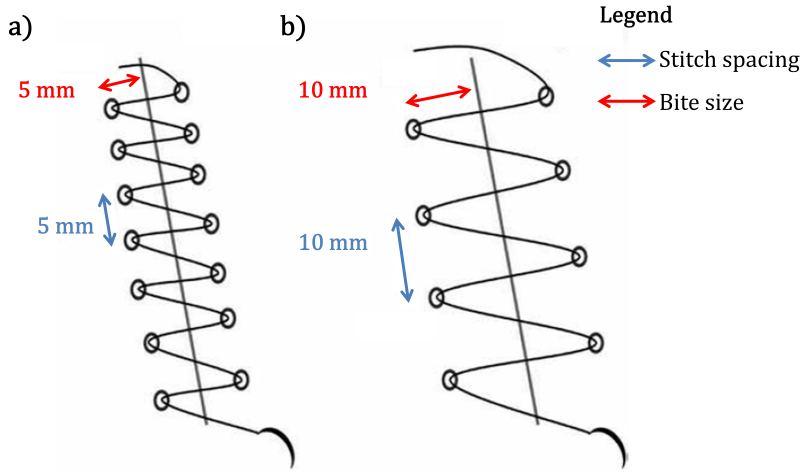

Figure 20.: Scheme of two sutures with different stitch spacing and bite size (distance from the wound, thickness of tissue trapped in the suture)
Legend: **a)** 5*5 mm **b)** 10*10 mm. Figure inspired from Meijer *et al.*, study (Meijer et al. 2016)

Minimising relative movement between the abdominal wall and the implant is crucial for successful healing and reducing postoperative pain (Kallinowski et al. 2021). The suture thread diameter also plays a mechanical role; a thicker thread increases its

strength but also requires a larger needle, leading to more tissue trauma. Repair failure often results from insufficient implant fixation strength relative to the stresses on the abdominal wall. As shown in Figure 21, significant stresses can accumulate at the implant-wall interface (Junge, Klinge, et al. 2001; DuBay, Xue Wang, et al. 2006; Simón-Allué, Calvo, et al. 2017; Simón-Allué, Ortillés, et al. 2018).

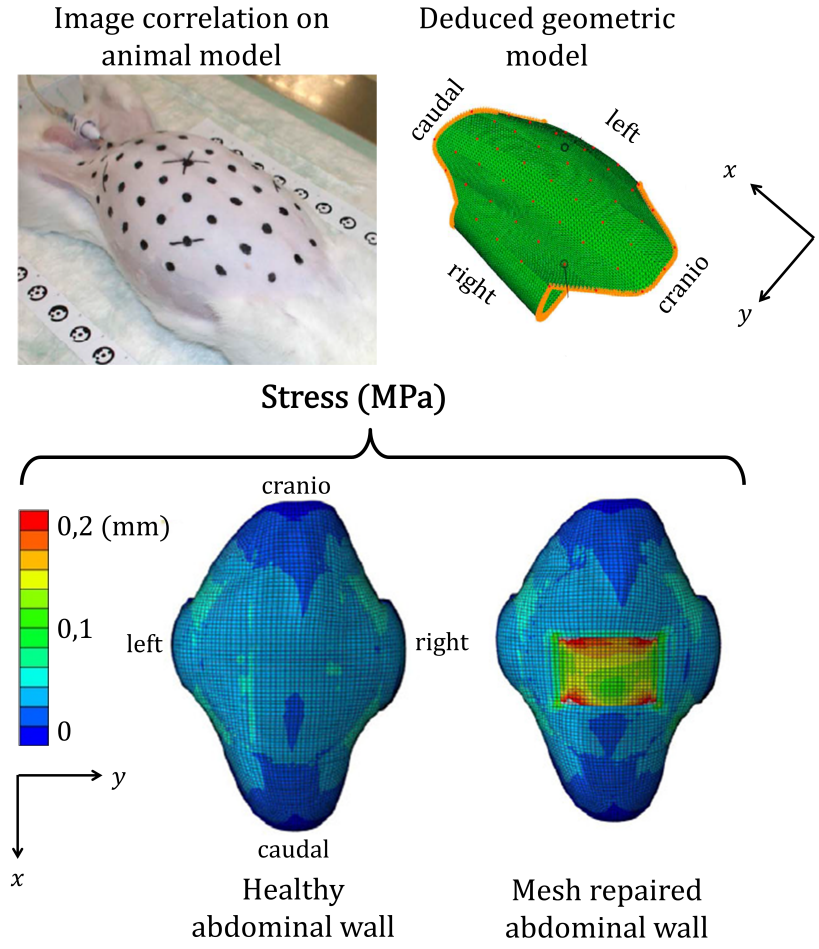

Figure 21.: Numerical model of abdominal wall, stresses obtained during a 12 mmHg increase in IAP with visible peak at mesh-wall interface. Figure from Simón-Allué *et al.* study (Simón-Allué, Calvo, et al. 2017; Simón-Allué, Ortillés, et al. 2018)

The tension applied to the suture during closure seems to influence recurrence risk. Studies suggest that optimal healing requires a mechanical stress that exceeds a minimum threshold, stimulating fibroblast activity, which is essential for collagen synthesis (Franz 2006). Therefore, the «tension-free repair» technique, which avoids placing any load on the scar, may not always be the most appropriate approach (Franz

2006). However, excessive tension can lead to ischemia and necrosis of the sutured tissues (Roca et al. 2018). Additionally, suture tension decreases by half within the first 24 hours postoperatively, indicating that high initial tension is unnecessary (A. Schachtrupp et al. 2016).

Although the choice of incision location is often dictated by surgical procedure, when possible, a transverse incision, i.e., following the left-right direction schematised on Figure 1, is preferable, as it is more resistant to rupture and reduces the hernia recurrence rate by half compared to a sagittal incision (S. R. Brown et al. 2005; Greenall et al. 1980; Le Huu Nho et al. 2012; Nilsson 1982). This is due to the anisotropic properties of the abdominal wall, where the tissues exhibit different elasticities in different directions. A transverse scar will experience lower perpendicular forces compared to a sagittal scar.

In cases where component separation is necessary to close the abdominal wall, this technique generally has minimal adverse effects on its mechanical behaviour (Daes et al. 2022). The lateral muscles, which can tolerate some degree of atrophy due to their composite configuration, compensate for the surgical procedure, preserving the overall muscle physiology.

A recent study has introduced the innovative concept of biomechanically optimised hernia repairs, which aim to customise surgical treatment based on standardised biomechanical assessments of the abdominal wall (Lesch et al. 2024). This approach moves beyond traditional «one-size-fits-all» repairs by tailoring the procedure to the unique mechanical properties and functional demands of each patient's anatomy. The study demonstrated that patients who underwent these biomechanically calculated repairs experienced a significant reduction in hernia recurrence rates, as well as a marked decrease in post-operative pain both at rest and during activities. These findings confirm that incorporating biomechanical considerations into hernia repair can lead to improved long-term outcomes, making it a promising advancement in personalised surgical care.

Influence of abdominal wall loading

The tensile force exerted on the suture is directly related to the IAP. A high IAP increases the forces on the suture and consequently the risk of repair failure (Konerding et al. 2011; Alexander Schachtrupp et al. 2019). Additionally, fluctuations in IAP, both pre- and postoperatively, are statistically associated with recurrence (Mureşan et al. 2016). In clinical practice, the use of an abdominal binder, which is stiffer than the abdominal wall, can help reduce the load on the abdominal wall by redistributing IAP-induced stresses. However, overly rigid abdominal binders are not recommended due to decreased comfort and increased IAP (H.-Y. Zhang et al. 2016).

Muscle contraction also plays a role in the pathophysiology of incisional hernia formation (Lien et al. 2015). The use of a muscle relaxant prior to closing the fascial defect can reduce the force required for closure during surgery and seems to decrease the risk of hernia recurrence, as well as the size of the defect in cases of recurrence.

Early signs of recurrence

Incisional hernia surgery typically occurs within two years following the initial repair (Helgstrand 2016; Gignoux et al. 2021), although early signs of recurrence may appear within a month postoperatively, illustrating the delay between their appearance and clinical diagnosis (Romain et al. 2020; DuBay, Xue Wang, et al. 2006; Luján et al. 2004). The primary early signs include fluid accumulation in the hernia sac (Loftus et al. 2017) or widening of the linea alba (Burger et al. 2005; J. J. Harlaar et al. 2017; Pollock et al. 1989). In general, patients with a wider linea alba, particularly those with diastasis (abnormal distance between the rectus muscle without fascial defect), are at greater risk of incisional hernia (Köhler et al. 2015). This may be due to the reduced thickness of the linea alba in the anteroposterior direction, leading to a smaller cross-sectional area subjected to forces, and consequently, higher stresses (see Equation 0.1).

Figure 22 below illustrate, among a group of high-risk laparotomies (Gignoux et al. 2021). According to Gignoux *et al.* study, 56% of incisional hernias repairs occurred during the first year after laparotomy and 79% during the first 2 years, the median duration was 9.6 months.

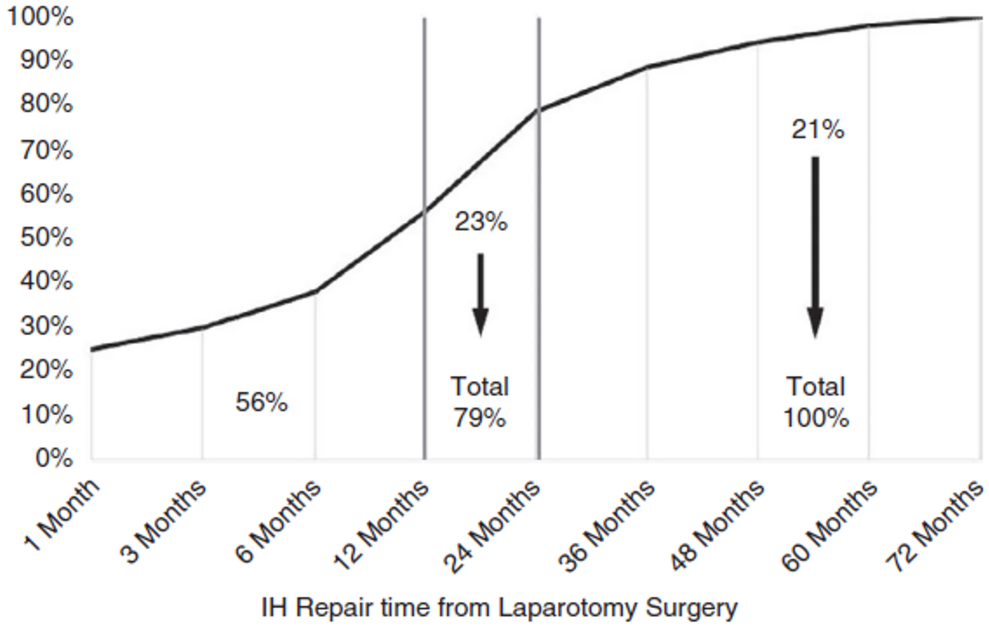

Figure 22.: Time to incidence of incisional hernia (IH) repair for the high-risk laparotomy list. Figure from Gignoux *et al.* study (Gignoux et al. 2021)

Key points

- Repairing a herniated abdominal wall with a prosthetic implant partially restores its mechanical properties, increasing its stiffness. Compared to simple sutures, the addition of a prosthetic implant allows for greater mobility in the repaired abdominal wall.

- The implant should have mechanical properties similar to those of the abdominal wall to optimise repair success and reduce postoperative pain (anisotropic elasticity, deformation). A small bite suture technique, is associated with a lower risk of recurrence.

Imaging of abdominal wall

Brief definitions of imaging techniques

MRI uses strong magnetic fields and radiofrequency (RF) waves to generate highly detailed images of internal body structures. The hydrogen nuclei (protons) present in the body's water and fat align themselves with the magnetic field. When this alignment is disturbed by an RF pulse, the protons emit signals as they return to their original alignment. The signals are then captured and converted into images. The primary benefit of MRI is the excellent soft tissue contrast it offers, especially for muscles, brain, and organs. Additionally, it is a non-invasive imaging technique that does not involve ionising radiation. The primary disadvantages of MRI are its high cost and long acquisition time, the need for specialised equipment, and its contraindication for patients with certain metallic implants.

CT scan uses X-rays to create detailed cross-sectional images (slices) of the body. A rotating X-ray tube sends beams to the opposite side of the patient, where detectors measure the intensity of X-rays that pass through the body. Unlike conventional X-rays which produce a 2D image, CT scans combine multiple X-ray images taken from different angles around the body to produce a 3D representation of internal structures. The main advantages of CT scan are the high-resolution imaging of internal structures, including bones, soft tissues, and blood vessels. CT is particularly effective for visualising bones, fractures, and calcifications, which may be challenging to discern with other imaging techniques, such as MRI. CT scans are a considerably faster alternative to MRI and can capture images in seconds, rendering them a valuable asset in emergency settings. However, the primary drawbacks are that CT scans expose patients to ionising radiation, which are significantly higher than regular X-rays. Repeated exposure can increase the risk of cancer over time. Additionally, while CT is highly effective for examining bones and dense structures, it exhibits inferior contrast resolution compared to MRI for soft tissues like the brain, muscles, and ligaments.

Ultrasound uses high-frequency sound waves emitted by a transducer. These waves penetrate the body and are reflected back when they encounter different tissues. The echoes are converted into real-time images that can show the structure of organs, tissues, and blood flow. The main advantages of ultrasound are to be portable, fast, widely available, non-invasive, without ionising radiation, relatively inexpensive, and

providing real-time imaging. The main disadvantages are the limited by penetration depth and poor image quality for air-filled or dense structures (e.g., bones, lungs), its lower soft tissue contrast compared to MRI.

Shear-wave elastography is an ultrasound-based technique that uses focused ultrasound pulses to generate shear waves in tissues. These shear waves propagate through the tissue, and their speed is measured to infer tissue stiffness. Stiffer tissues generally exhibit faster shear wave propagation. The main advantages of shear-wave elastography is to provide quantitative measurements of tissue stiffness (useful for liver fibrosis, muscle stiffness, etc.), it is a non-invasive and relatively quick imaging technique which can be integrated into conventional ultrasound systems. The main disadvantages are, as ultrasound, the limited penetration depth (less effective for deep tissues) and imaging resolution compared to MRI.

The above-mentioned imaging modalities are illustrated in Figure 23.

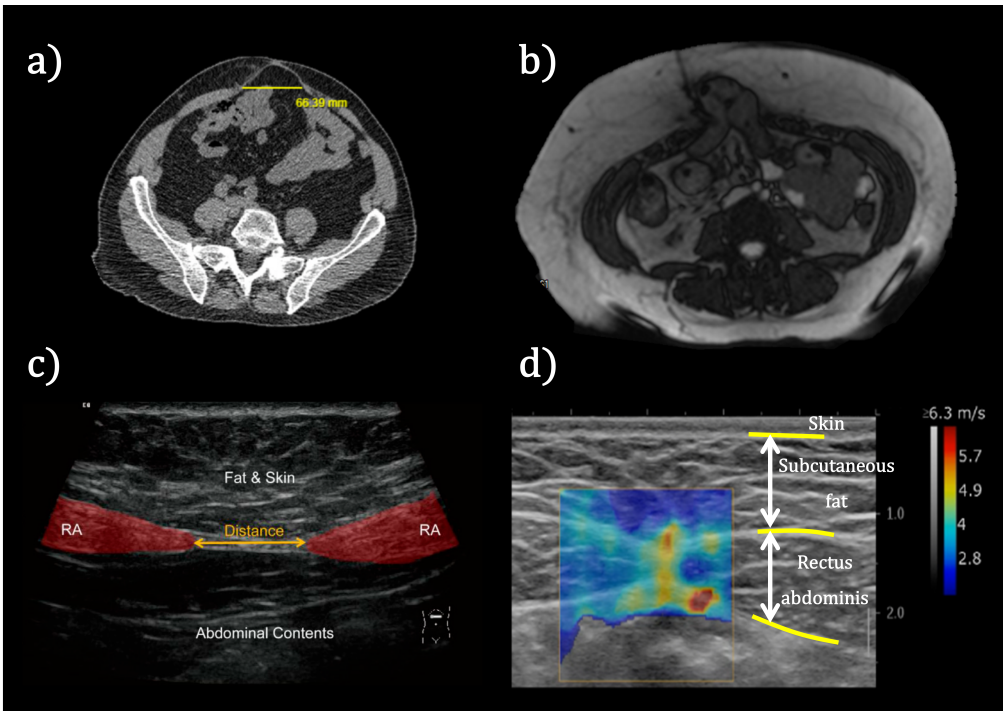

Figure 23.: Example of different abdominal wall imaging modalities
Legend: **a)** Axial CT scan from Frommer *et al.* study (Frommer et al. 2024)
b) Axial MRI
c) Ultrasound from Wang *et al.* study (F. Wang et al. 2023)
d) Shear-wave elastography, adapted from Vergari *et al.* study (Vergari et al. 2023)

Current imaging techniques and limitations

Imaging the abdominal wall is essential for diagnosing, monitoring, and understanding various pathologies, as well as for studying the biomechanics of this complex structure. Magnetic resonance imaging (MRI) and computed tomography (CT) are the primary imaging modalities employed for abdominal wall assessment, due to their superior contrast resolution for soft tissues (Plumb et al. 2021).

CT scan is the most common imaging modality for the detection of hernias (Muysoms, S. A. Antoniou, et al. 2015) and for post-operative follow-up (Gutiérrez de la Peña et al. 2001; Gossios et al. 2003). It has been demonstrated that a more functional-based preoperative imaging of the abdominal wall can markedly enhance the comprehension of ventral hernia defects, thereby facilitating the development of efficient surgical plans that result in minimal recurrence rates and optimal functional outcomes (Read et al. 2022). The use of Valsalva maneuver is helpful in diagnosing hernias in patients, due to the increased visibility of the hernia sac during physical exertion (Plumb et al. 2021; Dallaudiere et al. 2024). Continuous dynamic CT scans are not feasible because prolonged exposure to ionising radiation poses significant health risks to patients. In that respect, other imaging techniques including ultrasound, shear-wave elastography and MRI provide valuable pre or post-operative information on hernia detection which is sometimes challenging (Jaffe et al. 2005; Baucom et al. 2014; Bellio et al. 2019; Read et al. 2022).

Ultrasound proved its efficacity in detection of early sign of recurrence such as a large distance between rectus abdominis (J. J. Harlaar et al. 2017; F. Wang et al. 2023). Shear-wave elastography was used to estimate the mechanical properties of the abdominal wall, reporting a higher shear wave speed in patients with incisional hernia than in controls (Xiaohong Wang et al. 2020). Shear-wave elastography was also used on healthy subjects during normal breathing, highlighting the anisotropic stiffness on linea alba and the increasing shear wave speed when inflating the abdomen (Vergari et al. 2023).

However, ultrasound and shear-wave elastography methods can only be used to assess locally restricted area. CT scan provides an in-depth assessment of the abdominal wall but is a radiating imaging technique offering only static views that fail to capture the dynamic nature of hernias during physiological activities like breathing and coughing.

Different studies also showed that CT scan was not associated with reliable diagnosing in ventral hernia recurrence (Holihan et al. 2016), and CT reports often fail to include important pre-operative hernia feature (Kushner et al. 2021). In that respect, MRI appears to be an interesting and non-invasive alternative for its ability to visualise muscles, fat, and connective tissues without exposing patients to ionising radiation that extends the in-depth study of the various muscle groups in the abdominal wall.

Benefits of MRI in abdominal wall study

MRI allows for the real-time visualisation of the movement and interaction of abdominal structures during various physiological and pathological conditions (Randall et al. 2017). MRI has also been used for muscle denervation or atrophy (Rodriguez-Acevedo et al. 2020). Dynamic magnetic resonance imaging (MRI), often referred to as cine-MRI, represents a significant advancement in this field. Unlike static MRI, cine-MRI captures continuous sequences of images over time, offering detailed insights into the dynamic behaviour of the abdominal wall and surrounding tissues. It has multiple applications, such as observing the abdominal wall ability to move and deform (Vlot et al. 2013; Blanchard et al. 2016; Jourdan, Rapacchi, et al. 2022), enabling a better understanding of how muscles behave during pneumoperitoneum or activities such as breathing, coughing, and physical exertion.

Cine-MRI has also proven valuable in detecting and assessing abdominal adhesions, a common complication following surgery, by allowing clinicians to observe the movement restrictions between organs and tissues (Randall et al. 2017; Yasemin et al. 2020). Moreover, dynamic MRI can be used to study the biomechanical effects of external support devices, such as abdominal binder which are frequently used post-operatively or in the management of conditions like hernias. Research has shown that cine-MRI provides insight into how these binders influence muscle contraction and abdominal wall mechanics during physical activity (Miyamoto et al. 2002). Additionally, it has been employed in the study of chronic groin pain in inguinal hernias (Dallaudiere et al. 2024). Another important application of cine-MRI is in post-operative follow-up, particularly in patients with implanted mesh following hernia repair. The real-time imaging capability allows for the assessment of mesh positioning, integration with surrounding tissues, and potential complications such as mesh migration or folding

(Fischer et al. 2007; Ciritsis et al. 2014).

Image post-processing

In clinical practice, the most frequent use of imaging is done by the radiologist, who need both knowledge of radio-anatomy and surgical principles a prerequisite (Rousset et al. 2023). The radiologist provides the surgeon the necessary information, on the basis of a standardised report such as those proposed by the European Hernia Society (Muysoms, Miserez, et al. 2009; L. F. Kroese, Sneiders, et al. 2018), to enable the most appropriate surgical strategy and thus optimise effective and lasting repair.

Other image processing techniques, such as those employed for the enhancement of image quality (including contrast adjustment, filtering, and denoising), registration, segmentation, and feature extraction, are primarily used for research purposes. The registration process entails aligning images from different time points, subjects, or modalities (such as MRI and CT) to facilitate comparative studies. It is crucial for monitoring disease progression and evaluating pre- and post-operative conditions. The process of segmentation involves the division of an image into meaningful regions, such as the delineation of organs or muscles, as represented in Figure 11. This step is of particular importance for quantitative analysis, where the objective is to gain insight into the specific structures within the abdominal cavity. Following the segmentation stage, feature extraction consists in identifying and measuring key characteristics such as volume, texture, or shape of the structures. These features are frequently employed for diagnostic purposes or the assessment of the biomechanical properties of the abdominal wall. Precise segmentation of abdominal structures is crucial for in-depth analysis of anatomy and for assessing physiological and pathological responses of the abdominal wall. However, all the above mentioned imaging techniques face challenges such as the manual segmentation of images, which is labour-intensive and prone to variability. To achieve accurate segmentation, automatic or semi-automatic segmentation techniques, such as thresholding, geometric models, and multi-atlas approaches (Karlsson et al. 2015), have been widely applied, primarily targeting MRI and CT images for clinical analysis (A. C. Ogier et al. 2021; Lenchik et al. 2019).

However, the rise of deep learning, specifically Convolutional Neural Networks (CNNs), has revolutionised the field of medical image processing, leading to a new generation of automatic segmentation techniques. CNNs have demonstrated impressive

performance across different imaging modalities, including CT scans for fat, muscles and organs segmentation (Weston et al. 2019; Park et al. 2020), MRIs for adipose tissue assessment (Kway et al. 2021), and even ultrasound imaging for rectus muscle segmentation (F. Wang et al. 2023). Among these advanced neural network architectures, the nnUNet has emerged as a leading choice in biomedical image segmentation (Isensee et al. 2021), delivering remarkable results across various clinical applications (Verdier et al. 2024). (Ferrante et al. 2022). Despite these advancements, there remains a notable gap in the literature concerning highly automated methods for abdominal wall analysis (Borga 2018). Currently, abdominal muscles are often manually segmented to evaluate their mechanical function, a time-consuming task and operator-dependent. This highlights the pressing need for more efficient, automated segmentation tools, which would significantly reduce the manual labour involved and enhance the precision and reproducibility of abdominal wall studies.

Key points

- Imaging techniques like MRI, CT, ultrasound, and shear-wave elastography each provide unique insights into the abdominal wall, from tissue contrast to mechanical properties.
- MRI stands out for its good soft tissue contrast and non-invasive nature, while CT is preferred for its rapid imaging and detailed anatomical visualization.
- Dynamic MRI offers a substantial advancement in capturing real-time abdominal wall mechanics, enabling the study of muscle deformation and interactions during activities such as breathing and coughing.
- Emerging AI tools are transforming abdominal imaging by enhancing segmentation precision and reducing manual workload. These tools improve the accuracy and reproducibility of segmentation across imaging modalities, offering new possibilities for in-depth anatomical and biomechanical analyses.

Conclusion

The antero-posterior abdominal wall is a complex, multi-layered structure that plays a vital role in protecting internal organs or regulating intra-abdominal pressure during daily-life activities. However, despite its robust design, the abdominal wall is vulnerable to pathologies such as hernias, where defects in the musculo-aponeurotic layers allow the protrusion of abdominal contents. Hernia repair presents significant surgical challenges due to high recurrence rates and the variability in patient outcomes. Currently, surgeons have few objective tools to quantitatively assess the biomechanical parameters of their patients. Factors like patient-specific anatomy, insufficient biomechanical data, and the lack of advanced imaging tools further complicate the understanding and treatment of abdominal wall dysfunctions.

The study of abdominal wall biomechanics is critical for understanding the complexities of its function under different physiological conditions, as well as consequences associated with abdominal wall surgery. The abdominal wall is a dynamic structure that plays an essential role in maintaining intra-abdominal pressure, protecting vital organs, and supporting various bodily functions such as respiration, digestion, and movement.

In the preoperative phase, these tools would allow for a more personalised surgical approach (whether open or minimally invasive) and help in selecting the appropriate implant to reduce mechanical discrepancies between the abdominal wall and the implant. During surgery, they could objectively inform the decision on whether to use component separation techniques, assist in the implant positioning, and guide the choice of implant overlap and closure type. In the postoperative phase, these tools could improve patient recovery monitoring and enable the early detection of recurrences.

Objectives of the doctoral project

This PhD aims to address these challenges by advancing the biomechanical knowledge of the abdominal wall and developing new tools for improving diagnostic and therapeutic approaches. The primary objective of this thesis is to develop tools for evaluating the mechanical behaviour of the abdominal wall, providing quantitative data, and characterising the in vivo mechanical properties of healthy and pathological abdominal walls under physiological conditions. This characterisation relies on acquiring a dedicated medical imaging dataset as part of this work, followed by its post-processing.
The work presented in this manuscript is the result of a collaboration between two research laboratories with complementary expertise:

- The *Laboratory of Applied Biomechanics*, specialised in the biomechanical study and virtual modelling of the human body.
- The *Center for Magnetic Resonance in Biology and Medicine*, which develops MRI imaging methods for exploring pathologies affecting the cardiovascular, central nervous, and musculoskeletal systems.

The section below outlines each chapter's purpose by focusing on key research gaps, hypotheses, and the expected contribution of each section. A brief description of the scientific question each chapter aims to answer, the corresponding objective and challenge it addresses, and how the chapter contributes to the overall objectives of this PhD work is proposed.

Scientific question 1: How is intra-abdominal pressure (IAP) correlated with abdominal wall deformation during physiological activities, and how can this relationship be quantified using MRI?

Objective 1: To establish the correlation between intra-abdominal pressure (IAP) and abdominal wall deformation using MRI.

Challenge 1: IAP plays a critical role in hernia formation and recurrence, yet its dynamic *in vivo* relationship with abdominal wall motion is not fully understood.

Quantifying these interactions in real time using MRI is essential for improving diagnostic and treatment approaches. To address Objective 1, chapter 1 seeks to enlighten the *in vivo* correlation between IAP and the mechanical behaviour of the abdominal wall through MRI-based quantification during both passive (breathing) and active (Valsalva maneuver) exercises. These measurements were done in vivo during a clinical study involving 18 healthy subjects, aiming to improve the understanding of the abdominal wall's mechanical behaviour during various physiological activities.

Scientific question 2: How can the stresses experienced by the abdominal wall be approximated using a cylindrical model, and how accurate is this model in predicting real-world biomechanical loads?

Objective 2: To develop a cylindrical model to approximate stresses on the abdominal wall and validate it using real-world data.

Challenge 2: Predicting stresses within the abdominal wall under physiological loads requires a precise, yet simplified model. Existing models often fall short of capturing the complexity of the wall's biomechanics under varying conditions. To address Objective 2, chapter 2 develops a theoretical cylindrical model to estimate the abdominal wall's mechanical stresses during dynamic breathing, using the above mentioned *in vivo* temporal measurements of pressure and abdominal wall motion.

Scientific question 3: How does the 3D anatomical analysis of the linea alba (in terms of width, length, and curvature) across different patient demographics (age, gender, BMI) may help for understanding the structural variability of the abdominal wall and its vulnerability to hernia formation or diastasis recti?

Objective 3: To provide a comprehensive 3D anatomical description and variability of the linea alba based on demographics like age, BMI, and gender.

Challenge 3: Analysing and interpreting the impact of anatomical variability on the biomechanical properties of the abdominal wall is complicated by diverse patient-specific factors such as BMI and age. Capturing this variability accurately through 3D reconstructions is critical to understanding its clinical implications. To address

Objective 3, chapter 3 focuses on a 3D anatomical analysis of the linea alba, describing its length, width, and curvature across different patient groups. The findings lay the groundwork for understanding the relationship between anatomy and pathology, offering crucial insights for subsequent biomechanical modelling.

Scientific question 4: How can deep learning techniques, such as automatic segmentation and synthetic data generation, be used to enhance the analysis of abdominal MRI, improving accuracy and efficiency while addressing data variability and limitations?

Objective 4: To automate abdominal wall imaging analysis by integrating AI-driven segmentation and data synthesis techniques.

Challenge 4: The integration of AI into medical imaging presents challenges in developing models that are both accurate and generalizable. Balancing the need for large, diverse datasets with the limitations of available clinical data is crucial. Creating a workflow that combines automated segmentation with synthetic data generation to enhance model performance requires careful validation to ensure that these tools support and enhance real-world applications. To address Objective 4, chapter 4 merges the development of different tools. Automatic abdominal muscles segmentation using nnUNet was detailed in chapter 4.1, while the generation of synthetic MRI data is presented in chapter 4.2. The goal is to create a comprehensive framework for abdominal wall imaging with automated analysis of real-world datasets supplemented by synthetic ones.

Scientific question 5: How does abdominal wall biomechanics change after hernia surgery, and what are the key factors influencing post-operative muscle behaviour?

Objective 5: To analyse the biomechanical changes in patients' post-hernia surgery and compare pre- and post-operative conditions.

Challenge 5: While hernia surgeries aim to restore the structural integrity of the abdominal wall, post-operative changes in muscle behaviour are not fully understood. Studying these changes using MRI can offer insights into the factors that influence recovery and potential recurrence. To address Objective 5, chapter 5 investigates the

impact of hernia repair surgery on the biomechanics of the abdominal wall in patients comparing pre- and post-surgical states with the tools developed throughout this thesis.

Scientific question 6: How do the biomechanical and imaging findings from this thesis contribute to the improvement of hernia repair techniques, and what are the implications for future clinical practice?

Objective 6: To reflect on how the methods and findings from each chapter provide new insights into the biomechanical behaviour of the abdominal wall.

Challenge 6: Integrating biomechanical data, imaging techniques, and deep learning-based analysis into a cohesive framework that can inform clinical decision-making remains a complex task. To address Objective 6, chapter 6 synthesises the findings from previous chapters, discussing how each piece of research contributes to understanding and improving abdominal wall hernia repairs. It will also outline the broader implications for personalised patient care and future surgical planning.

1. Towards a better understanding of abdominal wall biomechanics: in vivo relationship between dynamic intra-abdominal pressure and magnetic resonance imaging measurements

This chapter refers to a published work (Victoria Joppin, Jourdan, et al. 2025). This article version is available on HAL, has been accepted for publication after peer-review, is subject to Elsevier's terms of use, is licensed under the terms of the CC BY-NC-ND license, and is not the editor's version.

Table of contents

1.1. Introduction 91
1.2. Methods 93
1.2.1. Participants 93
1.2.2. Protocol 94
1.2.3. Data processing 94
1.2.4. Correlation intra-abdominal pressure - abdominal wall motion 98
1.3. Results 99
1.3.1. Intra-abdominal pressure and MRI time-dependent changes . . 99
1.3.2. Relationship between intra-abdominal pressure and visceral area 101

1.3.3. Relationship between intra-abdominal pressure and displacement 103
1.4. Discussion 105
1.5. Conclusion 108

Victoria Joppin [1,2], **Arthur Jourdan** [1], **David Bendahan** [2], **Andréa Soucasse** [1], **Maxime Guye** [2,3], **Catherine Masson** [1], **Thierry Bege** [1,4]

[1]Univ Gustave Eiffel, Aix-Marseille Univ, LBA, F-13016 Marseille, France

[2]Aix Marseille Univ, CNRS, CRMBM UMR 7339, Marseille France

[3]Assistance Publique-Hopitaux de Marseille, Hôpital Universitaire Timone, CEMEREM, Marseille, France

[4]Department of General Surgery, Aix-Marseille Univ, North Hospital, APHM, Marseille, France

Corresponding author

Victoria Joppin victoria.joppin@proton.me

Laboratoire de Biomécanique Appliquée

UMRT24 Université Gustave Eiffel - Aix Marseille Université

Faculté des Sciences Médicales et Paramédicales - Secteur Nord

51 Boulevard Pierre Dramard, F-13016 Marseille, France

Preface

This chapter 1 addresses the Objective 1. The aim of the study was to investigate the *in vivo* relationship between intra-abdominal pressure and MRI-based abdominal wall motion. By combining dynamic MRI with measurements from ingestible pressure sensor in 20 healthy participants, this study aims to enhance our understanding of the mechanical behaviour of the abdominal wall. The impact of different physiological activities (passive or active) and the specific abdominal muscles engaged will be examined. The data (intra-abdominal pressure and MRI) was collected during Arthur Jourdan's doctoral project.

Abstract

Background: *In vivo* mechanical behaviour of the abdominal wall has been poorly characterised and important details are missing regarding the occurrence and post-operative recurrence rate of hernias which can be as high as 30%. This study aimed to assess the correlation between abdominal wall displacement and intra-abdominal pressure, as well as abdominal compliance.

Methods: Eighteen healthy participants performed audio-guided passive (breathing) and active (coughing, Valsalva maneuver) exercises. Axial dynamic changes of abdominal muscles and visceral area were measured using MRI, and intra-abdominal pressure with ingested pressure sensor.

Findings: Correlations between abdominal wall displacement and intra-abdominal pressure were specific to participant, exercise, and varying between rectus abdominis and lateral muscles. Strong correlations were found between rectus abdominis displacement and intra-abdominal pressure during breathing ($r = 0.92 \pm 0.06$), as well as lateral muscles displacement with intra-abdominal pressure during coughing and Valsalva maneuver ($r = -0.98 \pm 0.03$ and -0.94 ± 0.05 respectively). The abdominal pseudo-compliance varied greatly among participants during muscular contraction, the coefficient of variation reaching up to 70%.

Interpretation: The combination of intra-abdominal pressure and dynamic MRI measurements enables the identification of participant-specific behaviour pattern. Intra-abdominal pressure and abdominal wall dynamic undergo consistent and predictable interactions. However, this relationship is subject-specific and may not be extrapolated to other individuals. Therefore, both intra-abdominal pressure and abdominal wall motion must be measured in the same participant in order to accurately characterise the abdominal wall behaviour. These results are of great importance for mesh design, surgical decision-making, and personalised healthcare.

1.1. Introduction

The abdominal wall is a multi-layered structure crucial for organ protection, upper body movement and intra-abdominal pressure (IAP) control. However, our understanding of the relationship between IAP and abdominal wall motion is limited, largely due to inadequate investigative methods. Enhanced knowledge of abdominal wall mechanical behaviour could provide valuable insights into physiological and pathological phenomena, such as hernia development. Hernias, characterised by the protrusion of abdominal contents through defects in the musculo-aponeurotic structure, can cause pain and diminish quality of life (O. A. Smith et al. 2022). Despite advances in surgical treatment, hernia recurrence remains high i.e. 30% (Romain et al. 2020; Flum et al. 2003), likely due to a conflict between the increased IAP leading to an increased

abdominal wall loading and the ability of the abdominal wall to cope with this load by moving and deforming.

Abdominal wall displacements and strains have been assessed *in vivo* mostly externally by image correlation. These studies quantified abdominal motion during exercises (Klinge et al. 1998; Silvia Todros, de Cesare, Pianigiani, et al. 2019) and showed that strain depends on anatomical zones (Czesław Szymczak et al. 2011; Śmietański, Bury, et al. 2012). However, to fully understand hernia pathophysiology, a detailed examination of the different abdominal wall layers is necessary. Recent research using 2D dynamic MRI has reported specific abdominal muscle displacements (Jourdan, Rapacchi, et al. 2022). While these studies provide valuable data, integrating IAP is critical to fully understand the relationship between abdominal wall motion and pressure, which is essential for understanding both normal and pathological conditions such as hernias.

Most studies on IAP have focused on intraperitoneal hypertension and abdominal compartment syndrome (Malbrain, M. L. Cheatham, et al. 2006), with fewer investigations into its role in hernia formation, although it has been recognised as a potentially important factor (Mureşan et al. 2016). IAP changes can modulate external abdominal wall surface strain, internal muscular deformations and abdominal volume. Several studies using laparoscopic peritoneal gas insufflation in post-mortem conditions (Le Ruyet et al. 2020), anesthetised patients (Song et al. 2006) and rabbits (Simón-Allué, Calvo, et al. 2017) have confirmed the anisotropic behaviour of the abdominal wall, with greater curvature radius (Song et al. 2006) and shear modulus (Simón-Allué, Calvo, et al. 2017) in the longitudinal direction. Song *et al.* showed a near linear correlation between antero-posterior displacement of the abdominal wall and increasing IAP (Song et al. 2006). In post mortem human species, Konerding *et al.* observed a linear correlation between IAP and transverse forces on the linea alba (Konerding et al. 2011). *In vivo* studies also showed that IAP was correlated with electrical muscle activity (Misuri et al. 1997; Kawabata et al. 2023).

Abdominal compliance, defined as the ratio of intra-abdominal volume change to IAP change, reflects the abdominal wall's ability to distend in response to pressure (Malbrain, De Laet, et al. 2014). Abdominal compliance has been mainly investigated *in vivo* during laparoscopic peritoneal gas insufflation in porcine models (McDougall et al. 1994; Vlot et al. 2013) and humans (McDougall et al. 1994; Abu-Rafea et al.

2006; Mulier et al. 2009; Becker et al. 2017). In a porcine model, Vlot *et al.* (Vlot et al. 2013) reported a 93% abdominal volume increase when pressure rose from 5 to 10 mmHg. Using CT and surface image correlation, Becker *et al.* (Becker et al. 2017) reported an exponential relationship between in subcutaneous fat thickness and compliance. In healthy humans, body position (upright or supine) and abdominal binders were shown to influence compliance (Cala et al. 1993). However, compliance during voluntary muscle activation has yet to be studied.

Despite these advances, gaps remain in our understanding of *in vivo* real-time interactions between IAP and abdominal wall response. Current clinical practices measure IAP invasively via the bladder, but ingestible sensors offer a safer, non-invasive alternative (Soucasse, Jourdan, Edin, Meunier, et al. 2024; Soucasse, Jourdan, Edin, J. F. Gillion, et al. 2022). Surface imaging techniques are limited to external observations, while ultrasound and elastography only provide localised data. CT scanning, though in-depth, involves radiation. In this context, MRI stands out as a non-invasive, non-radiating alternative that extends the in-depth study of the various muscle groups in the abdominal wall.
To our knowledge, this is the first study to dynamically assess the *in vivo* relationship between IAP and MRI-based metrics of abdominal wall movement and deformation. Through the combination of dynamic MRI and ingestible pressure sensor measurements in healthy human participants, this study aims to enhance our understanding of the mechanical behaviour of the abdominal wall during various physiological activities that could contribute to hernia development.

1.2. Methods

1.2.1. Participants

Eighteen healthy participants (8 females) volunteered to take part in the study after providing their informed written consent. The average age and BMI were 29.3 ± 8.1 years old and 22.6 ± 2.5 kg/m^2 respectively.
This study was approved by the French ethics committee (IDRCB: 2019-A00806–51) and was conducted according to national legislation related to interventional research and the Declaration of Helsinki.

1.2.2. Protocol

Participants were positioned supine in the MRI scanner (MAGNETOM Verio, Siemens Healthineers, Erlangen, Germany) with integrated and flexible body coils on the abdomen. Dynamic (2D+t) MRI captured axial changes every 182 ms during three audio-guided exercises, as previously described (Jourdan, Rapacchi, et al. 2022). Breathing (inhale-exhale deeply during 10 s), coughing and the Valsalva maneuver (forceful expiration against closed nostrils and mouth (Srivastav et al. 2022) during 8 s), chosen as representative of daily activities and clinical exam (Jaffe et al. 2005), were performed after training. Breathing was considered passive (Campbell et al. 1953) while coughing and the Valsalva maneuver were active exercises involving abdominal contraction (Urquhart et al. 2005).

In a separate session, participants repeated the same exercises after swallowing a SmartPill^{TM} capsule (Medtronic, Minneapolis, MN, USA) to measure IAP (± 3.6 mmHg precision) (McCaffrey et al. 2008) with a 500 ms sampling time.

1.2.3. Data processing

As illustrated in Figure 1.1-a, muscles of interest were manually delineated in MR images using FSLeyes (S. M. Smith et al. 2004), then a semi-automatic segmentation algorithm was used to obtain the segmentation masks at each timestep (A. Ogier et al. 2017). Segmentation masks included the rectus abdominis (RA) and lateral muscles (LM, including the transverse abdominis, internal and external obliques), as represented in Figure 1.1-b.

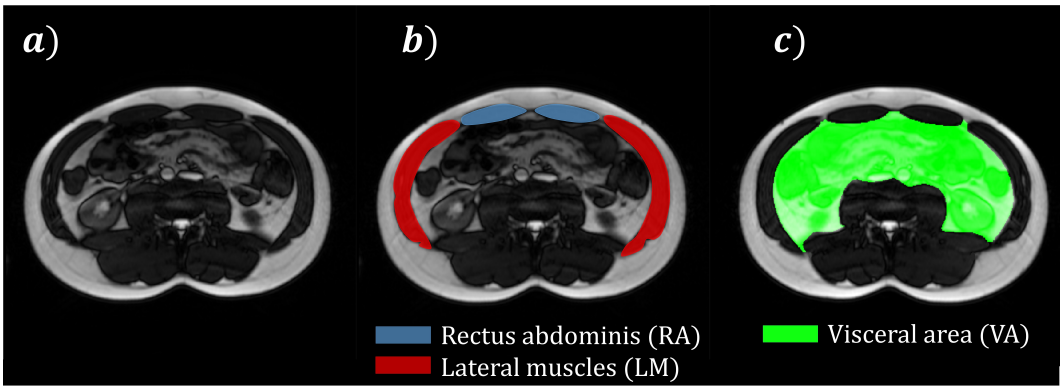

Figure 1.1.: Typical 2D axial abdominal MRI slice
Legend: **a)** MRI without annotation **b)** Segmentation masks of muscles **c)** Segmentation masks of visceral area

Radial displacements (Figure 1.2-b) were computed for each pixel of the segmented muscles (Jourdan, Le Troter, et al. 2021) (Figure 1.2-c), then averaged across the LM and RA muscles (Figure 1.2-d).

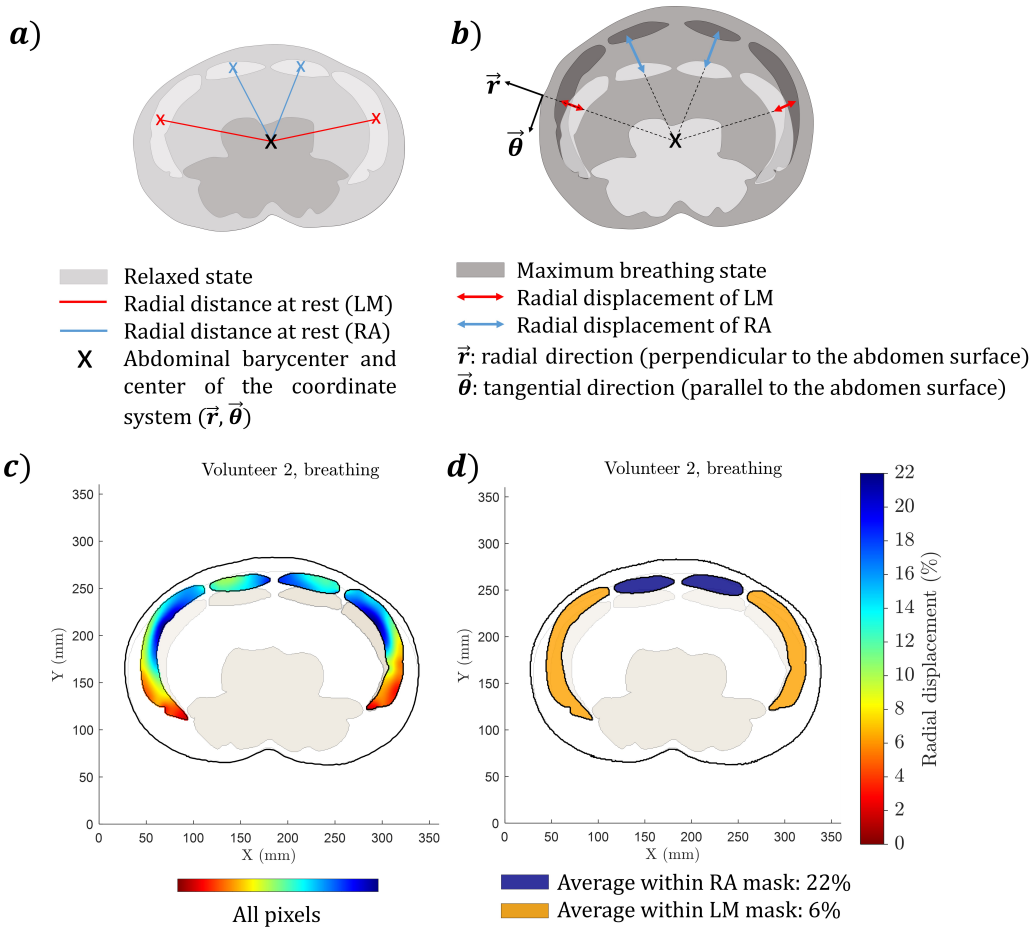

Figure 1.2.: Metrics derived from MRI
a) Abdominal radial distances at rest
b) Radial displacement scheme
c) Radial displacement of each pixel of the segmentation masks
d) Radial displacement averaged among LM and RA segmentation masks

The visceral area (Figure 1.1-c), defined as the region delimited by the internal surface of the abdominal muscles and dorsal structures (quadratus lumborum, psoas major, erector spinae, vertebral disc and body), was computed.
Radial displacement of LM and RA muscles and visceral area metrics were normalised to their resting values, defined as the endpoint of a calm exhalation without visible contraction, ensuring no variation at rest. For standardisation between participants,

these metrics were expressed relative to the resting state: the visceral area was divided by its resting value, and the radial displacements were divided by the radial distance between the barycenter of each muscle group (LM and RA) at resting state and the abdominal barycenter (Figure 1.2-a). The barycenter of a muscle is defined as the mean position of all pixels that constitute its segmentation mask. Meanwhile, the abdominal barycenter is the average location of all pixels composing the LM segmentation masks. As illustrated in Figure 1.3-a for each exercise, specific timepoints, i.e. onset and peak, were manually identified so as to delimit the different repetitions using MATLAB.
Then, all repetitions were linearly oversampled to n points, corresponding to the longest repetition across participants. This equates to n = 60, 12 and 54 points for breathing, coughing and the Valsalva maneuver, respectively, due to varying exercise durations. This approach was chosen to achieve a slight upsampling of the shorter repetitions, while avoiding the loss of information associated with downsampling the longer ones. For each participant, the resulting repetitions of n points were averaged to generate a representative average cycle of n points of each exercise (Figure 1.3-b). As illustrated in Figure 1.3-a, the maximum values of the each set of repetitions were aligned for signal averaging in order to prevent the peak from being smoothed out.

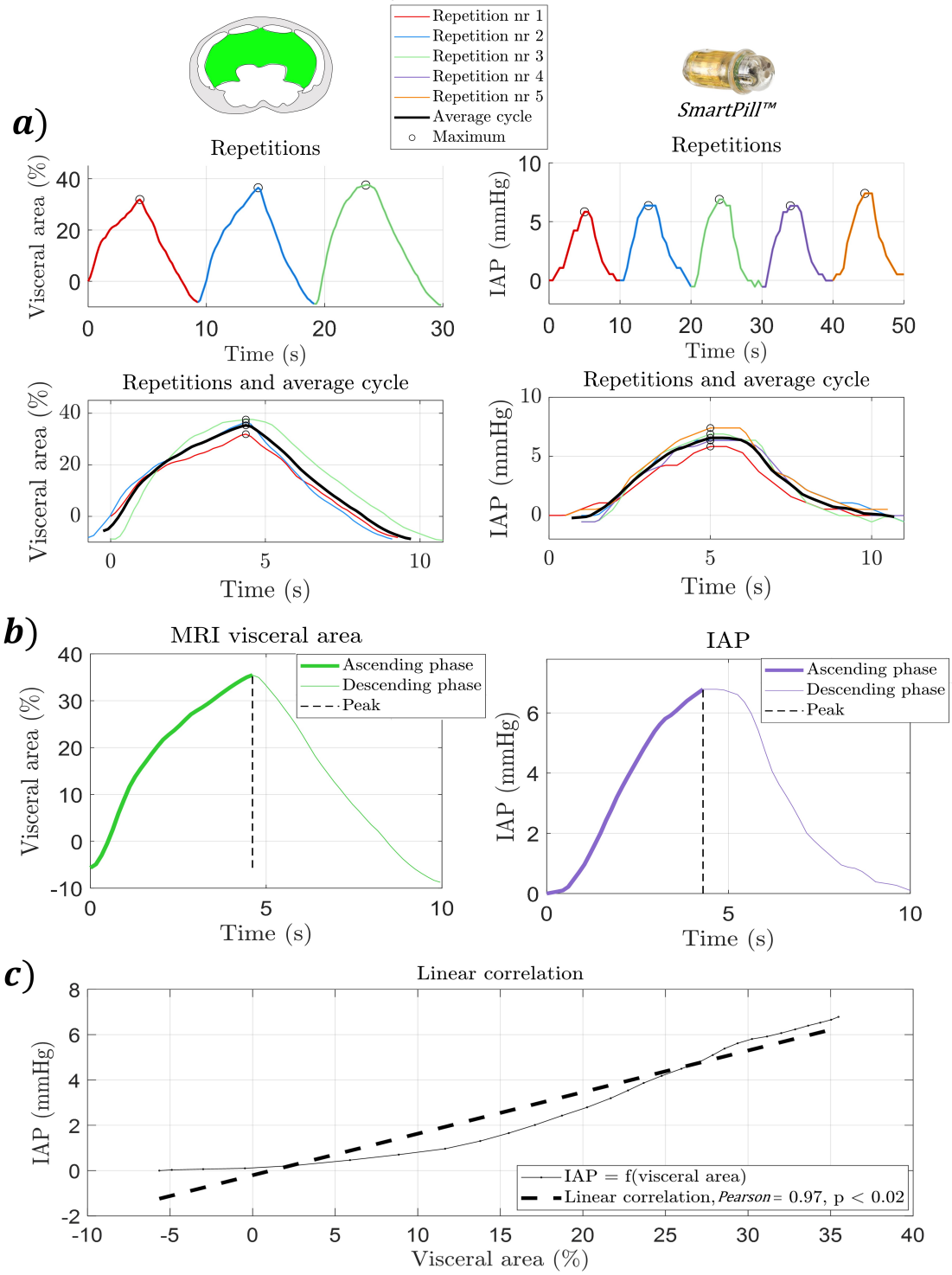

Figure 1.3.: Example of selected timepoints and averaging repetitions during breathing
a) Repetitions delimitation (left: visceral area, right: intra-abdominal pressure (IAP))
b) Average cycle (left: visceral area, right: IAP)
c) Linear correlation between the average cycles of IAP and visceral area during ascending phase, i.e. from the beginning until the IAP reaches its maximum value

The IAP values were exported using the SmartPill^{TM} 3.1 software with the temperature-compensated mode. The IAP repetitions were oversampled to reach n points by linear interpolation and averaged similarly to the MRI data. This process standardised the cycle lengths across repetitions, allowing for the correlation of MRI-based abdominal data and IAP values, despite non-simultaneous measurements. This approach enabled consistent comparison between abdominal motion and IAP across different participants and exercises.

1.2.4. Correlation intra-abdominal pressure - abdominal wall motion

This study investigates the relationship between intra-abdominal pressure (IAP) and MRI-based metrics of abdominal wall movement and deformation. Pearson correlation coefficients r were calculated for each participant and exercise to evaluate the direction (positive or negative) and strength of correlations between IAP and visceral area, as well as IAP and radial displacement of LM and RA. These correlations were assessed during the ascending phase of each exercise (until maximum or plateau for the Valsalva, as illustrated in Figure 1.3-c), with statistical significance considered for p-value $P \leq 0.05$ and $r \geq 0.468$, critical threshold of an acceptable correlation strength (Cunningham et al. 2013).

Abdominal pseudo-compliance was computed as the ratio between the maximum changes in visceral area $\Delta_{max}VA$ (value before normalisation, expressed in cm^2) and intra-abdominal pressure $\Delta_{max}IAP$:

$$C_{ab} = \frac{\Delta_{max}VA}{\Delta_{max}IAP}(\frac{cm^2}{mmHg})$$

The maximum change was defined as the difference between the beginning and the end of the ascending phase (Figure 1.3-b). This metric differs from the conventional compliance using volume given that it is applied to 2D MRI slices.

Results were presented as average across all participants (n = 18) ± standard deviation σ, with their [minimum/maximum] range and coefficient of variation CV, defined as the standard deviation divided by the absolute r value: $CV = \sigma/|r|$ (%).

The correlation between IAP and MRI measurements was further analysed in relation to morphologic parameters, including BMI (kg/m^2), waist circumference (mm), radial distance at rest of LM and RA (mm) and muscle mass ratio (%), defined as the area

occupied by abdominal muscles divided by the whole abdomen area (delimited by the external surface of the abdomen). The difference according to the sex assigned at birth (female or male) was assessed using a two-sided Wilcoxon-Mann-Whitney test, with a $P \leq 0.05$ considered statistically significant.

1.3. Results

1.3.1. Intra-abdominal pressure and MRI time-dependent changes

Temporal changes of IAP, visceral area and radial displacement of LM and RA during the different exercises are displayed in Figure 1.4, with maximum changes summarised in Table 1.1. Radial displacement and visceral area were analysed for 17 participants as one MRI dataset was excluded due to poor quality.

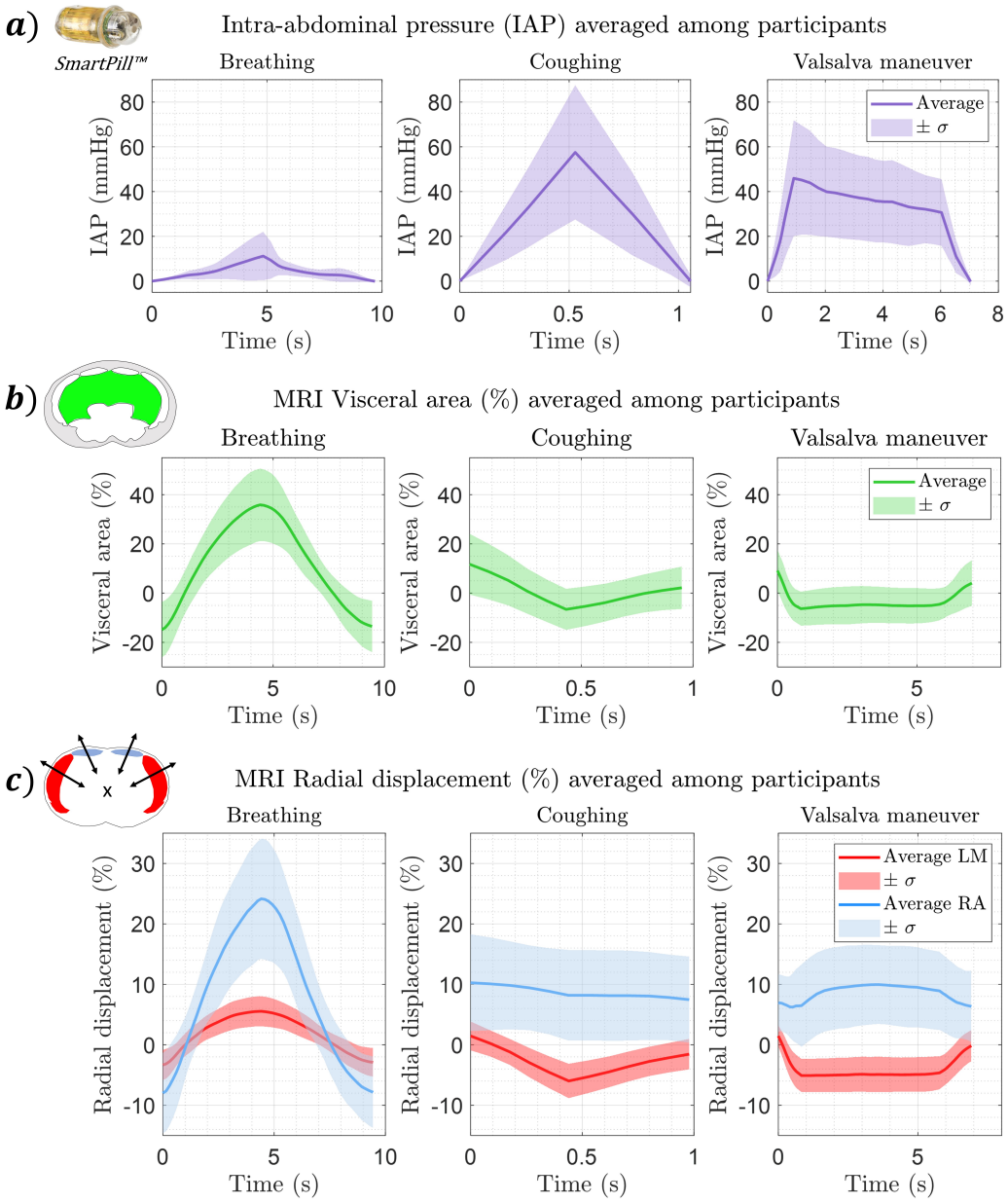

Figure 1.4.: Temporal changes for different exercises of
a) Intra-abdominal pressure (IAP, mmHg)
b) Visceral area (%)
c) Radial displacement of LM and RA (%)
Results are presented as mean values ± one standard deviation σ

During breathing, IAP, visceral area and radial displacement of LM and RA muscles followed a bell shape pattern with ascending and descending phases. Breathing induced a large visceral area increase and an outward/positive radial displacement. Coughing also exhibited these two phases, but visceral area and LM displacement

initially decreased during contraction, contrasting with IAP's initial rise. Radial displacement of RA was limited ($-2.63 \pm 6.38\%$) compared to LM ($-7.32 \pm 2.86\%$), with notable inter-participant variability, RA being pulled in or out according to the participant's coughing execution. The positive RA displacement at the onset was related to a short intake of air before coughing.

For the Valsalva maneuver, three phases where observed: IAP and RA displacement increased initially, while LM displacement and visceral area decreased. Variability in RA displacement was higher than LM, highlighting again differences in execution among participants (standard deviation of 6.15% for RA compared to 2.99% for LM).

Activities with muscular activation led to a visceral area decrease accompanied by an inward, negative displacement of LM and a higher $\Delta_{max}IAP$. IAP during coughing was 11 mmHg higher than during the Valsalva maneuver. For the Valsalva maneuver, a significant correlation between $\Delta_{max}IAP$ and the muscle mass ratio was found ($r = 0.71$, $P \leq 0.05$), with males showing higher IAP compared to females (59.14 and 29.49 mmHg, respectively).

Exercise	**Maximum IAP** $\Delta_{max}IAP$ **(mmHg)**	**Maximum visceral area** $\Delta_{max}VA$ **(%)**	**Maximum radial displacement (%)**	
			Lateral muscles (LM)	**Rectus abdominis (RA)**
Breathing	11.20 ± 11.15	48.27 ± 20.69	8.86 ± 4.04	30.16 ± 12.33
Coughing	57.52 ± 30.88	-18.99 ± 8.13	-7.32 ± 2.86	-2.63 ± 6.38
Valsalva	45.96 ± 26.62	-16.32 ± 8.04	-6.52 ± 2.99	-1.14 ± 6.15

Table 1.1.: Maximum changes in intra-abdominal pressure $\Delta_{max}IAP$, visceral area $\Delta_{max}VA$ and radial displacement of LM and RA for different exercises
Results are presented as mean values ± one standard deviation σ

1.3.2. Relationship between intra-abdominal pressure and visceral area

The relationship between IAP and visceral area changes was assessed in order to provide information related to the dynamic behaviour of the abdominal wall on a global scale, i.e. without distinction between LM and RA muscles. The mean r values

are presented in Table 1.2.

Exercise	***r***	**Range [min/max]**	**CV (%)**
Breathing	0.90 ± 0.09	[0.64/1]	10
Coughing	-0.99 ± 0.02	$[-1/-0.91]$	2.02
Valsalva	-0.92 ± 0.07	$[-1/-0.76]$	7.61

Table 1.2.: Pearson correlation coefficients (r) for the correlations between intra-abdominal pressure (IAP) and visceral area, range [min/max] and coefficient of variation (CV)
Results are presented for the different exercises as mean values ± one standard deviation σ

The correlation between IAP and visceral area changes was significant ($P \leq 0.05$ and $|r| \geq 0.468$) and very subject-specific for each participant and each exercise. For coughing and the Valsalva maneuver, r values were negative indicating that IAP was increasing while the visceral area was decreasing. The correlation was strong, with an absolute mean r value larger than 0.9 for the whole set of exercises.
Figure 1.5 illustrates the maximum changes of intra-abdominal pressure $\Delta_{max}IAP$ and visceral area $\Delta_{max}VA$ for all the participants and the three exercises. Both variables were normalised by their highest values among the 18 participants to be scaled from 0 to 1. The largest IAP change did not always correspond to the largest visceral area change. For example, participant 7 had large area changes with moderate IAP during breathing, whereas participant 5 showed the opposite during the Valsalva maneuver. No significant correlation was found between participants between maximum changes in IAP and visceral area, indicating that their relationship is participant-specific and cannot be generalised to the whole cohort.

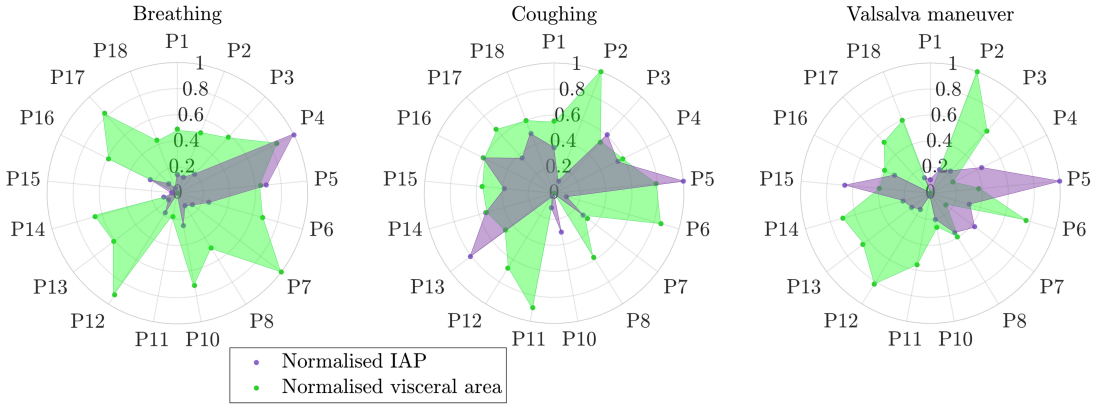

Figure 1.5.: Intra-abdominal pressure maximum change $\Delta_{max}IAP$ as a function of visceral area maximum change $\Delta_{max}VA$ for all participants and all exercises
Each spoke represents one participant (Pn: participant n)
Data normalised by the highest value (among all participants) to be scaled from 0 to 1

The mean abdominal pseudo-compliances C_{ab} were 7.65 ± 3.97, -0.54 ± 0.38 and -0.56 ± 0.39 $cm^2/mmHg$ for breathing, coughing and the Valsalva maneuver, respectively. The corresponding [minimum/maximum] ranges were [1.78/13.68], [−1.63/ − 0.13] and [−1.40/ − 0.12] $cm^2/mmHg$, and coefficients of variation CV of 51.90, 70.37 and 69.64%.

Participants with high pseudo-compliance during breathing did not necessarily have high pseudo-compliance during muscle contraction (coughing and the Valsalva maneuver). A significant difference in pseudo-compliance was found between males and females for breathing and the Valsalva maneuver exercises. During breathing, females had higher pseudo-compliance than males (9.73 versus 5.79 $cm^2/mmHg$ respectively). Inversely, with muscular activation during the Valsalva maneuver, females had lower pseudo-compliance than males (−0.82 versus −0.34 $cm^2/mmHg$, respectively).

1.3.3. Relationship between intra-abdominal pressure and displacement

The correlation between IAP and abdominal muscles displacements was assessed to explore the dynamic behaviour of the abdominal wall at a local level, distinguishing LM and RA muscles. The mean r values related to the correlations are presented in Table 1.3.

Exercise	**Lateral muscles (LM)**			**Rectus abdominis (RA)**		
	r	**Range [min/max]**	**CV (%)**	***r***	**Range [min/max]**	**CV (%)**
Breathing	0.78 ± 0.45	$[-0.94/0.99]$	57.69	0.92 ± 0.06	$[0.79/0.99]$	6.52
Coughing	-0.98 ± 0.03	$[-1/-0.86]$	0.03	$-0.16^{(¤)} \pm 0.91$	$[-0.99/1]$	600
Valsalva	-0.94 ± 0.05	$[-0.99/-0.81]$	5.32	$0.06^{(¤)} \pm 0.91$	$[-0.99/1]$	1517

Table 1.3.: Pearson correlation coefficients (r) for the correlations between intra-abdominal pressure (IAP) and radial displacement of lateral muscles (LM) and rectus abdominis (RA), range [min/max] and coefficient of variation (CV)
Results are presented for different exercises as mean values ± one standard deviation
σ
$^{(¤)}$ indicates that the correlation is not significant for all participants

A significant correlation was found between IAP and radial displacement of LM for all participants and all exercises. For RA, all participants had a significant correlation during breathing. There were 5 participants who did not have a significant correlation during coughing and 2 participants during the Valsalva maneuver with a $P \geq 0.05$.
The correlation between IAP and radial displacement varied depending on the muscle group (LM or RA) and the type of exercise performed (breathing, coughing or the Valsalva maneuver). IAP and radial displacement of RA were strongly correlated ($r = 0.92 \pm 0.06$) during breathing whereas very weak correlations were observed for coughing ($r = -0.16 \pm 0.91$) and the Valsalva maneuver ($r = 0.06 \pm 0.91$). On the contrary, the correlation between IAP and radial displacement of LM was better and had a lower standard deviation during active exercises ($r = -0.98 \pm 0.03$ and -0.94 ± 0.05 respectively for coughing and the Valsalva maneuver) than breathing ($r = 0.78 \pm 0.45$). As for visceral area, no significant linear correlation was found between participants, between maximum changes in IAP and radial displacement of LM or RA. The relationship between the IAP and radial displacement is very different among the participants.

1.4. Discussion

This work is the first study to investigate the correlation between IAP and MRI-based abdominal wall metrics. The present results provide valuable insights regarding the *in vivo* relationship between IAP and the structural and functional characteristics of the abdominal wall. This relationship was studied on both global (through the quantification of visceral area) and local scales (though radial displacement of LM and RA muscles), during passive (breathing) and active (coughing, Valsalva maneuver) exercises.

The IAP, visceral area and muscular radial displacement followed a specific pattern for each exercise. During coughing and Valsalva exercises, the recruitment of abdominal muscles led to a compression of the viscera, thus a decrease in visceral area (-18.99 ± 8.13 and -16.32 ± 8.04% for coughing and the Valsalva maneuver respectively, as compared to $+48.27 \pm 20.69$% for breathing). The slight differences in IAP, visceral area and radial displacement between coughing and the Valsalva maneuver may be related to the faster IAP increase during coughing reported by Soucasse *et al.* (Soucasse, Jourdan, Edin, J. F. Gillion, et al. 2022), thereby further supporting that the loading rate influences the behaviour of the abdominal wall tissue (Ben Abdelounis et al. 2013).

The present results allowed to assess the correlation between IAP and visceral area. During passive exercise such as breathing, this linear and positive correlation was in agreement with the results reported *in vivo* by Song *et al.* (Song et al. 2006), showing that the displacement of the abdominal outer surface evolved almost linearly with the insufflated pressure. As a measure of *in vivo* abdominal compliance, Papavramidis *et al.* also showed a linear correlation between abdominal pressure and ascitic fluid drained volume in patients (Papavramidis et al. 2011).
Our results showed that abdominal pseudo-compliance based on area rather than volume, was positive and larger during breathing (7.65 ± 3.97 for breathing versus -0.54 ± 0.38 and -0.56 ± 0.39 for coughing and the Valsalva maneuver respectively), with the abdominal wall shape being markedly stretched without being contracted, leading to a slight IAP increase but an important visceral area increase (Campbell et al. 1953).
On the contrary, active muscular exercises induced a visceral area decrease accompanied by high IAP increase, thereby resulting in a negative and smaller pseudo-

compliance. In most biological tissues (veins, lungs), increased pressure leads to tissue expansion and positive compliance. However in this case, a decrease in visceral area results in negative pseudo-compliance, likely due to muscle activation (e.g., LM/RA). A review article also reported that abdominal muscles decreased the abdominal compliance (Malbrain, De Laet, et al. 2014). During the Valsalva maneuver, males had a significantly higher IAP than females (59.14 and 29.49 mmHg, respectively), and a higher pseudo-compliance (−0.34 versus −0.82 $cm^2/mmHg$ respectively). While previous studies found no correlation between IAP and gender (Cobb et al. 2005; Sanchez et al. 2001), males generally have a higher muscle mass ratio than females (Jourdan, Soucasse, et al. 2020; Rankin et al. 2006), as seen in this cohort (16.25 versus 13% for males and females respectively, $P \leq 0.05$). The muscle mass ratio being correlated with IAP changes during Valsalva, males can generate a higher contraction. During breathing, females had a higher pseudo-compliance than males (9.73 versus 5.79 $cm^2/mmHg$ respectively), in line with the fact that females had a higher abdominal distention capacity (Junge, Klinge, et al. 2001).

Our findings indicate that correlations between IAP and radial displacement differ according to the type of exercise and the muscular group. Breathing resulted in a stronger correlation between IAP and the radial displacement of RA (r = 0.92 for RA versus 0.78 for LM). Conversely, during active exercise, the LM appeared more involved than RA with a stronger correlation with IAP (for LM, $r = -0.98$ and -0.94 for coughing and the Valsalva maneuver respectively compared -0.16 and 0.06 for RA). The correlation between IAP and radial displacement of RA was not significant for all participants during coughing and Valsalva, with a $P \leq 0.05$. This may be due to the fact that these muscles are less involved than LM during contraction, and these specific participants moved their RA minimally during these exercises. Also, the p-value P is affected by the number of datapoints, and these exercises are shorter than breathing. Misuri *et al.* (Misuri et al. 1997) also reported that IAP was linearly related to the thickness of the transverse muscle, being part of the LM considered in this study. Urquhart *et al.* also showed that LM were more recruited than RA during voluntary exercises (Urquhart et al. 2005).

At the intra-individual level, a robust correlation has been identified between IAP and abdominal wall motion, suggesting that these variables are tightly linked by participant-specific relationship. Each participant exhibits a unique pseudo-compliance

for each exercise, which can be modelled as IAP = f(abdominal wall motion). Once this function f has been identified for a participant, one variable can be predicted from the other. This relationship encompasses factors like anatomy, abdominal wall behaviour, and exercise execution. Regardless of the exercise, the correlation between changes in IAP and visceral area was strong, with r values above 0.9. The correlation between IAP and the radial displacement of LM during active exercises and the RA during passive ones was also strong for each participant.

Nevertheless, at the inter-individual level, the results showed a high variability in IAP and abdominal wall motion. No consistent pattern was identified in which a high IAP was systematically accompanied by a large visceral area or radial displacement of LM and RA. In other words, a participant with high pseudo-compliance may experience substantial change in visceral area with minimal IAP increases. The compliance parameter accounts for a considerable range of combinations between pressure values and visceral areas. The variability in the above-mentioned function f between participants reflects anatomical and mechanical differences. Previous studies have highlighted these inter-individual differences in abdominal anatomy (Jourdan, Soucasse, et al. 2020) and mechanical properties both *ex vivo* (Junge, Klinge, et al. 2001; Martins et al. 2012) and *in vivo* (John et al. 2007). Szepietowska *et al.* (Szepietowska et al. 2023) also reported recently an apparent lack of correlation between the maximum IAP values and abdominal strains between participants, further reinforcing the need for individualised measurements of both IAP and abdominal wall motion to accurately assess mechanical behaviour.

Several limitations should be acknowledged in this study. Dynamic MRI was recorded in a single axial plane, perpendicular to the RA muscle fibres. A 3D dynamic analysis would lengthen the time resolution to 1s instead of 182 ms, insufficient to capture contraction. Also, it has been documented that abdominal muscles movement in the cranio-caudal direction is minimal (Jourdan, Rapacchi, et al. 2022). Another limitation is the non-simultaneous IAP and MRI measurements, as the SmartPill^{TM} sensor, with a different sampling frequency, is not MRI compatible. To the best of our knowledge, there are no MRI-compatible IAP sensor. To ensure exercise repeatability and accurate motion capture, participants were trained under similar conditions. Before each MRI and SmartPill^{TM} session, the exercises were audio-guided and repeated multiple times. Oversampling shorter repetitions to match the longest repetition may introduce

bias. Secondly, the hypothesis that maximum pressure and maximum abdominal wall displacement occur simultaneously is supported by *in vivo* animal study (Vlot et al. 2013) where the antero-posterior distance and abdominal volume reached their maximum values when pressure reached its maximum. Human studies combining pressure and trunk motion (Hodges and Gandevia 2000) are limited.

This study on healthy participants is a prerequisite for assessing patients with abdominal wall pathologies, such as hernias. Extending these investigations to such groups would provide insights into mechanical alterations related to these conditions. It is reasonable to assume that the heterogeneity in mechanical characteristics amongst participants may impact the outcomes (pain, recurrence) of hernia repair procedures. A patient-based study could lead to the development of personalised mesh solutions, surgical interventions, thereby enhancing the effectiveness of hernia repair and minimising associated complications through the early diagnosis of abdominal wall changes.

1.5. Conclusion

This work is the first to investigate the relationship between intra-abdominal pressure and dynamic MRI-based abdominal wall metrics through continuous temporal *in vivo* measurements in healthy human subjects. The present results illustrate the interest of combining these two measurements to assess dynamically the mechanical behaviour of the abdominal wall. There was a strong correlation between abdominal wall motion and IAP, which was dependent on the participant. The corresponding results provide interesting information related to abdominal wall dynamics and could be used for the evaluation of patients with abdominal wall hernias.

2. Stress approximation of in vivo human abdominal wall during breathing

Table of contents

2.1. Introduction 111
2.2. Material and methods 113
2.2.1. Cohort and participant protocol 113
2.2.2. MRI data processing 113
2.2.3. Analytical stress computation 114
2.2.3.1. Cylinder radius 114
2.2.3.2. Cylinder stress 115
2.2.4. Young modulus approximation 117
2.3. Results 117
2.3.1. Cylinder geometry 117
2.3.2. Cylinder stress 118
2.3.3. Cylinder elastic moduli 120
2.4. Discussion 121
2.5. Conclusion 125

2. Stress approximation of in vivo human abdominal wall during breathing –

Victoria Joppin [1,2], **Thierry Bege** [1,3], **Catherine Masson** [1]

[1]Univ Gustave Eiffel, Aix-Marseille Univ, LBA, F-13016 Marseille, France

[2]Aix Marseille Univ, CNRS, CRMBM UMR 7339, Marseille France

[3]Aix Marseille Université, Département de Chirurgie, Hôpital Nord, APHM, Marseille, France

Preface

The capacity to visualise and quantify muscle motion in relation to intra-abdominal pressure offers invaluable insight into the dynamic behaviour of the abdominal wall. These results pave the way for further analysis done in this chapter 2. This chapter seeks to address Objective 2 by focusing on the distribution of forces across the abdominal wall. A cylindrical model representing the abdominal wall of the aforementioned participants, which employs the same dataset to quantify the mechanical stresses exerted during a passive breathing exercise. This model provides a simplified method for approximating the distribution of forces, enabling the identification of regions where stress is concentrated.

Abstract

Background: Abdominal wall hernias represent a significant clinical challenge, with intra-abdominal pressure and muscle deformation playing a crucial role in their occurrence. This study explores the *in vivo* mechanical behaviour of the abdominal wall using a novel combination of intra-abdominal pressure measurements and dynamic MRI-based assessments of abdominal wall displacement.

Methods: Seventeen healthy participants performed controlled breathing, during which intra-abdominal pressure was measured using a swallowable sensor, and the motion of the abdominal muscles, particularly the rectus abdominis (RA) and lateral muscles (LM), was analysed through 2D+t dynamic MRI at the L3-L4 vertebral level. The abdominal wall was approximated as two separate pressurised cylinders for the RA and LM groups, and the corresponding circumferential and radial stresses were calculated using Laplace's formula for thick-walled cylinders.

Findings: Results indicated that circumferential stress was higher in the RA compared

to the LM, with peak values of 8.76 ± 7.82 kPa in the RA and 7.75 ± 7.25 kPa in the LM. The radial stress, although negative and inward-oriented, was minimal in both muscle groups. Young's moduli for circumferential stress were 458.2 ± 155.83 kPa for the RA and 315.31 ± 244.81 kPa for the LM.

Interpretation: The combination of intra-abdominal pressure and dynamic MRI-based measurements provides enables quantitative estimation on how internal forces are transmitted to the abdominal wall and how it reacts to pressure variations. These findings highlight significant inter-individual variability in mechanical properties, reinforcing the importance of personalised approaches in abdominal surgery, particularly for hernia prevention and treatment. Future studies will extend these investigations to pathological conditions, including hernia patients, and compare these results with subject-specific finite element models for further validation and biomechanical insights.

2.1. Introduction

The study of the mechanical behaviour of the abdominal wall is of crucial importance in understanding parietal pathologies and developing effective treatment strategies. It is known for a long time that mechanical stress has an influence on healthy and wounded tissue (Urschel et al. 1988). The abdominal wall is a multi-layered structure that is permanently subjected to loads, principally intra-abdominal pressure (IAP) and deformations during daily activities. The development of a hernia, main pathology of the abdominal wall, can be better understood using a biomechanical approach.

Numerous *ex vivo* studies have described the material properties of the abdominal wall (Deeken and Lake 2017), the main investigated properties being elastic modulus and ultimate tensile strength. Van Ramshorst *et al.* (Ramshorst et al. 2008) investigated the relationship between IAP and abdominal wall tension in human cadavers. The tension was calculated using Laplace's law, based on distance and force measurements obtained from indentation tests on insufflated abdomens. Based on tensile tests, Hernández *et al.* (B. Hernández-Gascón et al. 2011) developed a constitutive model for characterising the passive elastic behaviour of the rabbit abdominal wall, confirmed by finite element (FE) uniaxial simulations reproducing the experiments. This study confirmed that the circumferential direction was stiffer than the cranio-caudal one.

Förstemann *et al.* (Förstemann et al. 2011) performed uniaxial tensile tests on the human linea alba and used MRI scans to calculate abdominal curvature radii. The Laplace's formula was employed to deduce the lineic forces, which were found to be equal to 3.4 and 1.45 N/mm in the circumferential and cranio-caudal directions, respectively, for an IAP of 150 mmHg. Consequently, the ratio of the Young modulus between the two directions was found to be 8. Konerding *et al.* (Konerding et al. 2011) experimentally confirmed these lineic forces during intra-abdominal inflation of a balloon on human species. Lyons *et al.* (Mathew Lyons et al. 2014) developed a FeBio computational model to fit experimental tensile data done on porcine rectus sheath. They approximated the circumferential stress within the abdominal wall by considering the abdomen as a 2cm thick cylinder of 20cm radius. Under known IAP and by using Laplace law, it is possible to quickly have an estimation of the circumferential stress of approx. 1 MPa during coughing. Although *ex vivo* tests are essential for characterising the abdominal wall and providing inputs for numerical models, they fail to reflect the physiological loading conditions of the tissues.

In vivo, Song *et al.* (Song et al. 2006) measured the motion of the abdominal wall, as well as curvature radii, strain and thickness, in anesthetised patients undergoing insufflation of gas with a known IAP. They deduced the tensile stress-strain curve, confirming once again the anisotropic behaviour of the abdominal wall, stiffer in circumferential direction. Tran *et al.* (Tran, Podwojewski, et al. 2016) measured shear modulus using elastography and local stiffness with indentation tests during different activities on healthy participants. Although *in vivo* experiments provide dynamic measurements of the abdomen under physiological conditions, they do not offer a direct evaluation of the level of stress applied to the abdominal wall.

Numerical studies investigated stress within the abdominal wall. Hernández *et al.* (Hernández-Gascón et al. 2013) developed an abdominal FE passive model based on healthy MRI to evaluate stress during physiological situations (standing, Valsalva maneuver, cough and jumping) with varying IAP. Stress has been evaluated within linea alba, rectus abdominis (RA) and lateral muscles (LM). This study highlights the maximum stress being on linea alba, the stiffest structure of the abdomen. Grasa *et al.* (Grasa et al. 2016) incorporated muscle activation to find stress values up to 1MPa.

However, few *in vivo* experimental data is available to feed the numerical models. In

order to assess the evolution of stresses during physiological situations and validate numerical models, a combined approach integrating experimental measurements and theoretical models may be necessary. Analytical formulas can be used to approximate the stress as a function of various measurements such as displacement, deformation or pressure. Few models exist to evaluate stress within the aorta using Laplace's law (Åstrand et al. 2007).

This is, to our knowledge, the first study approximating the stresses with *in vivo* temporal data of IAP and motion of the abdominal wall. IAP evaluation was performed using a swallowable pressure sensor, while the motion of the abdominal wall was assessed using dynamic MR images and advanced post-processing techniques.

2.2. Material and methods

2.2.1. Cohort and participant protocol

The corresponding French ethics committee authorised this monocentric study (IDRCB: 2019-A00806–51), which followed national legislation on interventional research and the declaration of Helsinki. The study recruited a cohort of seventeen healthy participants, including eight women, who provided informed written consent. The mean age was 28.6 ± 7.8 years old [min = 22, max = 54], and the mean body mass index (BMI) was 22.5 ± 2.6 kg/m^2 [min = 17.5, max = 28.5]. Each participant provided written consent after an information session held one week prior to the examination.
Participants realised audio-guided breathing within the MRI while dynamic 3-Tesla MRI (MAGNETOM Verio, Siemens Healthineers) captured 2D axial images (2D+t MRI) of their abdomen every 182 ms. The acquisition parameters were defined by Jourdan et al (Jourdan, Rapacchi, et al. 2022). Following MRI, participants ingested a Smartpill^{TM} capsule (Medtronic, Minneapolis, MN, U.S.A) and repeated the same audio-guided breathing while their IAP was recorded.

2.2.2. MRI data processing

As shown in Figure 2.1-a, the rectus abdominis (RA) and lateral muscles (comprising the transversus abdominis, internal, and external obliques, called LM) were manually delineated from MR images using FSLeyes (S. M. Smith et al. 2004), followed by a

semi-automatic segmentation algorithm (A. Ogier et al. 2017) to obtain segmentation masks at each timestep.
Radial displacements (Figure 2.1-b) were computed for each pixel of the segmented muscles (Jourdan, Le Troter, et al. 2021) and then averaged across the LM and RA muscle groups. Muscle thickness was computed as the maximum distance from the medial axis of each muscle to its contour.
Circumferential and radial strains respectively noted ε_θ and ε_r are computed for both LM and RA muscles. These metrics are defined respectively for the considered group (LM or RA) as the medial axis length and thickness variation with respect to its resting state value, i.e. $l - l_0/l_0$, expressed in percentage (%) (Jourdan, Rapacchi, et al. 2022). The resting state is defined as the endpoint of calm exhalation without visible contraction of the abdominal wall muscles.

2.2.3. Analytical stress computation

2.2.3.1. Cylinder radius

To model the abdominal wall, each muscle group (LM and RA) was approximated as a cylinder with specific radius and thickness, as shown in Figure 2.1-g and -h for LM and RA cylinders respectively. LM and RA were modelled separately as cylinders due to their different behaviour in terms of length, thickness, and motion. The steps for cylinder radius computation are represented in Figure 2.1 and are as follows:

1. The barycenter of each muscle group was calculated by averaging the (x, y) coordinates of all pixels composing its segmentation masks (represented by cross symbols on Figure 2.1-c).

2. The abdominal barycenter B_{abdo} was determined by averaging the barycenters of the right and left LM muscles (represented by a star symbol on Figure 2.1-c). The barycenter was determined in the resting state.

3. The radial distance at rest of each cylinder was computed as the distance between the abdominal barycenter B_{abdo} and the barycenter of each muscle group.

4. The effective cylinder radius was computed by summing the radial distance at rest with the radial displacement, averaged between left and right muscles of each muscle group, LM and RA respectively.

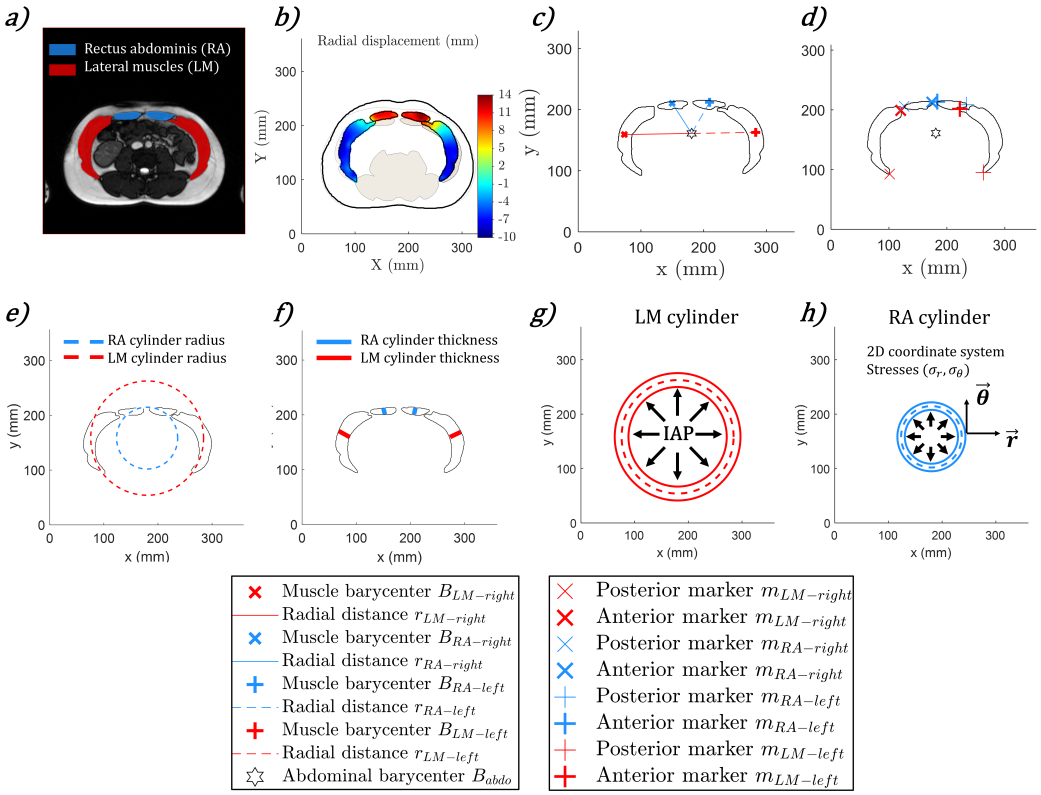

Figure 2.1.: Steps for abdominal cylinder design
Legend : **a)** Segmentation masks of abdominal muscles from MRI **b)** Radial displacement computed within muscle masks **c)** Radial distance between the barycenter of each muscle and the abdominal barycenter B_{abdo} **d)** Muscles extremities **e)** Cylinder radii **f)** Cylinder thicknesses **g)** Final pressurised lateral muscles (LM) cylinder **h)** Final pressurised rectus abdominis (RA) cylinder with cylindrical coordinate system

In order to assess the assumption of a cylindrical abdominal wall, the roundness of the abdominal wall was assessed with the ratio of LM cylinder radius over the RA cylinder radius.

2.2.3.2. Cylinder stress

The stress within abdominal wall cylinders provides a quantitative overview of the internal forces within the abdominal wall. The stress was computed using analytical formulas based on the assumption of a thick-walled cylinder. In order to use the simpler thin-wall approximation, the ratio of radius to thickness must be greater than 10, to ensure that Lame's formula remains valid and that the effects of wall curvature

do not significantly affect the result. However, as illustrated in Figure 2.2, none of the participants' MRI scans met this condition. The average radius-to-thickness ratio across all participants (n=17) was 4.46 ± 0.88 for the LM and 4.86 ± 0.80 for the RA cylinders. Consequently, the thick-walled cylinder model was employed in this study.

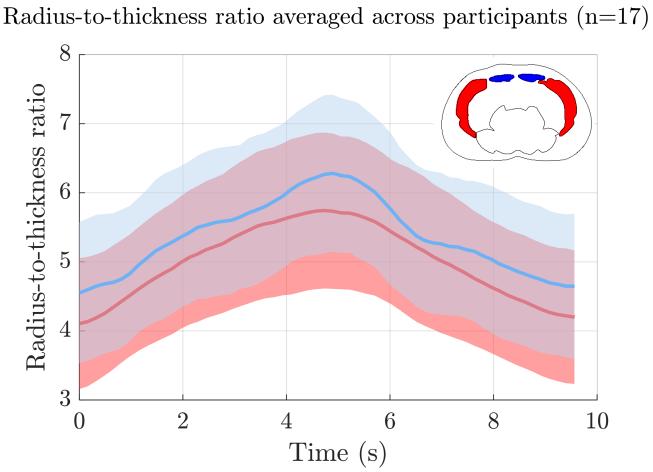

Figure 2.2.: Radius-to-thickness ratio of lateral muscles (LM) and rectus abdominis (RA) cylinders averaged among all participants (n=17)
Results are presented as mean values ± one standard deviation σ

For thick-walled cylinders, the stress σ (in Pascals) was computed using Lamé's formula, which is frequently employed to analyse structures like blood vessels and thick-walled reservoirs. The stresses were decomposed into two components in cylindrical coordinates, as represented on Figure 2.1-h. The circumferential stress, or hoop stress in the circumferential direction $\overrightarrow{\theta}$, tangential to the cylinder surface, is computed as follow :

$$\sigma_\theta(t,r) = \frac{IAP(t) * r^2_{internal}(t)}{r^2_{external}(t) - r^2_{internal}(t)}(1 + \frac{r^2_{external}(t)}{r^2(t)})(Pa) \tag{2.1}$$

The radial stress in the radial direction $\overrightarrow{r}$, normal to the cylinder surface, is computed as follow :

$$\sigma_r(t,r) = \frac{IAP(t) * r^2_{internal}(t)}{r^2_{external}(t) - r^2_{internal}(t)}(1 - \frac{r^2_{external}(t)}{r^2(t)})(Pa) \tag{2.2}$$

The external radius r_{external} was defined as the sum of the abdominal radial distance at rest, the radial displacement, and half the muscle thickness (either LM or RA). This approximates the external surface of the abdomen, assuming that subcutaneous fat and skin thicknesses are neglected. The internal radius r_{internal} was computed as the

radial distance at rest plus the radial displacement minus half of the muscle thickness. This represents the approximate location of the parietal peritoneum, beneath the abdominal muscles. Both stresses are dependent on time and the radial position. For simplicity, they were evaluated at the mean radius r_{mean}, defined as the sum of the radial distance at rest and the radial displacement, which corresponds to the middle of the muscle thickness.

Thin-wall assumption will be used to evaluate stress within the linea alba, considered being 1.5 mm thick (Axer et al. 2001a) and having the same displacement as RA muscles. The circumferential stress, or hoop stress, is thus computed by $\sigma_\theta = IAP * radius/thickness$ (Pa). The radial stress is inward-oriented, being equals to the intra-abdominal pressure $\sigma_r = -IAP$ (Pa).

2.2.4. Young modulus approximation

Once the stress-strain curves were generated for each cylinder (LM and RA) and each direction (along circumferential $\overrightarrow{\theta}$ and radial $\overrightarrow{r}$ directions), the Young's modulus E (in Pascals) of the cylinder was estimated by evaluating the slope of the linear portion of the increasing phase of the stress-strain curve, i.e. from the beginning until the end of inhale. Linear correlation between the stress (either σ_θ or σ_r) and strain (either ε_θ or ε_r) was assessed by a Pearson correlation coefficients r to evaluate the direction (positive or negative) and strength of correlations, with statistical significance threshold set to $p \leq 0.05$ and $r \geq 0.468$, critical threshold of an acceptable correlation strength (Cunningham et al. 2013). Therefore, if the linearity of the stress-strain relationship is not significant, the Young's modulus cannot be calculated for the corresponding participant. Thus, for each participant, circumferential and radial moduli E_θ and E_r were computed within each LM and RA cylinder.

2.3. Results

2.3.1. Cylinder geometry

The radius of both LM and RA cylinders evolving along time during the breathing exercise is shown in Figure 2.3. The ratio of these two radii (LM over RA cylinders) is plotted beside. The LM cylinder is approximately 1.66 larger than the RA cylinder. During breathing, both LM and RA cylinder become larger, with a more pronounced

changed for RA cylinder.

The thickness of these two cylinders is also shown. The LM cylinder is approximately 1.81 thicker than the RA cylinder. During breathing, the thickness of RA cylinder is mostly unchanged whereas LM cylinder become thinner.

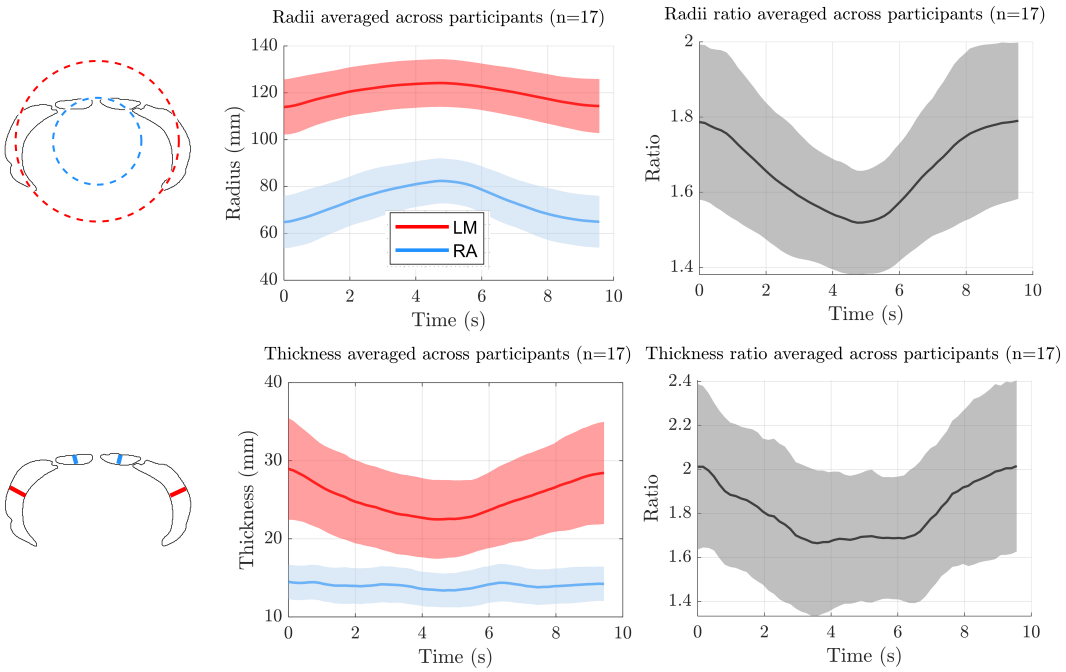

Figure 2.3.: LM and RA cylinders radii and thicknesses along time

2.3.2. Cylinder stress

The Figure 2.4 represents the circumferential stress σ_θ for the two cylinders. As the stresses are dependent of cylinder radius and thickness, its evolution follows the same pattern as these variables.

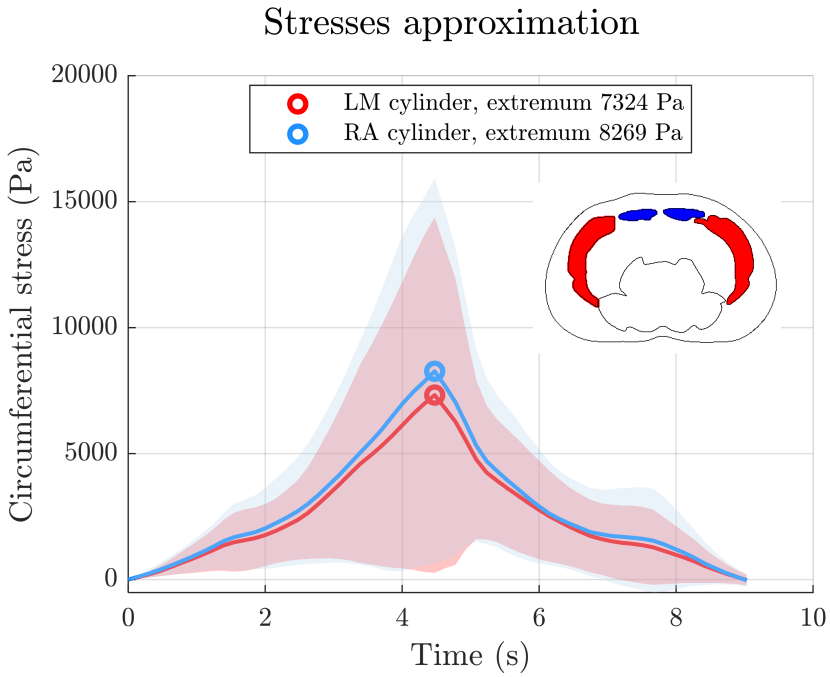

Figure 2.4.: Circumferential stress σ_θ temporal evolution for lateral muscles (LM) and rectus abdominis (RA) cylinders, averaged across participants (n=17)
Results are presented as mean values ± one standard deviation σ

Maximum stresses of both LM and RA cylinders are reported Table 2.1.

Direction - Cylinder	**Lateral muscles (LM)**	**Rectus abdominis (RA)**
Stress σ (kPa)		
Radial σ_r	-0.66 ± -0.64	-0.68 ± -0.66
Circumferential σ_θ	7.75 ± 7.25	8.76 ± 7.82
Young modulus E (kPa)		
Radial E_r	24 ± 22.56	35.7 ± 20.08
Circumferential E_θ	315.31 ± 244.81	458.2 ± 155.83

Table 2.1.: Theoretical stresses and associated Young moduli averaged among participants
Columns represent the different considered cylinders (i.e. cylinder of lateral muscles (LM), cylinder of rectus abdominis (RA), averaged cylinder)
Results are presented as mean ± one standard deviation

The maximum stresses were averaged among the whole cohort (n=17). The radial stress is negative in both cylinders being oriented inward of the abdomen. The radial stress is almost similar on both LM and RA cylinders, and very low in absolute value compare to the circumferential stress. The circumferential stress is higher in the RA cylinder than LM, reaching up to 8.76 kPa. Only this stress will be considered for the remainder of the study as it is the principal stress involved in hernia occurrence. High inter-individual variability is observed.

The computed circumferential stress σ_θ within the linea alba is 141.92 ± 141.44 kPa.

2.3.3. Cylinder elastic moduli

Elastic Young moduli of both LM and RA cylinders are reported Table 2.1.
The Young modulus was assessed on both LM and RA cylinders, along both radial and circumferential direction. Along the radial direction, for LM cylinder, the linear correlation between radial stress σ_r was and strain ε_r was statistically significant for

all participants. One participant was removed because negative Young modulus.
For RA cylinder, another participant has been removed for the same reason. Additionally, 6 participants were removed because the linearity of the relationship between σ_r and strain ε_r was not statistically significant. Thus, the Young modulus E_r for RA cylinder is based on 10 participants.

Considering the circumferential direction, the linear correlation between circumferential stress σ_θ was and strain ε_θ over the LM cylinder was statistically significant for all participants. The same participant as for radial direction was removed because negative Young modulus.
For the RA cylinder, 4 participants were removed because negative Young modulus. Additionally, 8 participants were removed because the linearity of the relationship between σ_θ and strain ε_θ was not statistically significant. Thus, the Young modulus E_θ for RA cylinder is based on 5 participants.

2.4. Discussion

This study aimed to improve our understanding of the mechanical behaviour of the abdominal wall by approximating the abdominal wall as a pressurised cylindrical structure and calculating the corresponding stresses and strains. To do so, *in vivo* measurements of intra-abdominal pressure (IAP) and abdominal wall geometry and motion using dynamic MRI were used. Using Laplace's formula, which assumes thick-wall conditions, both circumferential stress and radial stress were computed.

The radial stress σ_r was found to be negative (inward-directed), compensating the intra-abdominal pressure, and much smaller in magnitude than the circumferential stress σ_θ. The circumferential direction is the main fibers direction of the lateral muscles (Axer et al. 2001a; B. Hernández-Gascón et al. 2011). It has also been shown that the abdominal wall has an anisotropic behaviour, being stiffer in the transverse plane than in the sagittal plane. This aligns wit the result that, when possible, a transverse incision (along left-right direction) is preferable, as it is more resistant to rupture and reduces the hernia recurrence rate by half compared to a vertical incision (along cranio-caudal direction) (Helgstrand 2016; Le Huu Nho et al. 2012; S. R. Brown et al. 2005).

The circumferential stress was higher in the RA compared to the LM, suggesting that the RA muscles endure more stress during physiological activities. The stress being correlated with structure thickness (Equation 2.1), circumferential stress is higher in RA muscles which are thinner than LM (Jourdan, Rapacchi, et al. 2022). This heterogeneous distribution of stress, where lateral part of the abdomen is less subjected to stress than the midline area, is confirmed by different numerical studies under passive conditions (Hernández-Gascón et al. 2013; Simón-Allué, Calvo, et al. 2017).
In order to interpret the stress the RA cylinder is subjected to, the tensile strength of the rectus composite (composed of rectus muscle, the rectus sheaths and peritoneum) was 530 kPa in Kriener *et al.* study (Kriener et al. 2023). The computed stress of 8.76 ± 7.82 kPa representing only 1.6% of this threshold. On the *ex vivo* experimental part of Grasa *et al.* study, when subjected to electrical pulses of 100V, the RA muscles experienced a maximum isometric stress of 64 ± 12 kPa.

In our study, the computation of stress σ and strain ε on both directions (circumferential $\vec{\theta}$ and radial $\vec{r}$) allowed for the derivation of Young's modulus, when the linearity between stress and strain was statistically significant.

For **LM cylinder**, the stress-strain linear relationship was statistically significant for all participants on both radial and circumferential directions. One participant was removed because negative Young modulus. When observing the corresponding MRI and MRI-derived data, this may be due to an incorrect breathing performance inducing a slight abdominal muscle contraction. The LM became shorter (along the medial axis length, in the circumferential direction $\vec{\theta}$) whereas the circumferential stress σ_θ increased. In the same time, the LM became thicker (along the radial direction $\vec{r}$) whereas the radial stress σ_r decreased (oriented inward), resulting in a negative Young modulus.

For **RA cylinder**, respectively 6 and 8 participants have been removed due to non-statistically significant linear relationship between stress and strain along radial and circumferential directions, making not possible to calculate Young's modulus. This may be explained by the fact that RA muscles of the anterior abdominal wall are oriented vertically (cranio-caudally) along the midline of the body, at the contrary of LM which are mainly circumferential. Thus, the shape along radial and circumferential

directions almost did not change, leading to an almost zero strain during the breathing performance.
Along radial direction, one participant was removed because negative Young modulus. When looking at the corresponding MRI and MRI-derived data, this may be due to the very light deformation of the RA, where the shape almost did not change whereas the radial stress decreased, resulting in a negative Young modulus. Since the RA deformation along circumferential direction and thus the corresponding strain ε_θ did not change either during the increase in circumferential stress σ_θ, it resulted in a non-statistical significance of the linearity between the circumferential stress and strain.

The Young's moduli on both LM and RA cylinders were found to be significantly higher in the circumferential direction $\overrightarrow{\theta}$ than in the radial direction $\overrightarrow{r}$. This results brings new elastic values about the behaviour of the abdominal wall in the circumferential direction (i.e, transverse plane). Along this direction, the Young moduli was higher in the RA cylinder than in the LM one. This aligns with various studies showing that the different abdominal wall muscles play specific roles in the mechanical response of the abdominal wall (Jourdan, Rapacchi, et al. 2022; Cardoso 2012; Silvia Todros, de Cesare, Pianigiani, et al. 2019; Silvia Todros, Paola Pachera, et al. 2018). In Song *et al.* study where *in vivo* participants were insufflated with gas, they found an elastic modulus of the whole abdomen about 42.5 kPa in circumferential direction (Song et al. 2006). The elastic modulus measured on *ex vivo* rectus composite (composed of rectus muscle, the rectus sheaths and peritoneum) was 112 kPa in Kriener *et al.* study (Kriener et al. 2023). The elastic modulus measured on *ex vivo* lateral muscles composite (composed of internal and external obliques, and the transversus abdominis) was about 100 kPa in Cardoso *et al.* study (Kriener et al. 2023). These values are lower than the one measured here. This may be due to either the studies design which are very different, and also from the approximation made in this study.

A thin-wall approximation was used to estimate the circumferential stress within the linea alba, which was larger compared to the RA and LM cylinders. This highlights the high level of loading of this structure in comparison to other abdominal wall components. The large stresses observed in the linea alba suggest that this area is particularly vulnerable to herniation.

Other studies found values of stress in the range. From Hernández *et al.* numerical study, the stress on linea alba during passive situation at an IAP = 20 mmHg was 100 kPa (Hernández-Gascón et al. 2013). This is closer to the theoretical circumferential stress of our study 141.92 ± 141.44 kPa at an average breathing pressure of 10 mmHg. In Grasa *et al.* numerical study, the maximum principal stress is around 100 kPa at the end of the contraction on the central region of the model (Grasa et al. 2016). The experimental *ex vivo* tensile test of Förstemann *et al.* (Förstemann et al. 2011) or the constitutive model of Pachera *et al.* (P. Pachera et al. 2016) who resulted in a Cauchy stress in the circumferential direction of approximately 600 kPa for a stretch around 1.07 of the linea alba, equals to a strain ε_θ of about 7%. These values are higher than the ones obtained in this study. In Förstemann *et al.* study, the calculated Young modulus of linea alba in circumferential direction was about 50 kPa. In Cooney *et al.* tensile test study, the Young modulus of linea alba in the circumferential direction was about 72 MPa, highlighting the very high inter-subjects and inter-studies variability. In order to compare the stress experienced by the linea alba during breathing, the tensile strength $\sigma_{rupture}$ of linea alba in the circumferential direction (i.e., the main fibers direction (Axer et al. 2001b)), is about 10 MPa and 8.4 MPa on epigastric and hypogastric regions respectively (Hollinsky et al. 2007).

The high inter-individual variability in both stresses and Young's moduli suggests that the mechanical properties of the abdominal wall are highly subject-specific. This has important implications for clinical applications, such as the design of personalised surgical meshes or tailored treatments for conditions like hernias. Each patient's unique mechanical profile must be considered when planning interventions, which reinforces the importance of using *in vivo* measurements like those presented in this study.

Several limitations must be acknowledged in this study. First, 2D imaging was used, and the analysis was limited to the breathing exercise, leading for some participants to a quasi-zero deformation of the rectus abdominis (RA) muscles. When intra-abdominal pressure (IAP) increases during passive actions such as breathing or movements without active muscular loading, the RA fibers, which are oriented vertically, tend to align with the loading direction (diaphragmatic downward motion and chest expansion), the cranio-caudal curvature radius of the abdomen changing more

than the circumferential (Song et al. 2006; Hernández-Gascón et al. 2013; P. Pachera et al. 2016; Förstemann et al. 2011; Simón-Allué, Calvo, et al. 2017). Incorporating 3D dynamic MRI could provide a more comprehensive understanding of the abdominal wall mechanics, enabling a better assessment of stress distribution, particularly for addressing regional heterogeneity within the wall structure.

Another limitation stems from the need to validate our results using finite element models (FEM) that are specific to the participants of this study. While we compared our results with properties derived from *ex vivo* tensile tests, it is important to note that *in vivo* conditions may lead to different mechanical behaviour, complicating the direct comparison. This highlights the importance of coupling *in vivo* data with computational modelling to validate and refine the mechanical properties observed experimentally.

The assumption that the abdominal wall can be approximated as a cylindrical structure should also be discussed. Our analysis shows that the cylinder based on lateral muscles (LM) is, on average, 1.8 times wider than the RA, which supports the cylindrical approximation to some extent. Therefore, while the cylindrical approximation provides valuable insights, it is important to consider that it is a simplified model and may not fully capture the biomechanical complexities of the abdominal wall in all situations.

Finally, this study was conducted on healthy individuals. Future work should extend these investigations to pathological conditions, such as hernia patients. Comparing the mechanical properties of healthy individuals with those of hernia patients could provide valuable insights into how diseased tissue behaves differently. This information would be crucial for developing personalised treatment approaches and improving surgical outcomes.

2.5. Conclusion

This study provides critical insights into the mechanical behaviour of the abdominal wall, particularly regarding the differences in stress distribution between the rectus abdominis (RA) and lateral muscles (LM). The findings indicate that circumferential stress may be the principal factor responsible for abdominal wall failure, and the high inter-individual variability in mechanical properties emphasises the need for personalised approaches in clinical practice. By laying the groundwork for understanding

abdominal wall mechanics in healthy subjects, this study opens new avenues for future research, particularly in the prevention and treatment of hernias. Extending this work to include pathological conditions, such as hernia patients, will allow for more personalised and effective interventions in the clinical setting.

3. Linea alba 3D morphometric variability by CT scan exploration

This chapter refers to a published work (Gueroult et al. 2024). This article version is available on HAL, has been accepted for publication after peer-review, is subject to Springer Nature's accepted manuscript terms of use, and is not the editor's version.

Table of contents

3.1. Introduction . . . 129
3.2. Materials and Methods . . . 131
3.2.1. Cohort's selection . . . 131
3.2.2. CT scans . . . 131
3.2.3. Output metrics from CT scans . . . 132
3.2.4. Statistical analysis . . . 134
3.3. Results . . . 135
3.3.1. Demographic data . . . 135
3.3.2. Linea alba measurements . . . 135
3.3.3. Influence of age . . . 139
3.3.4. Influence of gender . . . 139
3.3.5. Influence of BMI . . . 140
3.3.6. Correlations . . . 141
3.4. Discussion . . . 142
3.4.1. Limitations . . . 145
3.5. Conclusion . . . 146

Pierre Gueroult [1,2], **Victoria Joppin** [1], **Kathia Chaumoitre** [3,4], **Mathieu Di Bisceglie** [3], **Catherine Masson** [1], **Thierry Bege** [1,5]

[1]Univ Gustave Eiffel, Aix-Marseille Univ, LBA, F-13016 Marseille, France

[2]Service de chirurgie viscérale et endocrinienne, Angers, University Hospital, Rue Larrey, 49933, CEDEX 9 Angers, France

[3]Department of Medical Imaging, Aix Marseille Univ, North Hospital, APHM, Marseille, France

[4]Anthropologie Biologique UMR 7268ADES, Aix Marseille Univ, Marseille, France

[5]Department of General Surgery, Aix Marseille Univ, North Hospital, APHM, Marseille, France

Author contributions

PG: collected the data

PG and **VJ**: processed the data and made figures

VJ: created the Matlab code

PG: drafted the article

VJ, **KC**, **MDB**, **CM** and **TB**: did the revision of the article.

Funding

Pierre GUEROULT disclaimed an «Association Française de Chirurgie» grant and a state research grant. Grants had no influence on scientifical content of the manuscript.

Data availability

All data supporting the findings are available within the paper and its Supplementary Information.

Preface

As previously highlighted in chapter 2, the midline zone is particularly subjected to circumferential stress. In particular, the linea alba is exposed to the highest degree of stress within the abdominal wall. This finding leads to the necessity of addressing the Objective 3 about the anatomical variability of the linea alba, essential for addressing issues such as hernia formation. The objective of this chapter 3 is to present a

three-dimensional anatomical analysis of the linea alba, with a view to uncovering its variability across different patient demographics (age, body mass index, gender) and geometrical variables (width, length, and curvature).

Abstract

Purpose: The width of the Linea alba, which is often gauged by inter-rectus distance, is a key risk factor for incisional hernia and recurrence. Previous studies provided limited descriptions with no consideration for width, location variability, or curvature. We aimed to offer a comprehensive 3D anatomical analysis of the Linea alba, emphasizing its variations across diverse demographics.

Methods: Using open source software, 2D sagittal plane and 3D reconstructions were performed on 117 patients' CT scans. Linea alba length, curvature assessed by the sagitta (the longest perpendicular segment between xipho-pubic line and the Linea alba), and continuous width along the height were measured.

Results: The Linea alba had a rhombus shape, with a maximum width at the umbilicus of 4.4 ± 1.9 cm and a larger width above the umbilicus than below. Its length was 37.5 ± 3.6 cm, which increased with body mass index (BMI) (p<0.001), and was shorter in women (p<0.001). The sagitta was 2.6 ± 2.2 cm, three times higher in the obese group (p<0.001), majorated with age (p=0.009), but was independent of gender (p=0.212). Linea alba width increased with both age and BMI (p<0.001, p=0.002), being notably wider in women halfway between the umbilicus and pubis (p=0.007).

Conclusion: This study provides an exhaustive 3D description of Linea Alba's anatomical variability, presenting new considerations for curvature. This method provides a patient-specific anatomy description of the Linea alba. Further studies are needed to determine whether 3D reconstruction correlates with pathologies, such as hernias and diastasis recti.

3.1. Introduction

The abdominal wall is a complex, multilayer structure composed of muscles, aponeurosis, fat, and skin. It provides essential functions such as trunk mobility, abdominal pressure regulation, breathing, and organ protection. The Linea alba comprises the

entanglement of anterior and posterior rectus sheath (Goldberg et al. 2023; Axer et al. 2001b), with a three-layer structure made of collagen fibers of different orientations (Axer et al. 2001b) and presenting with anisotropic properties (Astruc et al. 2018; Levillain et al. 2016; Gerard M. Cooney et al. 2016). It plays an important role in stabilizing the abdominal wall complex. Its dysfunction leads to parietal pathologies such as hernias and diastasis recti, or participates in syndromes such as postpartum abdominal wall insufficiency (PPAWI) (Śmietański, Śmietańska, et al. 2022).

The usual anatomic treatise descriptions of the Linea alba are not very detailed (Rouvière 2002; Kamina 2014; Netter 2023), and few authors have made more precise descriptions based on dissection (Rath, Attali, et al. 1996; Testut et al. 1948). Modern postprocessing techniques using CT scans, such as multiplanar reformation, three-dimensional (3D) visualization, and organ delineation, make it possible to study anatomy *in vivo* (Kirchgeorg et al. 1998; Maher et al. 2004). Several authors have described the Linea alba from a radiological point of view (Goldberg et al. 2023; Kaufmann et al. 2022; Jourdan, Soucasse, et al. 2020; Fredon et al. 2021). It has been shown to be enlarged in obese people, during pregnancy and postpartum, at higher ages, and with diabetes mellitus (Jourdan, Soucasse, et al. 2020; Cavalli et al. 2021; P. Mota et al. 2018; Yuan et al. 2021). However, these studies have been limited to axial planes, with no consideration of their sagittal length and 3D shape. Furthermore, axial studies are limited to selected slices, with no consideration for the entire anatomic profile.

Most of the literature studying the Linea alba has been driven by the problem of defining diastasis recti (Kaufmann et al. 2022; Cavalli et al. 2021; P. Mota et al. 2018; Reinpold et al. 2019; P. G. F. d. Mota et al. 2015). The European Hernia Society recommendations define it as an inter-rectus distance (IRD) exceeding 2 cm that should be measured 3 cm above the umbilicus (Hernández-Granados et al. 2021). With this definition, 35.6-57% of the population should be considered as presenting a diastasis recti (Kaufmann et al. 2022; Ugurlu et al. 2023). Diastasis recti is often associated with umbilical, small midline, and groin hernia (Ugurlu et al. 2023; Köhler et al. 2015; Bellido Luque et al. 2015; Nishihara et al. 2021). IRD is also a risk factor for recurrence after umbilical and midline hernia sutured repair (Köhler et al. 2015; Bellido Luque et al. 2015). The appropriate treatment in patients presenting a hernia associated with diastasis recti is still debated in the surgical field. A recent meta-analysis concluded

that both open and laparoscopic approaches are effective, as evidenced by very low recurrence rates (ElHawary et al. 2021).

The width of the Linea alba depends on the level of its measurement (Rath, Attali, et al. 1996; Kaufmann et al. 2022), but the assessments that have been carried out to date are «discontinuous» because of the limited number of measurements at different levels of the Linea alba. The variation of its width throughout the height and its curvature has never been considered in anatomy or in rectus diastasis repair. The IRD is not a constant distance over the entire height of the wall, which should be taken into account.

We aimed to provide a complete description of the Linea alba's width, shape, and curvature and to determine which factors influenced its parameters.

3.2. Materials and Methods

3.2.1. Cohort's selection

We conducted a retrospective study on a cohort of patients that was previously designed to describe abdominal wall axial morphometrics (Jourdan, Soucasse, et al. 2020). The inclusion criteria of the original cohort were as follows: adult patients over 18 years or older performing a CT scan for renal colic from October 2017 to April 2019 at the medical imaging department of the North Hospital, Marseille (France). The exclusion criteria of the original cohort were visible abdominal wall tissue disorder and the presence of a significant medical record (cancer, immunodeficiency, etc.).

A total of 841 patients met the criteria, and 120 CTs were randomly chosen to make four comparable groups of age (18–30 years, 31–45 years, 46–60 years, and older than 60 years, n = 30/group, n = 15 women in each group) , gender (n = 60/gender), and body mass index (BMI) (under and normal weight [BMI≤25, n = 52], overweight [BMI 25–30, n = 41], and obese [BMI≥30, n = 27]).

3.2.2. CT scans

CTs were performed on a Revolution HD GSI (GE Healthcare, USA) in a supine position. Patients were told to hold their breath after maximal inhalation during acquisition. No

contrast agent was injected. Exposure resulted in a dose of radiation of 120 kV, and the exposure time (mAS) and scan field of view varied according to the patient's weight. Slice thickness was 1.25 mm, and pitch was 1.375. The matrix size of the images was 512×512 pixels.

3.2.3. Output metrics from CT scans

CT scan measurements were performed by the same operator (PG, medical doctor) using Osirix Lite imaging software (v.13.0.2 Pixmeo SARL, Switzerland). Afterward, 3D multiplanar reconstruction (MPR) median sagittal reconstructions were systematically performed. Reconstruction of the whole Linea alba was not possible in three patients who only had upper abdomen images; those patients were discarded from the analysis.

Measurements were taken to quantify the length, curvature, and width of the Linea alba. These measurements are shown in Figure 3.1.

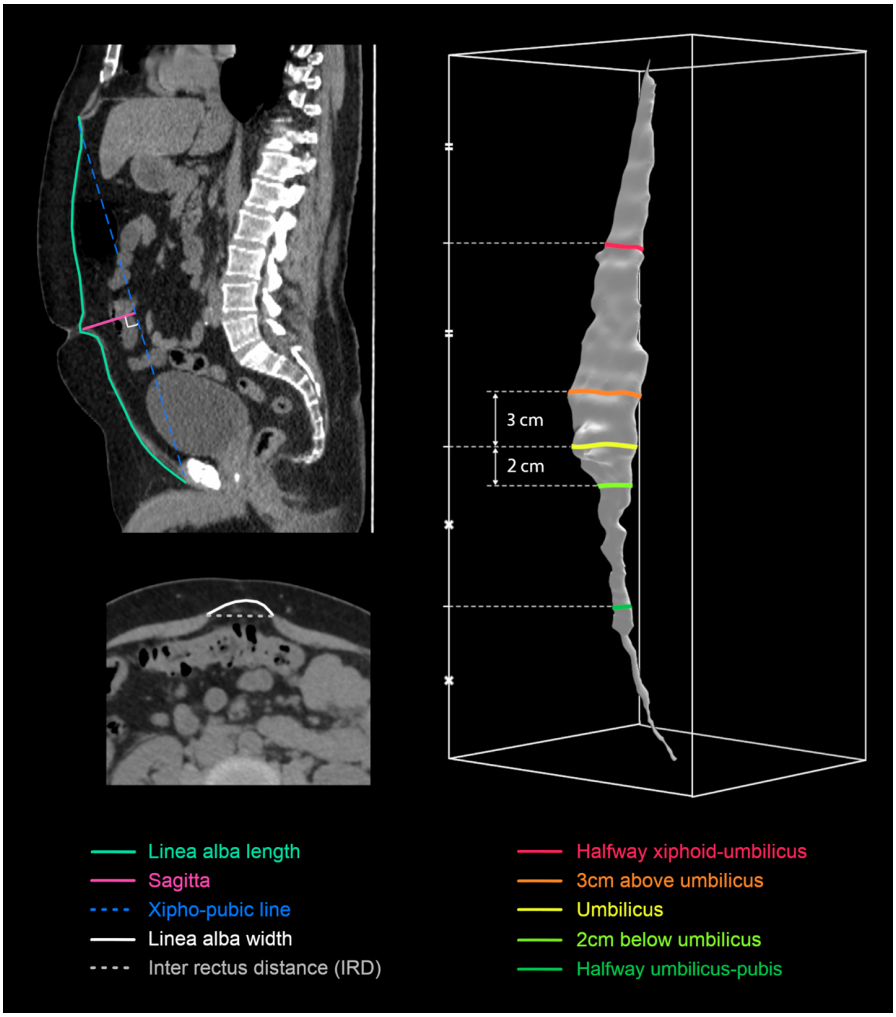

Figure 3.1.: Sagittal, axial and 3D measurements performed on the Linea alba: Linea alba length (light blue), sagitta (pink), Linea alba width (white), Inter rectus distance (grey), width halfway xiphoid-umbilicus (red), width 3 cm above umbilicus (orange), width at umbilicus (yellow), width 2 cm below umbilicus (light green), width halfway umbilicus-pubis (green)

The Linea alba length was defined as the distance between its insertion on the xiphoid process and on the pubic bone along the Linea alba. Curvature was described with the sagitta. In geometry, the sagitta of a circular arc is the distance from the center of the arc to the center of its base. Here, the base corresponded to the xipho-pubic line, and the sagitta was defined as the longest perpendicular segment between the xipho-pubic line and the Linea alba. All presented measures were rounded to millimeters.

A 3D reconstruction of the Linea alba was made for every patient on the open source 3D Slicer software (Version 4.13.0). Delineations of the Linea alba were performed

semiautomatically using the 2 mm paintbrush segmentation tool. The Linea alba was delineated manually on approximately 25% of axial and sagittal slices. The delineation was then propagated using the «fill between slice» tool. After propagation, the remaining holes were filled manually. Final 3D rendering is presented with a smoothing factor of 0.5.

The width of the Linea alba was calculated from the 3D axial plane geometry along its entire height using a specially designed Matlab algorithm (MathWorks ink, Version R2023a). The IRD distance corresponded to the shortest segment between the lateral edges of the Linea alba. The IRD is measured as a straight line, whereas the length of the Linea alba, as measured in this study, is a curve. Maximal and average Linea alba widths were calculated. The width was measured in specific landmarks of Linea alba (from top to bottom): halfway xiphoid–umbilicus, 3 cm above umbilicus, at umbilicus, 2 cm below umbilicus, and halfway umbilicus–pubis. These landmarks corresponded to those used to define diastasis recti and to those usually found in the literature (Kaufmann et al. 2022; P. Mota et al. 2018; Hernández-Granados et al. 2021). A relative Linea alba length scale suitable for all patients, regardless of their body size, was established for the location of maximal width and graphical comparison between individuals. The average width of the Linea alba at each level of its standardized height was then plotted on the same axis, group by group, with key anatomical landmarks.

Morphometric measurements performed at the upper edge of the fourth lumbar vertebrae and previously described in Jourdan *et al.* study (Jourdan, Soucasse, et al. 2020) were extracted and analyzed in the present cohort: total abdominal area, total visceral area, muscular area, abdominal muscles area, subcutaneous fat area, visceral fat area, subcutaneous fat thickness, and waist circumference.

3.2.4. Statistical analysis

Statistical analysis was performed using RStudio (Version 2022.7.2.576 RStudio, Inc., Boston, MA). Quantitative variables were expressed as means ± one standard deviation, minimal values, and maximal values. The normality of the distribution was checked using a Shapiro–Wilk test. The normally distributed variable was Linea alba length. Non-normally distributed variables were sagitta and all Linea alba width measurements. When required, equality of variance was checked before the statistical

analysis. Differences between sex groups were tested using the Student t-test for normally distributed variables and the Mann–Whitney for non-normally distributed variables. The differences between age groups and BMI groups were tested using an analysis of variance (ANOVA) for normally distributed variables and a Kruskal–Wallis test when not normally distributed. The normality of residuals was checked using a Shapiro–Wilk test. Alpha risk was 5%, two-tailed. Here, *p*-values under 0.025 were considered to be statistically significant. The correlation between variables was calculated using Pearson's correlation coefficient *r*. Data are presented using a correlation matrix plot coding Pearson's correlation coefficient with a gradation of colors. In this figure, BMI and age are treated as continuous variables. For the reader's convenience, the raw correlation coefficients have not been presented in the corresponding figure. The most representative patient of each subgroup was the one with the shortest Euclidean distance to the mean of all variables in each subgroup.

3.3. Results

3.3.1. Demographic data

The final cohort was made up of 117 patients: 58 women and 59 men. The mean age was 45.5 ± 16.4 years old, and the mean BMI was 26.1 ± 4.9 kg/m^2.

3.3.2. Linea alba measurements

The average length of the Linea alba in the sagittal plane was 37.5 ± 3.6 cm (range [30.5/47.7 cm]). The mean sagitta was 2.6 ± 2.2 cm (range [-3.4/8.1 cm]). Some patients (n=9) had a negative sagitta because of an inward curved Linea alba.
Linea alba width measurement showed a tendency to be rhombus shaped (Figure 3.1, Figure 3.2, Figure 3.3). The average maximal width was 4.4 ± 1.9 (range [1.4/11.4 cm]) an was located at the umbilicus level. Linea alba widths at specific landmarks are presented in Table 3.1.

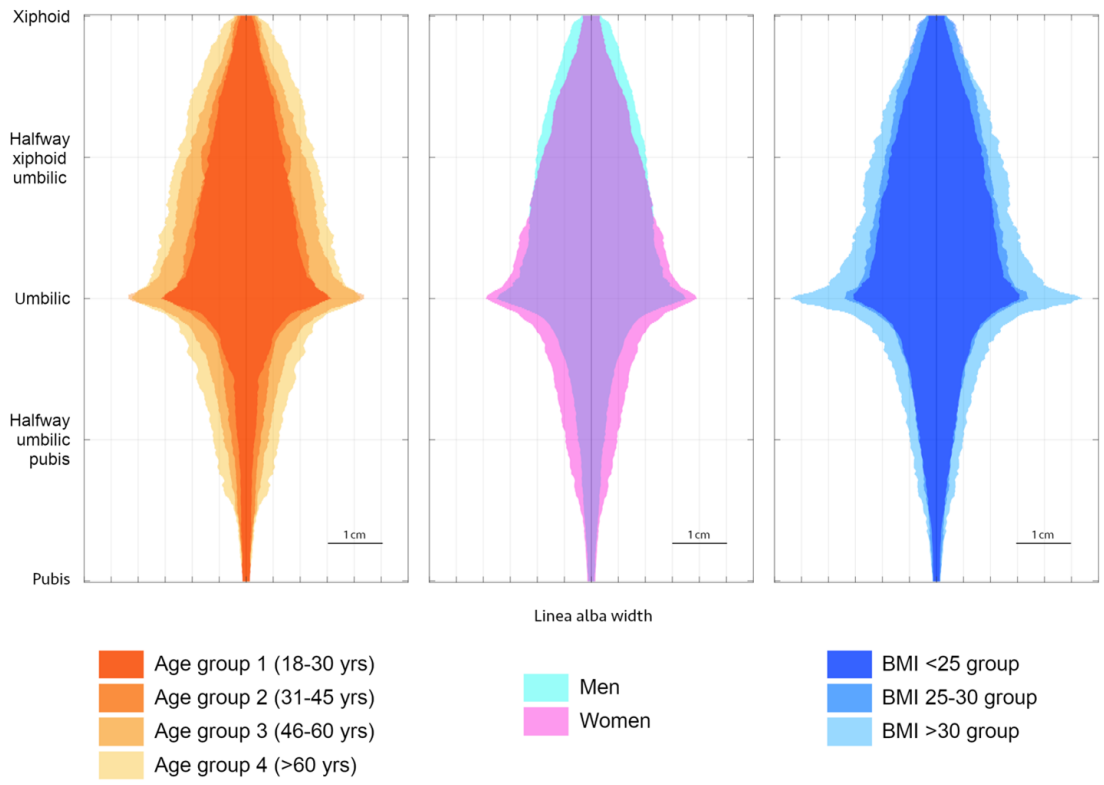

Figure 3.2.: Linea alba width calculated on 3D reconstruction according to age, gender, and BMI groups. Linea alba length has been standardized between individuals to allow for a comparison of key landmarks

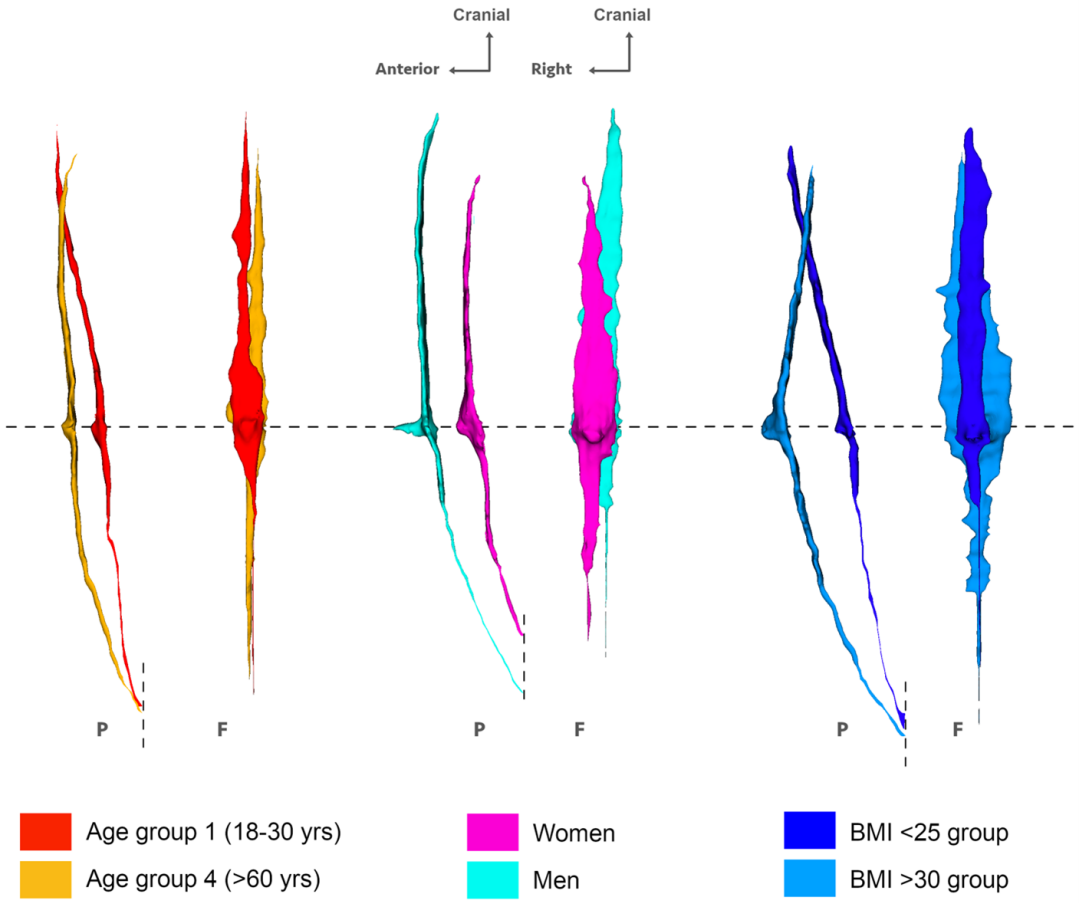

Figure 3.3.: 3D reconstruction of the Linea alba in the most representative patient in each group. The face (F) and profile (P) of the reconstructions are presented. Linea alba are aligned on the umbilicus and pubic insertion levels. The most representative patients are those with the shortest Euclidean distance to the mean of all variables in each subgroup. Reconstructions has been generated with a 3D slicer

	Mean ± Standard deviation	**Range [min/max]**
Demographic data		
Age ($years$)	45.5 ± 16.4	[18.0/86.0]
Size (m)	1.69 ± 0.10	[1.45/1.92]
BMI (kg/m^2)	26.1 ± 4.9	[15.6/43.3]
Linea alba measurements (cm)		
Sagitta	2.6 ± 2.2	[-3.4/8.1]
Length	37.5 ± 3.6	[30.5/47.7]
Width (cm)		
Halfway xiphoid-umbilicus	1.9 ± 1.2	[0.2/8.1]
3 cm above the umbilicus	2.6 ± 1.4	[0.6/9.6]
At the umbilicus	3.7 ± 1.9	[0.9/11]
2 cm below the umbilicus	1.7 ± 1.2	[0.4/9.6]
Halfway umbilicus-pubis	0.7 ± 0.9	[0.1/5.6]
Maximal width	4.4 ± 1.9	[1.4/11.4]
Maximal inter-rectus distance (IRD)	3.1 ± 1.4	[1.1/9.4]
Other abdominal measurements		
Length (cm)		
Subcutaneous fat thickness	2.3 ± 0.9	[0.4/4.4]
Waist circumference	95.2 ± 13.3	[68.2/135.3]
Areas (cm^2)		
Total abdominal area	678.4 ± 199.0	[309.1/1318.4]
Total visceral area	270.0 ± 102.9	[87.0/626.0]
Muscular area	133.2 ± 32.4	[74.2/215.3]
Abdominal muscles area	55.6 ± 16.6	[24.4/102.1]
Subcutaneous fat area	249.3 ± 125.9	[44.9/752.7]
Visceral fat area	147.0 ± 94.0	[17.2/449.0]

Table 3.1.: Demographic data, Linea alba measurements, and other abdominal measurements for the whole cohort (n=117)
Data are presented as mean ± standard deviation

3.3.3. Influence of age

Age had a significant impact on all abdominal metrics, except Linea alba length (Table 3.2, Figure 3.2 and Figure 3.3). The Linea alba widened with age in all landmarks, regardless of the size (p<0.001, p=0.002), but did not lengthen (p=0.252).
Its curvature, as reflected by the sagitta metric, increased significantly toward the front with age (p=0.009).

Linea alba measurements* (cm)	**Age group 1** (18–30 years) n=29	**Age group 2** (31–45 years) n=30	**Age group 3** (46–60 years) n=30	**Age group 4** (>60 years) n=28	***p*-value**
Sagitta	2.2 ± 2.2	2.0 ± 2.0	3.1 ± 2.1	3.3 ± 2.2	0.009 **
Length	37.7 ± 3.1	38.0 ± 4.2	38.0 ± 3.5	36.4 ± 3.2	0.252
Width					
Halfway xiphoid-umbilicus	1.4 ± 0.7	1.7 ± 1.0	2.2 ± 1.1	2.5 ± 1.5	<0.001 **
3 cm above the umbilicus	2.1 ± 0.9	2.2 ± 1.0	3.0 ± 1.2	3.1 ± 2.0	0.002 **
At the umbilicus	3.2 ± 1.7	3.1 ± 1.6	4.4 ± 1.7	4.2 ± 2.1	0.002 **
2 cm below the umbilicus	1.1 ± 0.5	1.3 ± 0.6	1.9 ± 1.2	2.3 ± 1.8	<0.001 **
Halfway umbilicus-pubis	0.3 ± 0.3	0.5 ± 0.5	0.9 ± 0.9	1.2 ± 1.2	<0.001 **
Maximal width	3.6 ± 1.6	3.7 ± 1.5	5.1 ± 1.8	5.4 ± 2.2	<0.001 **
Maximal inter-rectus distance (IRD)	2.4 ± 0.9	2.6 ± 0.9	3.5 ± 1.2	4.1 ± 1.8	<0.001 **

Table 3.2.: Influence of age on Linea alba measurements
*Data are presented as mean ± standard deviation
**Indicate statistically significant p-values (p<0.025)

3.3.4. Influence of gender

Gender had a significant impact on several measurements (Table 3.3, Figure 3.2 and Figure 3.3).
Women had a significantly wider Linea alba at the halfway umbilicus–pubis landmark (p=0.007). No statistical difference between men and women was found for width at other landmarks. Linea alba length (p<0.001) was significantly lower in women. The curvature reflected by the sagitta metric was not statistically different between men and women (p=0.212). This suggests the stability of this measurement between genders.
Visually, men tended to have a wider Linea alba toward the top but without statistical significance.

Linea alba measurements* (cm)	**Men** n=59	**Women** n=58	***p*-value**
Sagitta	2.9 ± 2.0	2.4 ± 2.3	0.212
Length	38.6 ± 3.8	36.4 ± 2.9	<0.001 **
Width			
Halfway xiphoid–umbilicus	2.0 ± 1.1	1.8 ± 1.2	0.184
3 cm above the umbilicus	2.5 ± 1.3	2.7 ± 1.5	0.281
At the umbilicus	3.5 ± 1.6	3.9 ± 2.1	0.417
2 cm below the umbilicus	1.4 ± 0.6	2.0 ± 1.6	0.058
Halfway umbilicus–pubis	0.5 ± 0.5	1.0 ± 1.1	0.007 **
Maximal width	4.2 ± 1.6	4.6 ± 2.2	0.515
Maximal inter-rectus distance (IRD)	3.0 ± 1.2	3.3 ± 1.6	0.689

Table 3.3.: Influence of gender on Linea alba measurements
*Data are presented as mean ± standard deviation
**Indicate statistically significant p-values (p<0.025)

3.3.5. Influence of BMI

BMI had a huge impact on abdominal metrics (Table 3.4, Figure 3.2 and Figure 3.3). Linea alba width was greater at the level of the umbilicus and around the umbilicus in obese people (p<0.001), whereas it was not greater from halfway xiphoid–umbilicus and halfway umbilicus–pubis (p=0.142 and p=0.071). Linea alba length was significantly greater with BMI increase (p<0.001).
The curvature, as reflected by the sagitta metric, was statistically higher with BMI increase (p<0.001). The sagitta was even three times higher in the BMI>30 group than in the BMI<25 group (4.8 ± 2.0 cm versus 1.6 ± 1.7 cm).
This indicates an overall widening of the Linea alba along its entire length, with a maximum in the periumbilical area in obese people.

Linea alba measurements* (*cm*)	**BMI<25** n=51	**BMI 25–30** n=40	**BMI>30** n=26	***p*-value**
Sagitta	1.6 ± 1.7	2.5 ± 1.8	4.8 ± 2.0	<0.001 **
Length	35.9 ± 2.9	37.6 ± 3.3	40.7 ± 3.0	<0.001 **
Width				
Halfway xiphoid–umbilicus	1.7 ± 1.0	1.9 ± 1.0	2.4 ± 1.7	0.142
3 cm above the umbilicus	2.3 ± 1.3	2.5 ± 1.4	3.3 ± 1.3	<0.001 **
At the umbilicus	3.1 ± 1.8	3.4 ± 1.2	5.4 ± 1.9	<0.001 **
2 cm below the umbilicus	1.5 ± 1.4	1.5 ± 0.7	2.3 ± 1.3	<0.001 **
Halfway umbilicus–pubis	0.6 ± 1.0	0.7 ± 0.6	1.0 ± 0.9	0.071
Maximal width	3.7 ± 1.8	4.2 ± 1.5	6.3 ± 1.8	<0.001 **
Maximal inter-rectus distance (IRD)	2.7 ± 1.3	3.1 ± 1.1	4.1 ± 1.5	<0.001 **

Table 3.4.: Influence of BMI on Linea alba measurements
*Data are presented as mean ± standard deviation
**Indicate statistically significant *p*-values (p<0.025)

3.3.6. Correlations

The correlations between sagittal measurements, axial measurements, and other abdominal measurements are presented in Figure 3.4.

Curvature measurements by the mean of sagitta metric were quasi totally independent of size (r=0.06) and poorly influenced by age (r=0.24), but these measurements were well correlated with mensuration related to obesity such as umbilical–spinal distance (r=0.83), total abdominal area (r=0.74), total visceral area (r=0.70), visceral fat area (r=0.69), and waist circumference (r=0.71).

Linea alba length was weakly associated with Linea alba width at the umbilicus (r=0.22). Linea alba length was totally independent of Linea alba width in other locations, such as halfway xiphoid–umbilicus (r=0.01), 3 cm above umbilicus (r=0.05),

2 cm below umbilicus (r=-0.01), and halfway umbilicus–pubis (r=-0.04). Linea alba length was more strongly correlated with BMI (r=0.57) than with the size of the patient (r=0.46).

The widths of the Linea alba showed similar correlation profiles, regardless of the landmark. However, the width at the umbilical level was slightly better correlated with the other variables: r=0.52 with total abdominal area and r=0.51 with waist circumference. Linea alba width at the umbilicus was well associated with its width 2 cm below and 3 cm above (r=0.62 and r=0.72). Overall, the other measurements were only weakly associated with the Linea alba width.

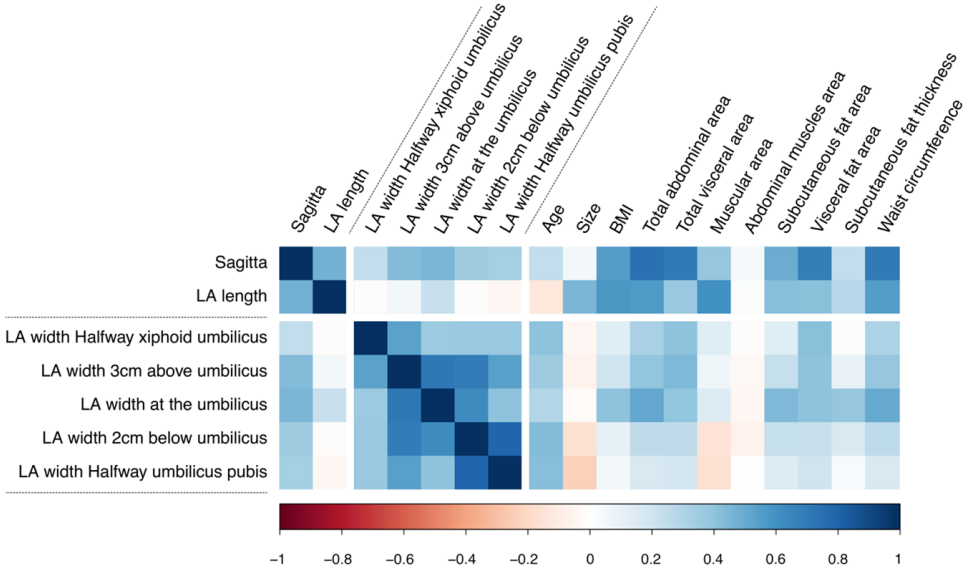

Figure 3.4.: Graphical representation of Pearson's correlation coefficient r between sagittal measurements, axial measurements, and other abdominal measurements. Positive Pearson's correlation coefficient r are shown in shades of blue and negative Pearson's correlation coefficient r in shades of red

3.4. Discussion

The present work has provided a continuous measurement of the width, curvature, and 3D shape of the Linea alba over its entire height. The current study has shown that the maximum width is located at the umbilicus level and that the Linea alba widens and curves forward with age and BMI. Our data have confirmed the previous anatomical descriptions in the axial plane of the Linea alba (Rath, Attali, et al. 1996; Testut et al.

1948; Kaufmann et al. 2022; Liaw et al. 2011; P. Mota et al. 2015) while adding important nuances based on known risk factors for diastasis and hernia surgery.

Until now, *in vivo* sagittal measures of the Linea alba have never been described. Numerous authors have previously ruled on Linea alba width, describing its variability on cranio–caudal axis (Axer et al. 2001b; Rath, Attali, et al. 1996; Testut et al. 1948; Kaufmann et al. 2022; Liaw et al. 2011; P. Mota et al. 2015). We found similar results with a mean Linea alba width of 2.6 cm measured 3 cm above the umbilicus and a mean of 1.7 cm measured 2 cm below the umbilicus. These data were in accordance with the literature, even if the measurement levels were not homogeneous between the authors (Rath, Attali, et al. 1996; Testut et al. 1948; Kaufmann et al. 2022; Liaw et al. 2011; P. Mota et al. 2015). Nevertheless, the Linea alba width at the umbilicus was higher in our study (3.7 ± 1.9 cm) than in the literature. We found a mean maximal width 1.3 cm higher than the mean maximal inter-rectus distance (IRD). This could be explained by the systematic use of IRD in the literature, while we chose to measure the Linea alba. As visible in Figure 3.3, the Linea alba is curved anteriorly by umbilical defect. As a result, the width of the Linea alba is measured on a curved surface, which means that this measurement is systematically greater than the IRD. The IRD is often chosen because this is how the diastasis recti is defined (Hernández-Granados et al. 2021). Most of the literature available on the Linea alba is clinical, aiming to define a cut-off for diastasis recti diagnosis. We chose to specifically focus on the Linea alba's shape, with no consideration for the rectus abdominis muscles.

In our study, the average length of the Linea alba was 37.5 ± 3.6 cm. This was greater than the length described on cadaver. Rath *et al.* found a mean of 29.11 cm on 40 subjects, while Axer *et al.* described 26.2 ± 3.64 cm (Axer et al. 2001b; Rath, Attali, et al. 1996). This observation could be explained by the specificity of the cadaver: the use of often old subjects, the conservation process responsible for shrinkage, and rigidity could bias the measurement of Linea alba. This underlines the need for *in vivo* studies to characterize abdominal wall structures.

In the present study, we introduced the concept of measuring the sagitta in the anatomy of the abdominal wall. Sagitta has never been used to characterize the Linea alba *in vivo*. We found this measurement interesting in assessing the anterior

deformation of Linea alba. Our data suggest that the sagitta is higher in obese and elderly patients. Moreover, it is not influenced by gender. It is well correlated with obesity-related measures such as total abdominal area (r=0.74), total visceral area (r=0.70), visceral fat area (r=0.69), and waist circumference (r=0.71). This could be an indirect indicator of Linea alba dehiscence or intra-abdominal pressure. In 2012, Naraynsingh *et al.* supported the hypothesis of a «Sick Linea Alba Complex» influenced by age, BMI, and parity, resulting in a thin and large Linea alba (Naraynsingh et al. 2012). A measure as easy to obtain as the sagitta could be added to this definition.

A 3D reconstruction of the Linea alba had never been seen in previous anatomical studies. This recent approach based on affordable tools provides a better understanding of real-life *in vivo* anatomy of Linea alba. Reconstruction was based on axial and sagittal delineation before 3D reconstruction. This allowed for better individualization of the Linea alba and the anterior rectus sheaths. Thus, there was no confusion between Linea alba and IRD. This misunderstanding is often found in the literature (Kaufmann et al. 2022; Liaw et al. 2011; P. Mota et al. 2015), even if it has been well illustrated by Beer *et al.*'s dissections and in traditional anatomy treatises that the Linea alba is a structure that can be differentiated from the anterior rectus sheath (Kamina 2014; Beer et al. 2009).

The use of 3D reconstruction and 3D models is becoming increasingly widespread in the field of medical research. Recently, some authors used finite element simulation to simulate wound healing (Karkhaneh Yousefi et al. 2023) or the stability of hernia-damaged abdominal wall (Karrech et al. 2023). These models are not intended to describe patient-specific anatomy and are based on images of a single healthy or cadaveric subject. However, the delineation of the Linea alba is precise, allowing the authors to draw observations based on reliable anatomy.

Our data have suggested a widening of Linea alba with age and BMI, which is in line with the data in the literature (Kaufmann et al. 2022; Jourdan, Soucasse, et al. 2020; Fredon et al. 2021). Gender only influences lower width, with larger Linea alba halfway umbilicus–pubis in women. One explanation could be parity, which is known to be a risk factor for diastasis recti (Śmietański, Śmietańska, et al. 2022; P. Mota et al. 2015). However, these data were not available in the initial cohort, so we cannot conclude

the influence of this parameter on our observations.

Most of the articles available on the Linea alba deal with diastasis recti. According to the European Hernia Society guidelines on the management of diastasis recti, this is defined as an IRD greater than 2 cm. The classification is D1 for an IRD between 2 and 3 cm, D2 for an IRD between 3 and 5 cm, and D3 for an IRD of 5 cm or greater (Hernández-Granados et al. 2021). IRD of 2 cm up to 3 cm at umbilical level is usually accepted to be physiological (Reinpold et al. 2019). Regarding our findings, the definition of diastasis recti should be rethought and based on Linea alba width charts. Current data available on Linea alba width could make it possible to represent normal curves and corridors according to age, BMI, and parity. These tools, analogous to growth curves, could be useful in everyday abdominal wall and plastic surgeries. The need for precision is even greater in the context of an aging population prone to obesity. It seems that the pathophysiology of umbilical hernia and diastasis recti is part of a continuous process of degeneration. The delineation of the Linea alba almost systematically revealed a depression corresponding to the umbilical orifice that seemed to widen with age and increasing BMI. This makes it all the more difficult to set a radiological cut-off for umbilical hernia, corroborating the «Sick Linea Alba Complex» theory of Naraynsingh *et al.* (Naraynsingh et al. 2012). We agree with Kaufmann *et al.*'s conclusions, which called for more population-based studies and a critical re-evaluation of the morphological definition of diastasis recti (Kaufmann et al. 2022).

3.4.1. Limitations

This study has several limitations. Our algorithm, which was designed to measure Linea alba width, was not able to identify it in 16% of all data measured in the cohort. This mainly corresponds to near pubis infraumbilical Linea alba, where it is too thin to allow the software to find two separate points. We chose to use a linear implementation to correct data, but the results near extremities should be taken with caution. The use of CT has sometimes made it difficult to identify the beginning of the Linea alba, particularly in patients with a cartilaginous xiphoid process, which is difficult to identify with this imaging modality. The thickness of the Linea alba could not be assessed in this study. This is mainly due to the resolution of the propagation tool used to create the 3D shapes which fails when used for thicknesses of less than 2

mm. This limitation forced us to use the 2 mm brush tool, which is sometimes greater than the expected thickness of the Linea Alba (Axer et al. 2001b). Finally, the static decubitus position required for the CTs means that we cannot extrapolate these data to the standing position. This last remark argues in favor of carrying out dynamic studies in more physiological positions.

To the best of our knowledge, the present study is the first to deal with an *in vivo* description of the Linea alba from a multiaxial point of view. It provides a new vision of this structure, which is known to be implicated in parietal pathology. Further studies are needed to evaluate the link between sagittal measurements as risk factors for abdominal wall pathologies. The study of the Linea alba from a dynamic and *in vivo* perspective is still not the standard, even though this point has been raised by Rath *et al.* since 1996 (Rath, Attali, et al. 1996). This opens the door to other explorations using dynamic imaging of the abdominal wall in the axial, sagittal, and even possibly frontal planes and 3D reconstruction. We hope that these data will enrich future 3D models to make abdominal wall surgery simulations more reliable.

3.5. Conclusion

The present study has provided an exhaustive 3D description of the anatomical variability of the Linea alba with new considerations for curvature expressed by the sagitta. This method, based on open source affordable software, provided a patient-specific anatomy description of the Linea alba, which could be automated in the future. Further studies are needed to determine whether 3D reconstruction correlates with pathologies, such as hernias and diastasis recti, which could make it a standard in patient management.

Declarations

Conflict of interest

The authors state that they do not have any conflicts of interest.

Ethical approval

The Local Ethics Committee approved this study.

Human and animal rights

This article does not contain any studies with human or animal subjects performed by any of the authors.

Consent to participate

All participants in this study provided informed consent.

Consent for publication

Not required.

4. AI applications in abdominal MRI

The previous chapter 3 on the linea alba study was based on CT scan manual segmentation using CT which, while accurate, is a time-consuming and error-prone process. These limitations underscore the necessity for the incorporation of more automated techniques, such as AI-based tools, which directly supports Objective 4 of this thesis. This chapter 4 serves as a key methodological component, facilitating the automation and enhancement of abdominal wall analysis and enabling a more comprehensive understanding of its biomechanical study. The proposed approaches facilitate the feasibility of large-scale data analysis, thereby offering novel methodologies to compensate for time-consuming and operator-dependent processing issues, as well as data scarcity, which is a particular challenge encountered in clinical trials and *in vivo* studies. This chapter is composed of two parts. The first chapter 4.1 proposes an automated segmentation of abdominal muscles using nnUNet framework. The second chapter 4.2 develops the generation of synthetic MRI data.

4.1. Automatic muscle segmentation on healthy abdominal MRI using nnUNet

This chapter 4.1 is available online (Victoria Joppin, Belton, et al. 2024).

Table of contents

4.1.1 Introduction . . . 151
4.1.2 Material and methods . . . 153
4.1.2.1 Dataset . . . 153
4.1.2.1.1 MRI scans . . . 153
4.1.2.1.2 Ground truth segmentation . . . 153
4.1.2.2 Neural network . . . 154
4.1.2.3 Assessment of segmentation quality . . . 154
4.1.3 Results . . . 155
4.1.4 Discussion and conclusion . . . 155

4.1. Automatic muscle segmentation on healthy abdominal MRI using nnUNet –

Victoria Joppin [1,2], **Niamh Belton** [3,4], **Marc-Adrien Hostin** [5], **Marc-Emmanuel Bellemare** [5], **Aonghus Lawlor** [6], **Kathleen M. Curran** [3], **Thierry Bege** [1,7], **Catherine Masson** [1], **David Bendahan** [2]

[1]Univ Gustave Eiffel, Aix-Marseille Univ, LBA, F-13016 Marseille, France

[2]Aix Marseille Univ, CNRS, CRMBM UMR 7339, Marseille France

[3]School of Medicine, University College Dublin, Dublin, Ireland

[4]Science Foundation Ireland Center for Research Training in Machine Learning

[5]Aix Marseille Université, Université de Toulon, CNRS, LIS UMR 7020, Marseille France

[6]School of Computer Science, University College Dublin, Dublin, Ireland

[7]Aix Marseille Université, Département de Chirurgie, Hôpital Nord, APHM, Marseille, France

Author contributions

MAH and **NB**: brought their expertise in AI and set up the nnUNet model

VJ and **NB**: processed and analysed the segmentation masks generated by nnUNet, assessed the nnUNet segmentation quality

VJ: drafted the article

VJ, **NB**, **MAH**, **MEB**, **AL**,**KC**, **TB**, **CM** and **DB**: did the revision of the article.

Preface

The chapter 4.1 focuses on automating the segmentation of abdominal wall muscles to facilitate the study of their mechanical properties. Manually segmenting muscles from MRI is a time-consuming and labour-intensive task. By using the nnUNet, a state-of-the-art deep learning model, the segmentation process can be automated with high accuracy. This allows for large-scale analysis of dynamic MRI data, enabling the extraction of key biomechanical insights in a much more efficient manner.

Abstract

Understanding the dynamics of the abdominal wall is essential in both physiology and surgery. To study the mechanical functionality of the abdominal wall, segmentation of the abdominal muscles could be useful but is a manual, tedious and time-consuming

process. In this study, we assessed the capability of Deep Learning to automatically segment the abdominal muscles from the axial plane of a unique dynamic abdominal MRI (2D+t) dataset. The 2D slices were acquired while the subject performed various exercises. The State-of-the-Art segmentation model, nnUNet was trained on 5,492 images from fifteen healthy subjects and tested it on 1,801 images from five different subjects. We assessed the segmentation accuracy using dice similarity coefficient (DSC), Hausdorff distance, as well as motion of the abdominal muscles. The ground truth and nnUNet segmentation showed high concordance, with a DSC over 0.87 for all exercises and muscles, and minimal differences in abdominal muscles motion. nnUNet effectively automates abdominal muscle segmentation, offering efficiency and new clinical applications in abdominal physiology.

4.1.1. Introduction

Abdominal wall pathologies represent a clinical challenge, with a significant prevalence of up to 30% recurrence after hernia repair (Romain et al. 2020). Hernias are a common medical condition that involves the protrusion of abdominal contents through a defect in the abdominal wall, specifically at the level of the musculoaponeurotic structure. Understanding and treating this condition requires in-depth analysis and understanding of the abdominal wall anatomy, the mechanical characterisation of tissue and its physiological and pathological response.

Imaging techniques, including shear-wave elastography, ultrasound, CT scans, and MRI provide valuable pre or post-operative information such as hernia detection which is sometimes challenging (Jaffe et al. 2005; Baucom et al. 2014; Bellio et al. 2019; Read et al. 2022), detection of early sign of recurrence such as a large distance between rectus abdominis (J. J. Harlaar et al. 2017; F. Wang et al. 2023), fluid collection (Loftus et al. 2017) or mesh fixation (Fischer et al. 2007; Ciritsis et al. 2014). Other information about the abdominal wall mechanical properties (Tran, Podwojewski, et al. 2016), muscle denervation or atrophy (Rodriguez-Acevedo et al. 2020), abdominal adhesion (Randall et al. 2017) or abdominal wall ability to move and deform (Vlot et al. 2013; Blanchard et al. 2016; Jourdan, Rapacchi, et al. 2022) help having a better understanding of these conditions.

These approaches often need precise segmentation of structures, as they allow for in-depth analysis of the anatomy, physiological and pathological response of the abdominal wall. In the field of medical image processing, various techniques automatic or semi-automatic, including thresholding, geometric models, multi-atlas segmentation (Karlsson et al. 2015) have been deployed to segment images which are mainly MRI and CT for good soft tissue contrast (A. C. Ogier et al. 2021; Lenchik et al. 2019). However, with the advent of neural networks, in particular Convolutional Neural Networks (CNN), a new era of automatic segmentation methods has emerged covering different regions of the body and various anatomical structures. CNNs have demonstrated their effectiveness on a variety of medical images, such as CT scans for fat, organs and muscles segmentation (Weston et al. 2019; Park et al. 2020), MRIs for adipose tissue assessment (Kway et al. 2021) and ultrasounds rectus muscles segmentation (F. Wang et al. 2023).

Among neural network architectures, nnUNet has stood out as a reference of choice for biomedical image segmentation (Isensee et al. 2021), demonstrating exceptional performance in various clinical contexts (Ferrante et al. 2022; Verdier et al. 2024). However, despite significant progress in the field, few articles' studies have used highly automated analysis methods (Borga 2018). At present, researchers manually segment abdominal muscle to quantify their mechanical functionality. Given that over 300 slices is acquired per subject, this is a tedious and costly process.

To our knowledge, no study has explored the automatic segmentation of abdominal muscles from MRI images. This gap in the literature motivates our study, in which we propose the innovative application of the nnUNet neural network for abdominal muscle segmentation. Our approach is based on the use of dynamic abdominal MRI scans acquired from healthy subjects performing different exercises with and without muscle contraction, thus providing a detailed understanding of abdominal muscle dynamics under a variety of conditions.

4.1.2. Material and methods

4.1.2.1. Dataset

4.1.2.1.1. MRI scans

Twenty healthy participants (8 women) volunteered to take part to the study after providing their informed written consent. The average age and BMI were 29.3 ± 8.1 years old and 22.6 ± 2.5 kg/m^2 respectively.
This study was approved by the French ethics committee (IDRCB : 2019-A00806–51) and was conducted according to national legislation related to interventional research and the declaration of Helsinki.
Participants were positioned supine in the MRI scanner (MAGNETOM Verio, Siemens Healthineers) and the radiofrequency coils used were those integrated in the bed scanner and a flexible body coil positioned on the abdomen. Dynamic MRI was performed as previously described (Jourdan, Rapacchi, et al. 2022) so as to capture axial 2D changes every 182 ms while performing consecutively three audio-guided exercises after training by an examinator. Breathing (inhale-exhale deeply during 10s), coughing and Valsalva maneuver (forceful expiration against closed nostrils and mouth during 8s) were chosen as representative of daily activities and also commonly used by the surgeons as part of the clinical exam (Jaffe et al. 2005). The dataset is thus composed of 60 dynamic MRI volumes (1 volume per exercise per participant), of 2D slices of the abdominal region at L3-L4 disc level over time.

4.1.2.1.2. Ground truth segmentation

This set of 7,293 axial images (Figure 4.1.1-a) was segmented with four distinct labels corresponding to left and right rectus abdominis (RA) and lateral muscles (LM, including transversus abdominis, internal and external obliques) as represented in Figure 4.1.1-b. A dedicated algorithm (A. Ogier et al. 2017) was used allowing a semi-automatic transversal propagation of a limited amount of manually-drawn masks (8% of total images). This segmentation technique has already been validated (Jourdan, Le Troter, et al. 2021), and the resulting masks serve as the ground truth for evaluating the quality of the segmentation performed by the nnUNet network.

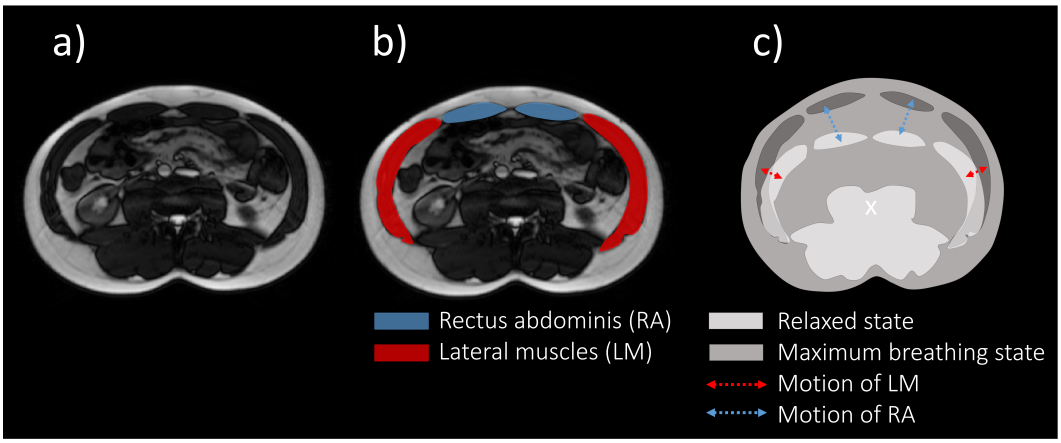

Figure 4.1.1.: 2D axial abdominal MRI
Legend : **a)** Without annotation **b)** Segmentation mask of the rectus abdominis (RA) and lateral muscles (LM) **c)** Motion quantification of the muscles

4.1.2.2. Neural network

nnUNet (*MIC-DKFZ/nnUNet* 2024) (V2) for deep learning segmentation with automatic learning hyperparameter selection was used. Parameters such as batch size and network depth were determined based on GPU size and input image size. Additional parameters were selected through 5-fold cross-validation (Isensee et al. 2021). Traditional data augmentation methods were applied, excluding horizontal flip as this caused issues due to the symmetrical nature of the abdominal muscles. The data was decomposed into 416×416 frames, resampled to 256×256, and randomly split into a 15-subject training set (5,492 images) and a 5-subject test set (1,801 images). Training was conducted with PyTorch 1.2 on an NVIDIA GeForce RTX 2080 Ti GPU, with a training time of approximately 55 hours per fold.

4.1.2.3. Assessment of segmentation quality

To evaluate nnUNet's ability to segment abdominal wall muscles, dice similarity coefficient (DSC) (Zou et al. 2004) and Hausdorff distance (Beauchemin et al. 1998) were calculated between the ground truth masks and the nnUNet segmented masks. Additionally, biomechanical metric such as radial displacement of LM and RA muscles were computed from both ground truth and nnUNet masks, as previously described (Jourdan, Rapacchi, et al. 2022) and shown in Figure 4.1.1-c.

4.1.3. Results

Figure 4.1.2 shows the DSC and Hausdorff distance of each label. The nnUNet performs better on the LM muscles than the RA muscles, likely due to the increased motion of the RA muscles during the exercises. The DSC is quite similar throughout the different exercises. The Hausdorff distance is higher for LM, this muscle being bigger than RA.
The difference of motion between the ground truth and nnUNet masks is lower than 0.8 mm for both LM and RA, for the three exercises.

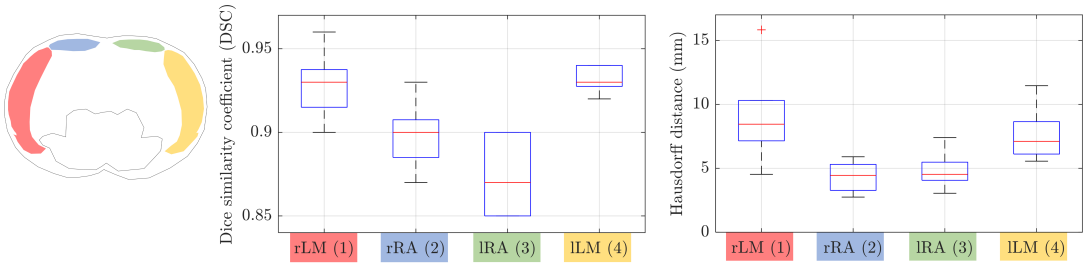

Figure 4.1.2.: Dice similarity coefficient (DSC) and Hausdorff distance results depending on the label

4.1.4. Discussion and conclusion

In conclusion, this study demonstrates the effectiveness of nnUNet in segmenting dynamic axial MRI images of healthy subjects, which could significantly reduce researchers' manual workload and accelerates research progress. Moving forward, enhancing the network's performance will involve diversifying the training set with additional axial planes, thereby reducing dependence on body location. Increasing the number of subjects will add anatomical variability, while incorporating more exercises will capture greater dynamics and motion, ultimately enhancing the network's robustness and applicability. It's worth noting that this study represents ongoing work, with the ultimate goal of applying these advancements to segment patients' images. The MRI dataset presented in this study will be made available upon request on a public repository.

4.2. Dynamic MRI generation for abdominal wall analysis

This chapter 4.2 is available online (Belton et al. 2024). In order to provide further context, the preface of this section aims to contextualize this study, and enhance the understanding of the method used.

Table of contents

4.2.1 Introduction 158
4.2.2 Methods 159
4.2.3 Results 160
4.2.4 Discussion 162
4.2.5 Conclusion 163

Niamh Belton [1,2], **Victoria Joppin** [3,4], **Aonghus Lawlor** [3,6], **Kathleen M. Curran** [1,2], **Catherine Masson** [4], **Thierry Bege** [4,7], **David Bendahan** [5]

[1]Science Foundation Ireland Center for Research Training in Machine Learning

[2]School of Medicine, University College Dublin, Dublin, Ireland

[3]School of Computer Science, University College Dublin, Dublin, Ireland

[4]Univ Gustave Eiffel, Aix-Marseille Univ, LBA, F-13016 Marseille, France

[5]Aix Marseille Univ, CNRS, CRMBM UMR 7339, Marseille France

[6]Insight Centre for Data Analytics, University College Dublin, Dublin, Ireland

[7]Aix Marseille Université, Département de Chirurgie, Hôpital Nord, APHM, Marseille, France

Author contributions

NB: Conceptualisation, Investigation, Data curation, Writing - original draft

VJ: Conceptualisation, Data curation, Writing - review & editing

AL,**KC**, **CM**, **TB** and **DB**: Conceptualisation, Writing - review & editing

Preface

The second part of this chapter explores the use of a Denoising Diffusion Probabilistic Model (DDPM) to generate synthetic MRI data. This synthetic data generation is highly pertinent to improving model training, especially when real patient data is limited. The ability to synthesise realistic MRI volumes based on existing anatomical structures enhances the training and validation of AI models like nnUNet, while also enabling new insights into abdominal wall biomechanics without the need for exhaustive patient datasets. Moreover, this tool has potential applications in simulating different clinical scenarios, contributing to a better understanding of both healthy and pathological conditions.

Abstract

An abdominal hernia is a protrusion of intestine or tissue in the abdominal wall and is known to cause debilitating pain. The recurrence rate of abdominal hernia varies from 30% to 80%, meaning it is paramount to improve our understanding of the mechanical functionality and physiology of the abdominal wall. This work

proposes DyABD, a dataset of dynamic abdominal MRIs (2D+t) of hernia patients and a 3D dual class and anatomically conditioned Denoising Diffusion Probabilistic Model (DDPM) that can perform the unique task of synthesising hernia patients performing any of three exercises, breathing, coughing or a Valsalva maneuver, whilst also taking into account whether the patient is pre or post corrective abdominal surgery. DyABD requires a subject prior as input which consists of the first 2D slice of the dynamic MRI sequence and the associated abdominal muscle masks of the first 2D slice which ensures anatomical correctness is preserved during synthesis. This work is based on 121 dynamic MRI volumes which will be made available for sharing as part of the complete dataset of approximately 300 volumes. The preliminary results of DyABD demonstrate its ability to model the mechanical functionality of the abdominal wall. Examples of generated volumes are made available at https://github.com/niamhbelton/DyABD/.

4.2.1. Introduction

An abdominal hernia is a protrusion of viscera through a rupture between muscles in the abdominal wall (Stedman 1920) and is known to cause debilitating discomfort. The recurrence rate of abdominal hernia post corrective surgery varies from 30% to 80% (Bhardwaj et al. 2024), meaning it is paramount to improve our understanding of the mechanical functionality and physiology of the abdominal wall. Dynamic MRI has recently been shown to be effective in quantifying abdominal wall motion and deformation during various exercises such as breathing and muscular contraction (Jourdan, Rapacchi, et al. 2022; Miyamoto et al. 2002). Therefore, this work has acquired a unique dynamic abdominal MRI dataset, named DyABD that contains patients with abdominal hernias performing various exercises pre and post corrective surgery. However, data scarcity, missing data and other issues relating to ability of the patient to perform the exercises remain a challenge to progressing the field.

This work proposes DyABD, a dataset of dynamic abdominal MRIs of hernia patients and a 3D dual class and anatomically conditioned Denoising Diffusion Probabilistic Model (DDPM). This technique is designed to synthesise dynamic abdominal MRI sequences for patients with pathologic abdominal wall, both with hernia before surgery and repair abdominal wall after surgery. The goal of the research is to model and simulate the mechanical functionality of the abdominal wall during different exer-

cises, such as breathing, coughing, and Valsalva maneuver, at both pre-operative and post-operative stages. It requires a subject prior as input which consists of the first 2D axial slice of the dynamic MRI sequence and the associated abdominal muscle masks which ensures anatomical correctness is preserved during synthesis. This means the muscles and organs in the images align with how they really look and move in real patients. The research proposes a new computer model that can generate realistic, synthetic MRIs of patients even if they have not been physically scanned. This work can help better understand the abdominal wall's behaviour under various conditions and assist clinicians in improving surgical planning and patient outcomes.

4.2.2. Methods

Dataset: The dataset consists of 121 dynamic MRI volumes (2D+t), where each volume consists of a 2D axial slice acquired at the same position over time whilst performing three exercises, coughing, breathing and Valsalva maneuver from eight patients with abdominal hernias pre-corrective surgery and from three of the eight patients post-corrective surgery. The abdominal muscle masks for the first slice of the sequence were annotated manually.

Figure 4.2.1 outlines the DyABD architecture. A training dataset $X_{train} \in \mathbb{R}^{h \times w \times s}$ consists of volumes where h and w are the height and width of a 2D slice and s is the number of slices in the time sequence. The dynamic volumes are resized so that $h = 128$, $w = 128$ and $s = 128$.

This study combines deep learning, which is a type of artificial intelligence (AI), and MRI data. The core AI model used in this work is called a Denoising Diffusion Probabilistic Model (DDPM) (Ho et al. 2020) that synthesises new MRI sequences by learning from real dynamic MRI data. The process behind DDPMs can be broken down into two steps: a forward and reverse diffusion processes. The **forward diffusion process**, noted q, is the step where a small amount of Gaussian noise; $\epsilon \sim \mathcal{N}(0, 1)$; is gradually added to the input MRI volume $x \in X_{train}$ over several steps T, making it progressively blurrier or more distorted.

The **reverse diffusion process**, noted p, is the step where a U-Net (Ronneberger et al. 2015), denoted as ϵ_θ, learns how to reverse the process by predicting the noise added at each step and gradually recovering the original, clean image, at each timestep t. During training, the model learns to recover the original image. This process

essentially teaches the model how to generate images from noise. The **UNet** is the backbone neural network architecture used to carry out the reverse diffusion process. UNets are widely used in medical imaging due to their ability to capture both local and global information from images. This is particularly important in MRI generation, as the model needs to preserve both the detailed structure of the abdominal muscles and the overall anatomical correctness. The key feature of UNets is their encoder-decoder structure, which captures context through downsampling (making the image smaller) and then reconstructs the image through upsampling (making it bigger again). In this study, the UNet is enhanced to be 3D, meaning it processes 3D MRI volumes instead of flat 2D images, which is essential for capturing the dynamic nature of the abdominal wall's motion.

In order to model the sequential nature of the data, the U-Net from the original DDPM (Ho et al. 2020) implementation is modified to have a 3D U-Net architecture (Dorjsembe, Odonchimed, et al. 2022). A recent work, Med-DDPM (Dorjsembe, Pao, et al. 2024) demonstrated how concatenating a conditional image with the MRI volume, x at timestep t, improves 3D image synthesis. This work therefore, concatenates the subject prior, sub with the MRI volume, x_t at each timestep t to ensure anatomical accuracy. The subject prior, $sub \in \mathbb{R}^{c \times h \times w}$ for each $x \in X_{train}$ has five channels, c, where a channel exists for the first slice in the sequence and the associated masks for each of the four abdominal muscles. The subject prior, sub is stacked s times along the time axis before concatenation, meaning the input to the U-Net at timestep t is of shape $(c+1) \times h \times w \times s$, denoted as x'_t.

The dual class conditioning aspect of the model enables it to generate MRI sequences based on two factors: the exercise type and whether the patient is pre- or post-surgery. Two label embedding layers for the class of exercise, l_e and operative stage, l_o are used to class condition the model. They are added to the time embedding layers of the U-Net. The training minimises the L1 loss between the predicted noise and the actual noise, $||\epsilon - \epsilon_\theta(x_t, t, l_e, l_o)||$ across all timesteps. The model is trained with $T = 250$ (as per (Dorjsembe, Pao, et al. 2024) implementation) for 50,000 steps.

4.2.3. Results

The model was trained using four fold cross validation, where each training fold had an average of 91 volumes and each test fold had an average of 30 volumes. Table 4.2.1

presents the results averaged over four test folds. The Structural Similarity Index Measure (SSIM) and Mean Squared Error (MSE) was calculated between the generated volumes and the ground truth volumes. Examples of the generated volumes are available at https://github.com/niamhbelton/DyABD/. DyABD shows promising initial results that demonstrates its ability to model the mechanical functionality of the abdomen performing each of the exercises. Future work will focus on improving the resolution.

Table 4.2.1.: Results of four fold cross validation in terms of SSIM and MSE and one standard deviation with and without conditioning on the abdominal muscle mask (w/o mask).

	Cough		Breathe		Valsalva Maneuver		Overall	
Method	**SSIM ↑**	**MSE ↓**	**SSIM ↑**	**MSE ↓**	**SSIM ↑**	**MSE ↓**	**SSIM ↑**	**MSE ↓**
DyABD	$\mathbf{0.84 \pm 0.0}$	$\mathbf{0.003 \pm 0.0}$	$\mathbf{0.71 \pm 0.1}$	$\mathbf{0.005 \pm 0.0}$	$\mathbf{0.78 \pm 0.1}$	$\mathbf{0.004 \pm 0.0}$	$\mathbf{0.78 \pm 0.1}$	$\mathbf{0.004 \pm 0.0}$
w/o mask	0.75 ± 0.2	0.004 ± 0.0	0.58 ± 0.3	0.010 ± 0.0	0.72 ± 0.1	0.005 ± 0.0	0.69 ± 0.2	0.006 ± 0.0

The figure Figure 4.2.1 shows the forward and reverse diffusion process of DyABD. In the reverse diffusion process, the U-Net model, ϵ_θ, takes x'_t as input which is the concatenation of the MRI volume x_t with the subject prior, sub. ϵ_θ is conditioned on the timestep, t and the class conditions, exercise, (l_e) and operative stage (l_o).

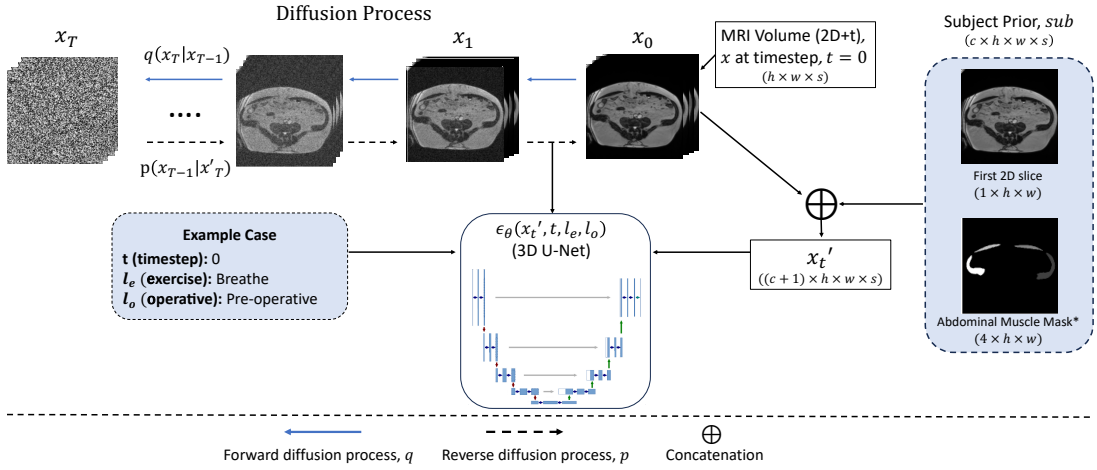

Figure 4.2.1.: Forward and reverse diffusion process of DyABD*
The mask of all four abdominal muscles are shown on one image for visualisation purposes

4.2.4. Discussion

The denoising task and image synthesis might seem like different processes, but in the context of DDPMs, they are closely related. Once the model is trained to reverse the noise-adding process, it can be used not just to denoise, but to generate entirely new images. Starting with random noise, the model can predict how an MRI should look, even if that MRI is not real. In essence, it learns the structure and patterns of MRI data and can then create similar, anatomically plausible MRI sequences by reversing the diffusion (noise addition) process.

Once trained, this model can take an input MRI slice from a patient, and generate a full sequence of images showing how the abdominal muscles would move, based on the exercise performed (e.g., breathing, coughing, Valsalva) and whether the patient has had surgery. The synthesised data helps in visualising and understanding the mechanical functionality of the abdominal wall, which could help in improving hernia treatments and surgical outcomes. To summarise, this model can generate new MRIs starting from noise, and can also generate new variations of existing patients' MRI sequences using the subject prior as a guide (e.g., simulating a new exercise for the same patient).

Although anatomically guided diffusion models exist (Konz et al. 2024), there is a lack of models that do not require anatomical guidance for the complete volume, whilst also being class conditional and capable of modelling the sequential nature of dataset, highlighting the uniqueness of DyABD's problem set-up. To provide context to the results, we also report the performance of DyABD without conditioning on the abdominal muscle mask. The results demonstrate the importance of providing anatomical context to the model.

Strengths of this study include its use of a rare dynamic MRI dataset and its ability to model real-time anatomical behaviour of the abdominal wall. It is particularly relevant for investigating hernias and the impacts of various exercises on patients pre- and post-surgery. The use of muscle masks ensures the anatomical correctness of the generated images, making it highly valuable in medical imaging research.

However, the study also has limitations. The relatively small dataset may restrict (121 MRI volumes from 8 patients pre-surgery and 3 post-surgery) the model's ability to generalise to broader populations. The model's reliance on subject priors limits its potential for fully synthetic, general-purpose applications. Moreover, the computational

demands of the diffusion process can be intensive, which might limit its practical scalability in clinical settings. The synthesised MRIs may look anatomically correct, but their clinical utility (e.g., using these images to make diagnostic or treatment decisions) would require validation through experiments with healthcare professionals. In other words, looking real does not always mean medically useful.

4.2.5. Conclusion

This work has outlined DyABD, a unique dynamic abdominal MRI dataset and technique for the novel task of synthesising hernia patients performing various exercises given a subject prior. Future work will include a qualitative study with clinicians to assess the synthesised volumes in terms of anatomical accuracy and the correctness of the functionality of the abdominal wall muscles for each exercise performed for both pre and post operative patients. The Github repository will be updated when the dataset is available for sharing.

5. Assessing the effects of hernia repair on abdominal wall biomechanics using dynamic MRI

Table of contents

5.1. Introduction . . . 167
5.2. Methods . . . 169
5.2.1. Participants . . . 169
5.2.2. MRI protocol . . . 169
5.2.3. Data processing . . . 170
5.2.3.1. Axial MRI . . . 171
5.2.3.2. Sagittal MRI . . . 174
5.2.3.3. Statistical analysis . . . 176
5.3. Results . . . 177
5.3.1. Cohort description . . . 177
5.3.2. MRI parameters . . . 179
5.3.3. Principal component analysis . . . 180
5.3.4. Axial displacement of lateral muscles and rectus abdominis . . . 181
5.3.5. Shape of lateral muscles and rectus abdominis . . . 184
5.3.6. Sagittal displacement of linea alba . . . 186
5.3.7. Inter-recti distance and hernia defect angle . . . 187
5.3.8. Hernia sac and ratio . . . 189
5.3.9. Visceral area . . . 190
5.3.10. Total abdomen area . . . 190
5.4. Discussion . . . 191
5.5. Conclusion . . . 195

5.6. Appendix 196
5.6.1. Segmentation of MRI 196
5.6.2. Registration of axial MRI 196
5.6.3. Registration of sagittal MRI 197
5.6.4. Influence of sex assigned at birth 198
5.6.5. Principal component analysis 198

Victoria Joppin [1,2], **David Bendahan** [2], **Catherine Masson** [1], **Thierry Bege** [1,3]

[1]Univ Gustave Eiffel, Aix-Marseille Univ, LBA, F-13016 Marseille, France

[2]Aix Marseille Univ, CNRS, CRMBM UMR 7339, Marseille France

[3]Aix Marseille Université, Département de Chirurgie, Hôpital Nord, APHM, Marseille, France

Preface

In light of the knowledge and tools developed in the preceding chapters of this doctoral project, the logical subsequent step is to apply these tools to pathological conditions by investigating the impact of surgery on these parameters in patients. This chapter 5 addresses the Objective 5, providing a more comprehensive view of how surgical intervention affects abdominal wall anatomy and function.

Abstract

Background: While the success of hernia repair surgery can still be improved and is typically measured by recurrence rates and comorbidities, there is a lack of objective evaluations of the functional and biomechanical outcomes of the abdominal wall pre and post-surgery. Although some studies have explored *in vivo* abdominal wall function using electromyography and dynamometers, there is limited literature on the use of magnetic resonance imaging (MRI) for this purpose.

Methods: This study enrolled 11 patients undergoing abdominal wall hernia repair surgery. Dynamic MRI was utilised to capture both axial and sagittal planes (2D+t) as patients performed various exercises within the MRI scanner. Segmentation of the abdominal muscles and linea alba, viscera and hernia sac was performed to analyse the muscles and linea alba displacement, shape, and function of the abdominal wall pre- and post-surgery.

Findings: Significant changes in muscle displacement and shapes were observed following hernia repair. Post-surgical evaluations revealed a lengthening of all abdominal muscles, accompanied by a higher inward displacement of lateral muscles during the Valsalva maneuver, an enhanced rectus abdominis displacement during coughing, and the increased displacement of linea alba suggest an overall improved functionality.

These results highlight the importance of considering dynamic muscle behaviour in surgical outcomes.

Interpretation: Our findings suggest that dynamic MRI is a valuable tool for assessing the biomechanical impact of hernia surgery, offering a more comprehensive evaluation of surgical success beyond traditional metrics. This approach provides a deeper understanding of the functional recovery of the abdominal wall and could enhance clinical decision-making and postoperative care.

5.1. Introduction

Abdominal wall hernias, characterised by the protrusion of abdominal contents through a weakened abdominal wall, are prevalent and associated with significant health and economic burdens (Bhardwaj et al. 2024; Schlosser et al. 2023). If not properly managed, they can lead to severe complications, making surgical intervention crucial (Gillies et al. 2023).

Hernia surgery success is traditionally measured by recurrence rates and comorbidities. While health-related quality of life significantly gain interest and has been shown to improves following ventral incisional hernia repair (Mussack et al. 2006; O. A. Smith et al. 2022), there has been insufficient focus on the objective evaluation of abdominal wall function before and after hernia surgery (Jensen et al. 2014).

Previous studies have explored the impact of hernia on muscle functionality using methods such as surface electromyography, revealing significantly reduced abdominal muscle strength in patients with incisional hernia compared to healthy (Roy et al. 2023). Various studies using isokinetic dynamometer (Strigård et al. 2016; García Moriana et al. 2023) and strain gauge (Sánchez Arteaga et al. 2024) showed a negative correlation between abdominal wall muscle strength and hernia defect width.

Criss *et al.* showed that hernia repair with linea alba restoration improved abdominal wall functionality through isokinetic and isometric measurements of the rectus muscle (Criss et al. 2014). Preoperative core training was found to significantly enhance muscle strength after ventral hernia repair (Ahmed et al. 2018). However, while these studies provide valuable insights, they are often limited by their reliance on static,

strength-based measurements rather than evaluations of abdominal wall behaviour during physiological activities.

Computed tomography (CT) is the most common imaging modality for hernia detection (Muysoms, S. A. Antoniou, et al. 2015) and post-operative follow-up (Gutiérrez de la Peña et al. 2001; Gossios et al. 2003). Changes in abdominal wall morphometry induced by hernia surgery were investigated on CT scans (Lisiecki et al. 2015), showing a decrease of the cross-sectional anterior-posterior distance, area and circumference of the abdomen after the surgery. However, different studies showed that CT scan was not associated with reliable diagnosing in ventral hernia recurrence (Holihan et al. 2016), and CT reports often fail to include important pre-operative hernia feature (Kushner et al. 2021). Moreover, CT is a radiating tool offering static views that fail to capture the dynamic nature of hernias during physiological activities like breathing and coughing. It has been demonstrated that a more functional-based preoperative CT imaging of the abdominal wall can markedly enhance the comprehension of ventral hernia defects, thereby facilitating the development of efficient surgical plans that result in minimal recurrence rates and optimal functional outcomes (Read et al. 2022). Dynamic magnetic resonance imaging (MRI), also called cine-MRI, represents a significant advancement in this field. It provides real-time insights into the movement and interaction of abdominal structures (Randall et al. 2017) and has multiple applications, such as the quantification of cross-sectional abdominal wall motion (Jourdan, Rapacchi, et al. 2022), abdominal adhesions (Yasemin et al. 2020), studying the effect of wearing an abdominal binder during contraction (Miyamoto et al. 2002), study of chronic groin pain in inguinal hernias (Dallaudiere et al. 2024), visualise the implanted mesh (Fischer et al. 2007; Ciritsis et al. 2014) etc.

This study aims to fill the gap in the objective, functional evaluation of the abdominal wall by investigating the anatomical and biomechanical changes in hernia patients before and after surgery. Using dynamic MRI during various exercises, this study provides a real-time, *in vivo* assessment of abdominal wall function, offering a more detailed understanding of post-surgical outcomes.

5.2. Methods

5.2.1. Participants

Eleven participants (6 females) volunteered to take part in the study after providing their informed written consent. This study was approved by the French ethics committee (IDRCB: 2021-A02119-32) and was conducted according to national legislation related to interventional research and the Declaration of Helsinki.

The participants must meet the following inclusion criteria: being of legal age, have abdominal wall pathology (primary or incisional hernias) requiring laparotomy surgery at the time of the study, having a hernia defect of 10 cm maximum, having a social security coverage. Exclusion criteria include pregnant or breast-feeding women, people under guardianship, people requiring emergency hernia/ventricular surgery, people with an active digestive pathology other than hernia, the usual contraindications for an MRI examination (claustrophobia, magnetized foreign bodies). A person will be withdrawn from the study if no longer meets the inclusion criteria or withdraws consent.

Participants had a pre-operative MRI and then get a hernia surgery at APHM (Assistance Publique des Hôpitaux de Marseille) Hospital, Marseille, France. Once their state of healing and pain allowed it, participants underwent post-operative MRI. The hernias were classified according the EHS classification (Muysoms, Miserez, et al. 2009).

5.2.2. MRI protocol

The participants were positioned in a supine position within the 3-Tesla MRI scanner (MAGNETOM Verio, Siemens Healthineers, Erlangen, Germany). The radiofrequency coils utilised were those integrated within the bed scanner and a flexible body coil placed on the abdomen, which was not attached to the bed. This was done to ensure that the anteroposterior movement of the abdomen was not restricted.

First, three-dimensional volumes with T2 haste and T1 vibe contrasts, respectively, were performed during apnea after inhalation (from the pubis to the xiphoid process). Subsequently, dynamic acquisitions were conducted in both the axial and consecutive sagittal planes, with the participant performing three audio-guided exercises. Each exercise was performed several times by the participant who had been trained before

the MRI, in order to obtain various repetitions of the exercise execution. These were activities that could be done in everyday life: deep breathing for 10 seconds, coughing, and performing the Valsalva maneuver, which involves forcing air out against closed mouth and nostrils for 8 seconds. In the pre-operative MRI, dynamic axial acquisitions were performed over the cross-sectional plane where the hernia neck was the largest, as identified from the 3D volumes. The sagittal plane was selected to be situated at the midpoint of the hernia neck, as illustrated in Figure 5.1. In the case of the post-operative MRI, the axial and sagittal planes were selected with the intention of maintaining as much similarity as possible to those chosen for the pre-operative MRI.

The MRI acquisition parameters, including field of view (window size) and temporal resolution (timestep between two images), were tailored to the individual participant based on their body size.

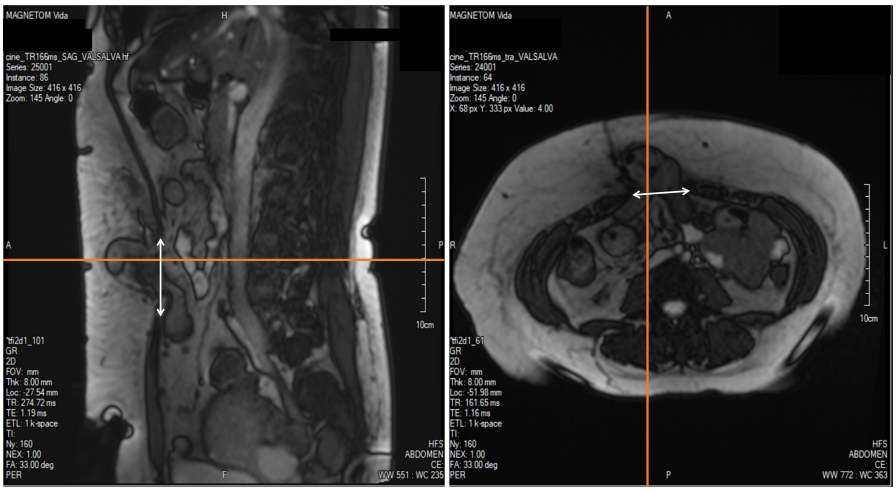

Figure 5.1.: Selection of sagittal and axial planes for dynamic acquisitions. Example of a pre-operative MRI. The white arrows represent the hernia defect measurements at the resting state, respectively the height on sagittal MRI, and width on axial MRI

5.2.3. Data processing

To improve understanding of how hernia surgery affects abdominal wall functionality during different exercises, this paper proposes an investigation of abdominal wall anatomy and motion before and after hernia surgery, with various metrics and anatomical areas explored. To do so, the MRI scans were initially converted from DICOM to Nifti format using the dcm2niix software (Li et al. 2016). The selection of images of interest was conducted by an operator, who identified the first image

that exhibited no abdominal wall contraction, which was defined as the resting state. Subsequently, both objective assessments; based on DICE and mutual information from the Python medical image processing library (*MedPy* 2024); and subjective visual assessment by the same operator were done to truncate the MRI sequence to be at resting state at the end as well.

5.2.3.1. Axial MRI

Each patient (n=11) had dynamic axial acquisition during which they performed audio-guided breathing, coughing and Valsalva maneuver. The hernia defect width was measured at the resting state (Figure 5.1). The rectus abdominis (RA) and lateral muscles (LM) as shown in Figure 5.2-b, which include the transversus abdominis, internal obliques, and external obliques, were delineated in the MR images using FSLeyes, the image viewer included in the FSL toolbox, and a semi-automatic segmentation method as previously described by Ogier *et al.* (A. Ogier et al. 2017). Appendix 5.6.1 details the percentage of manually segmented slices for both pre and post-operative MRI required to obtain anatomically accurate masks using the semi-automatic propagation method (A. Ogier et al. 2017).

It should be noted that the deep learning based segmentation method described in chapter 4.1 was not used in this chapter. In fact, the masks obtained with this network on the patients' MRI scans were of poor quality. This could be due to the fact that the network was trained exclusively on MRI scans of healthy subjects, whose anatomy was quite different (high BMI, presence of a hernia, fatty infiltration between the different lateral muscles, location of the axial plane fixed by the position of the hernia versus always at the L3/L4 disc level for the healthy subjects' MRI). Therefore, the segmentations obtained here could serve as ground truth for later re-training of the networks to segment pathological abdominal MRIs.

Additionally, the visceral area as shown in Figure 5.2-c was defined as the region enclosed by the internal surface of the abdominal muscles and the dorsal area, which includes the quadratus lumborum, psoas major, erector spinae muscles, vertebral discs and body, as previously described (Victoria Joppin, Jourdan, et al. 2025). The total cross-sectional area of the abdomen was also segmented, delimited by the external surface of the abdomen, thereby enabling the computation of the waist circumference (in millimeters). The muscle mass ratio (in %) was also computed, as previously defined as the ratio between the area occupied by abdominal muscles and the total

area of the abdomen (Jourdan, Rapacchi, et al. 2022). Both waist circumference and muscle mass ratio were assessed at the resting state. All the segmented masks were post-processed using Python codes.

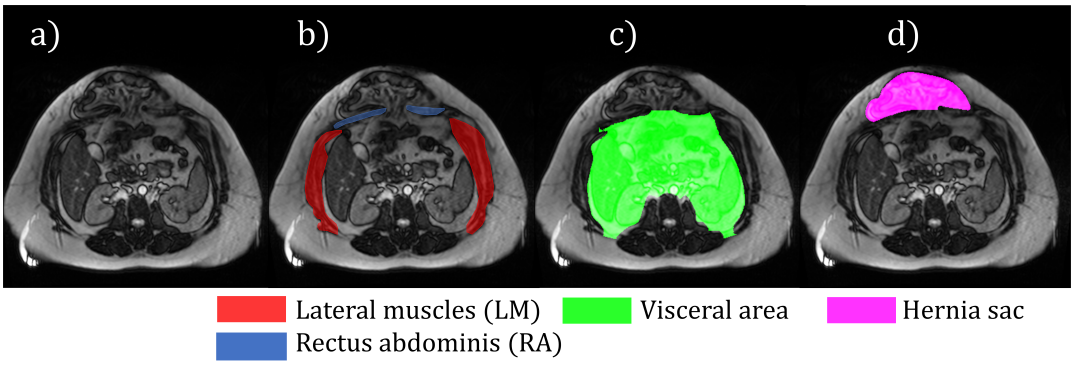

Figure 5.2.: Segmentation masks of axial MRI. **Legend** : **a)** Raw MRI **b)** Abdominal muscles : lateral muscles (LM) and rectus abdominis (RA) **c)** Visceral area **d)** Hernia sac (for pre-operative patients)

In the case of pre-operative MRI, the hernia sac was segmented whenever feasible, as illustrated Figure 5.2-d. The cross-sectional ratio between hernia sac area and total area was computed for each patient, similarly to the ratio between the incisional hernia volume over the peritoneal volume, also known as IHV/PV ratio, already described in 3D by Sabbagh *et al.* (Sabbagh et al. 2011). Additionally, the hernia sac area variation with respect to its resting state area, i.e. $area - area_0/area_0$ was computed, expressed in percentage (%).

The distance between the two inner tips of the rectus abdominis muscles was measured and defined as the inter-recti distance, also called RAM distance. Additionally, the abdominal aorta was segmented, and the hernia defect angle (in °), defined as the angle between the inter-recti distance and the aorta barycenter. The hernia defect angle reflects both the anatomical separation of the rectus muscles (how wide apart they are) and their positional relationship to the central axis of the body, represented by the aorta.

As illustrated in Figure 5.3 for the Valsalva exercise, the radial displacement was calculated for each pixel within the segmented abdominal wall muscles in accordance with the registration methodology proposed by Jourdan *et al.* (Jourdan, Rapacchi, et al.

2022). Some registration parameters have been adapted to this study, as mentioned in Appendix 5.6.2. The displacement of all pixels was then averaged across the LM and RA muscles. This displacement is subject to change at each time point.

As a separate measurements, the radial distance is defined as the distance between the barycenter of each muscle group (calculated by averaging the location of all pixels in the segmentation masks of the considered muscle group, i.e. LM and RA respectively) and the abdominal barycenter (averaged from the pixels composing the left and right LM segmentation masks). This measurement is done at the resting state, provides insight into the depth and width (along the left-right body axis) of the abdomen.

As previously introduced by Jourdan *et al.* on healthy subject abdominal wall MRI (Jourdan, Rapacchi, et al. 2022), circumferential and radial strains respectively noted ε_θ and ε_r are computed for both LM and RA muscles. These variables are defined respectively for the considered group (LM or RA) as the medial axis length and thickness variation with respect to its resting state value, i.e. $length - length_0/length_0$ for ε_θ, and $thickness - thickness_0/thickness_0$ for ε_r, expressed in percentage (%). The total muscular strap length was assessed, by summing the length of all abdominal muscles.
The different repetitions, each exercise performed multiple times by each participant, were then averaged using Matlab R2024a software, in order to obtain a representative average cycle of each exercise for each patient for the two abdominal wall condition before and after the surgery, as previously described (Victoria Joppin, Jourdan, et al. 2025).

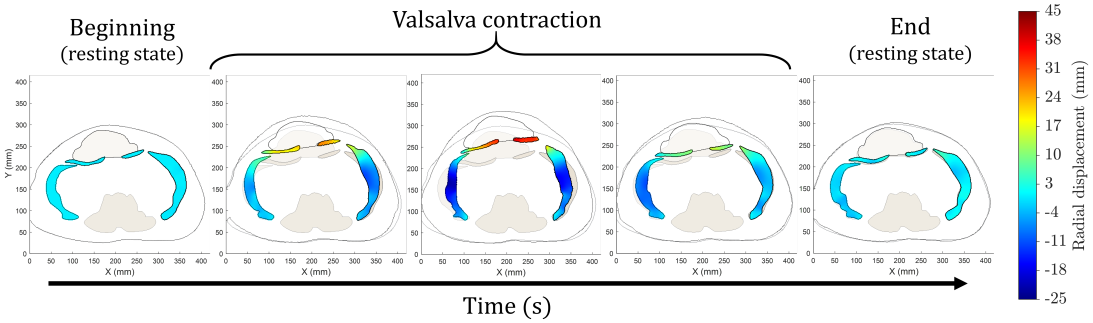

Figure 5.3.: Radial displacement of the abdominal muscles of a preoperative patient performing the Valsalva maneuver. The abdominal wall is at rest; without contraction; at the beginning and end of the exercise

5.2.3.2. Sagittal MRI

For sagittal dynamic acquisition, the post-processing has been focused on Valsalva maneuver. The hernia defect height was measured at the resting state (Figure 5.1). The linea alba, illustrated in Figure 5.4-b, was delineated in the sagittal MR images for the Valsalva exercise using the same semi-automatic segmentation method employed for axial MRI.
As with the axial MRI, the visceral area, shown in Figure 5.4-c was defined as the region enclosed by the internal surface of the linea alba and the vertebral arch. Additionally, the total sagittal area was delineated, delimited by the external surface of the abdomen.

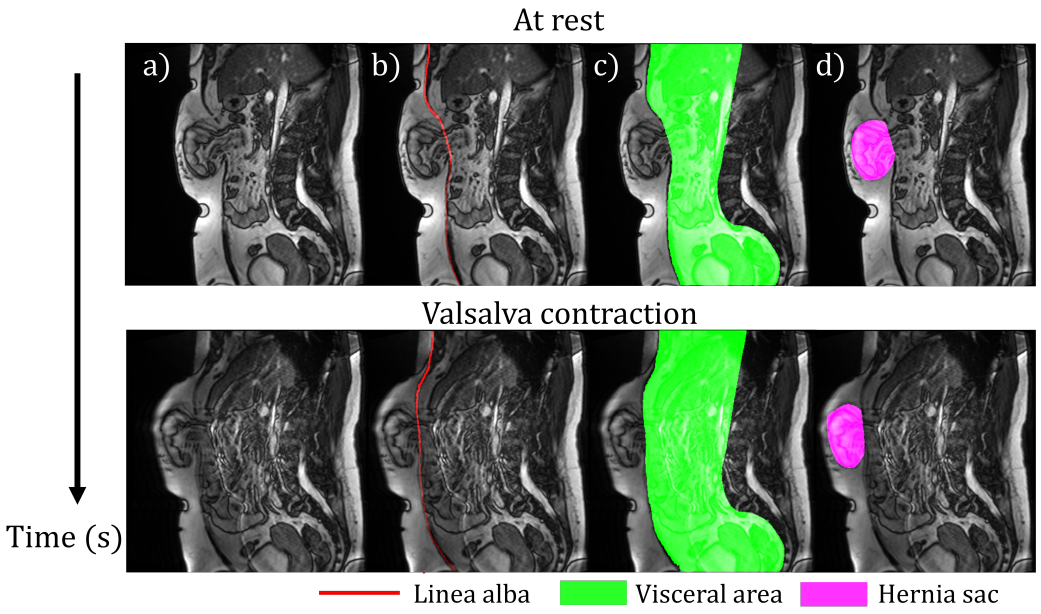

Figure 5.4.: Segmentation masks on sagittal pre-operative MRI
Legend : **a)** Raw MRI **b)** Linea alba segmentation **c)** Visceral area **d)** Hernia sac (for pre-operative patients)

As shown in Figure 5.5, the cartesian displacement within the segmented mask of the linea alba was computed. Some registration parameters has been adapted, as detailed in Appendix 5.6.3. This displacement evolves at each timestep. The linea alba mask was divided into discrete regions for each patient in order to facilitate assessment within specific areas.
As illustrated in Figure 5.5-a, the initial approach entailed the division of the mask into three regions of interest, according to the specific hernia or scar location for

pre-operative and post-operative MRI respectively. The lowest region, called infra, encompasses the area from the bottom of the image to a point 3 cm below the largest hernia neck, where the axial plane was selected. The second region, called hernia-scar, is centered on the hernia neck (or scar) ± 3 cm. The upper and third region, called supra, extends from 3 cm above the hernia neck to the top of the image. This approach allows for intra-patient comparisons between pre-operative and post-operative stages, with a particular emphasis on the hernia region. The displacement was then averaged within these regions.

To facilitate inter-patient comparisons, the location of the upper border of the L4 vertebral disc was measured, and the distance with the hernia defect location was assessed. These measurements were done along the cranio-caudal axis.

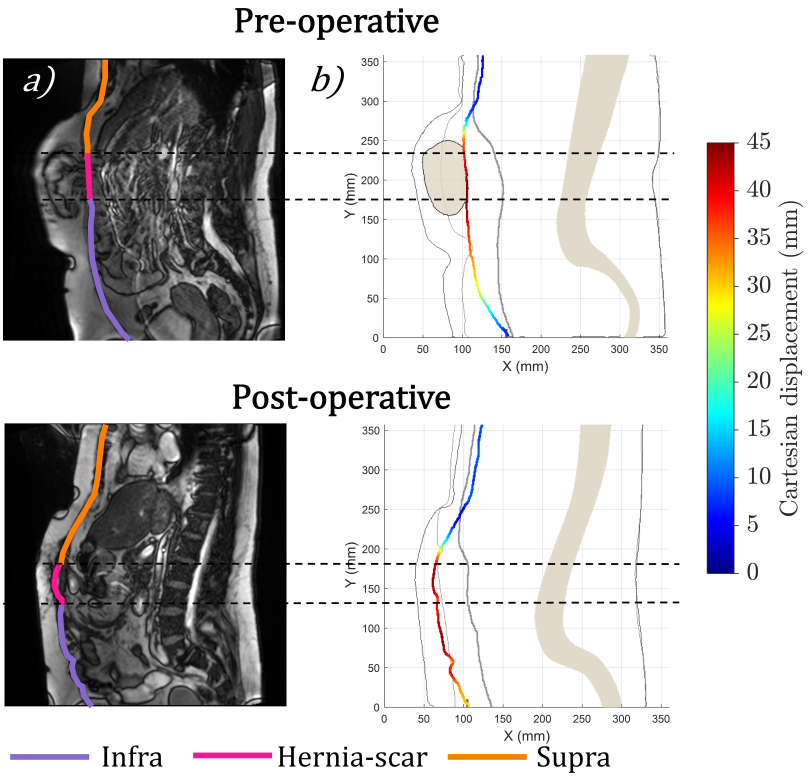

Figure 5.5.: Sagittal MRI during Valsalva contraction, pre-operative (first row) and post-operative (second row)
Legend : **a)** Linea alba divided into the 3 regions : infra, hernia-scar and supra
b) Cartesian displacement of the linea alba

5.2.3.3. Statistical analysis

The results are presented as an average of all participants (n = 11) ± one standard deviation noted σ, with their corresponding [minimum/maximum] range. The difference according to pre-operative or post-operative stage was assessed on the maximum values of the different variables mentioned above. The maximum value corresponds to the end of inhalation for breathing, cough peak for coughing, and onset plateau for Valsalva. A paired t-test or Wilcoxon test was used according to hypothesis validation of a Shapiro-Wilk normality test. Statistical significance was considered for p-value $\leq$ 0.05.

Linear correlation between the maximum values of different variables was assessed by a Pearson correlation coefficients r to evaluate the direction (positive or negative) and strength of correlations, with statistical significance threshold set to $p \leq 0.05$.

To further visualise the distribution of maximum values among participants before and after surgery, radar plots (also called circular graphs or spider plots) were employed to represent the spread of data, often obscured by the averages. These graphs aimed to highlight the variability in biomechanical changes induced by surgery across different participants, emphasising the individualised impact of the surgical intervention on abdominal wall dynamics.

Principal component analysis (PCA) was performed to explain and compare the pre-operative and post-operative behaviour of participants. Since a lot of abdominal metrics are considered in this study, this statistical tool was used to reduce the dimensionality of the data, allowing for the identification of key patterns and variations among participants by highlighting the most significant factors contributing to differences in their biomechanical behaviour before and after surgery. In order to simplify the interpretation of the principal components, it was decided to carry out different PCAs by dividing the metrics into 3 different categories: the morphometric data, which are independent of the dynamic nature of the acquisition, and the dynamic axial and sagittal values obtained from the MRI.

A PCA was done on the morphometric data including sex, hernia defect dimensions (height and width, in cm), the location of the hernia defect with respect to the upper boundary of L4 disc (mm), the muscle mass ratio (%), the BMI (kg/m^2), the radial distance of LM and RA muscles (in mm), the waist circumference (mm) and the age (yo).

Another PCA was done on both pre-operative and post-operative axial maximum values including the visceral area (cm^2), the muscular strap length (mm), the total cross-sectional area (cm^2), the radial displacement of both LM and RA (mm), the inter-recti distance (mm), and the hernia defect angle (°). The pre-operative hernia defect width (mm) was also added to this analysis.

Finally, another PCA was done on both pre-operative and post-operative sagittal maximum values (i.e. assessed at the onset plateau of Valsalva), including the visceral area (cm^2), the total sagittal area (cm^2), and the radial displacement of the three regions of linea alba (infra, hernia/scar, supra, in mm). The pre-operative hernia defect height (mm) was also added to this analysis.

5.3. Results

5.3.1. Cohort description

The morphometric data of the patients (n=11, 6 females) cohort is reported in Table 5.1.

Morphometric data (n=11 patients)	**Average** $\pm\ \sigma$	**Range [min/max]**
Global data		
Age at pre-operative MRI (yo)	57.9 ± 15.1	[27.9 / 75.2]
BMI $(\frac{kg}{m^2})$	30.8 ± 3.1	[27.7 / 38.9]
Hernia defect width (cm)	4.2 ± 2.3	[1.5 / 10]
Hernia defect height (cm)	4.8 ± 1.5	[3.1 / 8.2]
Location of hernia defect with respect to the upper boundary of L4 disc (mm)	−0.2 ± 36.9	[−71.3 / 66.6]
Pre-operative data		
Waist circumference (mm)	1133 ± 95	[1042 / 1378]
Muscle mass ratio (%)	9.5 ± 2.3	[5.1 / 12.7]
Radial distance of LM (mm)	155.4 ± 18.4	[124.7 / 187.7]
Radial distance of RA (mm)	99.8 ± 28.8	[64 / 159.7]
Post-operative data		
Waist circumference (mm)	1132 ± 94	[1019 / 1333]
Muscle mass ratio (%)	9.4 ± 2.3	[4.8 / 12.6]
Radial distance of LM (mm)	156.9 ± 18.1	[126.5 / 183.1]
Radial distance of RA (mm)	100.7 ± 25	[58.3 / 142]

Table 5.1.: Morphometric data of the cohort
Results are presented as mean values ± one standard deviation σ

The waist circumferences before and after surgery were very similar (1133 ± 95 mm and 1132 ± 94 mm, pre-operatively and post-operatively respectively) and well corre-

lated (r=0.92, $p \leq 0.05$).

The muscle mass ratios before and after surgery were very similar (9.5 ± 2.3% and 9.4 ± 2.3%, pre-operatively and post-operatively respectively) and well correlated (r=0.94, $p \leq 0.05$). The difference in muscle mass ratio between post-operative and pre-operative stages is not correlated with the initial muscle mass ratio before the surgery.

Same observation for radial distance at rest of LM, being similar before and after surgery (155.4 ± 18.4 mm and 156.9 ± 18.1 mm, pre-operatively and post-operatively respectively) and well correlated (r=0.97, $p \leq 0.05$). As well, radial distances of RA before and after surgery are very similar (99.8 ± 28.8 mm and 100.7 ± 25 mm, pre-operatively and post-operatively respectively) and well correlated (r=0.95, $p \leq 0.05$).

The influence of sex assigned at birth was examined, and significant differences were observed between males and females for muscle mass ratio and radial distance at rest of the LM. The results are detailed in the Appendix 5.6.4, but will not be used in the rest of the study, which will focus more on the differences between pre- and post-operative stages than on sex.

According to EHS classification (Muysoms, Miserez, et al. 2009), among the 11 patients, there were four occurrences of incisional midline M2 hernia, two incisional midline M3 hernia, one incisional midline M4 hernia, three primary midline umbilical hernias, and one incisional lateral L4 hernia. Concerning the mesh placement, six patients had an Intra-Peritoneal Onlay Mesh with defect closure (IPOM+), two had a sublay retro-muscular, two had an underlay pre-peritoneal, and one had a retro-muscular pre-peritoneal mesh placement.

5.3.2. MRI parameters

The duration between the surgery and the post-operative MRI, as well as acquisition parameters such as field of view, temporal and spatial resolution for both axial and sagittal MR sequences are reported in Table 5.2. The acquisition parameters were the same across the exercises.

Data	Average $\pm \sigma$	Range [min/max]
Duration between surgery and post-operative MRI $(days)$	137 ± 84	[76 / 362]
Axial MRI		
Field of view (mm)	409 ± 31	[360 / 470]
Temporal resolution (ms)	160 ± 4	[154 / 166]
Spatial resolution (mm)	0.983 ± 0.075	[0.865 / 1.130]
Sagittal MRI		
Field of view (mm)	374 ± 28	[360 / 450]
Temporal resolution (ms)	214 ± 57	[156 / 275]
Spatial resolution (mm)	0.898 ± 0.068	[0.865 / 1.082]

Table 5.2.: Acquisition parameters of pre-operative MRI
Results are presented as mean values ± one standard deviation σ

The average duration of sequences is 41 ± 2s, 23 ± 3s and 54 ± 6s for breathing, coughing and Valsalva respectively.

5.3.3. Principal component analysis

About the PCA done on morphometric data, the variables contributing positively the most to this first principal component (explaining 38% of the variance) are respectively the radial distance of LM, i.e. a large abdomen along the left-right axis, the radial distance of RA, i.e. a deep abdomen along the antero-posterior axis, the BMI, the waist circumference, the age and in last the location of the hernia defect with respect to the upper boundary of L4 disc. The corresponding loadings are respectively 0.5, 0.46, 0.4, 0.39, 0.22, 0.17, and 0.16. The sex variables had a negative contribution to this

principal component, with a loading of -0.32.

According to the PCA done on the axial maximum values (i.e. assessed at the end of inhalation for breathing, cough peak for coughing, onset plateau for Valsalva), the variables contributing positively the most to this first principal component (explaining 38% of the variance) are respectively the visceral area, the muscular strap length, and the total cross-sectional area. The corresponding loadings are respectively 0.55, 0.5, 0.44. The radial displacement of LM variable had a negative contribution to this principal component, with a loading of -0.4.

According to the PCA done on the sagittal maximum values, the variables contributing positively the most to this first principal component (explaining 44% of the variance) are respectively the sagittal visceral area, the linea alba displacement of hernia/scar and supra regions, and the total sagittal area. The corresponding loadings are respectively 0.52, 0.52, 0.45, and 0.43.

5.3.4. Axial displacement of lateral muscles and rectus abdominis

The radial displacement of both RA and LM before and after surgery is shown in Figure 5.6. For the LM muscles, the post-operative averaged displacement (Figure 5.6-a) was significantly higher (in absolute value) during Valsalva maneuver compared to the pre-operative one, and is similar for breathing and coughing. The maximum radial displacement of LM muscles before and after surgery is respectively 1.6 ± 7.6 mm and 2.7 ± 4.6 mm for breathing (p=0.4350), -11.7 ± 7 mm and -11.9 ± 6.7 mm for coughing (p=0.8764), -8.2 ± 4 mm and -11.2 ± 7.1 mm for Valsalva (p=0.046).
The post-operative averaged radial displacement of RA is higher than pre-operative for the three exercises (Figure 5.6-c). The maximum radial displacement of RA muscles before and after surgery is respectively 15.3 ± 8.2 mm and 19.5 ± 7.8 mm for breathing (difference almost significant, p=0.086), 21.2 ± 9 mm and 22.4 ± 9.7 mm for coughing (p=0.0485), 15.3 ± 8.7 mm and 19.2 ± 11.6 mm for Valsalva (p=0.245).

The corresponding circular plots (Figure 5.6-b and Figure 5.6-d) show the maximum values (i.e. assessed at the end of inhalation for breathing, cough peak for coughing, onset plateau for Valsalva) of displacement before and after the surgery for each patient, for LM and RA muscles respectively.
Concerning the LM group, the pre-operative displacement is higher than the post-

operative one for the three exercises only for patients nr 3 and 5. According to the three PCA done, any specific characteristics for these individuals were highlighted. Concerning the RA group, no patients had a higher pre-operative displacement of RA for the three exercises. The RA displacement was higher after surgery than before for the three exercises for the patients nr 1, 5, 6, and 7. As mentioned above for the LM, according to the three PCA, there is no specific characteristics were highlighted for these patients.

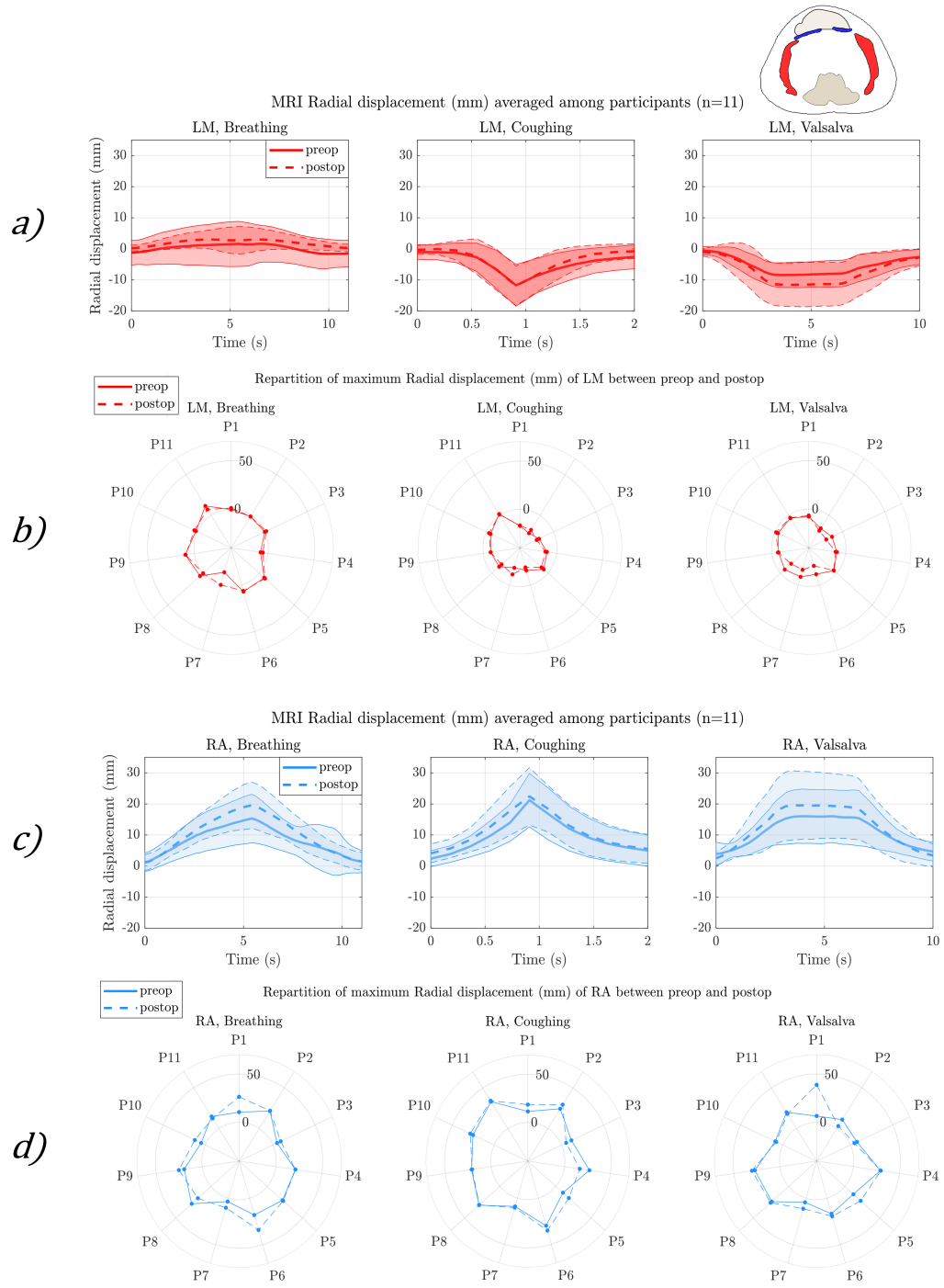

Figure 5.6.: Pre-operative and post-operative radial displacement of lateral muscles (LM) and rectus abdominis (RA) for the three exercises
Legend: **a)** LM displacement averaged among patients **b)** Corresponding maximum values (i.e. assessed at the end of inhalation for breathing, cough peak for coughing, onset plateau for Valsalva) for all patients **c)** RA displacement averaged among patients **d)** Corresponding maximum values for all patients

5.3.5. Shape of lateral muscles and rectus abdominis

The Table 5.3 shows the results according to abdominal muscle length, thickness, circumferential and radial strains.

When looking at the difference in muscle thickness after the surgery, indeed a slight tendency of being thinner post-operatively, these differences in thickness for LM and RA muscles were not statistically significant. At the contrary , the maximum length of both LM and RA muscles was higher after surgery than before. For LM muscles, this increase was significant for coughing and Valsalva ($p \leq 0.05$), and almost significant for breathing ($p = 0.066$). For RA muscles, the post-operative increase in length was significant for the three exercises ($p \leq 0.05$). This change in muscle length can be also assessed in the muscular strap length which is a more global variable, with the post-operative increase significant for the three exercises as well.

Concerning the circumferential and radial strains ε_θ and ε_r, there were not significant differences between pre-operative and post-operative stages for both LM and RA muscles.

The pre-operative maximum value of RA muscles radial strain ε_r among the whole cohort are negatively correlated with the hernia defect width during coughing exercise (r=-0.72, $p \leq 0.05$).

Exercise	Muscle group	Pre-operative	Post-operative	*p*-value
Thickness (mm)				
Breathing	**LM**	25.2 ± 3.9	24.6 ± 4.1	0.54
	RA	13.1 ± 1.7	13 ± 3.3	0.83
Coughing	**LM**	31.6 ± 7.3	30.8 ± 7.3	0.52
	RA	13.5 ± 2	13 ± 3.2	0.49
Valsalva	**LM**	31.4 ± 6	31.6 ± 7	0.86
	RA	14 ± 3.5	13.5 ± 3.9	0.41
Length (mm)				
Breathing	**LM**	169.8 ± 50.1	177 ± 50.6	0.07
	RA	81.1 ± 24.4	90.4 ± 26.6	0.01*
Coughing	**LM**	143.9 ± 48.6	151.7 ± 44.6	0.02*
	RA	84.7 ± 23.2	91.4 ± 23.9	0.04*
Valsalva	**LM**	146.2 ± 52.6	155.7 ± 53.4	0.03*
	RA	82 ± 23.1	90.9 ± 23.1	0.03*
Muscular strap length (mm)				
Breathing	-	501.9 ± 118.3	531.3 ± 121.6	0.009*
Coughing	-	457.3 ± 107.5	485 ± 112.2	0.004*
Valsalva	-	456.5 ± 124.9	489.5 ± 121.4	0.022*
Radial strain ε_r (%)				
Breathing	**LM**	−7.9 ± 13.3	−11.1 ± 5.6	0.43
	RA	−3.1 ± 8.8	−0.9 ± 8.7	0.55
Coughing	**LM**	16.1 ± 19.8	14.4 ± 18.4	0.76
	RA	1.3 ± 9.9	−4.7 ± 9.2	0.08
Valsalva	**LM**	11.8 ± 13.5	16.7 ± 18.2	0.21
	RA	4 ± 13.3	0.6 ± 10.9	0.58
Circumferential strain ε_θ (%)				
Breathing	**LM**	6.1 ± 12.4	10.4 ± 9.9	0.15
	RA	2.2 ± 5.9	5.9 ± 4.7	0.24
Coughing	**LM**	−12.8 ± 9.8	−9.1 ± 8.3	0.29
	RA	9.6 ± 14.5	6.5 ± 8.5	0.28
Valsalva	**LM**	−9.2 ± 7.3	−6.5 ± 8.9	0.35
	RA	5.1 ± 8.3	5.9 ± 8.2	0.78

Table 5.3.: Maximum radial and circumferential strains of lateral muscles (LM) and rectus abdominis (RA) during breathing, coughing and Valsalva peak exercise averaged among participants (n=11)
Results are presented as mean values (n=11) ± one standard deviation σ, the star symbol (*) indicate a significant p-value ≤ 0.05

5.3.6. Sagittal displacement of linea alba

The cartesian displacement of the three regions of linea alba (infra defect, defect, supra defect) before and after surgery is shown in Figure 5.7. The average among the whole cohort is displayed on Figure 5.7-a. For visualisation purpose, the standard deviation was plotted for each region on Figure 5.7-c.
The averaged post-operative displacement is slightly higher compared to the pre-operative one for the three regions of linea alba, however the difference is not statistically significant ($p = 0.686$, 0.519 and 0.898 respectively for infra, defect and supra regions).

The maximum displacement; assessed at the onset plateau of Valsalva; before and after surgery for these three linea alba regions is displayed on Figure 5.7-b for the 11 patients. On the contrary of average tendency, it can be observed that the post-operative displacement of the three linea alba regions is lower than the pre-operative one for participants nr 2 and 8. According to the PCA done on morphometric data, these two participants are ones of the first three patients having the highest scores along the first principal component (x-values in the new coordinate system defined by the first two principal components) Figure 5.10 in Appendix 5.6.5 displays the corresponding PCA. According to the PCA done on the axial maximum values, these two participants are also the ones having the highest scores along the first principal component. Figure 5.11 in Appendix 5.6.5 displays the corresponding PCA. Interestingly, these patients were not highlighted in the results of the PCA done on the sagittal maximum values (i.e. assessed at the onset plateau of Valsalva). Figure 5.12 in Appendix 5.6.5 displays the corresponding PCA.

The pre-operative and post-operative displacement for participants nr 3 and 10 are very similar for the three linea alba regions. According to the PCA done on the sagittal maximum values, these are the two participants having the lowest scores along the first principal component (Figure 5.12 in Appendix 5.6.5). No particular characteristic stands out from the PCA done on morphometric data and axial data on these patients (Figure 5.10 and Figure 5.11 in Appendix 5.6.5).

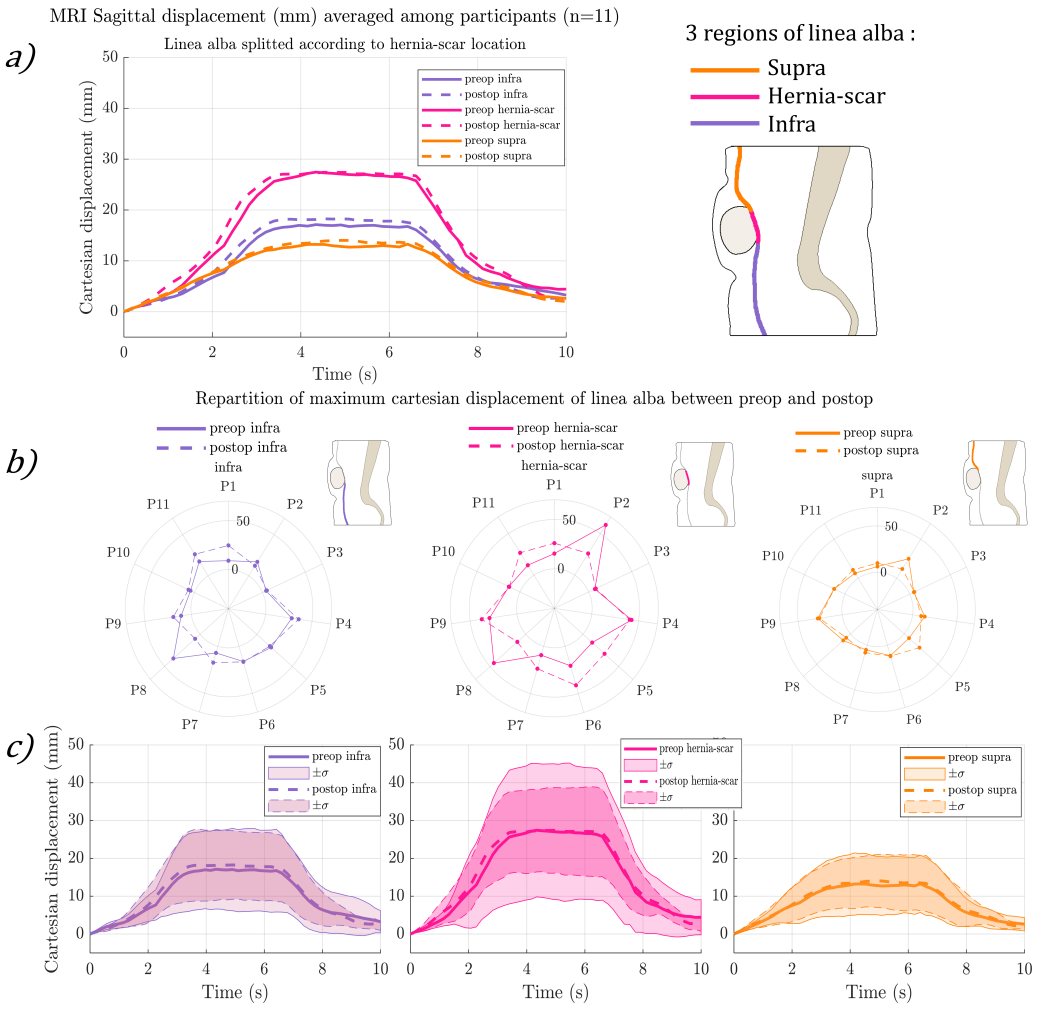

Figure 5.7.: Pre-operative and post-operative sagittal displacement of the 3 regions of linea alba (infra - hernia/scar - supra) for the Valsalva maneuver
Legend: **a)** Displacement averaged among patients (n=11) **b)** Corresponding maximum values of each region for all patients **c)** Corresponding average ± one standard deviation σ for each region

5.3.7. Inter-recti distance and hernia defect angle

The averaged inter-recti distance before and after surgery is shown in Table 5.4 for the three exercises. The inter-recti distance is shorter after the surgery, the difference is statistically significant for almost all the exercises ($p = 0.053$ for breathing, $p \leq 0.05$ for coughing and Valsalva maneuver).

Exercise	Pre-operative	Post-operative	*p*-value
Inter-recti distance (mm)			
Breathing	48.2 ± 15.1	38.2 ± 17	0.053
Coughing	51.4 ± 15.9	39.4 ± 18.3	0.0407*
Valsalva maneuver	49.7 ± 13.5	36.6 ± 15.6	0.0350*
Hernia defect angle (°)			
Breathing	28.8 ± 9.4	22.7 ± 11.6	0.0405*
Coughing	26.7 ± 8.6	20.2 ± 8.7	0.0192*
Valsalva maneuver	28.4 ± 10.3	19.9 ± 9.7	0.0098*

Table 5.4.: Inter-recti distance before and after surgery assessed at exercise peak (i.e., end of inhalation for breathing, cough peak for coughing, onset plateau for Valsalva) Results are presented as mean values (n=11) ± one standard deviation σ, the star symbol (*) indicate a significant p-value ≤ 0.05

The hernia defect angle α is schematised in Figure 5.8 where its evolution along time is plotted before and after surgery. The values at exercises peak are reported in Table 5.4. This angle is significantly smaller after the surgery for all the exercises ($p \leq 0.05$). No correlation was found either at pre-operative or post-operative stages between the maximum value of radial displacement of RA with the inter-recti distance or the hernia defect angle.

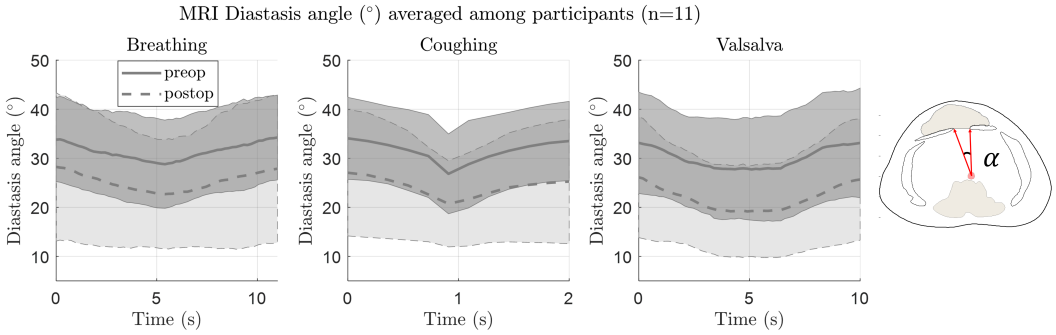

Figure 5.8.: Hernia defect angle before and after surgery averaged among participants (n=11)
Results are presented as mean values ± one standard deviation σ

5.3.8. Hernia sac and ratio

The hernia sac was segmented for eight patients over the 11, being too difficult to delimit for the three remaining patients. The hernia sac area in axial plane at exercises peak were 21.5 ± 26.4 cm^2, 21.8 ± 23.3 cm^2, 22.6 ± 21.1 cm^2 for breathing, coughing and Valsalva maneuver respectively. The differences between exercises are not significant. No correlation was found between the hernia defect width and the axial hernia sac area, neither at resting state nor at exercise peaks.
With respect to the hernia sac area at resting state, the area increased by 17.3 ± 57.4%, 128.4 ± 199.2% and 35 ± 44% during breathing, coughing and Valsalva respectively.

The cross-sectional ratio between hernia sac area and total area at exercises peak were 6.2 ± 6.8%, 6.6 ± 5.8%, 7.3 ± 4.9% for breathing, coughing and Valsalva maneuver respectively. It was superior than 20% only for patient.

The hernia sac area in sagittal plane at Valsalva peak was 19.1 ± 11.4 cm^2. The cross-sectional ratio between hernia sac area and total area at Valsalva peak was 3.9 ± 2.1%. As for axial plane, o correlation was found between the hernia defect height and the sagittal hernia sac area, both at resting state or at Valsalva peak.
There are strong correlation between axial and sagittal hernia sac area both at rest or at Valsalva peak (r=0.98 and r=0.97 respectively, $p \leq 0.05$). Hernia defect width and height are also correlated (r=0.65, $p \leq 0.05$).

5.3.9. Visceral area

The visceral area before and after surgery is shown in Figure 5.9 for the three exercises in axial plane, and for Valsalva in sagittal plane. The axial visceral area is slightly higher after the surgery. The visceral area in axial plane at exercises peak before surgery were 337.9 ± 118.9 cm^2, 318.5 ± 99.3 cm^2, 305.6 ± 101.3 cm^2 for breathing, coughing and Valsalva maneuver respectively. After surgery, they were 353.9 ± 118.3 cm^2, 323.4 ± 92.9 cm^2, 315.2 ± 93.9 cm^2 for breathing, coughing and Valsalva maneuver respectively. The difference is almost significant for the breathing exercise ($p = 0.058$). Pre-operatively, the difference between max visceral area during breathing and Valsalva is significant ($p = 0.01$). Post-operatively, the difference between max visceral area during breathing and coughing, as well as between breathing and Valsalva, are significant.
The sagittal visceral area at Valsalva peak is significantly lower before the surgery than after, being 514.6 ± 106.6 cm^2 and 546.3 ± 107.5 cm^2 respectively ($p = 0.0345$).

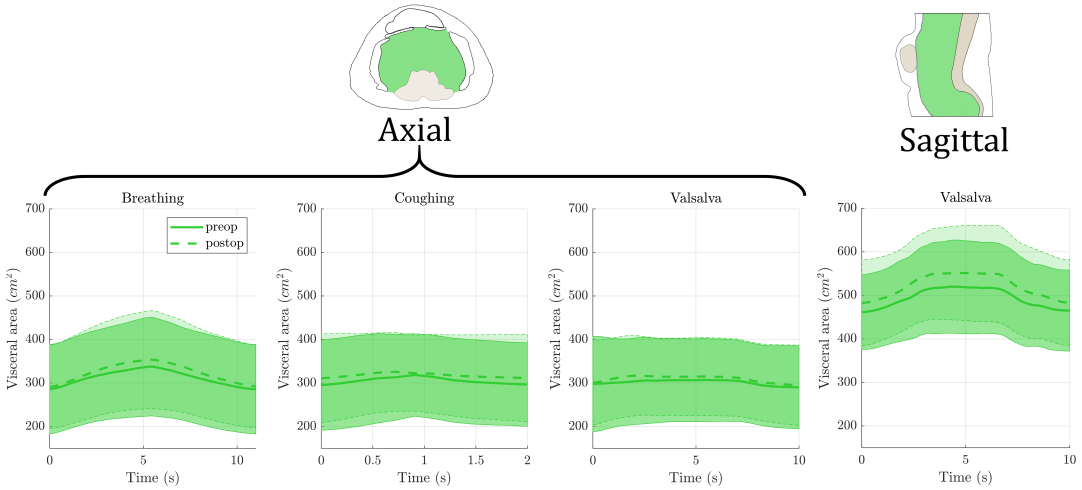

Figure 5.9.: Visceral area before and after hernia surgery averaged among participants (n=11)
Results are presented as mean values ± one standard deviation σ

5.3.10. Total abdomen area

The total cross-sectional area in axial plane at exercises peak before surgery were 882.4 ± 177 cm^2, 877.8 ± 180.9 cm^2, 874.1 ± 181.9 cm^2 for breathing, coughing and Valsalva maneuver respectively. After surgery, they were 895.9 ± 165.6 cm^2, 875.1 ± 159.2 cm^2, 874.8 ± 142.6 cm^2 for breathing, coughing and Valsalva maneuver respectively.

The total area in sagittal plane at Valsalva peak before and after surgery were 1072.6 ± 172.1 cm^2 and 1036.9 ± 167.2 cm^2 respectively.
The difference between the total cross-sectional areas and sagittal areas of the abdomen before and after surgery was not statistically significant, being very similar pre-operatively and post-operatively.

5.4. Discussion

This study is the first to evaluate both anatomical and functional changes in the abdominal wall using dynamic MRI in axial and sagittal views before and after abdominal hernia surgery. By allowing real-time, *in vivo* visualisation of the abdominal muscles, linea alba, hernia sac, and visceral area, this approach offers a more comprehensive understanding of post-surgical dynamic changes.

When examining the morphometric data, no significant changes were observed before and after the surgery in waist circumferences, muscle mass ratios, or radial distance at rest of LM and RA muscles. This study did not show that patients with high muscle mass ratio before surgery had significantly stronger abdominal muscles after ventral hernia repair, at the contrary of Ahmed *et al.* study who conclude that pre-operative abdominal muscle training was effective for strengthening abdominal muscles after ventral hernia repair with isokinetic dynamometer measurements (Ahmed et al. 2018). The discrepancy may be due to differences in cohort characteristics. Ahmed *et al.* 's cohort was younger (20-45 years) compared to our study's older population (57.9 ± 15.1 years). Additionally, our cohort's BMI averaged 30.8 ± 3.1 kg/m^2, indicating an obese population according to the classification of overweight and obesity established by the World Health Organisation (WHO Consultation on Obesity et al. 2000), which might have impacted the outcomes, the BMI of Ahmed *et al.* study cohort was not indicated. Various studies have showed that the risk of complication increased significantly with a BMI ≥ 30 kg/m^2 (Owei et al. 2017; van Silfhout et al. 2021). Previous studies have shown that older age, male sex, daily smoking, postoperative wound complication, and relaparotomy were independently associated with incisional hernia (Sørensen et al. 2005; Le Huu Nho et al. 2012).

This study detailed the characterisation of muscle motion and linea alba behaviour pre- and post-surgery. The radial displacement of rectus abdominis and lateral muscles,

measured in a cross section plane, follow a pattern which is specific to each exercise. The rectus abdominis are mainly involved during breathing, also observed on healthy cohort (Jourdan, Rapacchi, et al. 2022).

By analysing the axial and sagittal planes over time, we were able to highlights differences between pre and post-operative stages. Primarily, there is a significantly more pronounced inward displacement of lateral muscles during Valsalva after surgery, as well as a higher displacement of rectus muscle during coughing for all patients. The higher displacement on the whole linea alba post-operatively, although not statistically significant. These could suggest a positive trend towards improved muscle function after surgery. This might imply better engagement of muscles during physiological activities, reflecting improved biomechanical function, which is crucial for patients' postoperative recovery and long-term outcomes. This result is supported by Criss *et al.* study which showed that hernia repair with linea alba restoration improved abdominal wall functionality (Criss et al. 2014).

Interestingly, many studies have shown a repaired abdominal wall tends to be more rigid (DuBay, Xue Wang, et al. 2006; Le Ruyet et al. 2020), with reduced mobility compared to a healthy or herniated abdominal wall (Junge, Klinge, et al. 2001; Silvia Todros, Paola Pachera, et al. 2018; He et al. 2020)

In our cohort, patients with less displacement of the linea alba post-surgery tended to have characteristics associated with higher recurrence risk, such as high visceral area, long muscular strap (Figure 5.11), high radial distance of both LM and RA, high BMI, high waist circumference, and male sex (Owei et al. 2017; van Silfhout et al. 2021; Sørensen et al. 2005; Le Huu Nho et al. 2012).

Figure 5.7-b highlights that there is no clear tendency in the complex and patient-specific nature of displacements in the linea alba before and after hernia surgery.

The differences between pre-operative and post-operative stages of abdominal muscles shapes suggest a significant change in the absolute length, but no change in muscle ability to deform (i.e., the relative circumferential and radial strains ε_θ, and ε_r). The length of muscular strap is significantly higher after surgery. This may due to the fact that when surgeon is closing the hernia neck, they try to bring the defect sides close together, lengthening the muscles. This result may suggest that the surgery has changed the anatomy of the abdominal muscles but preserved their functional behaviour. Before and after surgery, when the muscles are subjected to the same

physiological loading like breathing, coughing or Valsalva maneuver, they deform similarly relative to their new baseline size l_0, indicating that their capacity to stretch and contract are unchanged.

A negative correlation between rectus abdominis radial strain ε_r and hernia defect width was observed, echoing findings from García Moriana *et al.* and Gunnarsson*et al.* who both measured rectus abdominis strength using isokinetic dynamometer (García Moriana et al. 2023; Gunnarsson et al. 2015).

In García Moriana *et al.* study, a negative correlation was found between hernia defect width measured in CT scan and abdominal muscle strength on 40 patients before their hernia surgery (García Moriana et al. 2023).

In Gunnarsson *et al.* study, a negative correlation was found between abdominal rectus diastasis width under the umbilicus and abdominal muscle strength on 57 patients before their abdominal recti diastasis surgery (Gunnarsson et al. 2015). However, in our study, this correlation focused on muscle deformation capacity during coughing rather than muscle strength, with the width of the hernia defect. Our results emphasise that dynamic muscle behaviour may be just as critical to consider as static muscle strength measurements in evaluating surgical outcomes.

One of the contributions of this study is the quantification of the inter-recti distance and hernia defect angle during various exercises, before and after the surgery. The reduction in the inter-recti distance following surgery, coupled with a significant decrease in the hernia defect angle in axial MRI views, suggests successful repair. For a given distance to the aorta, if the rectus muscles become closer due to the closure of the defect, the defect angle is likely to decrease. For a given inter-recti distance, if the muscles motion increased (further from the aorta), the defect angle is also likely to decrease. Here the reduced inter-recti distance and increased radial RA displacement further supports this conclusion. The combined effects of surgical closure and enhanced muscle mobility may play an important role in the reduction of the hernia defect angle post-operatively.

In addition, our study quantified changes over time of the hernia sac area. The hernia sac area in axial plane at exercises peak were quite similar across the exercises, with a slightly higher value during coughing and Valsalva compared to breathing. The variation of hernia sac, although not significant between exercise, is much higher during coughing. The variation is very important during coughing for two patients

in particular, reflected by the very high standard variation (57.4%). The difference observed between coughing and breathing (128.4 ± 199.2% and 17.3 ± 57.4% respectively) is consistent with the increased intra-abdominal pressure generated during these exercises (Soucasse, Jourdan, Edin, J. F. Gillion, et al. 2022). However, one can expect the same result with the Valsalva maneuver, during which the hernia sac area varied more than during breathing (35 ± 44%) but lower than coughing. This can be explained when looking at the resting value of hernia sac area. Indeed, the hernia sac area was significantly higher at the beginning of Valsalva maneuver than at the beginning of coughing (20.8 ± 23.2 cm^2 and 18.8 ± 24.8 cm^2 for Valsalva and coughing respectively), the differences being mostly significant (p=0.054). This may be attributed to the order in which exercises were performed during the clinical trial, the first exercise performed by the patient was breathing, then coughing, then Valsalva maneuver. The exercises were always performed in the same order, with the hernia sac potentially remaining in an extended position after coughing, making the hernia sac at rest (i.e. at the beginning of the acquisition) of Valsalva higher.

In addition, our study quantified changes in the internal visceral area. The corresponding slight increase post-surgery may be explained by the fact that the surgeons is pushing back to abdomen the hernia sac content. This post-operative increase is statistically significant for sagittal plane during Valsalva maneuver.
Interestingly, our study did not corroborate the findings of Lisiecki *et al.* regarding post-operative reductions in cross-sectional waist circumference or abdominal area (Lisiecki et al. 2015). Differences in measurement locations and cohort characteristics likely explain this divergence. In Lisiecki *et al.* study, the measurements were done and averaged on cross-sectional slices from L4 to T12 disc, which is higher in body that the studied cross-sectional planes in this study, determined by the hernia location. This may explain the differences in total body cross-sectional area, pre-operative and post-operative values being 968.0 and 928.6 cm^2 for Lisiecki *et al.* study cohort, and 835.9 cm^2 for both pre and post-operative stages if this study cohort, although Lisiecki *et al.* study cohort BMI is higher than this cohort (35.1 ± 5.6 versus 30.8 ± 3.1 kg/m^2). However, the waist circumferences of both studies are very close (113.6 versus 1133 for Lisiecki and present study cohorts).

Despite the novel insights provided by this study, several limitations should be ac-

knowledged. The small sample size of 11 patients and the high inter-individual variability among the results limit the generalisability of our findings, larger studies are required to confirm these results. There is great variability in the time at which postoperative MRI was performed after surgery, which depended mainly on the patient's state of recovery. It would be interesting to assess the impact of this duration on surgery outcome. While we observed significant improvements post-surgery on some metrics, the long-term durability of these changes remains to be studied.
Recovery from hernia surgery involves complex interactions between patient anatomy (muscular, fascial, and visceral structures), hernia characteristics, and surgical techniques, which may not manifest uniformly across different outcomes. The study focuses on anatomical and biomechanical changes, but the inclusion of more diverse types of outcomes (e.g. pain, quality of life, physical activity levels) would provide a more comprehensive assessment of the impact of surgery. The effect of mesh type, surgery type, and mesh positioning on postoperative outcomes was not analysed. The effect of pain immediately after surgery would be interesting to analyse in conjunction with the outcomes. Here, the postoperative MRI scan was performed when the patient was free of postoperative pain, so as not to limit the exercises the patient performed and bias the results.
Lastly, while dynamic MRI offered valuable insights, it was limited to single axial and sagittal planes. The axial plane was chosen where the hernia neck is the largest, and was perpendicular to the RA muscle fibres maybe not fully capturing its contraction. In sagittal plane was placed in the middle on the hernia neck, often within the linea alba. Thus, the motion of muscles in the sagittal plane was not studied. A full 3D dynamic analysis could provide a more complete understanding of abdominal wall motion, though it would require adjustments to the time resolution.

5.5. Conclusion

This study provides a novel and comprehensive assessment of abdominal wall biomechanics before and after hernia surgery using dynamic MRI in both axial and sagittal planes. The findings suggest that while certain anatomical parameters, such as muscle mass ratio and waist circumference, remain unchanged post-surgery, significant improvements in muscle displacement and linea alba behaviour were observed. These results indicate potential functional recovery following surgery, a promising indicator

of surgical success, although variability among patients emphasises the need for personalised approaches. Future research should focus on expanding these findings in larger, more diverse cohorts and exploring the integration of functional and long-term outcomes into dynamic MRI assessments. This approach could be adopted in clinical practice to evaluate the functional outcomes of hernia surgeries more comprehensively, potentially leading to more tailored and effective treatment strategies.

5.6. Appendix

5.6.1. Segmentation of MRI

The percentage of manually segmented slices are reported on Table 5.5. Coughing exercise required more manual segmentation due to the fast nature of motion which was more difficult to propagate.

Exercise	Pre-operative MRI	Post-operative MRI
Breathing	7.4	6.5
Coughing	15.6	16.9
Valsalva	8.7	8.7

Table 5.5.: Percentage of manually segmented slices
Results are presented as mean values ± one standard deviation σ

5.6.2. Registration of axial MRI

As described by Jourdan *et al.* (Jourdan, Le Troter, et al. 2021), displacement fields were obtained for each timestep by registering the initial segmented mask, M_0, with the ith target mask M_i ($1 \leqslant i \leqslant n$, where n is the total number of timesteps). Registration was performed using the *TimeVaryingVelocityField* transformation model from the ANTs library (*ANTsX/ANTs* 2024). Large deformations sometimes caused distortions in the displacement field, which were corrected by increasing the smoothing-sigmas parameter which controls the amount of Gaussian smoothing applied to the images at each multi-resolution level during the registration process. The registration is typically performed in a coarse-to-fine manner, where the images are first smoothed

and downsampled. This process helps in capturing large-scale deformations at lower resolutions, progressively refining them at higher resolutions.
The registration was performed with the parameters:

- *TimeVaryingVelocityField*[2,10,1,0,0.05,0]
- cost functions (mean squares and demons)
- five multi-resolution steps with 1000x500x100x20x0 iterations per level
- convergence threshold was 0
- window size was 5
- shrink factors were 8x6x4x2x1
- smoothing sigmas were 12x10x8x4x1 voxels

The Demons metric minimized the sum of squared intensity differences (SSD) between images and accounted for local image structures, guiding the registration and helping to handle large smooth deformations.

5.6.3. Registration of sagittal MRI

For sagittal MRI registration of the linea alba, the displacement field is close to zero at the upper and lower y-axis bounds due to the segmentation mask being a vertical curvilinear line moving mainly along the x-axis Figure 5.5-b. The *TimeVaryingVelocityField* algorithm initially struggled with boundary conditions and large displacements. Registration algorithms, such as *SyN* or *TimeVaryingVelocityField* *ANTsX/ANTs* 2024, often impose smoothness constraints, anchoring the edges and resulting in near-zero displacements at the boundaries. To mitigate this, a buffer zone of background pixels was added at the top and bottom of the image, giving the algorithm more room to apply deformations and reduce boundary effects. Both *TimeVaryingVelocityField* and *SyN* transformations produced similar results, but *SyN* was retained due to its lower computational time for sagittal MRI registration. The registration was performed with the following parameters:

- *SyN*[0.1,3,0]
- cost functions (mean squares and demons)

- five multi-resolution steps with 1000x500x100x20x0 iterations per level
- convergence threshold was 0
- window size was 5
- shrink factors were 12x10x8x4x1
- smoothing sigmas were 12x10x8x4x1 voxels

5.6.4. Influence of sex assigned at birth

A significant difference was found between males and females in muscle mass ratio (%), at both pre-operative and post-operative stages ($p = 0.0493$ and $p = 0.0237$ respectively) . Females had lower muscle mass ratio than males; pre-operatively (10.7 ± 1.9 % and 8 ± 1.9 % for males and females respectively) and post-operatively (10.8 ± 1.7 % and 7.8 ± 1.9 % for males and females respectively).
A significant difference was also found in radial distance at rest of LM (mm), at both pre-operative and post-operative stages ($p = 0.0486$ and $p = 0.0292$ respectively), where females had lower radial distance at rest of LM than males; pre-operatively (165.1 ± 17.3 mm and 143.8 ± 12.7 mm for males and females respectively) and post-operatively (167.2 ± 15.2 mm and 144.5 ± 13.4 mm for males and females respectively).
No significant differences were found between males and females for the other morphometric parameters such as hernia defect dimensions (height and width), the location of the hernia defect with respect to the upper boundary of L4 disc, the BMI, the radial distance at rest of RA muscles, the waist circumference or age. A strong correlation was found between BMI and waist circumference.

5.6.5. Principal component analysis

Figure 5.10 relates to the PCA done on both pre-operative and post-operative **morphometric** data including sex, hernia defect dimensions (height and width, in cm), the location of the hernia defect with respect to the upper boundary of L4 disc (mm), the muscle mass ratio (indicated as MR in the figure) (%), the BMI (kg/m^2), the radial distance of LM and RA muscles (in mm), the waist circumference (mm) and the age (yo). On this figure, participants nr 2 and 8 are surrounded in green because they both had a higher post-operative sagittal displacement, as referred in subsection 5.3.6,

and there are ones on the first three patients having the highest scores along the first principal component (x-values in the new coordinate system defined by the first two principal components). Participants nr 3 and 10 are surrounded in yellow because they both had an equal sagittal displacement before and after surgery, as referred in subsection 5.3.6, however there is no particular characteristic that stands out for these patients from the following PCA.

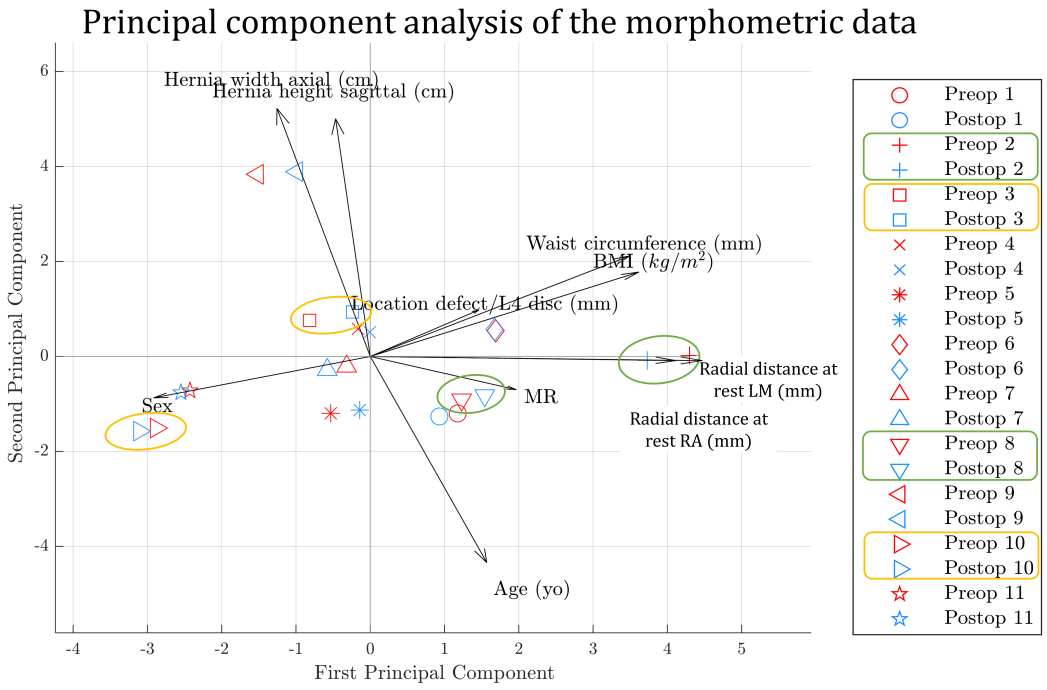

Figure 5.10.: PCA done on pre-operative and post-operative morphometric data

Figure 5.11 relates to the PCA done on both pre-operative and post-operative **axial** maximum values including the visceral area (cm^2), the muscular strap length (mm), the total cross-sectional area (cm^2), the radial displacement of both LM and RA (mm), the inter-recti distance (mm), the hernia defect angle (°) and pre-operative hernia defect width (mm). On this figure, participants nr 2 and 8 are surrounded in green because they both had a higher post-operative sagittal displacement, as referred in subsection 5.3.6, and these patients are the ones having the highest scores along the first principal component. Participants nr 3 and 10 are surrounded in yellow because they both had an equal sagittal displacement before and after surgery, as referred in subsection 5.3.6, and there are the two patients having the lowest scores along the first principal component.

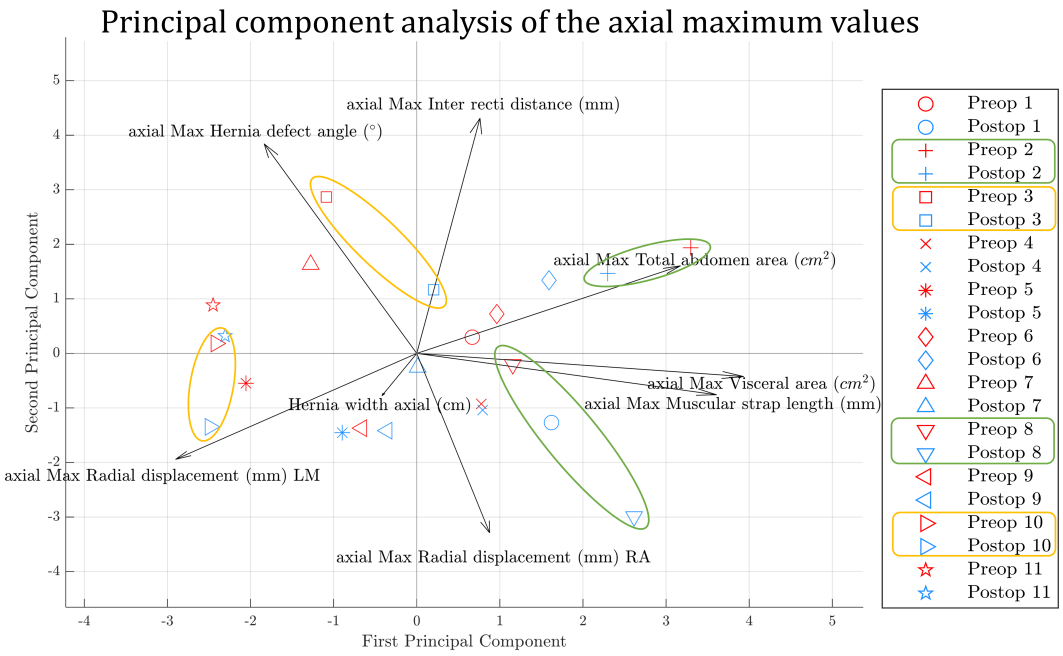

Figure 5.11.: PCA done on pre-operative and post-operative axial maximum values

Figure 5.12 relates to the PCA done on both pre-operative and post-operative **sagittal** maximum values including the visceral area (cm^2), the total sagittal area (cm^2), the radial displacement of the three regions of linea alba (infra, hernia/scar, supra, in mm), and the pre-operative hernia defect height (mm). On this figure, participants nr 2 and 8 are surrounded in green because they both had a higher post-operative sagittal displacement, as referred in subsection 5.3.6, however there is no particular characteristic that stands out for these patients from the following PCA. Participants nr 3 and 10 are surrounded in yellow because they both had an equal sagittal displacement before and after surgery, as referred in subsection 5.3.6, however there is no particular characteristic that stands out for these patients from the following PCA.

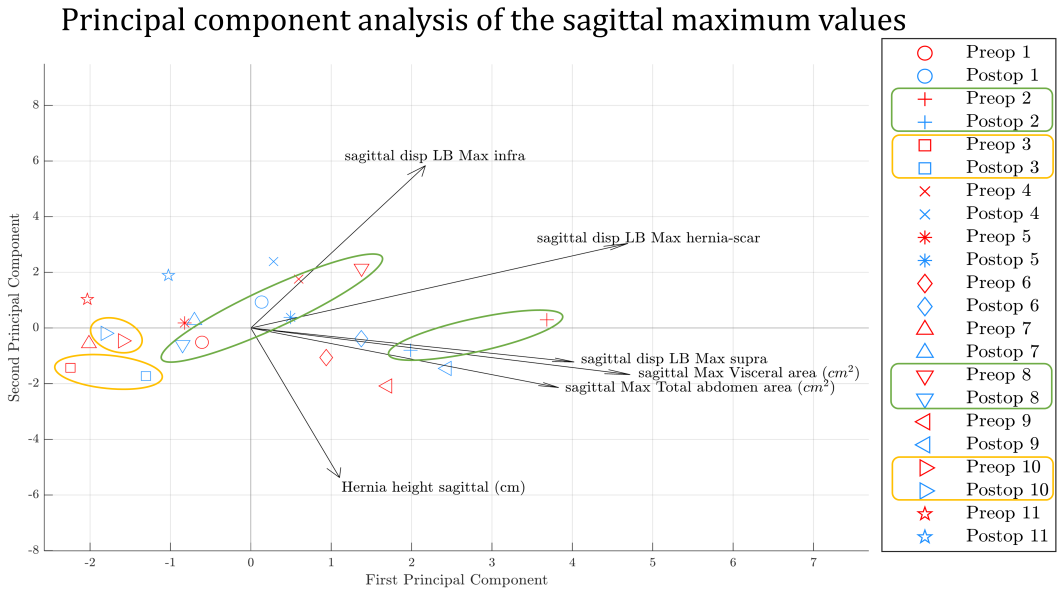

Figure 5.12.: PCA done on pre-operative and post-operative sagittal maximum values

6. Discussion

Table of contents

6.1. Contribution of the findings 203
6.1.1. Intra-abdominal pressure and abdominal wall motion 203
6.1.2. Cylindrical model for abdominal wall stress approximation . . . 203
6.1.3. Anatomical variability of the linea alba 204
6.1.4. AI for MRI segmentation and synthetic data generation 204
6.1.5. Post-operative changes and MRI analysis 205
6.2. Clinical significance 205
6.3. Limitations and perspectives 206
6.3.1. Imaging limitations 206
6.3.2. Simplifying assumptions 208
6.3.3. AI model generalisability 208
6.3.4. Sample size generalisability 209

Preface

This thesis presents a comprehensive study of the abdominal wall, focusing on its dynamic behaviour in both healthy and pathological conditions. By employing a variety of tools such as dynamic MRI-based measurements, biomechanical modelling, and AI-driven analysis, the work not only improves our understanding of abdominal wall biomechanics but also addresses key clinical challenges in hernia surgery.
This chapter aims to synthesise the results from the previous chapters, to reflect on the significance of the findings, to tie together the diverse elements of this doctoral project, showing how each chapter contributes to the overall understanding of abdominal wall biomechanics and surgical interventions. By connecting the various elements explored, we highlight how the advancements in imaging, biomechanical modelling, and AI-driven analysis contribute to improving patient-specific care in abdominal

wall hernia surgery. Lastly, this chapter will discuss limitations, and to propose future directions to further optimize the developed tools and models.

6.1. Contribution of the findings

6.1.1. Intra-abdominal pressure and abdominal wall motion

To address Objective 1, chapter 1 of the thesis focused on establishing the *in vivo* relationship between intra-abdominal pressure (IAP) and abdominal wall motion using dynamic MRI. The type of physiological activity (passive or active) undertaken, such as breathing, coughing or the Valsalva maneuver, affects changes in IAP and muscle displacement in distinctive ways. Correlations were found to be strong between displacement of the rectus abdominis and IAP during breathing, whereas lateral muscle displacement demonstrated a stronger correlation with IAP elevation during coughing and the Valsalva maneuver. This relationship is subject-specific and may not be extrapolated to other individuals. Consequently, in order to characterise the *in vivo* abdominal wall behaviour, it is essential to measure both intra-abdominal pressure and abdominal wall motion in the same participant. The ability to visualise and quantify muscle motion in relation to IAP provides valuable insight into the distribution of forces across the abdominal wall, laying the foundation for further analysis in chapter 2, which uses the same dataset to compute mechanical stress in the abdominal wall.

6.1.2. Cylindrical model for abdominal wall stress approximation

To address Objective 2, chapter 2 focused on developing a cylindrical model representing the abdominal wall. The objective was to quantify the mechanical stresses exerted during a passive breathing exercise. This model offers a streamlined approach to approximating the distribution of forces, facilitating the identification of regions where stress is concentrated. Notably, the midline zone is particularly subjected to circumferential stress. In particular, the linea alba is exposed to the highest stress. This finding gives rise to the question addressed in chapter 3 of understanding its anatomical variability, which is essential for addressing issues such as hernia formation.

6.1.3. Anatomical variability of the linea alba

To meet Objective 3, chapter 3 focused on the three-dimensional anatomical analysis of the linea alba, with the objective of uncovering its variability across different patient demographics (age, body mass index, gender) and geometrical variables (width, length, and curvature). These new insights into the anatomical variability of the linea alba is beneficial for the development of personalised surgical approaches and may enhance our comprehension of the risk factors associated with conditions such as hernias or diastasis recti. This anatomical study was based on manual segmentation using CT scans, which, while accurate, is a time-consuming and error-prone process. These limitations highlight the need for the introduction of more automated analysis, such as AI-based tools, as discussed in chapter 4, to automate and enhance the process of abdominal wall imaging segmentation. In addition to addressing these limitations, the proposed approach makes large-scale data analysis more feasible, thereby providing new methods to compensate for data scarcity, which is a particular problem encountered in clinical trials and *in vivo* studies.

6.1.4. AI for MRI segmentation and synthetic data generation

In order to address Objective 4, chapter 4 introduces the use of AI-based tools for the analysis of abdominal wall imaging. This may assist in overcoming limitations associated with dataset availability and manual tasks, which are time-consuming and susceptible to variability.
In chapter 4.1, the incorporation of nnUNet for the segmentation of abdominal wall muscles effectively automates this task, offering a more efficient and reliable analysis of abdominal MRI and the potential for new clinical applications in abdominal physiology. Furthermore, the Denoising Diffusion Probabilistic Model developed in chapter 4.2 demonstrated its capacity to simulate the mechanical functionality of the abdominal wall by generating synthetic MRI of hernia patients engaged in activities such as breathing, coughing, or a Valsalva maneuver, while accounting for the patient's surgical history, whether pre- or post-corrective abdominal surgery. The chapter 4 also shifts the focus from healthy subjects to patients undergoing ventral hernia surgery. Once the biomechanical stresses and the anatomical structure of the abdominal wall in healthy conditions have been understood, the logical next step is to investigate how surgery impacts these parameters in patients. This chapter is based on methodologies

developed in the earlier chapters (i.e., MRI-based motion analysis, segmentation) which are now applied to pathologic conditions, providing a more comprehensive view of how surgical intervention affects abdominal wall function.

6.1.5. Post-operative changes and MRI analysis

To address Objective 5, chapter 5 proposed a study based on dynamic MRI of patients before and after hernia surgery, which provided crucial information on the biomechanical recovery of the abdominal wall. The dynamic MRI analysis on both axial and sagittal planes revealed how muscle shape and displacement evolved post-surgery, thereby offering insights into the healing process and anatomical and functional changes. These findings indicate that real-time MRI evaluations have the potential to serve as a valuable tool for post-operative monitoring, enabling earlier interventions if complications arise and objective assessment of post-surgical outcomes.

6.2. Clinical significance

The findings of this thesis have several implications for clinical practice.
The integration of biomechanical models and dynamic MRI into pre-surgical evaluations represents a non-invasive and non-radiating method way for surgeons to gain insight into areas of high stress on the abdominal wall, assess tissue elasticity at the local level, and tailor their approaches based on patient-specific anatomy and biomechanics. This approach has the potential to enhance the selection of repair techniques and materials, as well as techniques that minimize tension. The 3D anatomical analysis of the linea alba offers a potential avenue for the development of personalized surgical techniques based on individual anatomical variations. The utilization of these tools in post-surgical follow-up could facilitate the assessment of repair integrity and muscle function recovery, in addition to the identification of high-stress areas susceptible to failure. This could help in detecting complications early, such as recurrences or weakened muscle regions.
Additionally, the model of synthetic MRI developed could provide dynamic synthetic sequences of the patient, thus assisting the surgeon in comprehending the patient's dynamic behaviour, both pre- and post-operatively. The implementation of automated segmentation in clinical practice could facilitate the real-time delineation of structures of interest.

The integration of AI-powered tools for segmentation, biomechanical models, and anatomical analysis paves the way for a more personalized approach to hernia repair, with implants and procedures tailored to the specific needs of each patient. Such an approach has the potential to reduce recurrence rates and improve recovery outcomes, particularly for high-risk groups (e.g., patients with a high BMI, smokers, or older patients).

6.3. Limitations and perspectives

While this thesis made valuable advancements in the biomechanical understanding of the abdominal wall, certain limitations should be acknowledged to contextualise the findings. This section will identify areas for further research and optimisation of the tools developed during this doctoral project.

6.3.1. Imaging limitations

The use of dynamic MRI throughout the thesis provided valuable insights into abdominal wall motion and pressure dynamics. However, this imaging modality was limited to 2D axial of sagittal views. This limited the study of motion and muscle deformation only on a given plane, missing to capture muscle contraction in other dimensions, as well as other surrounding structures such as diaphragm of pelvic floor. Nonetheless, this limitation allowed for high spatial (around 1mm in-plane) and temporal resolution (around 180ms between each image), necessary for dynamic acquisitions. Future work could address this limitation by adopting 3D+t MRI, with dedicated methods to reach an acceptable temporal resolution, or multi-slice acquisition, which would enable simultaneous acquisition of multiple planes, improving our ability to assess abdominal wall behaviour during complex physiological activities.
Moreover, simultaneous measurements of MRI and pressure were not feasible due to equipment incompatibilities (e.g., SmartPill sensor). The low sampling frequency (2 Hz) of the pressure sensor may be insufficient for accurately capturing maximum values and non-linearities. To reduce the errors based on these limitations, participants were trained several times on how to perform the exercises, and exercises were done several time in order to average all repetitions. Future research should focus on developing MRI-compatible pressure devices with higher sampling frequencies, ensuring accurate synchronization between pressure and motion data. Increasing the

sampling frequency of the SmartPill beyond 2Hz would be particularly beneficial in capturing rapid changes in IAP during dynamic activities.

Another notable limitation was the inability to segment the individual lateral muscles (external oblique, internal oblique, and transversus abdominis) due to insufficient spatial resolution, compromise found in order to visualise of the whole set of abdominal muscles. As a result, these muscles were treated as a composite in the analysis, geometrical characteristics of each individual muscle was not measured. Radial parcellation techniques (Jourdan, Rapacchi, et al. 2022) may offer a solution to this limitation, allowing for a more detailed analysis of individual muscle recruitment patterns.

In chapter 5, the mesh visibility of patients who underwent post-operative MRI after hernia repair was not investigated. The fat infiltration and muscle atrophy were not assessed, which can impact recovery and long-term outcomes after surgery, such as the biomechanical integration of the mesh with surrounding tissues. The lack of these measurements may limit the conclusions drawn about muscle function post-surgery. Incorporating quantitative MRI fat fraction analysis or DIXON imaging techniques could provide a more accurate assessment of muscle quality.

Lastly, although the MRI-based analysis has great potential, its accessibility and high cost limit its widespread use, particularly in low and middle income countries (Geethanath et al. 2019; Jalloul et al. 2023; *Magnetic Resonance Imaging (MRI) Units per Million People* 2024). It has recently been showed that Central Sub-Saharan Africa was the region with the highest age-standardized prevalence (existing cases) and incidence (new cases) rates of inguinal, femoral, and abdominal hernias (Ma et al. 2023), and increasing obesity burden (Steyn et al. 2014). To bridge this gap, research efforts should focus on developing cost-effective imaging techniques, and software solutions that can translate CT data into MRI-equivalent outputs as CT is a more common and affordable imaging modality globally (*Computed Tomography (CT) Imaging Units per Million People* 2024). For example, developing methods to convert CT abdominal data to MRI-like representations could be an impactful clinical solution. This is an ongoing work in others pathologies research field, including abdominal radiotherapy (Boulanger et al. 2021; McNaughton et al. 2023; S.-H. Hsu et al. 2020). Beyond imaging, the prevalence of hernias is closely linked to risk factors such as obesity and smoking. Public health efforts aimed at reducing these risk factors could help prevent hernias before they develop, rather than intervening after the pathology has already occurred. Policies and educational campaigns that promote healthy lifestyles,

such as maintaining a healthy weight and quitting smoking, could have a significant impact on reducing the incidence and recurrence of hernias, particularly in high-risk populations.

6.3.2. Simplifying assumptions

The cylindrical approximation of the abdominal wall in chapter 2 provided a useful framework for estimating stress distribution. However, this model simplifies the anatomy of the abdominal wall by assuming a uniform cylindrical shape with homogeneous properties throughout muscle group (e.g. lateral muscles or rectus abdominis), which does not fully capture the complex geometry and behaviour of the abdominal wall. More refined models, such as finite element analysis (FEA) using patient-specific geometries and non-linear tissue behaviours should be explored to validate the accuracy of stress predictions.
The relationship between pressure and abdominal wall motion in both chapter 1 and chapter 2 were considered as linear. Incorporating viscoelastic properties and non-linear pressure-motion relationships would result in more realistic models that better reflect clinical conditions. Additionally, the cylindrical model used Laplace's law, which is only suitable for passive activities like breathing. Future work should focus on extending this framework to include muscle activation and dynamic loading conditions (e.g., coughing or Valsalva maneuver).
In chapter 5, the variability in slice location based on hernia site complicated comparisons between patients. On the same chapter, due to the large number of variables, factors like physical activity level and smoking were not considered, even though they are known to influence hernia recurrence (Sørensen et al. 2005). Including these variables would provide a more comprehensive view of the factors contributing to hernia outcomes.

6.3.3. AI model generalisability

Although the nnUNet segmentation model performed well for the data presented in chapter 4.1, the training dataset was limited to 20 healthy subjects with dynamic acquisition at L3-L4 disc level, with relatively homogeneous characteristics in terms of physical activity, age, and BMI. This may limit the model's ability to generalize across more anatomically complex or pathological cases. Future studies should incorpo-

rate larger datasets that include more diverse anatomy range, patients with different anatomical variations, as well as subjects with hernias or other abdominal pathologies. Expanding the training set to include multiple axial planes (both above and below the umbilicus) would also increase the model's robustness by accounting for variability in muscle shape and insertion points.
Generative models for synthetic data augmentation should also be explored to mitigate data scarcity issues. The model presented in chapter 4.2 performed well the generative task, with good similarity results with the ground truth volumes. However, the synthetic data must be validated by clinicians and radiologists to assess its anatomical accuracy and clinical utility. In particular, some features such as the realistic appearance of the synthesised MRI, the consistency between the slices, if the exercise (whereas, breathing, coughing or Valsalva) is identifiable, whether the MRI concerns a pre-operative or post-operative stage, the anatomical correctness of the MRI, if we can differentiate between a real of synthesised MRI etc must be assessed .

6.3.4. Sample size generalisability

The relatively small cohort size used in this thesis (cohort of 18 healthy subjects in chapter 1, cohort of 17 healthy subjects in chapter 2, and cohort of 11 patients with an abdominal hernia in chapter 5) limits the generalisability of the findings. The studies of chapter 1 and chapter 2 were based on healthy subjects, whereas chapter 3 focused on subjects without abdominal wall pathology or aponeurosis defect. The chapter 5 studied patients with abdominal hernia. To confirm the validity of these results and strengthen the conclusions, it is essential to expand the study to include larger, more diverse populations. This could involve patients with different types of hernias (inguinal, hiatal, etc.) and post-operative conditions, which would allow researchers to better understand the factors influencing hernia recurrence and surgical outcomes across patient groups.

Conclusion

In conclusion, this thesis has contributed to the field of abdominal wall biomechanics and hernia surgery. By progressing from motion analysis to stress estimation, and ultimately applying these findings to clinical cases, this work links theory and practice, thereby offering new avenues of research on abdominal wall pathologies. By integrating imaging post-processing techniques, biomechanical modelling, and AI-based tools, the work provides a more comprehensive understanding of the abdominal wall's function in both healthy and pathological conditions. The tools developed during this thesis have the potential to improve patient-specific care, resulting in better surgical outcomes and fewer complications. Further research should focus on extending these methods and confirming their efficacy in a wider range of clinical settings, thus fully realising their potential to enhance patient outcomes.

Declaration of Generative AI and AI-assisted technologies in the writing process

During the writing of this PhD thesis, generative AI and AI-assisted technologies, such as ChatGPT or DeepL, were used to assist in language refinement and rephrasing of sections of the text. These tools were used to improve the clarity and flow of the text. However, all content, data interpretations, and conclusions were reviewed and edited by the author, who takes full responsibility for the content. Every effort has been made to ensure the integrity and scientific rigor of the thesis.

Funding

This doctoral project was funded by Université Gustave Eiffel. There were no conflicts of interest during the realization of this doctoral project. All research was conducted without external financial, personal, or institutional influences.

Data availability statement

The data that support the findings of this thesis is located in a main repository titled Experimental Abdominal Data that has been created on the **Recherche Data Gouv** platform.

Recherche Data Gouv is a national platform in France dedicated to the open sharing, management, and preservation of research data. It supports researchers in adhering to open science principles by providing a centralized repository where datasets from various research disciplines can be made publicly available. The platform ensures the accessibility, citation, and long-term preservation of data, fostering transparency and reproducibility in scientific research.

Within this https://entrepot.recherche.data.gouv.fr/dataverse/experimental-abdominal-dataExperimental Abdominal Data repository, two datasets are archived as of today in accordance with the FAIR principles (Findable, Accessible, Interoperable, and Reusable). Due to privacy and ethical concerns, data related to human participants are not publicly available. However, anonymized data can be shared with researchers who meet the criteria for access to confidential data in accordance with institutional guidelines.

These dataset on intra-abdominal pressure on healthy participants, used in chapter 1 and chapter 2, has been archived in a Recherche Data Gouv repository and can be accessed by contacting the research team. The corresponding README file containing detailed metadata and instructions for interpreting the data are included in Appendix C of this thesis.

These dataset on segmentation and registration of dynamic axial abdominal MRI of healthy participants, used in chapter 1 and chapter 2, has been archived in a Recherche Data Gouv repository and can be accessed by contacting the research team. The corresponding README file containing detailed metadata and instructions for interpreting the data are included in Appendix B of this thesis.

Another dataset will be released at the end of the generative MRI project, available on Belton's Github.

Bibliography

[Abu+06] Basim Abu-Rafea, George A. Vilos, Angelos G. Vilos, et al. “Effect of Body Habitus and Parity on Insufflated CO2 Volume at Various Intraabdominal Pressures during Laparoscopic Access in Women”. In: *Journal of Minimally Invasive Gynecology* 13.3 (2006), pp. 205–210. ISSN: 1553-4650. DOI: 10.1016/j.jmig.2006.02.004 (cit. on p. 92).

[Ahm+18] Mohamed G. Ahmed, Salah A. Mohamed, Walid A. ABOU EL-NAGA, et al. “Effect of Preoperative Abdominal Training on Abdominal Muscles Strength Outcomes after Ventral Hernia Repair”. In: *The Medical Journal of Cairo University* 86.12 (Dec. 2018), pp. 4495–4501. ISSN: 2536-9806. DOI: 10.21608/mjcu.2018.63151. (Visited on 08/26/2024) (cit. on pp. 68, 167, 191).

[Ang+16] A. M. Angelici, B. Perotti, C. Dezzi, et al. “Measurement of Intra-Abdominal Pressure in Large Incisional Hernia Repair to Prevent Abdominal Compartmental Syndrome”. In: *Il Giornale Di Chirurgia* 37.1 (2016), pp. 31–36. ISSN: 0391-9005. DOI: 10.11138/gchir/2016.37.1.031 (cit. on p. 70).

[Ant+00] T. Anthony, P. C. Bergen, L. T. Kim, et al. “Factors Affecting Recurrence Following Incisional Herniorrhaphy”. In: *World Journal of Surgery* 24.1 (Jan. 2000), 95–100, discussion 101. ISSN: 0364-2313. DOI: 10.1007/s002689910018 (cit. on p. 66).

[Ant+11] George A. Antoniou, George S. Georgiadis, Stavros A. Antoniou, et al. “Abdominal Aortic Aneurysm and Abdominal Wall Hernia as Manifestations of a Connective Tissue Disorder”. In: *Journal of Vascular Surgery* 54.4 (Oct. 2011), pp. 1175–1181. ISSN: 0741-5214. DOI: 10.1016/j.jvs.2011.02.065. (Visited on 09/28/2022) (cit. on p. 62).

[24a] *ANTsX/ANTs*. Advanced Normalization Tools Ecosystem. Aug. 2024. (Visited on 08/26/2024) (cit. on pp. 196, 197).

[ATO12] M. V. Anurov, S. M. Titkova, and A. P. Oettinger. “Biomechanical Compatibility of Surgical Mesh and Fascia Being Reinforced: Dependence of Experimental Hernia Defect Repair Results on Anisotropic Surgical Mesh Positioning”. In: *Hernia* 16.2 (Apr. 2012), pp. 199–210. ISSN: 1248-9204. DOI: 10.1007/s10029-011-0877-y. (Visited on 07/29/2022) (cit. on pp. 47, 69).

[Åst+07] H. Åstrand, A Rydén-Ahlgren, G. Sundkvist, et al. "Reduced Aortic Wall Stress in Diabetes Mellitus". In: *European Journal of Vascular and Endovascular Surgery* 33.5 (May 2007), pp. 592–598. ISSN: 1078-5884. DOI: 10.1016/j.ejvs.2006.11.011. (Visited on 06/05/2024) (cit. on p. 113).

[Ast+18] Laure Astruc, Maurice De Meulaere, Jean-François Witz, et al. "Characterization of the Anisotropic Mechanical Behavior of Human Abdominal Wall Connective Tissues". In: *Journal of the Mechanical Behavior of Biomedical Materials* 82 (June 2018), pp. 45–50. ISSN: 1751-6161. DOI: 10.1016/j.jmbbm.2018.03.012. (Visited on 11/23/2021) (cit. on pp. 47, 49, 130).

[AKP01a] Hubertus Axer, Diedrich Graf v Keyserlingk, and Andreas Prescher. "Collagen Fibers in Linea Alba and Rectus Sheaths: II. Variability and Biomechanical Aspects". In: *Journal of Surgical Research* 96.2 (Apr. 2001), pp. 239–245. ISSN: 0022-4804, 1095-8673. DOI: 10.1006/jsre.2000.6071. (Visited on 07/30/2022) (cit. on pp. 117, 121).

[AKP01b] Hubertus Axer, Diedrich Graf v. Keyserlingk, and Andreas Prescher. "Collagen Fibers in Linea Alba and Rectus Sheaths: I. General Scheme and Morphological Aspects". In: *Journal of Surgical Research* 96.1 (Mar. 2001), pp. 127–134. ISSN: 0022-4804. DOI: 10.1006/jsre.2000.6070. (Visited on 11/23/2021) (cit. on pp. 47, 53, 124, 130, 143, 146).

[Bar+07] U. Barbaros, O. Asoglu, R. Seven, et al. "The Comparison of Laparoscopic and Open Ventral Hernia Repairs: A Prospective Randomized Study". In: *Hernia* 11.1 (Feb. 2007), pp. 51–56. ISSN: 1248-9204. DOI: 10.1007/s10029-006-0160-9. (Visited on 10/04/2023) (cit. on p. 65).

[Bau+14] Rebeccah B. Baucom, William C. Beck, Michael D. Holzman, et al. "Prospective Evaluation of Surgeon Physical Examination for Detection of Incisional Hernias". In: *Journal of the American College of Surgeons* 218.3 (Mar. 2014), pp. 363–366. ISSN: 1072-7515. DOI: 10.1016/j.jamcollsurg.2013.12.007. (Visited on 01/19/2024) (cit. on pp. 79, 151).

[BTE98] M. Beauchemin, K.P.B. Thomson, and G. Edwards. "On the Hausdorff Distance Used for the Evaluation of Segmentation Results". In: *Canadian Journal of Remote Sensing* 24.1 (Mar. 1998), pp. 3–8. ISSN: 0703-8992. DOI: 10.1080/07038992.1998.10874685. (Visited on 10/10/2024) (cit. on p. 154).

[Bec+17] Chuck Becker, Margaret A. Plymale, John Wennergren, et al. "Compliance of the Abdominal Wall during Laparoscopic Insufflation". In: *Surgical Endoscopy* 31.4 (Apr. 2017), pp. 1947–1951. ISSN: 0930-2794, 1432-2218. DOI: 10.1007/s00464-016-5201-6. (Visited on 03/10/2022) (cit. on pp. 54, 93).

[Bee+09] Gertrude M. Beer, Antonius Schuster, Burkhardt Seifert, et al. “The Normal Width of the Linea Alba in Nulliparous Women”. In: *Clinical Anatomy* 22.6 (2009), pp. 706–711. ISSN: 1098-2353. DOI: 10.1002/ca.20836. (Visited on 10/11/2024) (cit. on p. 144).

[Bel+15] Juan Bellido Luque, A. Bellido Luque, J. Valdivia, et al. “Totally Endoscopic Surgery on Diastasis Recti Associated with Midline Hernias. The Advantages of a Minimally Invasive Approach. Prospective Cohort Study”. In: *Hernia* 19.3 (June 2015), pp. 493–501. ISSN: 1248-9204. DOI: 10.1007/s10029-014-1300-2. (Visited on 10/11/2024) (cit. on p. 130).

[Bel+19] Gabriele Bellio, Tommaso Cipolat Mis, Roberto Del Giudice, et al. “Preoperative Abdominal Computed Tomography at Rest and During Valsalva’s Maneuver to Evaluate Incisional Hernias”. In: *Surgical Innovation* 26.5 (Oct. 2019), pp. 519–527. ISSN: 1553-3506. DOI: 10.1177/1553350619849986. (Visited on 06/15/2022) (cit. on pp. 63, 79, 151).

[Bel+24] Niamh Belton, Victoria Joppin, Aonghus Lawlor, et al. “DyABD: A Dataset and Technique for Synthetically Generating Dynamic Abdominal MRIs with Dual Class and Anatomically Conditioned Diffusion Models”. In: *Medical Imaging with Deep Learning*. Apr. 2024. (Visited on 07/12/2024) (cit. on p. 156).

[Ben+13] H. Ben Abdelounis, S. Nicolle, M. Otténio, et al. “Effect of Two Loading Rates on the Elasticity of the Human Anterior Rectus Sheath”. In: *Journal of the Mechanical Behavior of Biomedical Materials* 20 (Apr. 2013), pp. 1–5. ISSN: 1751-6161. DOI: 10.1016/j.jmbbm.2012.12.002. (Visited on 11/03/2021) (cit. on pp. 51, 105).

[Bha+24] Priya Bhardwaj, Maria T. Huayllani, Molly A. Olson, et al. “Year-Over-Year Ventral Hernia Recurrence Rates and Risk Factors”. In: *JAMA Surgery* 159.6 (June 2024), pp. 651–658. ISSN: 2168-6254. DOI: 10.1001/jamasurg.2024.0233. (Visited on 07/16/2024) (cit. on pp. 56, 58, 158, 167).

[Bit+19] R. Bittner, K. Bain, V. K. Bansal, et al. “Update of Guidelines for Laparoscopic Treatment of Ventral and Incisional Abdominal Wall Hernias (International Endohernia Society (IEHS))—Part A”. In: *Surgical Endoscopy* 33.10 (Oct. 2019), pp. 3069–3139. ISSN: 1432-2218. DOI: 10.1007/s00464-019-06907-7. (Visited on 01/20/2025) (cit. on p. 65).

[BSG16] Trevor W. Blanchard, Camille Smith, and Sylvain G. Grenier. “In a Dynamic Lifting Task, the Relationship between Cross-Sectional Abdominal Muscle Thickness and the Corresponding Muscle Activity Is Affected by the Combined Use of a Weightlifting Belt and the Valsalva Maneuver”. In: *Journal of Electromyography and Kinesiology* 28 (June 2016), pp. 99–103. ISSN: 1050-6411. DOI: 10.1016/j.jelekin.2016.03.006. (Visited on 01/19/2024) (cit. on pp. 80, 151).

[Blá+15] Luis Alberto Blázquez Hernando, Miguel Ángel García Ureña, Javier López Monclús, et al. "Roturas de malla: una causa poco frecuente de recidiva herniaria". In: *Revista Hispanoamericana de Hernia* 3.4 (Oct. 2015), pp. 155–159. ISSN: 2255-2677. DOI: 10.1016/j.rehah.2015.02.006. (Visited on 09/28/2022) (cit. on p. 70).

[BMV24] Bruno Bordoni, Navid Mahabadi, and Matthew Varacallo. "Anatomy, Fascia". In: *StatPearls*. Treasure Island (FL): StatPearls Publishing, 2024. (Visited on 10/08/2024) (cit. on p. 36).

[Bor18] Magnus Borga. "MRI Adipose Tissue and Muscle Composition Analysis—a Review of Automation Techniques". In: *British Journal of Radiology* 91.1089 (Sept. 2018), p. 20180252. ISSN: 0007-1285. DOI: 10.1259/bjr.20180252. (Visited on 01/19/2024) (cit. on pp. 82, 152).

[Bou+21] M. Boulanger, Jean-Claude Nunes, H. Chourak, et al. "Deep Learning Methods to Generate Synthetic CT from MRI in Radiotherapy: A Literature Review". In: *Physica Medica* 89 (Sept. 2021), pp. 265–281. ISSN: 1120-1797. DOI: 10.1016/j.ejmp.2021.07.027. (Visited on 10/14/2024) (cit. on p. 207).

[BF10] CN. Brown and JG. Finch. "Which Mesh for Hernia Repair?" In: *Annals of The Royal College of Surgeons of England* 92.4 (May 2010), pp. 272–278. ISSN: 0035-8843. DOI: 10.1308/003588410X12664192076296. (Visited on 09/23/2022) (cit. on p. 69).

[BT05] Steven R. Brown and Jim Tiernan. "Transverse Verses Midline Incisions for Abdominal Surgery". In: *Cochrane Database of Systematic Reviews* 4 (2005). ISSN: 1465-1858. DOI: 10.1002/14651858.CD005199.pub2. (Visited on 10/19/2022) (cit. on pp. 74, 121).

[Bru17] BruceBlaus. *English: An Illustration Depicting Common Sites of a Hernia.* May 2017. (Visited on 10/08/2024) (cit. on p. 57).

[Bur+05] Jacobus W.A. Burger, Johan F. Lange, Jens A. Halm, et al. "Incisional Hernia: Early Complication of Abdominal Surgery". In: *World Journal of Surgery* 29.12 (Dec. 2005), pp. 1608–1613. ISSN: 1432-2323. DOI: 10.1007/s00268-005-7929-3. (Visited on 09/22/2022) (cit. on pp. 56, 71, 75).

[CEE93] S. J. Cala, J. Edyvean, and L. A. Engel. "Abdominal Compliance, Parasternal Activation, and Chest Wall Motion". In: *Journal of Applied Physiology* (Mar. 1993). DOI: 10.1152/jappl.1993.74.3.1398. (Visited on 09/21/2022) (cit. on p. 93).

[CG53] E. J. M. Campbell and J. H. Green. "The Variations in Intra-Abdominal Pressure and the Activity of the Abdominal Muscles during Breathing; a Study in Man". In: *The Journal of Physiology* 122.2 (Nov. 1953), pp. 282–290. ISSN: 0022-3751. (Visited on 09/21/2022) (cit. on pp. 52, 94, 105).

[Car12] Maria Helena Sequeira Cardoso. “Experimental Study of the Human Anterolateral Abdominal Wall”. In: (July 2012), p. 104 (cit. on pp. 49, 53, 123).

[Cas+97] A Casati, G Valentini, S Ferrari, et al. “Cardiorespiratory Changes during Gynaecological Laparoscopy by Abdominal Wall Elevation: Comparison with Carbon Dioxide Pneumoperitoneum”. In: *British Journal of Anaesthesia* 78.1 (Jan. 1997), pp. 51–54. ISSN: 0007-0912. DOI: 10.1093/bja/78.1.51. (Visited on 09/21/2022) (cit. on p. 54).

[Cav+21] M. Cavalli, A. Aiolfi, P. G. Bruni, et al. “Prevalence and Risk Factors for Diastasis Recti Abdominis: A Review and Proposal of a New Anatomical Variation”. In: *Hernia* 25.4 (Aug. 2021), pp. 883–890. ISSN: 1248-9204. DOI: 10.1007/s10029-021-02468-8. (Visited on 10/11/2024) (cit. on p. 130).

[CKM23] O. A. Cherkas, P. A. Kobeza, and D. G. Marchenko. “Basic Principles of the Structure and Organization of Connective Tissue”. In: *Morphologia* 1 (2023), pp. 77–85. ISSN: 1997-9665. (Visited on 10/08/2024) (cit. on p. 36).

[Cir+14] Alexander Ciritsis, Nienke Lynn Hansen, Alexandra Barabasch, et al. “Time-Dependent Changes of Magnetic Resonance Imaging–Visible Mesh Implants in Patients”. In: *Investigative Radiology* 49.7 (July 2014), pp. 439–444. ISSN: 0020-9996. DOI: 10.1097/RLI.0000000000000051. (Visited on 06/24/2022) (cit. on pp. 81, 151, 168).

[Cob+05] William S. Cobb, Justin M. Burns, Kent W. Kercher, et al. “Normal Intraabdominal Pressure in Healthy Adults”. In: *Journal of Surgical Research* 129.2 (Dec. 2005), pp. 231–235. ISSN: 0022-4804, 1095-8673. DOI: 10.1016/j.jss.2005.06.015. (Visited on 11/03/2021) (cit. on pp. 51, 52, 54, 106).

[CF10] Kerstyn Comley and Norman A. Fleck. “A Micromechanical Model for the Young’s Modulus of Adipose Tissue”. In: *International Journal of Solids and Structures* 47.21 (Oct. 2010), pp. 2982–2990. ISSN: 0020-7683. DOI: 10.1016/j.ijsolstr.2010.07.001. (Visited on 09/21/2022) (cit. on p. 49).

[] *Computed Tomography (CT) Imaging Units per Million People*. https://ourworldindata.org/g of-computed-tomography-ct-imaging. (Visited on 10/14/2024) (cit. on p. 207).

[CK99] J. Conze and U. Klinge. “Biocompatibility of Biomaterials - Clinical and Mechanical Aspects”. In: *Incisional Hernia*. Ed. by Volker Schumpelick and Andrew N. Kingsnorth. Berlin, Heidelberg: Springer, 1999, pp. 169–177. ISBN: 978-3-642-60123-1. DOI: 10.1007/978-3-642-60123-1_14 (cit. on p. 69).

[CKS01] Joachim Conze, Uwe Klinge, and V. Schumpelick. “Hernias”. In: *Surgical Treatment: Evidence-Based and Problem-Oriented*. Zuckschwerdt, 2001. (Visited on 10/08/2024) (cit. on p. 56).

[Coo+18] G. M. Cooney, A. Kiernan, D. C. Winter, et al. “Optimized Wound Closure Using a Biomechanical Abdominal Model”. In: *British Journal of Surgery* 105.4 (Mar. 2018), pp. 395–400. ISSN: 0007-1323. DOI: 10.1002/bjs.10753. (Visited on 11/04/2022) (cit. on p. 72).

[Coo+16] Gerard M. Cooney, Spencer P. Lake, Dominic M. Thompson, et al. “Uniaxial and Biaxial Tensile Stress–Stretch Response of Human Linea Alba”. In: *Journal of the Mechanical Behavior of Biomedical Materials* 63 (Oct. 2016), pp. 134–140. ISSN: 17516161. DOI: 10.1016/j.jmbbm.2016.06.015. (Visited on 03/02/2022) (cit. on pp. 47, 130).

[Cri+14] Cory N. Criss, Clayton C. Petro, David M. Krpata, et al. “Functional Abdominal Wall Reconstruction Improves Core Physiology and Quality-of-Life”. In: *Surgery* 156.1 (July 2014), pp. 176–182. ISSN: 0039-6060. DOI: 10.1016/j.surg.2014.04.010. (Visited on 07/16/2024) (cit. on pp. 68, 167, 192).

[CWP13] Christopher J. L. Cunningham, Bart L. Weathington, and David J. Pittenger. “Appendix B: Statistical Tables”. In: *Understanding and Conducting Research in the Health Sciences*. John Wiley & Sons, Ltd, 2013, pp. 479–520. ISBN: 978-1-118-64362-4. DOI: 10.1002/9781118643624.app2. (Visited on 11/27/2023) (cit. on pp. 98, 117).

[DOJ22] J. Daes, E. Oma, and L. N. Jorgensen. “Changes in the Abdominal Wall after Anterior, Posterior, and Combined Component Separation”. In: *Hernia* 26.1 (Feb. 2022), pp. 17–27. ISSN: 1248-9204. DOI: 10.1007/s10029-021-02535-0. (Visited on 09/23/2022) (cit. on p. 74).

[Dal+] Benjamin Dallaudiere, Hugo Sans, Gilles Reboul, et al. “Dynamic Magnetic Resonance Imaging (MRI) in Inguinal-Related Chronic Groin Pain (CGP): Comparison With Systematic Surgical Assessment”. In: *Cureus* 16.3 (), e55947. ISSN: 2168-8184. DOI: 10.7759/cureus.55947. (Visited on 07/16/2024) (cit. on pp. 79, 80, 168).

[deA+18] Nicola de’Angelis, Niccoló Petrucciani, Giusy Giannandrea, et al. “The Protocol of Low-Impact Laparoscopic Cholecystectomy: The Combination of Mini-Laparoscopy and Low-Pressure Pneumoperitoneum”. In: *Updates in Surgery* 70.4 (Dec. 2018), pp. 553–556. ISSN: 2038-3312. DOI: 10.1007/s13304-018-0591-8. (Visited on 09/20/2022) (cit. on p. 54).

[Dee+11] Corey R. Deeken, Michael S. Abdo, Margaret M. Frisella, et al. “Physicomechanical Evaluation of Absorbable and Nonabsorbable Barrier Composite Meshes for Laparoscopic Ventral Hernia Repair”. In: *Surgical Endoscopy* 25.5 (May 2011), pp. 1541–1552. ISSN: 1432-2218. DOI: 10.1007/s00464-010-1432-0. (Visited on 09/23/2022) (cit. on p. 69).

[DL17] Corey R. Deeken and Spencer P. Lake. “Mechanical Properties of the Abdominal Wall and Biomaterials Utilized for Hernia Repair”. In: *Journal of the Mechanical Behavior of Biomedical Materials* 74 (Oct. 2017), pp. 411–427. ISSN: 1751-6161. DOI: 10.1016/j.jmbbm.2017.05.008. (Visited on 11/11/2021) (cit. on pp. 49, 69, 111).

[Dee+16] E. B. Deerenberg, J. Verhelst, S. E. R. Hovius, et al. “Mesh Expansion as the Cause of Bulging after Abdominal Wall Hernia Repair”. In: *International Journal of Surgery Case Reports* 28 (2016), pp. 200–203. ISSN: 2210-2612. DOI: 10.1016/j.ijscr.2016.09.051 (cit. on p. 70).

[Dee+15] Eva B. Deerenberg, Joris J. Harlaar, Ewout W. Steyerberg, et al. “Small Bites versus Large Bites for Closure of Abdominal Midline Incisions (STITCH): A Double-Blind, Multicentre, Randomised Controlled Trial”. In: *The Lancet* 386.10000 (Sept. 2015), pp. 1254–1260. ISSN: 0140-6736, 1474-547X. DOI: 10.1016/S0140-6736(15)60459-7. (Visited on 11/14/2021) (cit. on p. 72).

[Die+10] Markus K. Diener, Sabine Voss, Katrin Jensen, et al. “Elective Midline Laparotomy Closure: The INLINE Systematic Review and Meta-Analysis”. In: *Annals of Surgery* 251.5 (May 2010), pp. 843–856. ISSN: 0003-4932. DOI: 10.1097/SLA.0b013e3181d973e4. (Visited on 10/13/2022) (cit. on p. 71).

[DOX22] Zolnamar Dorjsembe, Sodtavilan Odonchimed, and Furen Xiao. “Three-Dimensional Medical Image Synthesis with Denoising Diffusion Probabilistic Models”. In: *Medical Imaging with Deep Learning*. Apr. 2022. (Visited on 09/30/2024) (cit. on p. 160).

[Dor+24] Zolnamar Dorjsembe, Hsing-Kuo Pao, Sodtavilan Odonchimed, et al. “Conditional Diffusion Models for Semantic 3D Brain MRI Synthesis”. In: *IEEE Journal of Biomedical and Health Informatics* 28.7 (July 2024), pp. 4084–4093. ISSN: 2168-2208. DOI: 10.1109/JBHI.2024.3385504. (Visited on 09/30/2024) (cit. on p. 160).

[DuB+07] Derek A. DuBay, Winston Choi, Melanie G. Urbanchek, et al. “Incisional Herniation Induces Decreased Abdominal Wall Compliance via Oblique Muscle Atrophy and Fibrosis”. In: *Annals of Surgery* 245.1 (Jan. 2007), pp. 140–146. ISSN: 0003-4932. DOI: 10.1097/01.sla.0000251267.11012.85 (cit. on pp. 63, 66).

[DuB+06] Derek A. DuBay, Xue Wang, Belinda Adamson, et al. “Mesh Incisional Herniorrhaphy Increases Abdominal Wall Elastic Properties: A Mechanism for Decreased Hernia Recurrences in Comparison with Suture Repair”. In: *Surgery* 140.1 (July 2006), pp. 14–24. ISSN: 0039-6060. DOI: 10.1016/j.surg.2006.01.007 (cit. on pp. 62, 66, 69–71, 73, 75, 192).

[Edo11] Edoarado. *English: Anatomical Planes and Axis*. Nov. 2011. (Visited on 10/01/2024) (cit. on p. 31).

[] *EHS History – EHS*. (Visited on 10/08/2024) (cit. on p. 58).

[ElH+21] H. ElHawary, N. Barone, D. Zammit, et al. "Closing the Gap: Evidence-Based Surgical Treatment of Rectus Diastasis Associated with Abdominal Wall Hernias". In: *Hernia* 25.4 (Aug. 2021), pp. 827–853. ISSN: 1248-9204. DOI: 10.1007/s10029-021-02460-2. (Visited on 10/11/2024) (cit. on p. 131).

[Esp+22] A. Espinosa-de-los-Monteros, S. Dominguez-Arellano, J. Vazquez-Guadalupe, et al. "Immediate Changes in Intra-Abdominal Pressure and Lung Indicators in Patients Undergoing Complex Ventral Hernia Repair with the Transversus Abdominis Muscle Release, with and without Preoperative Botulinum Toxin". In: *Hernia* (Mar. 2022). ISSN: 1248-9204. DOI: 10.1007/s10029-022-02601-1. (Visited on 06/15/2022) (cit. on p. 70).

[Fed18a] Fedenko. *Diagram of Diastasis Recti*. 2018. (Visited on 10/01/2024) (cit. on p. 56).

[Fed18b] Fedenko. *Russian: Diagram of the White Line of the Abdomen, Cross-Section, above the Navel*. 2018. (Visited on 10/01/2024) (cit. on p. 56).

[Fed18c] Fedenko. *Scheme of Combination of Diastasis Recti with Hernia*. 2018. (Visited on 10/01/2024) (cit. on p. 56).

[Fer+22] Matteo Ferrante, Lisa Rinaldi, Francesca Botta, et al. "Application of nnU-Net for Automatic Segmentation of Lung Lesions on CT Images and Its Implication for Radiomic Models". In: *Journal of Clinical Medicine* 11.24 (Jan. 2022), p. 7334. ISSN: 2077-0383. DOI: 10.3390/jcm11247334. (Visited on 10/01/2024) (cit. on pp. 82, 152).

[Fin+14] C Fink, P Baumann, M N Wente, et al. "Incisional Hernia Rate 3 Years after Midline Laparotomy". In: *British Journal of Surgery* 101.2 (Jan. 2014), pp. 51–54. ISSN: 0007-1323. DOI: 10.1002/bjs.9364. (Visited on 10/08/2024) (cit. on p. 56).

[Fis+07] Tanja Fischer, Roland Ladurner, Alexander Gangkofer, et al. "Functional Cine MRI of the Abdomen for the Assessment of Implanted Synthetic Mesh in Patients after Incisional Hernia Repair: Initial Results". In: *European Radiology* 17.12 (Dec. 2007), pp. 3123–3129. ISSN: 1432-1084. DOI: 10.1007/s00330-007-0678-y. (Visited on 01/19/2024) (cit. on pp. 81, 151, 168).

[FHK03] David R. Flum, Karen Horvath, and Thomas Koepsell. "Have Outcomes of Incisional Hernia Repair Improved With Time?: A Population-Based Analysis". In: *Annals of Surgery* 237.1 (Jan. 2003), p. 129. ISSN: 0003-4932. (Visited on 11/10/2023) (cit. on p. 91).

[För+11] T. Förstemann, J. Trzewik, J. Holste, et al. “Forces and Deformations of the Abdominal Wall—A Mechanical and Geometrical Approach to the Linea Alba”. In: *Journal of Biomechanics* 44.4 (Feb. 2011), pp. 600–606. ISSN: 0021-9290. DOI: 10.1016/j.jbiomech.2010.11.021. (Visited on 11/03/2021) (cit. on pp. 47, 112, 124, 125).

[Fra06] Michael G. Franz. “The Biology of Hernias and the Abdominal Wall”. In: *Hernia* 10.6 (Dec. 2006), pp. 462–471. ISSN: 1248-9204. DOI: 10.1007/s10029-006-0144-9. (Visited on 11/17/2021) (cit. on pp. 59, 73).

[Fre+21] Fabien Fredon, Jérémy Hardy, Mélanie Germain, et al. “Correlations of the Rectus Abdominis Muscle Anatomy with Anthropometric Measurements”. In: *Surgical and Radiologic Anatomy* 43.4 (Apr. 2021), pp. 589–593. ISSN: 1279-8517. DOI: 10.1007/s00276-020-02655-9. (Visited on 10/11/2024) (cit. on pp. 130, 144).

[Fro+24] M. L. Frommer, R. Faderani, M. Kanapathy, et al. “Preoperative CT Imaging as a Tool to Predict Incisional Hernia Outcomes Following Abdominal Wall Reconstruction: A Retrospective Cohort Analysis”. In: *Journal of Plastic, Reconstructive & Aesthetic Surgery* 88 (Jan. 2024), pp. 369–377. ISSN: 1748-6815. DOI: 10.1016/j.bjps.2023.11.007. (Visited on 10/02/2024) (cit. on pp. 58, 78).

[FMC01] Mark A. Fusco, R. Shayn Martin, and and Michael C. Chang. “Estimation of Intra-Abdominal Pressure by Bladder Pressure Measurement: Validity and Methodology”. In: *Journal of Trauma and Acute Care Surgery* 50.2 (Feb. 2001), pp. 297–302. ISSN: 2163-0755. (Visited on 09/21/2022) (cit. on p. 51).

[Gar+23] A. J. García Moriana, A. Sánchez Arteaga, J. L. Gil Delgado, et al. “Evaluation of Rectus Abdominis Muscle Strength and Width of Hernia Defect in Patients Undergoing Incisional Hernia Surgery”. In: *Hernia* 27.4 (Aug. 2023), pp. 919–926. ISSN: 1248-9204. DOI: 10.1007/s10029-023-02834-8. (Visited on 08/23/2024) (cit. on pp. 59, 63, 167, 193).

[GAZ24] Adrianna Gatt, Sanjay Agarwal, and Patrick M. Zito. “Anatomy, Fascia Layers”. In: *StatPearls*. Treasure Island (FL): StatPearls Publishing, 2024. (Visited on 10/08/2024) (cit. on p. 36).

[Ge+20] Zhixing Ge, Junhua Zhao, Haibo Yu, et al. “Biomimetic Construction of Peritoneum to Imitate Peritoneal Metastasis Using Digital Micromirror Device-Based Optical Projection Lithography”. In: *Lab on a Chip* 20.17 (Aug. 2020), pp. 3109–3119. ISSN: 1473-0189. DOI: 10.1039/D0LC00361A. (Visited on 09/21/2022) (cit. on p. 49).

[GV19] Sairam Geethanath and John Thomas Vaughan Jr. “Accessible Magnetic Resonance Imaging: A Review”. In: *Journal of Magnetic Resonance Imaging* 49.7 (2019), e65–e77. ISSN: 1522-2586. DOI: 10.1002/jmri.26638. (Visited on 10/14/2024) (cit. on p. 207).

[Gig+21] Benoit Gignoux, Yves Bayon, Damien Martin, et al. “Incidence and Risk Factors for Incisional Hernia and Recurrence: Retrospective Analysis of the French National Database”. In: *Colorectal Disease* 23.6 (2021), pp. 1515–1523. ISSN: 1463-1318. DOI: 10.1111/codi.15581. (Visited on 10/07/2024) (cit. on pp. 58, 59, 75, 76).

[Gil+23] Madeline Gillies, Lakmali Anthony, Aymen Al-Roubaie, et al. “Trends in Incisional and Ventral Hernia Repair: A Population Analysis From 2001 to 2021”. In: *Cureus* 15.3 (Mar. 2023). ISSN: 2168-8184. DOI: 10.7759/cureus.35744. (Visited on 07/16/2024) (cit. on p. 167).

[GOR19] Jean-François Gillion, Pablo Ortega-Deballon, and Benoît Romain. *Eventrations Postopératoires : Rapport Présenté Au 121e Congrès Français de Chirurgie, 2019*. https://www.jle.com/fr/ouvrages/e-docs/eventrations_postoperatoires_313956/ouvrage.phtml. 2019. (Visited on 11/11/2021) (cit. on p. 66).

[GD23] Iliya Goldberg and Salvatore Docimo. “Normal Radiographic Anatomy of Anterior Abdominal Wall”. In: *Fundamentals of Hernia Radiology*. Ed. by Salvatore Docimo Jr., Jeffrey A. Blatnik, and Eric M. Pauli. Cham: Springer International Publishing, 2023, pp. 43–56. ISBN: 978-3-031-21336-6. DOI: 10.1007/978-3-031-21336-6_5. (Visited on 10/11/2024) (cit. on p. 130).

[Gos+03] K. Gossios, A. Zikou, P. Vazakas, et al. “Value of CT after Laparoscopic Repair of Postsurgical Ventral Hernia”. In: *Abdominal Imaging* 28.1 (Jan. 2003), pp. 0099–0102. ISSN: 1432-0509. DOI: 10.1007/s00261-001-0156-y. (Visited on 08/28/2024) (cit. on pp. 79, 168).

[GBS22] Aakansha Giri Goswami, Somprakas Basu, and Vijay Kumar Shukla. “Wound Healing in the Golden Agers: What We Know and the Possible Way Ahead”. In: *The International Journal of Lower Extremity Wounds* 21.3 (Sept. 2022), pp. 264–271. ISSN: 1534-7346. DOI: 10.1177/15347346211037841. (Visited on 10/08/2024) (cit. on p. 59).

[Grä+05] David Gräβel, Andreas Prescher, Sabine Fitzek, et al. “Anisotropy of Human Linea Alba: A Biomechanical Study”. In: *Journal of Surgical Research* 124.1 (Mar. 2005), pp. 118–125. ISSN: 0022-4804. DOI: 10.1016/j.jss.2004.10.010. (Visited on 11/23/2021) (cit. on p. 47).

[Gra+16] J. Grasa, M. Sierra, N. Lauzeral, et al. “Active Behavior of Abdominal Wall Muscles: Experimental Results and Numerical Model Formulation”. In: *Journal of the Mechanical Behavior of Biomedical Materials* 61 (Aug. 2016), pp. 444–454. ISSN: 1751-6161. DOI: 10.1016/j.jmbbm.2016.04.013. (Visited on 11/23/2021) (cit. on pp. 112, 124).

[Gra+24] Augusto Graziani e Sousa, Enrico Prajiante Bertolino, Amanda Godoi, et al. “Effect of an Abdominal Binder on Postoperative Outcomes after Ventral Hernia Repair: A Systematic Review and Meta-Analysis of Randomized Controlled Trials”. In: *Hernia* 29.1 (Nov. 2024), p. 20. ISSN: 1248-9204. DOI: 10.1007/s10029-024-03193-8. (Visited on 01/22/2025) (cit. on p. 65).

[GEP80] M J Greenall, Mary Evans, and A V Pollock. “Midline or Transverse Laparotomy? A Random Controlled Clinical Trial. Part I: Influence on Healing”. In: *British Journal of Surgery* 67.3 (Mar. 1980), pp. 188–190. ISSN: 0007-1323. DOI: 10.1002/bjs.1800670308. (Visited on 10/19/2022) (cit. on p. 74).

[Gud+02] F. Gudmundsson, A. Viste, H. Gislason, et al. “Comparison of Different Methods for Measuring Intra-Abdominal Pressure”. In: *Intensive Care Medicine* 28.4 (Apr. 2002), pp. 509–514. ISSN: 1432-1238. DOI: 10.1007/s00134-001-1187-0. (Visited on 07/28/2022) (cit. on p. 51).

[GT13] G. Guérin and F. Turquier. “Impact of the Defect Size, the Mesh Overlap and the Fixation Depth on Ventral Hernia Repairs: A Combined Experimental and Numerical Approach”. In: *Hernia: The Journal of Hernias and Abdominal Wall Surgery* 17.5 (Oct. 2013), pp. 647–655. ISSN: 1248-9204. DOI: 10.1007/s10029-013-1050-6 (cit. on pp. 67, 70, 71).

[Gue+24] P. Gueroult, V. Joppin, K. Chaumoitre, et al. “Linea Alba 3D Morphometric Variability by CT Scan Exploration”. In: *Hernia* 28.2 (Apr. 2024), pp. 485–494. ISSN: 1248-9204. DOI: 10.1007/s10029-023-02939-0. (Visited on 07/12/2024) (cit. on pp. 59, 127).

[Gun+15] Ulf Gunnarsson, Birgit Stark, Ursula Dahlstrand, et al. “Correlation between Abdominal Rectus Diastasis Width and Abdominal Muscle Strength”. In: *Digestive Surgery* 32.2 (Mar. 2015), pp. 112–116. ISSN: 0253-4886. DOI: 10.1159/000371859. (Visited on 10/03/2024) (cit. on p. 193).

[GVD01] C. Gutiérrez de la Peña, J. Vargas Romero, and J. Diéguez García. “The Value of CT Diagnosis of Hernia Recurrence after Prosthetic Repair of Ventral Incisional Hernias”. In: *European Radiology* 11.7 (July 2001), pp. 1161–1164. ISSN: 1432-1084. DOI: 10.1007/s003300000743. (Visited on 08/28/2024) (cit. on pp. 79, 168).

[Har+17] J. J. Harlaar, E. B. Deerenberg, R. S. Dwarkasing, et al. “Development of Incisional Herniation after Midline Laparotomy”. In: *BJS open* 1.1 (Feb. 2017), pp. 18–23. ISSN: 2474-9842. DOI: 10.1002/bjs5.3 (cit. on pp. 71, 75, 79, 151).

[Har+09] Joris J. Harlaar, Gabrielle H. van Ramshorst, Jeroen Nieuwenhuizen, et al. “Small Stitches with Small Suture Distances Increase Laparotomy Closure Strength”. In: *The American Journal of Surgery* 198.3 (Sept. 2009), pp. 392–

395. ISSN: 0002-9610. DOI: 10.1016/j.amjsurg.2008.10.018. (Visited on 09/23/2022) (cit. on pp. 67, 72).

[He+20] Wei He, Xiaoyu Liu, Shuai Wu, et al. "A Numerical Method for Guiding the Design of Surgical Meshes with Suitable Mechanical Properties for Specific Abdominal Hernias". In: *COMPUTERS IN BIOLOGY AND MEDICINE* 116 (Jan. 2020). ISSN: 0010-4825. DOI: 10.1016/j.compbiomed.2019.103531 (cit. on pp. 66, 67, 192).

[Hel16] F Helgstrand. "National Results after Ventral Hernia Repair". In: *Danish medical journal* 63.7 (July 2016). ISSN: 2245-1919. (Visited on 09/23/2022) (cit. on pp. 75, 121).

[Hel+13] Frederik Helgstrand, Jacob Rosenberg, Henrik Kehlet, et al. "Nationwide Prospective Study of Outcomes after Elective Incisional Hernia Repair". In: *Journal of the American College of Surgeons* 216.2 (Feb. 2013), pp. 217–228. ISSN: 1879-1190. DOI: 10.1016/j.jamcollsurg.2012.10.013. (Visited on 10/13/2022) (cit. on p. 59).

[Hen+20] N A Henriksen, A Montgomery, R Kaufmann, et al. "Guidelines for Treatment of Umbilical and Epigastric Hernias from the European Hernia Society and Americas Hernia Society". In: *British Journal of Surgery* 107.3 (Feb. 2020), pp. 171–190. ISSN: 0007-1323. DOI: 10.1002/bjs.11489. (Visited on 11/25/2024) (cit. on p. 65).

[Hen+15] Nadia A. Henriksen, Joachim H. Mortensen, Lars T. Sorensen, et al. "The Collagen Turnover Profile Is Altered in Patients with Inguinal and Incisional Hernia". In: *Surgery* 157.2 (Feb. 2015), pp. 312–321. ISSN: 0039-6060. DOI: 10.1016/j.surg.2014.09.006. (Visited on 10/08/2024) (cit. on p. 59).

[Her+11a] B. Hernández, E. Peña, G. Pascual, et al. "Mechanical and Histological Characterization of the Abdominal Muscle. A Previous Step to Modelling Hernia Surgery". In: *Journal of the Mechanical Behavior of Biomedical Materials* 4.3 (Apr. 2011), pp. 392–404. ISSN: 1751-6161. DOI: 10.1016/j.jmbbm.2010.11.012. (Visited on 11/03/2021) (cit. on pp. 47, 52).

[Her+13] B Hernández-Gascón, A Mena, E Peña, et al. "Understanding the Passive Mechanical Behavior of the Human Abdominal Wall". In: *Annals of biomedical engineering* 41.2 (Feb. 2013), pp. 433–444. ISSN: 1573-9686. DOI: 10.1007/s10439-012-0672-7. (Visited on 11/30/2021) (cit. on pp. 46, 69, 70, 112, 122, 124, 125).

[Her+11b] B. Hernández-Gascón, E. Peña, H. Melero, et al. "Mechanical Behaviour of Synthetic Surgical Meshes: Finite Element Simulation of the Herniated Abdominal Wall". In: *Acta Biomaterialia* 7.11 (Nov. 2011), pp. 3905–3913. ISSN: 1742-7061. DOI: 10.1016/j.actbio.2011.06.033. (Visited on 11/03/2022) (cit. on pp. 69, 111, 121).

[Her+21] P Hernández-Granados, N A Henriksen, F Berrevoet, et al. "European Hernia Society Guidelines on Management of Rectus Diastasis". In: *British Journal of Surgery* 108.10 (Oct. 2021), pp. 1189–1191. ISSN: 0007-1323. DOI: 10.1093/bjs/znab128. (Visited on 10/11/2024) (cit. on pp. 130, 134, 143, 145).

[HJA20] Jonathan Ho, Ajay Jain, and Pieter Abbeel. *Denoising Diffusion Probabilistic Models*. Dec. 2020. DOI: 10.48550/arXiv.2006.11239. arXiv: 2006.11239 [cs, stat]. (Visited on 09/30/2024) (cit. on pp. 159, 160).

[Hod+01] Paul W. Hodges, Andrew G. Cresswell, Karl Daggfeldt, et al. "In Vivo Measurement of the Effect of Intra-Abdominal Pressure on the Human Spine". In: *Journal of Biomechanics* 34.3 (Mar. 2001), pp. 347–353. ISSN: 0021-9290. DOI: 10.1016/S0021-9290(00)00206-2. (Visited on 09/28/2023) (cit. on p. 52).

[HG00] Paul W. Hodges and Simon C. Gandevia. "Changes in Intra-Abdominal Pressure during Postural and Respiratory Activation of the Human Diaphragm". In: *Journal of Applied Physiology* 89.3 (Sept. 2000), pp. 967–976. ISSN: 8750-7587, 1522-1601. DOI: 10.1152/jappl.2000.89.3.967. (Visited on 12/16/2021) (cit. on p. 108).

[Hol+16] Julie L. Holihan, Burzeen Karanjawala, Annie Ko, et al. "Use of Computed Tomography in Diagnosing Ventral Hernia Recurrence: A Blinded, Prospective, Multispecialty Evaluation". In: *JAMA Surgery* 151.1 (Jan. 2016), pp. 7–13. ISSN: 2168-6254. DOI: 10.1001/jamasurg.2015.2580. (Visited on 08/28/2024) (cit. on pp. 80, 168).

[HS07] C. Hollinsky and S. Sandberg. "Measurement of the Tensile Strength of the Ventral Abdominal Wall in Comparison with Scar Tissue". In: *Clinical Biomechanics* 22.1 (Jan. 2007), pp. 88–92. ISSN: 0268-0033. DOI: 10.1016/j.clinbiomech.2006.06.002. (Visited on 11/11/2021) (cit. on pp. 47, 48, 54, 124).

[Hol+92] David R. Holt, Stephen J. Kirk, Mark C. Regan, et al. "Effect of Age on Wound Healing in Healthy Human Beings". In: *Surgery* 112.2 (Aug. 1992), pp. 293–298. ISSN: 0039-6060, 1532-7361. DOI: 10.5555/uri:pii:003960609290223M. (Visited on 10/08/2024) (cit. on p. 59).

[Hop+18] William W. Hope, Zachary F. Williams, James W. Rawles, et al. "Rationale and Technique for Measuring Abdominal Wall Tension in Hernia Repair". In: *The American Surgeon* 84.9 (Sept. 2018), pp. 1446–1449. ISSN: 0003-1348. DOI: 10.1177/000313481808400947. (Visited on 09/22/2022) (cit. on p. 70).

[Hsu+20] Shu-Hui Hsu, Pamela DuPre, Qi Peng, et al. "A Technique to Generate Synthetic CT from MRI for Abdominal Radiotherapy". In: *Journal of Applied Clinical Medical Physics* 21.2 (2020), pp. 136–143. ISSN: 1526-9914. DOI: 10.1002/acm2.12816. (Visited on 10/14/2024) (cit. on p. 207).

[Hsu+12] Yvonne Hsu, Tanner J. Coleman, Robert W. Hitchcock, et al. "Clinical Evaluation of a Wireless Intra-Vaginal Pressure Transducer". In: *International Urogynecology Journal* 23.12 (Dec. 2012), pp. 1741–1747. ISSN: 1433-3023. DOI: 10.1007/s00192-012-1811-2. (Visited on 08/03/2022) (cit. on p. 51).

[Hun+02] Beverley J. Hunt, Lucilla Poston, Alison W. Halliday, et al. *An Introduction to Vascular Biology: From Basic Science to Clinical Practice*. Cambridge University Press, July 2002. ISBN: 978-0-521-79652-1 (cit. on p. 42).

[ILB89] Thomas J. Iberti, Charles E. Lieber, and Ernest Benjamin. "Determination of Intra-Abdominal Pressure Using a Transurethral Bladder Catheter: Clinical Validation of the Technique". In: *Anesthesiology* 70.1 (Jan. 1989), pp. 47–50. ISSN: 0003-3022. DOI: 10.1097/00000542-198901000-00011. (Visited on 09/21/2022) (cit. on p. 51).

[Ise+21] Fabian Isensee, Paul F. Jaeger, Simon A. A. Kohl, et al. "nnU-Net: A Self-Configuring Method for Deep Learning-Based Biomedical Image Segmentation". In: *Nature Methods* 18.2 (Feb. 2021), pp. 203–211. ISSN: 1548-7105. DOI: 10.1038/s41592-020-01008-z. (Visited on 01/19/2024) (cit. on pp. 82, 152, 154).

[Jaf+05] Tracy A. Jaffe, Martin J. O'Connell, John P. Harris, et al. "MDCT of Abdominal Wall Hernias: Is There a Role for Valsalva's Maneuver?" In: *American Journal of Roentgenology* 184.3 (Mar. 2005), pp. 847–851. ISSN: 0361-803X. DOI: 10.2214/ajr.184.3.01840847. (Visited on 06/15/2022) (cit. on pp. 63, 79, 94, 151, 153).

[Jal+23] Mohammad Jalloul, Monica Miranda-Schaeubinger, Abass M. Noor, et al. "MRI Scarcity in Low- and Middle-Income Countries". In: *NMR in Biomedicine* 36.12 (2023), e5022. ISSN: 1099-1492. DOI: 10.1002/nbm.5022. (Visited on 10/14/2024) (cit. on p. 207).

[Jan+04] P. Lynen Jansen, P. R. Mertens, U. Klinge, et al. "The Biology of Hernia Formation". In: *Surgery* 136.1 (July 2004), pp. 1–4. ISSN: 0039-6060. DOI: 10.1016/j.surg.2004.01.004. (Visited on 10/08/2024) (cit. on p. 59).

[Jen76] T P N Jenkins. "The Burst Abdominal Wound: A Mechanical Approach". In: *British Journal of Surgery* 63.11 (Nov. 1976), pp. 873–876. ISSN: 0007-1323. DOI: 10.1002/bjs.1800631110. (Visited on 11/04/2022) (cit. on p. 72).

[JKJ14] K. K. Jensen, M. Kjaer, and L. N. Jorgensen. "Abdominal Muscle Function and Incisional Hernia: A Systematic Review". In: *Hernia* 18.4 (Aug. 2014), pp. 481–486. ISSN: 1248-9204. DOI: 10.1007/s10029-014-1242-8. (Visited on 07/16/2024) (cit. on p. 167).

[JP20] Dr Somen Jha and Dr Pankaj. “A Study to Assess the Prevalence and Risk Factors of Inguinal Hernia”. In: *International Journal of Surgery Science* 4.3 (2020), pp. 330–332. ISSN: 2616-3470. DOI: 10.33545/surgery.2020.v4.i3e.514. (Visited on 10/08/2024) (cit. on p. 59).

[JB07] E. K. John and I. D. Beith. “Can Activity within the External Abdominal Oblique Be Measured Using Real-Time Ultrasound Imaging?” In: *Clinical Biomechanics* 22.9 (Nov. 2007), pp. 972–979. ISSN: 0268-0033. DOI: 10.1016/j.clinbiomech.2007.07.005. (Visited on 11/11/2021) (cit. on pp. 45, 107).

[Jol+20] Joshua S. Jolissaint, Bryan V. Dieffenbach, Thomas C. Tsai, et al. “Surgical Site Occurrences, Not Body Mass Index, Increase the Long-Term Risk of Ventral Hernia Recurrence”. In: *Surgery* 167.4 (Apr. 2020), pp. 765–771. ISSN: 0039-6060. DOI: 10.1016/j.surg.2020.01.001. (Visited on 09/22/2022) (cit. on p. 71).

[JMB23] V. Joppin, C. Masson, and T. Bege. “Chapitre 2 - Biomécanique de La Paroi Abdominale”. In: *Chirurgie Pariétale*. Ed. by Guillaume Passot and Yohann Renard. Paris: Elsevier Masson, Jan. 2023, pp. 15–25. ISBN: 978-2-294-77733-2. DOI: 10.1016/B978-2-294-77733-2.00002-5. (Visited on 09/16/2024) (cit. on pp. 41, 43, 44, 53, 61).

[Jop+24] Victoria Joppin, Niamh Belton, Marc Adrien Hostin, et al. “Automatic Muscle Segmentation on Healthy Abdominal MRI Using nnUNet”. In: *Medical Imaging with Deep Learning*. Apr. 2024. (Visited on 07/12/2024) (cit. on p. 149).

[Jop+25] Victoria Joppin, Arthur Jourdan, David Bendahan, et al. “Towards a Better Understanding of Abdominal Wall Biomechanics: *In Vivo* Relationship between Dynamic Intra-Abdominal Pressure and Magnetic Resonance Imaging Measurements”. In: *Clinical Biomechanics* 121 (Jan. 2025), p. 106396. ISSN: 0268-0033. DOI: 10.1016/j.clinbiomech.2024.106396. (Visited on 01/20/2025) (cit. on pp. 88, 171, 173, 257, 258, 264, 265).

[Jou21] Arthur Jourdan. “Explorations Combinées Biomécaniques et Physiologiques de La Paroi Abdominale in Vivo”. These de Doctorat. Aix-Marseille, Dec. 2021. (Visited on 10/26/2022) (cit. on p. 53).

[Jou+21] Arthur Jourdan, Arnaud Le Troter, Pierre Daude, et al. “Semiautomatic Quantification of Abdominal Wall Muscles Deformations Based on Dynamic MRI Image Registration”. In: *NMR in Biomedicine* 34.4 (2021), e4470. ISSN: 1099-1492. DOI: 10.1002/nbm.4470. (Visited on 11/03/2021) (cit. on pp. 95, 114, 153, 196).

[Jou+22] Arthur Jourdan, Stanislas Rapacchi, Maxime Guye, et al. “Dynamic-MRI Quantification of Abdominal Wall Motion and Deformation during Breathing and Muscular Contraction”. In: *Computer Methods and Programs in Biomedicine* 217 (Apr. 2022), p. 106667. ISSN: 1872-7565. DOI: 10.1016/j.cmpb.2022.106667 (cit. on pp. 49, 52, 53, 80, 92, 94, 107, 113, 114, 122, 123, 151, 153, 154, 158, 168, 172, 173, 192, 207, 257, 258, 260).

[Jou+20] Arthur Jourdan, Andrea Soucasse, Ugo Scemama, et al. “Abdominal Wall Morphometric Variability Based on Computed Tomography: Influence of Age, Gender, and Body Mass Index”. In: *Clinical Anatomy* 33.8 (2020), pp. 1110–1119. ISSN: 1098-2353. DOI: 10.1002/ca.23548. (Visited on 07/30/2022) (cit. on pp. 54, 55, 59, 106, 107, 130, 131, 134, 144).

[Jun+01] K. Junge, U. Klinge, A. Prescher, et al. “Elasticity of the Anterior Abdominal Wall and Impact for Reparation of Incisional Hernias Using Mesh Implants”. In: *Hernia: The Journal of Hernias and Abdominal Wall Surgery* 5.3 (Sept. 2001), pp. 113–118. ISSN: 1265-4906. DOI: 10.1007/s100290100019 (cit. on pp. 47, 66, 68, 69, 73, 106, 107, 192).

[Jun+06] K. Junge, R. Rosch, U. Klinge, et al. “Risk Factors Related to Recurrence in Inguinal Hernia Repair: A Retrospective Analysis”. In: *Hernia* 10.4 (Aug. 2006), pp. 309–315. ISSN: 1248-9204. DOI: 10.1007/s10029-006-0096-0. (Visited on 10/12/2024) (cit. on p. 58).

[Kal+21] Friedrich Kallinowski, Yannique Ludwig, Dominik Gutjahr, et al. “Biomechanical Influences on Mesh-Related Complications in Incisional Hernia Repair”. In: *Frontiers in Surgery* 8 (2021), p. 518. ISSN: 2296-875X. DOI: 10.3389/fsurg.2021.763957. (Visited on 11/11/2021) (cit. on pp. 62, 69, 72).

[Kam14] Pierre Kamina. *Anatomie clinique. Tome 3 : Thorax, abdomen, 4e éd. | Maloine*. https://www.maloine.fr/anatomie-clinique-tome-3-thorax-abdomen-4e-ed-maloine.html. 2014. (Visited on 10/11/2024) (cit. on pp. 130, 144).

[KPS14] Tovy Haber Kamine, Efstathios Papavassiliou, and Benjamin E. Schneider. “Effect of Abdominal Insufflation for Laparoscopy on Intracranial Pressure”. In: *JAMA Surgery* 149.4 (Apr. 2014), pp. 380–382. ISSN: 2168-6254. DOI: 10.1001/jamasurg.2013.3024. (Visited on 09/21/2022) (cit. on p. 54).

[Kar+23] Ali Akbar Karkhaneh Yousefi, Baptiste Pierrat, Anicet Le Ruyet, et al. “Patient-Specific Computational Simulations of Wound Healing Following Midline Laparotomy Closure”. In: *Biomechanics and Modeling in Mechanobiology* 22.5 (Oct. 2023), pp. 1589–1605. ISSN: 1617-7940. DOI: 10.1007/s10237-023-01708-3. (Visited on 10/11/2024) (cit. on p. 144).

[Kar+15] Anette Karlsson, Johannes Rosander, Thobias Romu, et al. "Automatic and Quantitative Assessment of Regional Muscle Volume by Multi-Atlas Segmentation Using Whole-Body Water–Fat MRI". In: *Journal of Magnetic Resonance Imaging* 41.6 (2015), pp. 1558–1569. ISSN: 1522-2586. DOI: 10.1002/jmri.24726. (Visited on 01/19/2024) (cit. on pp. 81, 152).

[KAH23] Ali Karrech, Hairul Ahmad, and Jeffrey M. Hamdorf. "Biomechanical Stability of Hernia-Damaged Abdominal Walls". In: *Scientific Reports* 13.1 (Mar. 2023), p. 4936. ISSN: 2045-2322. DOI: 10.1038/s41598-023-31674-w. (Visited on 10/11/2024) (cit. on p. 144).

[Kau+22] R. L. Kaufmann, C. S. Reiner, U. A. Dietz, et al. "Normal Width of the Linea Alba, Prevalence, and Risk Factors for Diastasis Recti Abdominis in Adults, a Cross-Sectional Study". In: *Hernia* 26.2 (Apr. 2022), pp. 609–618. ISSN: 1248-9204. DOI: 10.1007/s10029-021-02493-7. (Visited on 10/11/2024) (cit. on pp. 130, 131, 134, 143–145).

[KS23] Masashi Kawabata and Norihiro Shima. "Interaction of Breathing Pattern and Posture on Abdominal Muscle Activation and Intra-Abdominal Pressure in Healthy Individuals: A Comparative Cross-Sectional Study". In: *Scientific Reports* 13.1 (July 2023), p. 11338. ISSN: 2045-2322. DOI: 10.1038/s41598-023-37629-5. (Visited on 11/23/2023) (cit. on p. 92).

[Al-+11] Abdulla Al-Khan, Manan Shah, Mohamed Altabban, et al. "Measurement of Intraabdominal Pressure in Pregnant Women at Term". In: *The Journal of Reproductive Medicine* 56.1-2 (2011), pp. 53–57. ISSN: 0024-7758 (cit. on pp. 57, 59).

[KP98] Markus A. Kirchgeorg and Mathias Prokop. "Increasing Spiral CT Benefits with Postprocessing Applications". In: *European Journal of Radiology* 28.1 (Aug. 1998), pp. 39–54. ISSN: 0720-048X, 1872-7727. DOI: 10.1016/S0720-048X(98)00011-4. (Visited on 10/11/2024) (cit. on p. 130).

[Kir+11] Miglena Kirilova, Stoyan Stoytchev, Dessislava Pashkouleva, et al. "Experimental Study of the Mechanical Properties of Human Abdominal Fascia". In: *Medical Engineering & Physics* 33.1 (Jan. 2011), pp. 1–6. ISSN: 1350-4533. DOI: 10.1016/j.medengphy.2010.07.017. (Visited on 11/03/2021) (cit. on p. 47).

[Kir+13] Andrew W. Kirkpatrick, Derek J. Roberts, Jan De Waele, et al. "Intra-Abdominal Hypertension and the Abdominal Compartment Syndrome: Updated Consensus Definitions and Clinical Practice Guidelines from the World Society of the Abdominal Compartment Syndrome". In: *Intensive Care Medicine* 39.7 (July 2013), pp. 1190–1206. ISSN: 1432-1238. DOI: 10.1007/s00134-013-2906-z (cit. on p. 42).

[Kli+98] U. Klinge, M. Müller, C. Brücker, et al. “Application of Three-Dimensional Stereography to Assess Abdominal Wall Mobility”. In: *Hernia* 2.1 (Mar. 1998), pp. 11–14. ISSN: 1248-9204. DOI: 10.1007/BF01207767. (Visited on 06/15/2022) (cit. on p. 92).

[KLE15] Gernot Köhler, Ruzica-Rosalia Luketina, and Klaus Emmanuel. “Sutured Repair of Primary Small Umbilical and Epigastric Hernias: Concomitant Rectus Diastasis Is a Significant Risk Factor for Recurrence”. In: *World Journal of Surgery* 39.1 (Jan. 2015), pp. 121–126. ISSN: 1432-2323. DOI: 10.1007/s00268-014-2765-y. (Visited on 09/22/2022) (cit. on pp. 75, 130).

[Kon+11] Moritz A. Konerding, Michael Bohn, Tanja Wolloscheck, et al. “Maximum Forces Acting on the Abdominal Wall: Experimental Validation of a Theoretical Modeling in a Human Cadaver Study”. In: *Medical Engineering & Physics* 33.6 (July 2011), pp. 789–792. ISSN: 1873-4030. DOI: 10.1016/j.medengphy.2011.01.010 (cit. on pp. 50, 75, 92, 112).

[Kon+24] Nicholas Konz, Yuwen Chen, Haoyu Dong, et al. *Anatomically-Controllable Medical Image Generation with Segmentation-Guided Diffusion Models*. June 2024. DOI: 10.48550/arXiv.2402.05210. arXiv: 2402.05210 [cs, eess, stat]. (Visited on 09/30/2024) (cit. on p. 162).

[Kot+11] Efstathios V. Kotidis, Theodosis S. Papavramidis, Kostas Ioannidis, et al. “The Effect of Chronically Increased Intra-Abdominal Pressure on Rectus Abdominis Muscle Histology an Experimental Study on Rabbits”. In: *Journal of Surgical Research* 171.2 (Dec. 2011), pp. 609–614. ISSN: 0022-4804, 1095-8673. DOI: 10.1016/j.jss.2010.06.034. (Visited on 07/31/2022) (cit. on p. 51).

[Kri+23] Kyleigh Kriener, Raushan Lala, Ryan Anthony Peter Homes, et al. “Mechanical Characterization of the Human Abdominal Wall Using Uniaxial Tensile Testing”. In: *Bioengineering* 10.10 (Oct. 2023), p. 1213. ISSN: 2306-5354. DOI: 10.3390/bioengineering10101213. (Visited on 06/06/2024) (cit. on pp. 122, 123).

[Kro+17] L. F. Kroese, J. J. Harlaar, C. Ordrenneau, et al. “The ‘AbdoMAN’: An Artificial Abdominal Wall Simulator for Biomechanical Studies on Laparotomy Closure Techniques”. In: *Hernia* 21.5 (Oct. 2017), pp. 783–791. ISSN: 1248-9204. DOI: 10.1007/s10029-017-1615-x. (Visited on 09/22/2022) (cit. on pp. 67, 68).

[Kro+18a] L. F. Kroese, D. Sneiders, G. J. Kleinrensink, et al. “Comparing Different Modalities for the Diagnosis of Incisional Hernia: A Systematic Review”. In: *Hernia* 22.2 (Apr. 2018), pp. 229–242. ISSN: 1248-9204. DOI: 10.1007/s10029-017-1725-5. (Visited on 10/04/2023) (cit. on p. 81).

[Kro+18b] Leonard F. Kroese, Jean-Francois Gillion, Johannes Jeekel, et al. "Primary and Incisional Ventral Hernias Are Different in Terms of Patient Characteristics and Postoperative Complications - A Prospective Cohort Study of 4,565 Patients". In: *International Journal of Surgery* 51 (Mar. 2018), pp. 114–119. ISSN: 1743-9191. DOI: 10.1016/j.ijsu.2018.01.010. (Visited on 10/08/2024) (cit. on p. 56).

[Kro+18c] Leonard F. Kroese, Gert-Jan Kleinrensink, Johan F. Lange, et al. "External Validation of the European Hernia Society Classification for Postoperative Complications after Incisional Hernia Repair: A Cohort Study of 2,191 Patients". In: *Journal of the American College of Surgeons* 226.3 (Mar. 2018), 223–229.e1. ISSN: 1072-7515. DOI: 10.1016/j.jamcollsurg.2017.11.018. (Visited on 10/08/2024) (cit. on p. 58).

[KHN84] I L Kron, P K Harman, and S P Nolan. "The Measurement of Intra-Abdominal Pressure as a Criterion for Abdominal Re-Exploration." In: *Annals of Surgery* 199.1 (Jan. 1984), pp. 28–30. ISSN: 0003-4932. (Visited on 09/21/2022) (cit. on p. 51).

[Kus+21] Bradley Kushner, Carter Starnes, Maggie Sehnert, et al. "Identifying Critical Computed Tomography (CT) Imaging Findings for the Preoperative Planning of Ventral Hernia Repairs". In: *Hernia* 25.4 (Aug. 2021), pp. 963–969. ISSN: 1248-9204. DOI: 10.1007/s10029-020-02314-3. (Visited on 08/26/2024) (cit. on pp. 80, 168).

[Kwa+21] Yeshe Manuel Kway, Kashthuri Thirumurugan, Mya Thway Tint, et al. "Automated Segmentation of Visceral, Deep Subcutaneous, and Superficial Subcutaneous Adipose Tissue Volumes in MRI of Neonates and Young Children". In: *Radiology: Artificial Intelligence* 3.5 (Sept. 2021), e200304. DOI: 10.1148/ryai.2021200304. (Visited on 01/19/2024) (cit. on pp. 82, 152).

[Kyc09] Kychot. *English: The Needle EMG of Paravertebral Muscles*. May 2009. (Visited on 10/01/2024) (cit. on p. 45).

[Lac+87] S. R. Lacey, J. Bruce, S. P. Brooks, et al. "The Relative Merits of Various Methods of Indirect Measurement of Intraabdominal Pressure as a Guide to Closure of Abdominal Wall Defects". In: *Journal of Pediatric Surgery* 22.12 (Dec. 1987), pp. 1207–1211. ISSN: 0022-3468. DOI: 10.1016/S0022-3468(87)80739-X. (Visited on 08/03/2022) (cit. on p. 51).

[Le +12] R. Le Huu Nho, D. Mege, M. Ouaïssi, et al. "Incidence and Prevention of Ventral Incisional Hernia". In: *Journal of Visceral Surgery*. Hernia Surgery 149.5, Supplement (Oct. 2012), e3–e14. ISSN: 1878-7886. DOI: 10.1016/j.jviscsurg.2012.05.004. (Visited on 11/03/2021) (cit. on pp. 59, 60, 65, 74, 121, 191, 192).

[Le +20] A. Le Ruyet, Y. Yurtkap, F. P. J. den Hartog, et al. "Differences in Biomechanics of Abdominal Wall Closure with and without Mesh Reinforcement: A Study in Post Mortem Human Specimens". In: *Journal of the Mechanical Behavior of Biomedical Materials* 105 (May 2020), p. 103683. ISSN: 1751-6161. DOI: 10.1016/j.jmbbm.2020.103683. (Visited on 11/23/2021) (cit. on pp. 48, 53, 54, 66, 69, 72, 92, 192).

[Len+19] Leon Lenchik, Laura Heacock, Ashley A. Weaver, et al. "Automated Segmentation of Tissues Using CT and MRI: A Systematic Review". In: *Academic Radiology* 26.12 (Dec. 2019), pp. 1695–1706. ISSN: 1076-6332, 1878-4046. DOI: 10.1016/j.acra.2019.07.006. (Visited on 12/08/2023) (cit. on pp. 81, 152).

[Les+24] C. Lesch, R. Nessel, D. Adolf, et al. "STRONGHOLD First-Year Results of Biomechanically Calculated Abdominal Wall Repair: A Propensity Score Matching". In: *Hernia* 28.1 (Feb. 2024), pp. 63–73. ISSN: 1248-9204. DOI: 10.1007/s10029-023-02897-7. (Visited on 10/01/2024) (cit. on p. 74).

[Lev+16] A. Levillain, M. Orhant, F. Turquier, et al. "Contribution of Collagen and Elastin Fibers to the Mechanical Behavior of an Abdominal Connective Tissue". In: *Journal of the Mechanical Behavior of Biomedical Materials* 61 (Aug. 2016), pp. 308–317. ISSN: 1751-6161. DOI: 10.1016/j.jmbbm.2016.04.006. (Visited on 06/15/2022) (cit. on pp. 47, 130).

[Li+16] Xiangrui Li, Paul S. Morgan, John Ashburner, et al. "The First Step for Neuroimaging Data Analysis: DICOM to NIfTI Conversion". In: *Journal of Neuroscience Methods* 264 (May 2016), pp. 47–56. ISSN: 1872-678X. DOI: 10.1016/j.jneumeth.2016.03.001 (cit. on p. 170).

[Lia+17] Mike K. Liang, Julie L. Holihan, Kamal Itani, et al. "Ventral Hernia Management: Expert Consensus Guided by Systematic Review". In: *Annals of Surgery* 265.1 (Jan. 2017), pp. 80–89. ISSN: 0003-4932. DOI: 10.1097/SLA.0000000000001701. (Visited on 09/23/2022) (cit. on p. 68).

[Lia+20] Chien-Hung Liao, Chi-Tung Cheng, Chih-Chi Chen, et al. "An Ingestible Electronics for Continuous and Real-Time Intraabdominal Pressure Monitoring". In: *Journal of Personalized Medicine* 11.1 (Dec. 2020), p. 12. ISSN: 2075-4426. DOI: 10.3390/jpm11010012. (Visited on 02/17/2022) (cit. on p. 52).

[Lia+11] Lih-Jiun Liaw, Miao-Ju Hsu, Chien-Fen Liao, et al. "The Relationships Between Inter-Recti Distance Measured by Ultrasound Imaging and Abdominal Muscle Function in Postpartum Women: A 6-Month Follow-up Study". In: *Journal of Orthopaedic & Sports Physical Therapy* 41.6 (June 2011), pp. 435–443. ISSN: 0190-6011. DOI: 10.2519/jospt.2011.3507. (Visited on 10/11/2024) (cit. on pp. 143, 144).

[Lie+15] Samuel C. Lien, Yaxi Hu, Adi Wollstein, et al. “Contraction of Abdominal Wall Muscles Influences Size and Occurrence of Incisional Hernia”. In: *Surgery* 158.1 (July 2015), pp. 278–288. ISSN: 1532-7361. DOI: 10.1016/j.surg.2015.01.023 (cit. on p. 75).

[Lis+15] Jeffrey Lisiecki, Jeffrey H. Kozlow, Shailesh Agarwal, et al. “Abdominal Wall Dynamics after Component Separation Hernia Repair”. In: *Journal of Surgical Research* 193.1 (Jan. 2015), pp. 497–503. ISSN: 0022-4804. DOI: 10.1016/j.jss.2014.08.008. (Visited on 07/16/2024) (cit. on pp. 68, 168, 194).

[Lof+17] Tyler J. Loftus, Kristina L. Go, Janeen R. Jordan, et al. “CT Evidence of Fluid in the Hernia Sac Predicts Surgical Site Infection Following Mesh Repair of Acutely Incarcerated Ventral and Groin Hernias”. In: *The journal of trauma and acute care surgery* 83.1 (July 2017), pp. 170–174. ISSN: 2163-0755. DOI: 10.1097/TA.0000000000001503. (Visited on 09/22/2022) (cit. on pp. 75, 151).

[Lub+22] Izabela Lubowiecka, Katarzyna Szepietowska, Agnieszka Tomaszewska, et al. “A Novel in Vivo Approach to Assess Strains of the Human Abdominal Wall under Known Intraabdominal Pressure”. In: *JOURNAL OF THE MECHANICAL BEHAVIOR OF BIOMEDICAL MATERIALS* 125 (Jan. 2022). ISSN: 1751-6161. DOI: 10.1016/j.jmbbm.2021.104902 (cit. on p. 48).

[Lui+00] Roland W. Luijendijk, Wim C.J. Hop, M. Petrousjka van den Tol, et al. “A Comparison of Suture Repair with Mesh Repair for Incisional Hernia”. In: *New England Journal of Medicine* 343.6 (Aug. 2000), pp. 392–398. ISSN: 0028-4793. DOI: 10.1056/NEJM200008103430603. (Visited on 09/22/2022) (cit. on p. 71).

[Luj+04] Juan A. Luján, M. Dolores Frutos, Quiteria Hernández, et al. “Laparoscopic Versus Open Gastric Bypass in the Treatment of Morbid Obesity: A Randomized Prospective Study”. In: *Annals of Surgery* 239.4 (Apr. 2004), pp. 433–437. ISSN: 0003-4932. DOI: 10.1097/01.sla.0000120071.75691.1f. (Visited on 07/28/2022) (cit. on pp. 65, 75).

[Lyo+15] M Lyons, H Mohan, D C Winter, et al. “Biomechanical Abdominal Wall Model Applied to Hernia Repair”. In: *British Journal of Surgery* 102.2 (Jan. 2015), e133–e139. ISSN: 0007-1323. DOI: 10.1002/bjs.9687. (Visited on 11/03/2021) (cit. on p. 67).

[LWS14] Mathew Lyons, Des C. Winter, and Ciaran K. Simms. “Mechanical Characterisation of Porcine Rectus Sheath under Uniaxial and Biaxial Tension”. In: *Journal of Biomechanics* 47.8 (June 2014), pp. 1876–1884. ISSN: 0021-9290. DOI: 10.1016/j.jbiomech.2014.03.009. (Visited on 03/22/2022) (cit. on pp. 47, 52, 112).

[Ma+23] Qiuyue Ma, Wenzhan Jing, Xiaoli Liu, et al. “The Global, Regional, and National Burden and Its Trends of Inguinal, Femoral, and Abdominal Hernia from 1990 to 2019: Findings from the 2019 Global Burden of Disease Study – a Cross-Sectional Study”. In: *International Journal of Surgery* 109.3 (Mar. 2023), p. 333. DOI: 10.1097/JS9.0000000000000217. (Visited on 10/14/2024) (cit. on p. 207).

[] *Magnetic Resonance Imaging (MRI) Units per Million People*. https://ourworldindata.org/gra resonance-imaging-mri-units-availability. (Visited on 10/14/2024) (cit. on p. 207).

[Mah+04] Michael M. Maher, Mannudeep K. Kalra, Dushyant V. Sahani, et al. “Techniques, Clinical Applications and Limitations of 3D Reconstruction in CT of the Abdomen”. In: *Korean Journal of Radiology* 5.1 (Mar. 2004), pp. 55–67. ISSN: 1229-6929. DOI: 10.3348/kjr.2004.5.1.55. (Visited on 10/11/2024) (cit. on p. 130).

[MC11] Manu Malbrain and Michael Cheatham. “Definitions and Pathophysiological Implications of Intra-Abdominal Hypertension and Abdominal Compartment Syndrome”. In: *The American surgeon* 77 Suppl 1 (July 2011), S6–11 (cit. on p. 50).

[Mal+06] Manu Malbrain, Michael L. Cheatham, Andrew Kirkpatrick, et al. “Results from the International Conference of Experts on Intra-Abdominal Hypertension and Abdominal Compartment Syndrome. I. Definitions”. In: *Intensive Care Medicine* 32.11 (Nov. 2006), pp. 1722–1732. ISSN: 0342-4642. DOI: 10.1007/s00134-006-0349-5 (cit. on pp. 50, 54, 71, 92).

[Mal+04] Manu Malbrain, Davide Chiumello, Paolo Pelosi, et al. “Prevalence of Intra-Abdominal Hypertension in Critically Ill Patients: A Multicentre Epidemiological Study”. In: *Intensive Care Medicine* 30.5 (May 2004), pp. 822–829. ISSN: 0342-4642. DOI: 10.1007/s00134-004-2169-9 (cit. on p. 50).

[Mal+14] Manu Malbrain, Inneke De Laet, Jan J. De Waele, et al. “The Role of Abdominal Compliance, the Neglected Parameter in Critically Ill Patients - a Consensus Review of 16. Part 2: Measurement Techniques and Management Recommendations”. In: *Anaesthesiology Intensive Therapy* 46.5 (2014), pp. 406–432. ISSN: 1731-2531. DOI: 10.5603/AIT.2014.0063 (cit. on pp. 42, 43, 53, 92, 106).

[Mar+12] P. Martins, E. Peña, R. M. Natal Jorge, et al. “Mechanical Characterization and Constitutive Modelling of the Damage Process in Rectus Sheath”. In: *Journal of the Mechanical Behavior of Biomedical Materials* 8 (Apr. 2012), pp. 111–122. ISSN: 1751-6161. DOI: 10.1016/j.jmbbm.2011.12.005. (Visited on 11/03/2021) (cit. on pp. 47, 54, 107).

[McC+08] Colm McCaffrey, Olivier Chevalerias, Cian O'Mathuna, et al. "Swallowable-Capsule Technology". In: *IEEE Pervasive Computing* 7.1 (Jan. 2008), pp. 23–29. ISSN: 1558-2590. DOI: 10.1109/MPRV.2008.17 (cit. on pp. 52, 94).

[McD+94] Elspeth M. McDougall, Robert S. Figenshau, Ralph V. Clayman, et al. "Laparoscopic Pneumoperitoneum: Impact of Body Habitus". In: *Journal of Laparoendoscopic Surgery* 4.6 (Dec. 1994), pp. 385–391. ISSN: 1052-3901. DOI: 10.1089/lps.1994.4.385. (Visited on 09/21/2022) (cit. on pp. 54, 92).

[McN+23] Jake McNaughton, Samantha Holdsworth, Benjamin Chong, et al. "Synthetic MRI Generation from CT Scans for Stroke Patients". In: *BioMedInformatics* 3.3 (Sept. 2023), pp. 791–816. ISSN: 2673-7426. DOI: 10.3390/biomedinformatics3030050. (Visited on 10/14/2024) (cit. on p. 207).

[] *MedPy: Medical Image Processing in Python*. (Visited on 08/30/2024) (cit. on p. 171).

[Mei+16] E.-J. Meijer, L. Timmermans, J. Jeekel, et al. "The Principles of Abdominal Wound Closure". In: *Acta Chirurgica Belgica* 113.4 (2016), pp. 239–244. ISSN: 0001-5458. DOI: 10.1080/00015458.2013.11680920. (Visited on 09/22/2022) (cit. on pp. 71, 72).

[24b] *MIC-DKFZ/nnUNet*. MIC-DKFZ. Sept. 2024. (Visited on 09/30/2024) (cit. on p. 154).

[MCI09] Daniel Millbourn, Yucel Cengiz, and Leif A. Israelsson. "Effect of Stitch Length on Wound Complications After Closure of Midline Incisions: A Randomized Controlled Trial". In: *Archives of Surgery* 144.11 (Nov. 2009), pp. 1056–1059. ISSN: 0004-0010. DOI: 10.1001/archsurg.2009.189. (Visited on 11/04/2022) (cit. on p. 72).

[Mis+97] G. Misuri, S. Colagrande, M. Gorini, et al. "In Vivo Ultrasound Assessment of Respiratory Function of Abdominal Muscles in Normal Subjects". In: *European Respiratory Journal* 10.12 (Dec. 1997), pp. 2861–2867. ISSN: 0903-1936, 1399-3003. (Visited on 11/11/2021) (cit. on pp. 53, 92, 106).

[MSM02] Kei Miyamoto, Katsuji Shimizu, and Kazuaki Masuda. "Fast MRI Used to Evaluate the Effect of Abdominal Belts During Contraction of Trunk Muscles". In: *Spine* 27.16 (Aug. 2002), p. 1749. ISSN: 0362-2436. (Visited on 09/28/2023) (cit. on pp. 80, 158, 168).

[Mot+15a] Patrícia Mota, Augusto Gil Pascoal, Ana Isabel Carita, et al. "The Immediate Effects on Inter-Rectus Distance of Abdominal Crunch and Drawing-in Exercises During Pregnancy and the Postpartum Period". In: *Journal of Orthopaedic & Sports Physical Therapy* 45.10 (Oct. 2015), pp. 781–788. ISSN: 0190-6011. DOI: 10.2519/jospt.2015.5459. (Visited on 10/11/2024) (cit. on pp. 143, 144).

[Mot+18] Patrícia Mota, Augusto Gil Pascoal, Ana Isabel Carita, et al. "Normal Width of the Inter-Recti Distance in Pregnant and Postpartum Primiparous Women". In: *Musculoskeletal Science and Practice* 35 (June 2018), pp. 34–37. ISSN: 2468-7812. DOI: 10.1016/j.msksp.2018.02.004. (Visited on 10/11/2024) (cit. on pp. 130, 134).

[Mot+15b] Patrícia Gonçalves Fernandes da Mota, Augusto Gil Brites Andrade Pascoal, Ana Isabel Andrade Dinis Carita, et al. "Prevalence and Risk Factors of Diastasis Recti Abdominis from Late Pregnancy to 6 Months Postpartum, and Relationship with Lumbo-Pelvic Pain". In: *Manual Therapy* 20.1 (Feb. 2015), pp. 200–205. ISSN: 1356-689X. DOI: 10.1016/j.math.2014.09.002. (Visited on 10/11/2024) (cit. on p. 130).

[Mul+09] Jan Paul Mulier, Bruno Dillemans, Mark Crombach, et al. "On the Abdominal Pressure Volume Relationship". In: *The Internet Journal of Anesthesiology* 21.1 (Jan. 2009), pp. 5221–5231. ISSN: 1092-406X. (Visited on 03/10/2022) (cit. on p. 93).

[Mur+16] Mircea Mureşan, Simona Mureşan, Tivadar Bara, et al. "Hernia Recurrence Long Term Follow-up after Open Procedures of Abdominal Wall Plasty – Prospective Study Including 142 Patients". In: *Cirugía y Cirujanos (English Edition)* 84.5 (Sept. 2016), pp. 376–383. ISSN: 2444-0507. DOI: 10.1016/j.circen.2016.08.007. (Visited on 03/02/2022) (cit. on pp. 75, 92).

[Mus+06] T. Mussack, R. Ladurner, T. Vogel, et al. "Health-Related Quality-of-Life Changes after Laparoscopic and Open Incisional Hernia Repair". In: *Surgical Endoscopy And Other Interventional Techniques* 20.3 (Mar. 2006), pp. 410–413. ISSN: 1432-2218. DOI: 10.1007/s00464-005-0440-y. (Visited on 07/16/2024) (cit. on p. 167).

[Muy+15] F. E. Muysoms, S. A. Antoniou, K. Bury, et al. "European Hernia Society Guidelines on the Closure of Abdominal Wall Incisions". In: *Hernia* 19.1 (Feb. 2015), pp. 1–24. ISSN: 1248-9204. DOI: 10.1007/s10029-014-1342-5. (Visited on 08/28/2024) (cit. on pp. 58, 79, 168).

[Muy+09] F. E. Muysoms, M. Miserez, F. Berrevoet, et al. "Classification of Primary and Incisional Abdominal Wall Hernias". In: *Hernia* 13.4 (Aug. 2009), pp. 407–414. ISSN: 1248-9204. DOI: 10.1007/s10029-009-0518-x. (Visited on 09/22/2022) (cit. on pp. 58, 70, 81, 169, 179).

[Nar+12] V. Naraynsingh, R. Maharaj, D. Dan, et al. "Strong Linea Alba: Myth or Reality?" In: *Medical Hypotheses* 78.2 (Feb. 2012), pp. 291–292. ISSN: 0306-9877. DOI: 10.1016/j.mehy.2011.11.004. (Visited on 10/11/2024) (cit. on pp. 144, 145).

[Net23] Frank Henry Netter. *Atlas Netter d'anatomie humaine 8e édition*. https://www.elsevier.com/fr-fr/connect/atlas-netter-danatomie-humaine-8e-edition. 2023 (cit. on p. 130).

[Ngu+14] Mylan T. Nguyen, Rachel L. Berger, Stephanie C. Hicks, et al. “Comparison of Outcomes of Synthetic Mesh vs Suture Repair of Elective Primary Ventral Herniorrhaphy: A Systematic Review and Meta-Analysis”. In: *JAMA Surgery* 149.5 (May 2014), pp. 415–421. ISSN: 2168-6254. DOI: 10.1001/jamasurg.2013.5014. (Visited on 10/19/2022) (cit. on p. 47).

[Nil82] T. Nilsson. “The Relative Rate of Wound Healing in Longitudinal and Transverse Laparotomy Incisions. Animal Experiments”. In: *Acta Chirurgica Scandinavica* 148.3 (1982), pp. 251–256. ISSN: 0001-5482 (cit. on p. 74).

[Nis+21] Yuichi Nishihara, Momoko Asami, Takehiro Shimada, et al. “Comorbid Rectus Abdominis Diastasis Is a Risk Factor for Recurrence of Umbilical Hernia in Japanese Patients”. In: *Asian Journal of Endoscopic Surgery* 14.3 (2021), pp. 368–372. ISSN: 1758-5910. DOI: 10.1111/ases.12868. (Visited on 10/11/2024) (cit. on p. 130).

[Nov+21] Jakub Novak, Jakub Jacisko, Andrew Busch, et al. “Intra-Abdominal Pressure Correlates with Abdominal Wall Tension during Clinical Evaluation Tests”. In: *CLINICAL BIOMECHANICS* 88 (Aug. 2021). ISSN: 0268-0033. DOI: 10.1016/j.clinbiomech.2021.105426 (cit. on pp. 40, 51).

[Ogi+17] Augustin Ogier, Michael Sdika, Alexandre Fouré, et al. “Individual Muscle Segmentation in MR Images: A 3D Propagation through 2D Non-Linear Registration Approaches”. In: *2017 39th Annual International Conference of the IEEE Engineering in Medicine and Biology Society (EMBC)*. July 2017, pp. 317–320. DOI: 10.1109/EMBC.2017.8036826. (Visited on 10/09/2023) (cit. on pp. 94, 114, 153, 171).

[Ogi+21] Augustin C. Ogier, Marc-Adrien Hostin, Marc-Emmanuel Bellemare, et al. “Overview of MR Image Segmentation Strategies in Neuromuscular Disorders”. In: *Frontiers in Neurology* 12 (2021). ISSN: 1664-2295. (Visited on 01/19/2024) (cit. on pp. 81, 152).

[Ope13] OpenStax. *English: Caption:The Ventral Cavity Includes the Thoracic and Abdominopelvic Cavities and Their Subdivisions. The Dorsal Cavity Includes the Cranial and Spinal Cavities.* 2013. (Visited on 10/01/2024) (cit. on p. 32).

[Ope16] OpenStax. *Caption: (A) The Anterior Abdominal Muscles Include the Medially Located Rectus Abdominis, Which Is Covered by a Sheet of Connective Tissue Called the Rectus Sheath. On the Flanks of the Body, Medial to the Rectus Abdominis, the Abdominal Wall Is Composed of Three Layers. The External Oblique Muscles Form the Superficial Layer, While the Internal Oblique Muscles Form the Middle Layer, and the Transverses Abdominus Forms the Deepest Layer. (b) The Muscles of the Lower Back Move the Lumbar Spine but Also Assist in Femur Movements.* May 2016. (Visited on 10/08/2024) (cit. on p. 35).

[Ott19] Douglas E. Ott. "Abdominal Compliance and Laparoscopy: A Review". In: *JSLS : Journal of the Society of Laparoendoscopic Surgeons* 23.1 (2019), e2018.00080. ISSN: 1086-8089. DOI: 10.4293/JSLS.2018.00080. (Visited on 03/10/2022) (cit. on p. 54).

[Owe+17] Lily Owei, Robert A. Swendiman, Rachel R. Kelz, et al. "Impact of Body Mass Index on Open Ventral Hernia Repair: A Retrospective Review". In: *Surgery* 162.6 (Dec. 2017), pp. 1320–1329. ISSN: 0039-6060. DOI: 10.1016/j.surg.2017.07.025. (Visited on 09/20/2024) (cit. on pp. 58, 191, 192).

[Pac+16] P. Pachera, P. G. Pavan, S. Todros, et al. "A Numerical Investigation of the Healthy Abdominal Wall Structures". In: *Journal of Biomechanics* 49.9 (June 2016), pp. 1818–1823. ISSN: 0021-9290. DOI: 10.1016/j.jbiomech.2016.04.019. (Visited on 11/23/2021) (cit. on pp. 124, 125).

[Pap+11] Theodossis S. Papavramidis, Nick A. Michalopoulos, George Mistriotis, et al. "Abdominal Compliance, Linearity between Abdominal Pressure and Ascitic Fluid Volume". In: *Journal of Emergencies, Trauma, and Shock* 4.2 (Apr. 2011), pp. 194–197. ISSN: 0974-519X. DOI: 10.4103/0974-2700.82205 (cit. on p. 105).

[Par+20] Hyo Jung Park, Yongbin Shin, Jisuk Park, et al. "Development and Validation of a Deep Learning System for Segmentation of Abdominal Muscle and Fat on Computed Tomography". In: *Korean Journal of Radiology* 21.1 (Jan. 2020), pp. 88–100. ISSN: 1229-6929. DOI: 10.3348/kjr.2019.0470. (Visited on 01/19/2024) (cit. on pp. 82, 152).

[Par+21] S G Parker, S . Mallett, L Quinn, et al. "Identifying Predictors of Ventral Hernia Recurrence: Systematic Review and Meta-Analysis". In: *BJS Open* 5.2 (Mar. 2021), zraa071. ISSN: 2474-9842. DOI: 10.1093/bjsopen/zraa071. (Visited on 10/07/2024) (cit. on pp. 56, 59).

[PhD19] Dennis M. DePace PhD. *English: Cross Section through the Abdomen Showing the Continuity of the Parietal and Visceral Peritoneum through the Mesentery and the Principal Muscles That Contribute to the Abdominal Wall.* 2019. (Visited on 10/01/2024) (cit. on p. 36).

[PWR21] A. A. Plumb, A. C. J. Windsor, and D. Ross. "Contemporary Imaging of Rectus Diastasis and the Abdominal Wall". In: *Hernia* 25.4 (Aug. 2021), pp. 921–927. ISSN: 1248-9204. DOI: 10.1007/s10029-021-02463-z. (Visited on 10/01/2024) (cit. on p. 79).

[Pod+13] F. Podwojewski, M. Otténio, P. Beillas, et al. "Mechanical Response of Animal Abdominal Walls in Vitro: Evaluation of the Influence of a Hernia Defect and a Repair with a Mesh Implanted Intraperitoneally". In: *Journal of Biomechanics* 46.3 (Feb. 2013), pp. 561–566. ISSN: 0021-9290. DOI: 10.1016/j.jbiomech.2012.09.014. (Visited on 10/12/2022) (cit. on p. 62).

[Pod+14] F. Podwojewski, M. Otténio, P. Beillas, et al. “Mechanical Response of Human Abdominal Walls Ex Vivo: Effect of an Incisional Hernia and a Mesh Repair”. In: *Journal of the Mechanical Behavior of Biomedical Materials* 38 (Oct. 2014), pp. 126–133. ISSN: 1751-6161. DOI: 10.1016/j.jmbbm.2014.07.002. (Visited on 11/03/2021) (cit. on pp. 47, 62, 69).

[PE89] A. V. Pollock and M. Evans. “Early Prediction of Late Incisional Hernias”. In: *The British Journal of Surgery* 76.9 (Sept. 1989), pp. 953–954. ISSN: 0007-1323. DOI: 10.1002/bjs.1800760926 (cit. on p. 75).

[Por+16] K. E. Poruk, N. Farrow, F. Azar, et al. “Effect of Hernia Size on Operative Repair and Post-Operative Outcomes after Open Ventral Hernia Repair”. In: *Hernia* 20.6 (Dec. 2016), pp. 805–810. ISSN: 1248-9204. DOI: 10.1007/s10029-016-1542-2. (Visited on 09/22/2022) (cit. on p. 71).

[PG96] Paolo Primatesta and Michael J Goldacre. “Inguinal Hernia Repair: Incidence of Elective and Emergency Surgery, Readmission and Mortality”. In: *International Journal of Epidemiology* 25.4 (Aug. 1996), pp. 835–839. ISSN: 0300-5771. DOI: 10.1093/ije/25.4.835. (Visited on 10/12/2024) (cit. on p. 58).

[QO16] Haitham Qandeel and Patrick J. O’Dwyer. “Relationship between Ventral Hernia Defect Area and Intra-Abdominal Pressure: Dynamic in Vivo Measurement”. In: *Surgical Endoscopy* 30.4 (Apr. 2016), pp. 1480–1484. ISSN: 1432-2218. DOI: 10.1007/s00464-015-4356-x (cit. on p. 63).

[Qin+21] Changfu Qin, Huiqi Yang, Yingmo Shen, et al. “Development of Hernia and Abdominal Wall Surgery and Hernia Registry in China”. In: *Surgery in Practice and Science* 7 (Dec. 2021), p. 100043. ISSN: 2666-2620. DOI: 10.1016/j.sipas.2021.100043. (Visited on 10/12/2024) (cit. on p. 58).

[Ram+08] G. H. van Ramshorst, J. F. Lange, R. H. M. Goossens, et al. “Non-Invasive Measurement of Intra-Abdominal Pressure: A Preliminary Study”. In: *Physiological Measurement* 29.8 (July 2008), N41–N47. ISSN: 0967-3334. DOI: 10.1088/0967-3334/29/8/N01. (Visited on 11/26/2021) (cit. on p. 111).

[Ran+17] David Randall, Frank Joosten, Richard Peter Ten Broek, et al. “A Novel Diagnostic Aid for Intra-Abdominal Adhesion Detection in Cine-MRI: Pilot Study and Initial Diagnostic Impressions”. In: *British Journal of Radiology* 90.1077 (Sept. 2017), p. 20170158. ISSN: 0007-1285. DOI: 10.1259/bjr.20170158. (Visited on 08/28/2024) (cit. on pp. 80, 151, 168).

[RSN06] Gabrielle Rankin, Maria Stokes, and Dianne J. Newham. “Abdominal Muscle Size and Symmetry in Normal Subjects”. In: *Muscle & Nerve* 34.3 (2006), pp. 320–326. ISSN: 1097-4598. DOI: 10.1002/mus.20589. (Visited on 09/11/2024) (cit. on p. 106).

[Rat+96] A. Rath, P. Attali, JL. Dumas, et al. “The Abdominal Linea Alba: An Anatomo-Radiologic and Biomechanical Study”. In: *Surgical and Radiologic Anatomy* 18.4 (Dec. 1996), pp. 281–288. ISSN: 1279-8517. DOI: 10.1007/BF01627606. (Visited on 09/16/2024) (cit. on pp. 54, 130, 131, 142, 143, 146).

[RZC97] A. Rath, J. Zhang, and J. Chevrel. “The Sheath of the Rectus Abdominis Muscle: An Anatomical and Biomechanical Study”. In: *Hernia* (1997). DOI: 10.1007/BF02426420 (cit. on p. 54).

[Rea+22] John W. Read, Nabeel Ibrahim, Anita S. W. Jacombs, et al. “Imaging Insights Into Abdominal Wall Function”. In: *Frontiers in Surgery* 9 (2022). ISSN: 2296-875X. (Visited on 01/19/2024) (cit. on pp. 79, 151, 168).

[Rei+19] Wolfgang Reinpold, Ferdinand Köckerling, Reinhard Bittner, et al. “Classification of Rectus Diastasis—A Proposal by the German Hernia Society (DHG) and the International Endohernia Society (IEHS)”. In: *Frontiers in Surgery* 6 (Jan. 2019). ISSN: 2296-875X. DOI: 10.3389/fsurg.2019.00001. (Visited on 10/11/2024) (cit. on pp. 130, 145).

[Rob+16] Derek J. Roberts, Jan J. De Waele, Andrew W. Kirkpatrick, et al. “Intra-Abdominal Hypertension and the Abdominal Compartment Syndrome”. In: *Surgical Intensive Care Medicine*. Ed. by John M. O’Donnell and Flávio E. Nácul. Cham: Springer International Publishing, 2016, pp. 621–644. ISBN: 978-3-319-19668-8. DOI: 10.1007/978-3-319-19668-8_46. (Visited on 09/04/2023) (cit. on p. 50).

[Roc+18] Joan Roca, Miquel Nogués, Rafael Villalobos, et al. “Surgical Dynamometer to Simultaneously Measure the Tension Forces and the Distance between Wound Edges during the Closure of a Laparotomy”. In: *Sensors* 18.1 (Jan. 2018), p. 189. ISSN: 1424-8220. DOI: 10.3390/s18010189. (Visited on 09/23/2022) (cit. on p. 74).

[Rod+20] Omar Rodriguez-Acevedo, Kristen Elstner, John W Read, et al. “Functional 3DVR Imaging of Abdominal Wall Hernias”. In: *Journal of Medical Imaging and Radiation Oncology* 64.5 (2020), pp. 663–667. ISSN: 1754-9485. DOI: 10.1111/1754-9485.13085. (Visited on 01/19/2024) (cit. on pp. 80, 151).

[Rom+20] Benoît Romain, Yohann Renard, Christine Binquet, et al. “Recurrence after Elective Incisional Hernia Repair Is More Frequent than You Think: An International Prospective Cohort from the French Society of Surgery”. In: *Surgery* 168.1 (July 2020), pp. 125–134. ISSN: 0039-6060. DOI: 10.1016/j.surg.2020.02.016. (Visited on 07/28/2022) (cit. on pp. 56, 59, 66, 75, 91, 151).

[RFB15] Olaf Ronneberger, Philipp Fischer, and Thomas Brox. *U-Net: Convolutional Networks for Biomedical Image Segmentation*. May 2015. DOI: 10.48550/arXiv.1505.04597. arXiv: 1505.04597 [cs]. (Visited on 09/30/2024) (cit. on p. 159).

[RMH23] P. Rousset, V. Michel, and C. Hoeffel. “Chapitre 5 - Imagerie de La Paroi Abdominale”. In: *Chirurgie Pariétale*. Ed. by Guillaume Passot and Yohann Renard. Paris: Elsevier Masson, Jan. 2023, pp. 41–53. ISBN: 978-2-294-77733-2. DOI: 10.1016/B978-2-294-77733-2.00005-0. (Visited on 10/01/2024) (cit. on p. 81).

[Rou02] Henri Rouvière. *Anatomie humaine. Descriptive, topographique et fonctionnelle. Tronc | Livre | 9782294003929*. https://www.elsevier-masson.fr/anatomie-humaine-descriptive-topographique-et-fonctionnelle-tronc-9782294003929.html. 2002. (Visited on 10/11/2024) (cit. on p. 130).

[Roy+23] Nilanjan Barman Roy, Washim Firoz Khan, Asuri Krishna, et al. “A Comparative Study to Evaluate Abdominal Wall Dynamics in Patients with Incisional Hernia Compared to Healthy Controls”. In: *Surgical Endoscopy* 37.12 (Dec. 2023), pp. 9414–9419. ISSN: 1432-2218. DOI: 10.1007/s00464-023-10408-z. (Visited on 07/16/2024) (cit. on pp. 63, 167).

[Rut03] Ira M Rutkow. “Demographic and Socioeconomic Aspects of Hernia Repair in the United States in 2003”. In: *Surgical Clinics of North America*. Hernia Repair 83.5 (Oct. 2003), pp. 1045–1051. ISSN: 0039-6109. DOI: 10.1016/S0039-6109(03)00132-4. (Visited on 10/12/2024) (cit. on p. 58).

[RR93] Ira M. Rutkow and Alan W. Robbins. “Demographic, Classificatory, and Socioeconomic Aspects of Hernia Repair in the United States”. In: *Surgical Clinics of North America*. Hernia Surgery 73.3 (June 1993), pp. 413–426. ISSN: 0039-6109. DOI: 10.1016/S0039-6109(16)46027-5. (Visited on 10/12/2024) (cit. on p. 57).

[SH11] Richard J. Saad and William L. Hasler. “A Technical Review and Clinical Assessment of the Wireless Motility Capsule”. In: *Gastroenterology & Hepatology* 7.12 (Dec. 2011), pp. 795–804. ISSN: 1554-7914. (Visited on 09/21/2022) (cit. on p. 52).

[Sab+11] C. Sabbagh, F. Dumont, B. Robert, et al. “Peritoneal Volume Is Predictive of Tension-Free Fascia Closure of Large Incisional Hernias with Loss of Domain: A Prospective Study”. In: *Hernia* 15.5 (Oct. 2011), pp. 559–565. ISSN: 1248-9204. DOI: 10.1007/s10029-011-0832-y. (Visited on 10/03/2024) (cit. on p. 172).

[San+01] N. C. Sanchez, P. L. Tenofsky, J. M. Dort, et al. “What Is Normal Intra-Abdominal Pressure?” In: *The American Surgeon* 67.3 (Mar. 2001), pp. 243–248. ISSN: 0003-1348 (cit. on pp. 54, 57, 59, 106).

[Sán+24] Alejandro Sánchez Arteaga, José Luis Gil Delgado, Adrián Feria Madueño, et al. “Impact of Incisional Hernia on Abdominal Wall Strength”. In: *BJS Open* 8.3 (June 2024), zrae045. ISSN: 2474-9842. DOI: 10.1093/bjsopen/zrae045. (Visited on 09/20/2024) (cit. on pp. 63, 167).

[SWH16] A. Schachtrupp, O. Wetter, and J. Höer. “An Implantable Sensor Device Measuring Suture Tension Dynamics: Results of Developmental and Experimental Work”. In: *Hernia* 20.4 (Aug. 2016), pp. 601–606. ISSN: 1248-9204. DOI: 10.1007/s10029-015-1433-y. (Visited on 11/03/2022) (cit. on p. 74).

[SWH19] Alexander Schachtrupp, Oliver Wetter, and Jörg Höer. “Influence of Elevated Intra-Abdominal Pressure on Suture Tension Dynamics in a Porcine Model”. In: *Journal of Surgical Research* 233 (Jan. 2019), pp. 207–212. ISSN: 0022-4804. DOI: 10.1016/j.jss.2018.07.043. (Visited on 11/03/2022) (cit. on p. 75).

[SI98] M Schein and R Ivatury. “Intra-Abdominal Hypertension and the Abdominal Compartment Syndrome”. In: *British Journal of Surgery* 85.8 (Aug. 1998), pp. 1027–1028. ISSN: 0007-1323. DOI: 10.1046/j.1365-2168.1998.00831.x. (Visited on 07/28/2022) (cit. on p. 50).

[Sch+95] M. Schein, D. H. Wittmann, C. C. Aprahamian, et al. “The Abdominal Compartment Syndrome: The Physiological and Clinical Consequences of Elevated Intra-Abdominal Pressure”. In: *Journal of the American College of Surgeons* 180.6 (June 1995), pp. 745–753. ISSN: 1072-7515 (cit. on p. 50).

[Sch+23] K. A. Schlosser, S. M. Renshaw, R. M. Tamer, et al. “Ventral Hernia Repair: An Increasing Burden Affecting Abdominal Core Health”. In: *Hernia* 27.2 (Apr. 2023), pp. 415–421. ISSN: 1248-9204. DOI: 10.1007/s10029-022-02707-6. (Visited on 08/05/2024) (cit. on p. 167).

[SCK96] V. Schumpelick, J. Conze, and U. Klinge. “Die präperitoneale Netzplastik in der Reparation der NarbenhernieEine vergleichende retrospektive Studie an 272 operierten Narbenhernien”. In: *Der Chirurg* 67.10 (Oct. 1996), pp. 1028–1035. ISSN: 1433-0385. DOI: 10.1007/s001040050099. (Visited on 07/28/2022) (cit. on p. 65).

[SES97] A. Shafik, A. El-Sharkawy, and W. M. Sharaf. “Direct Measurement of Intra-Abdominal Pressure in Various Conditions”. In: *The European Journal of Surgery = Acta Chirurgica* 163.12 (Dec. 1997), pp. 883–887. ISSN: 1102-4151 (cit. on pp. 51, 63).

[Sim+17] R. Simón-Allué, B. Calvo, A. Oberai, et al. “Towards the Mechanical Characterization of Abdominal Wall by Inverse Analysis”. In: *Journal of the Mechanical Behavior of Biomedical Materials* 66 (Feb. 2017), pp. 127–137. ISSN: 1751-6161. DOI: 10.1016/j.jmbbm.2016.11.007. (Visited on 07/28/2022) (cit. on pp. 73, 92, 122, 125).

[Sim+16] R. Simón-Allué, B. Hernández-Gascón, L. Lèoty, et al. “Prostheses Size Dependency of the Mechanical Response of the Herniated Human Abdomen”. In: *Hernia: The Journal of Hernias and Abdominal Wall Surgery*

20.6 (Dec. 2016), pp. 839–848. ISSN: 1248-9204. DOI: 10.1007/s10029-016-1525-3 (cit. on pp. 67, 69, 70).

[SOC18] R. Simón-Allué, A. Ortillés, and B. Calvo. "Mechanical Behavior of Surgical Meshes for Abdominal Wall Repair: In Vivo versus Biaxial Characterization". In: *Journal of the Mechanical Behavior of Biomedical Materials* 82 (June 2018), pp. 102–111. ISSN: 1751-6161. DOI: 10.1016/j.jmbbm.2018.03.011. (Visited on 09/22/2022) (cit. on pp. 62, 67, 69, 73).

[Śmi+12] Maciej Śmietański, Kamil Bury, Agnieszka Tomaszewska, et al. "Biomechanics of the Front Abdominal Wall as a Potential Factor Leading to Recurrence with Laparoscopic Ventral Hernia Repair". In: *Surgical Endoscopy* 26.5 (May 2012), pp. 1461–1467. ISSN: 1432-2218. DOI: 10.1007/s00464-011-2056-8. (Visited on 11/23/2021) (cit. on pp. 47, 48, 92).

[ŚŚZ22] Maciej Śmietański, Irmina Anna Śmietańska, and Mateusz Zamkowski. "Post-Partum Abdominal Wall Insufficiency Syndrome (PPAWIS): Lessons Learned from a Single Surgeon's Experience Based on 200 Cases". In: *BMC Surgery* 22.1 (Dec. 2022), pp. 1–8. ISSN: 1471-2482. DOI: 10.1186/s12893-022-01757-y. (Visited on 10/11/2024) (cit. on pp. 130, 144).

[Smi+22] O. A. Smith, M. F. Mierzwinski, P. Chitsabesan, et al. "Health-Related Quality of Life in Abdominal Wall Hernia: Let's Ask Patients What Matters to Them?" In: *Hernia* 26.3 (June 2022), pp. 795–808. ISSN: 1248-9204. DOI: 10.1007/s10029-022-02599-6. (Visited on 06/30/2023) (cit. on pp. 56, 91, 167).

[Smi+04] Stephen M. Smith, Mark Jenkinson, Mark W. Woolrich, et al. "Advances in Functional and Structural MR Image Analysis and Implementation as FSL". In: *NeuroImage*. Mathematics in Brain Imaging 23 (Jan. 2004), S208–S219. ISSN: 1053-8119. DOI: 10.1016/j.neuroimage.2004.07.051. (Visited on 09/17/2024) (cit. on pp. 94, 113).

[Son+06] C. Song, A. Alijani, T. Frank, et al. "Mechanical Properties of the Human Abdominal Wall Measured in Vivo during Insufflation for Laparoscopic Surgery". In: *Surgical Endoscopy And Other Interventional Techniques* 20.6 (June 2006), pp. 987–990. ISSN: 1432-2218. DOI: 10.1007/s00464-005-0676-6. (Visited on 11/14/2023) (cit. on pp. 45, 47–49, 53, 54, 92, 105, 112, 123, 125).

[Sør+05] Lars Tue Sørensen, Ulla B. Hemmingsen, Lene T. Kirkeby, et al. "Smoking Is a Risk Factor for Incisional Hernia". In: *Archives of Surgery* 140.2 (Feb. 2005), pp. 119–123. ISSN: 0004-0010. DOI: 10.1001/archsurg.140.2.119. (Visited on 10/27/2022) (cit. on pp. 59, 191, 192, 208).

[Sou+22] Andrea Soucasse, Arthur Jourdan, Lauriane Edin, Jean F. Gillion, et al. "A Better Understanding of Daily Life Abdominal Wall Mechanical Solicitation: Investigation of Intra-Abdominal Pressure Variations by Intragastric Wireless Sensor in Humans". In: *Medical Engineering & Physics* 104 (June

2022), p. 103813. ISSN: 1350-4533. DOI: 10.1016/j.medengphy.2022.103813. (Visited on 11/05/2024) (cit. on pp. 51, 52, 93, 105, 194, 264, 265).

[Sou+24] Andrea Soucasse, Arthur Jourdan, Lauriane Edin, Elise Meunier, et al. "Assessment of the Smartpill, a Wireless Sensor, as a Measurement Tool for Intra-Abdominal Pressure (IAP)". In: *Sensors* 24.1 (Jan. 2024), p. 54. ISSN: 1424-8220. DOI: 10.3390/s24010054. (Visited on 01/11/2024) (cit. on p. 93).

[SJZ22] Shival Srivastav, Radia T. Jamil, and Roman Zeltser. "Valsalva Maneuver". In: *StatPearls*. Treasure Island (FL): StatPearls Publishing, 2022. (Visited on 10/08/2022) (cit. on pp. 52, 94).

[Ste20] Thomas Stedman. *Stedman's Medical Dictionary*. Dalcassian Publishing Company, Jan. 1920 (cit. on p. 158).

[SM14] Nelia P. Steyn and Zandile J. Mchiza. "Obesity and the Nutrition Transition in Sub-Saharan Africa". In: *Annals of the New York Academy of Sciences* 1311.1 (2014), pp. 88–101. ISSN: 1749-6632. DOI: 10.1111/nyas.12433. (Visited on 10/14/2024) (cit. on p. 207).

[24c] "Stress (Mechanics)". In: *Wikipedia* (July 2024). (Visited on 09/13/2024) (cit. on p. 40).

[Str+16] K. Strigård, L. Clay, B. Stark, et al. "Giant Ventral Hernia—Relationship between Abdominal Wall Muscle Strength and Hernia Area". In: *BMC Surgery* 16.1 (Dec. 2016), pp. 1–6. ISSN: 1471-2482. DOI: 10.1186/s12893-016-0166-x. (Visited on 09/20/2024) (cit. on pp. 63, 167).

[Sze+23] Katarzyna Szepietowska, Mateusz Troka, Monika Lichodziejewska-Niemierko, et al. "Full-Field in Vivo Experimental Study of the Strains of a Breathing Human Abdominal Wall with Intra-Abdominal Pressure Variation". In: *Journal of the Mechanical Behavior of Biomedical Materials* 147 (Nov. 2023), p. 106148. ISSN: 1751-6161. DOI: 10.1016/j.jmbbm.2023.106148. (Visited on 10/04/2023) (cit. on p. 107).

[Szy+10] C. Szymczak, I. Lubowiecka, A. Tomaszewska, et al. "Modeling of the Fascia-Mesh System and Sensitivity Analysis of a Junction Force after a Laparoscopic Ventral Hernia Repair". In: *undefined* (2010). (Visited on 03/24/2022) (cit. on p. 69).

[Szy+11] Czesław Szymczak, Izabela Lubowiecka, Agnieszka Tomaszewska, et al. "Investigation of Abdomen Surface Deformation Due to Life Excitation: Implications for Implant Selection and Orientation in Laparoscopic Ventral Hernia Repair". In: *Clinical Biomechanics* 27.2 (2011), pp. 105–110. ISSN: 0268-0033. DOI: 10.1016/j.clinbiomech.2011.08.008. (Visited on 03/24/2022) (cit. on pp. 47, 48, 50, 92).

[TKL11] Helena Talasz, Markus Kofler, and Monika Lechleitner. "Misconception of the Valsalva Maneuver". In: *International Urogynecology Journal* 22.9 (Sept. 2011), pp. 1197–1198. ISSN: 1433-3023. DOI: 10.1007/s00192-011-1397-0. (Visited on 10/08/2022) (cit. on p. 52).

[Tas+19] Luciano Tastaldi, David M. Krpata, Ajita S. Prabhu, et al. "The Effect of Increasing Body Mass Index on Wound Complications in Open Ventral Hernia Repair with Mesh". In: *The American Journal of Surgery* 218.3 (Sept. 2019), pp. 560–566. ISSN: 0002-9610. DOI: 10.1016/j.amjsurg.2019.01.022. (Visited on 10/08/2024) (cit. on p. 59).

[Tay+21] Salar Tayebi, Adrian Gutierrez, Ikram Mohout, et al. "A Concise Overview of Non-Invasive Intra-Abdominal Pressure Measurement Techniques: From Bench to Bedside". In: *Journal of Clinical Monitoring and Computing* 35.1 (Feb. 2021), pp. 51–70. ISSN: 1387-1307, 1573-2614. DOI: 10.1007/s10877-020-00561-4. (Visited on 02/01/2022) (cit. on p. 52).

[TL48] Léo Testut and André Latarjet. *Traité d'anatomie humaine: Ostéologie. Arthrologie. Myologie*. G. Doin et Cie, 1948 (cit. on pp. 130, 142, 143).

[TPN17] S. Todros, P. G. Pavan, and A. N. Natali. "Synthetic Surgical Meshes Used in Abdominal Wall Surgery: Part I—Materials and Structural Conformation". In: *Journal of Biomedical Materials Research Part B: Applied Biomaterials* 105.3 (2017), pp. 689–699. ISSN: 1552-4981. DOI: 10.1002/jbm.b.33586. (Visited on 09/23/2022) (cit. on p. 69).

[Tod+20] Silvia Todros, Niccolò de Cesare, Gianmaria Concheri, et al. "Numerical Modelling of Abdominal Wall Mechanics: The Role of Muscular Contraction and Intra-Abdominal Pressure". In: *Journal of the Mechanical Behavior of Biomedical Materials* 103 (Mar. 2020), p. 103578. ISSN: 1751-6161. DOI: 10.1016/j.jmbbm.2019.103578. (Visited on 11/23/2021) (cit. on p. 53).

[Tod+19] Silvia Todros, Niccolò de Cesare, Silvia Pianigiani, et al. "3D Surface Imaging of Abdominal Wall Muscular Contraction". In: *Computer Methods and Programs in Biomedicine* 175 (July 2019), pp. 103–109. ISSN: 0169-2607. DOI: 10.1016/j.cmpb.2019.04.013. (Visited on 11/23/2021) (cit. on pp. 50, 53, 92, 123).

[Tod+18] Silvia Todros, Paola Pachera, Nicola Baldan, et al. "Computational Modeling of Abdominal Hernia Laparoscopic Repair with a Surgical Mesh". In: *International Journal of Computer Assisted Radiology and Surgery* 13.1 (Jan. 2018), pp. 73–81. ISSN: 1861-6429. DOI: 10.1007/s11548-017-1681-7. (Visited on 11/23/2021) (cit. on pp. 62, 66, 67, 123, 192).

[Tom+13] A. Tomaszewska, I. Lubowiecka, C. Szymczak, et al. "Physical and Mathematical Modelling of Implant–Fascia System in Order to Improve Laparoscopic Repair of Ventral Hernia". In: *Clinical Biomechanics* 28.7 (Aug.

2013), pp. 743–751. ISSN: 0268-0033. DOI: 10.1016/j.clinbiomech.2013.06.009. (Visited on 10/19/2022) (cit. on p. 69).

[TLS18] Agnieszka Tomaszewska, Izabela Lubowiecka, and Czesław Szymczak. "Mechanics of Mesh Implanted into Abdominal Wall under Repetitive Load. Experimental and Numerical Study". In: *Journal of Biomedical Materials Research Part B: Applied Biomaterials* 107.5 (2018), pp. 1400–1409. ISSN: 1552-4981. DOI: 10.1002/jbm.b.34232. (Visited on 11/11/2021) (cit. on p. 67).

[Tra+14] D. Tran, D. Mitton, D. Voirin, et al. "Contribution of the Skin, Rectus Abdominis and Their Sheaths to the Structural Response of the Abdominal Wall Ex Vivo". In: *Journal of Biomechanics* 47.12 (Sept. 2014), pp. 3056–3063. ISSN: 0021-9290. DOI: 10.1016/j.jbiomech.2014.06.031. (Visited on 11/03/2021) (cit. on pp. 47, 48).

[Tra+16] D. Tran, F. Podwojewski, P. Beillas, et al. "Abdominal Wall Muscle Elasticity and Abdomen Local Stiffness on Healthy Volunteers during Various Physiological Activities". In: *Journal of the Mechanical Behavior of Biomedical Materials* 60 (July 2016), pp. 451–459. ISSN: 1751-6161. DOI: 10.1016/j.jmbbm.2016.03.001. (Visited on 11/03/2021) (cit. on pp. 112, 151).

[Tur+07] D. Turnbull, S. Webber, C. H. Hamnegard, et al. "Intra-Abdominal Pressure Measurement: Validation of Intragastric Pressure as a Measure of Intra-Abdominal Pressure". In: *British Journal of Anaesthesia* 98.5 (May 2007), pp. 628–634. ISSN: 0007-0912. DOI: 10.1093/bja/aem060 (cit. on p. 51).

[Tva10] Tvanbr. *English: Anatomy of the Human Abdomen, by Ties van Brussel / Tiesworks.Nl.* Sept. 2010. (Visited on 10/08/2024) (cit. on p. 33).

[Ugu+23] C. Ugurlu, H. Gok, A. Sahin, et al. "Prevalence of Rectus Diastasis Is Higher in Patients with Inguinal Hernia". In: *Hernia* 27.4 (Aug. 2023), pp. 943–956. ISSN: 1248-9204. DOI: 10.1007/s10029-023-02820-0. (Visited on 10/11/2024) (cit. on p. 130).

[Urq+05] Donna M. Urquhart, Paul W. Hodges, Trevor J. Allen, et al. "Abdominal Muscle Recruitment during a Range of Voluntary Exercises". In: *Manual Therapy* 10.2 (May 2005), pp. 144–153. ISSN: 1356-689X. DOI: 10.1016/j.math.2004.08.011. (Visited on 09/19/2023) (cit. on pp. 94, 106).

[USW88] J. D. Urschel, P. G. Scott, and H. T. G. Williams. "The Effect of Mechanical Stress on Soft and Hard Tissue Repair; a Review". In: *British Journal of Plastic Surgery* 41.2 (Mar. 1988), pp. 182–186. ISSN: 0007-1226. DOI: 10.1016/0007-1226(88)90049-5. (Visited on 11/14/2023) (cit. on p. 111).

[van+11] Gabrielle H. van Ramshorst, Mahdi Salih, Wim C. J. Hop, et al. "Non-invasive Assessment of Intra-Abdominal Pressure by Measurement of Abdominal Wall Tension". In: *The Journal of Surgical Research* 171.1 (Nov. 2011), pp. 240–244. ISSN: 1095-8673. DOI: 10.1016/j.jss.2010.02.007 (cit. on p. 54).

[van+21] L. van Silfhout, L. A. M. Leenders, J. Heisterkamp, et al. "Recurrent Incisional Hernia Repair: Surgical Outcomes in Correlation with Body-Mass Index". In: *Hernia* 25.1 (Feb. 2021), pp. 77–83. ISSN: 1248-9204. DOI: 10.1007/s10029-020-02320-5. (Visited on 09/20/2024) (cit. on pp. 59, 191, 192).

[VMJ99] S. Varshney, P. Manek, and C. D. Johnson. "Six-Fold Suture:Wound Length Ratio for Abdominal Closure." In: *Annals of The Royal College of Surgeons of England* 81.5 (Sept. 1999), pp. 333–336. ISSN: 0035-8843. (Visited on 11/04/2022) (cit. on p. 72).

[Ver+24] Margaux Verdier, Jeremy Deverdun, Nicolas Menjot de Champfleur, et al. "Evaluation of a nnU-Net Type Automated Clinical Volumetric Tumor Segmentation Tool for Diffuse Low-Grade Glioma Follow-Up". In: *Journal of Neuroradiology* 51.1 (Feb. 2024), pp. 16–23. ISSN: 0150-9861. DOI: 10.1016/j.neurad.2023.05.008. (Visited on 10/01/2024) (cit. on pp. 82, 152).

[VPR23] Claudio Vergari, Sylvain Persohn, and Pierre-Yves Rohan. "The Effect of Breathing on the *in Vivo* Mechanical Characterization of *Linea Alba* by Ultrasound Shearwave Elastography". In: *Computers in Biology and Medicine* 167 (Dec. 2023), p. 107637. ISSN: 0010-4825. DOI: 10.1016/j.compbiomed.2023.107637. (Visited on 10/02/2024) (cit. on pp. 78, 79).

[Ver+21] L. Verstoep, G. H. J. de Smet, D. Sneiders, et al. "Hernia Width Explains Differences in Outcomes between Primary and Incisional Hernias: A Prospective Cohort Study of 9159 Patients". In: *Hernia* 25.2 (Apr. 2021), pp. 463–469. ISSN: 1248-9204. DOI: 10.1007/s10029-020-02340-1. (Visited on 10/12/2024) (cit. on p. 56).

[Vlo+13] John Vlot, Rene Wijnen, Robert Jan Stolker, et al. "Optimizing Working Space in Porcine Laparoscopy: CT Measurement of the Effects of Intra-Abdominal Pressure". In: *Surgical Endoscopy* 27.5 (May 2013), pp. 1668–1673. ISSN: 1432-2218. DOI: 10.1007/s00464-012-2654-0. (Visited on 06/30/2023) (cit. on pp. 80, 92, 93, 108, 151).

[Wan+23] Fei Wang, Rongsong Mao, Laifa Yan, et al. "A Deep Learning-Based Approach for Rectus Abdominis Segmentation and Distance Measurement in Ultrasonography". In: *Frontiers in Physiology* 14 (2023). ISSN: 1664-042X. (Visited on 01/19/2024) (cit. on pp. 78, 79, 82, 151, 152).

[Wan+20] Xiaohong Wang, Kai He, Yulan Zhu, et al. "Use of Shear Wave Elastography to Quantify Abdominal Wall Muscular Properties in Patients With Incisional Hernia". In: *Ultrasound in Medicine & Biology* 46.7 (July 2020), pp. 1651–1657. ISSN: 0301-5629. DOI: 10.1016/j.ultrasmedbio.2020.03.027. (Visited on 10/02/2024) (cit. on p. 79).

[Wel+01] G. Welty, U. Klinge, B. Klosterhalfen, et al. "Functional Impairment and Complaints Following Incisional Hernia Repair with Different Polypropylene Meshes". In: *Hernia* 5.3 (Sept. 2001), pp. 142–147. ISSN: 1248-9204. DOI: 10.1007/s100290100017. (Visited on 09/28/2022) (cit. on p. 66).

[Wes+19] Alexander D. Weston, Panagiotis Korfiatis, Timothy L. Kline, et al. "Automated Abdominal Segmentation of CT Scans for Body Composition Analysis Using Deep Learning". In: *Radiology* 290.3 (Mar. 2019), pp. 669–679. ISSN: 0033-8419, 1527-1315. DOI: 10.1148/radiol.2018181432. (Visited on 02/17/2022) (cit. on pp. 82, 152).

[WO00] Switzerland) WHO Consultation on Obesity and World Health Organization. *Obesity : preventing and managing the global epidemic : report of a WHO consultation*. World Health Organization, 2000. ISBN: 978-92-4-120894-9. (Visited on 09/20/2024) (cit. on p. 191).

[Wil33] W. H. Wilson. "Effect of Breathing on the Intra-Abdominal Pressure". In: *The Journal of Physiology* 79.4 (Oct. 1933), pp. 481–486. ISSN: 0022-3751. DOI: 10.1113/jphysiol.1933.sp003061 (cit. on p. 52).

[Wis+17] R. D. Wise, R. N. Rodseth, L. Correa-Martin, et al. "Correlation between Different Methods of Intra-Abdominal Pressure Monitoring in Varying Intra-Abdominal Hypertension Models". In: *Southern African Journal of Critical Care (Online)* 33.1 (July 2017), pp. 15–18. ISSN: 1562-8264. DOI: 10.7196/SAJCC.2017.v33i1.327. (Visited on 09/04/2023) (cit. on p. 51).

[Wor+13] Blair Andrew Wormer, Amanda L. Walters, Joel F. Bradley, et al. "Does Ventral Hernia Defect Length, Width, or Area Predict Postoperative Quality of Life? Answers from a Prospective, International Study". In: *Journal of Surgical Research* 184.1 (Sept. 2013), pp. 169–177. ISSN: 0022-4804. DOI: 10.1016/j.jss.2013.04.034. (Visited on 09/22/2022) (cit. on p. 71).

[Yan+18] Yujia Yang, Liyun Wang, Feng Yan, et al. "Determination of Normal Skin Elasticity by Using Real-Time Shear Wave Elastography". In: *Journal of Ultrasound in Medicine* 37.11 (2018), pp. 2507–2516. ISSN: 1550-9613. DOI: 10.1002/jum.14608. (Visited on 09/21/2022) (cit. on p. 49).

[YMO20] Altıntas Yasemin, Bayrak Mehmet, and Alabaz Omer. "Assessment of the Diagnostic Efficacy of Abdominal Ultrasonography and Cine Magnetic Resonance Imaging in Detecting Abdominal Adhesions: A Double-Blind Research Study". In: *European Journal of Radiology* 126 (May 2020),

p. 108922. ISSN: 0720-048X. DOI: 10.1016/j.ejrad.2020.108922. (Visited on 07/16/2024) (cit. on pp. 80, 168).

[YWZ21] Sue Yuan, Honghong Wang, and Jie Zhou. "Prevalence and Risk Factors of Hernia in Patients With Rectus Abdominis Diastasis: A 10-Year Multicenter Retrospective Study". In: *Frontiers in Surgery* 8 (Sept. 2021). ISSN: 2296-875X. DOI: 10.3389/fsurg.2021.730875. (Visited on 10/11/2024) (cit. on p. 130).

[Zha+16] Hua-Yu Zhang, Dong Liu, Hao Tang, et al. "The Effect of Different Types of Abdominal Binders on Intra-Abdominal Pressure". In: *Saudi Medical Journal* 37.1 (Jan. 2016), pp. 66–72. ISSN: 0379-5284, 1658-3175. DOI: 10.15537/smj.2016.1.12865. (Visited on 09/28/2023) (cit. on p. 75).

[Zou+04] Kelly H. Zou, Simon K. Warfield, Aditya Bharatha, et al. "Statistical Validation of Image Segmentation Quality Based on a Spatial Overlap Index1". In: *Academic Radiology* 11.2 (Feb. 2004), pp. 178–189. ISSN: 1076-6332. DOI: 10.1016/S1076-6332(03)00671-8. (Visited on 10/10/2024) (cit. on p. 154).

Appendix

A. Appendix: Ethic committee approval

These two documents below are from the French Committee for the Protection of Individuals, which allow the clinical trial on patients to be carried out, explained in chapter 5.

CPP SUD-EST VI
Clermont-Ferrand

Clermont Ferrand, le 28 mars 2022

Avis du Comité de protection des personnes Sud-Est VI sur Demande Initiale

Informations promoteur

Organisme : Université Gustave Eiffel
Nom et prénom : Masson Catherine

Investigateur

Investigateur : Thierry Bege

Informations dossier

Numéro SI : 21.04187.000055
Numéro national : 2021-A02119-32
Règlementation : Loi Jardé
Qualification de recherche : Catégorie 1
Produit ou acte : Hors produits de santé (produits non mentionnés à l'article L.5311-11 du code de la santé publique)
Titre : Apports d'une caractérisation biomécanique des contraintes et déformations en chirurgie de la paroi abdominale

Ce dossier a été étudié en séance le 07/01/2022 et mandat a été donné au Bureau du CPP d'émettre l'avis à réception des réponses du déposant aux dernières demandes.

Au vu des réponses obtenues, l'avis suivant a donc été émis le 28/03/2022.

Avis favorable

Cet avis est valable deux ans. Si vous n'avez pas été en mesure d'inclure des participants dans ce délai, vous pouvez demander au CPP une prorogation de cet avis avant la fin de validité de ce dernier (voir en ce sens l'article R.1123-26 du code de la santé publique).

C'est la date de la notification de l'avis sur le SI qui fait foi.

Personnes ayant délibéré

Collège	Catégorie	Nom et prénom
Collège I	Qualification RIPH - Autre	DUBRAY Claude
Collège I	Qualification RIPH - Autre	LEVALLOIS Sylvain
Collège I	Qualification RIPH - Biostatistique ou épidémiologie	CABRESPINE Aurélie
Collège I	Qualification RIPH - Autre	TERRAL Daniel
Collège I	Spécialiste de médecine générale	TEISSANDIER Dorian
Collège I	Qualification RIPH - Autre	SAMALIN Ludovic
Collège I	Qualification RIPH - Autre	RICHARD Ruddy
Collège I	Qualification RIPH - Autre	BERNADACH Maureen
Collège II	Compétence juridique	LASSALAS Christine
Collège II	Représentant d'association agréée	BARRAUD René
Collège II	Représentant d'association agréée	VIGIER Daniel

Collège II	Compétence éthique	NOUAILLES Bertrand
Collège II	Compétence juridique	BORGES Rose-Marie
Collège II	Compétence éthique	SOUSTRE Julie
Collège II	Compétence juridique	PAGNAT Lucie-Hélène
Collège II	Compétence juridique	LIBERT Marion
Collège II	Compétence en sciences humaines et sociales ou action sociale	LUGEZ David

Documents analysés par le CPP

Catégorisation	Intitulé	Date de dépôt
ADD - Doc additionnel	*Document-additionnel.pdf*	23/11/2021
ASS - Assurance	*ATTESTATION D'ASSURANCE RC RECHERCHES BIOMEDICALES.pdf*	23/11/2021
ASS - Assurance	*ATTESTATION ASSURANCE RC RECHERCHES BIOMEDICALES_35 personnes.pdf*	27/01/2022
COU - Courrier	*Lettre_saisine_CPP_UGE.pdf*	23/11/2021
CVI - CV investigateurs	*CV.pdf*	23/11/2021
DEM - Demande autorisation	*Lettre_autorisation_promotion_UGE.pdf*	23/11/2021
DOC - Autres documents	*2021-A02119-32_formulaire_04112021_v1.pdf*	23/11/2021
DOC - Autres documents	*2021-A02119-32_courrierAEC_04112021_v1.pdf*	23/11/2021
DOC - Autres documents	*HPSAEC1-2021-11-0004_2021-A02119-32_CF_DA.pdf*	27/01/2022
DOC - Autres documents	*Protocole_soumission_2_modifications_rouge.pdf*	27/01/2022
DOC - Autres documents	*Reponse_CI_CPP_27_01_2022.pdf*	27/01/2022
DOC - Autres documents	*Note_information_V2_modifications_rouge.pdf*	11/02/2022
DOC - Autres documents	*Note_information_V3_modifications_rouge.pdf*	23/03/2022
INF - Doc Information	*Note_information.pdf*	23/11/2021
INF - Doc Information	*Note_information_soumission_2.pdf*	27/01/2022
INF - Doc Information	*Note_information_V3.pdf*	23/03/2022
JUS - Justification lieux de recherche	*Autorisation_lieux_recherche_CRMBM.pdf*	23/11/2021
PRO - Protocole	*Protocole.pdf*	23/11/2021
PRO - Protocole	*Protocole_soumission_2.pdf*	27/01/2022
RES - Résumé	*Resume_protocole.pdf*	23/11/2021
RES - Résumé	*Resume_protocole_soumission_2.pdf*	27/01/2022

Veuillez agréer, Madame, Monsieur, l'expression de nos salutations distinguées.

Le Président,
Dr. Daniel TERRAL

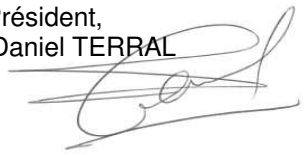

Comité de protection des personnes Sud-Est VI
Avis sur une modification substantielle

Promoteur / Demandeur

Promoteur : Université Gustave Eiffel
Représentant légal (UE) : -
Mandataire : -

Dossier

Numéro SI : 21.04187.000055-MS01
Numéro national : 2021-A02119-32
Référence interne : -

Règlementation : Loi Jardé
Qualification : Catégorie 1
Produit ou acte : Hors produits de santé (produits non mentionnés à l'article L.5311-11 du code de la santé publique)
Investigateur : Thierry Bege

Titre : **Apports d'une caractérisation biomécanique des contraintes et déformations en chirurgie de la paroi abdominale**

Informations MS

Numéro de la MS : 1
Motif de la MS : Nous souhaiterions modifier le formulaire de consentement afin de pouvoir partager les données anonymisées sur des plateformes de dépôt sécurisé et ajouter un formulaire de recueil d'informations afin de centraliser les informations recueillies

Récapitulatif des avis antérieurs

Dossier	Avis	Date d'émission (ou date de validation du dossier historique sur le SIRIPH 2G)
21.04187.000055	*Favorable*	28/03/2022

Ce dossier a été étudié en séance le 02/06/2023 et l'avis suivant a donc été émis.
Cet avis court à compter du changement de statut sur le SI.

Considérant que les conditions éthiques sont remplies notamment au regard des éléments de l'article L.1123-7 du code de la Santé Publique, l'examen du Comité permet de conclure que la recherche peut être réalisée et de rendre l'avis suivant :

Avis favorable

Personnes ayant délibéré

Collège	Catégorie	Nom et prénom
Collège I	Qualification RIPH - Biostatistique ou épidémiologie	CABRESPINE Aurélie
Collège I	Qualification RIPH - Autre	TERRAL Daniel
Collège I	Qualification RIPH - Autre	LEVALLOIS Sylvain

Collège I	Qualification RIPH - Autre	SAMALIN Ludovic
Collège I	Qualification RIPH - Autre	DUBRAY Claude
Collège I	Qualification RIPH - Autre	BERNADACH Maureen
Collège I	Qualification RIPH - Autre	GOLDSTEIN Anna
Collège I	Spécialiste de médecine générale	BLANQUET Marie
Collège I	Spécialiste de médecine générale	TEISSANDIER Dorian
Collège I	Pharmacien hospitalier	CIVIALE-COUDORE Marie-Ange
Collège I	Auxiliaire médical	MEYER Bénédicte
Collège I	Auxiliaire médical	MEYER Bertrand
Collège I	Auxiliaire médical	KEBOUR Anne
Collège II	Compétence éthique	NOUAILLES Bertrand
Collège II	Compétence juridique	LIBERT Marion
Collège II	Compétence juridique	BERTIN Lauriane
Collège II	Compétence juridique	COURTOUX-COUSSEAU Marie-Anne
Collège II	Compétence juridique	LASSALAS Christine
Collège II	Représentant d'association agréée	VIGIER Daniel
Collège II	Représentant d'association agréée	TRINCAL Sébastien
Collège II	Représentant d'association agréée	BONAFOUS Monique
Collège II	Représentant d'association agréée	REMY Stéphane
Collège II	Représentant d'association agréée	TIXIER Sandrine

Documents analysés par le CPP

Catégorie	Intitulé	Date de dépôt
Courrier de demande de modification substantielle	*2021-A02119-32_MS_COURRIER_v1_09052023.pdf*	09/05/2023
DOC - Autres documents	*2021-A02119-32_Note_information_v6_28032023.pdf*	09/05/2023
DOC - Autres documents	*2021-A02119-32_Formulaire_Consentement_v7_28032023.pdf*	09/05/2023
DOC - Autres documents	*2021-A02119-32_Informations_complementaires_v1_18012023.pdf*	09/05/2023
Formulaire de demande de MS	*2021-A02119-32_MS_Formulaire_ANSM_v1_09052023.pdf*	09/05/2023
Les informations justifiant le bien-fondé de chaque modification	*2021-A02119-32_MS_Informations_justificatives_v1_09052023.pdf*	09/05/2023
Tableau comparatif mettant en évidence les modifications apportées dans les documents de la demande initiale	*2021-A02119-32_MS_Tableau_comparatif_v1_09052023.pdf*	09/05/2023
Tableau récapitulatif de l'ensemble des MS et MNS survenues depuis le DI	*2021-A02119-32_MS_Tableau_recap_MS_MNS_v1_09052023.pdf*	09/05/2023

**Les documents étiquetés non-conformes sur le SI RIPH2G ou transmis pour information/notification dans le cadre de cette demande d'avis n'ont pas été évalués par le CPP.*

**L'intitulé des documents examinés par le comité, listés sur le présent avis, reprend la nomenclature des fichiers utilisée par le déposant sur le SI RIPH2G.*

La Vice-Présidente,
Me Marion LIBERT



B. Appendix: README file of dataset "Abdominal in vivo metrics derived from axial dynamic MRI of healthy participants"

The dataset on segmentation and registration of dynamic axial abdominal MRI of healthy participants, used in chapter 1 and chapter 2, has been archived in a Recherche Data Gouv repository and can be accessed by contacting the research team. This is the corresponding README file containing detailed metadata and instructions for interpreting the data.

This README was generated on 2024-01-23 by Victoria Joppin.
Last updated on 2025-01-16
DOI: https://doi.org/10.57745/R5AQRS

Dataset description

This dataset is related to the data presented in different scientific studies:

- 1st study, "Dynamic-MRI quantification of abdominal wall motion and deformation during breathing and muscular contraction" published in 2022 by Jourdan *et al.* (Jourdan, Rapacchi, et al. 2022)
- 2nd study, "Towards a better understanding of abdominal wall biomechanics: In vivo relationship between dynamic intra-abdominal pressure and magnetic resonance imaging measurements" published in 2024 by Joppin *et al.* (Victoria Joppin, Jourdan, et al. 2025)

The data were obtained from the segmentation masks of dynamic MRI. Dynamic axial abdominal MRI was acquired on twenty healthy in vivo participants performing three different exercises: breathing, coughing and the Valsalva maneuver. The data is in .csv format with comma delimiters.

Dataset acquisition

The article by Jourdan *et al.* (Jourdan, Rapacchi, et al. 2022) available here presents and explains the MRI acquisition parameters.
More details about the anatomical MRI and their segmentation masks can be found in the README of the corresponding dataset.

Dataset processing

The metrics are presented and explained in both articles by Jourdan *et al.* (Jourdan, Rapacchi, et al. 2022) available here and Joppin *et al.* (Victoria Joppin, Jourdan, et al. 2025) available here.
Although these data are extracted from the MRIs in dataset, they do not correspond directly to the MR images. In fact, the various metrics were first calculated from the MRIs and then averaged using different timepoints (available in this dataset). This means that all repetitions of exercises were averaged. For instance, if a participant realized three breathing motions (inhale-exhale three times), this data relates to the average of the 3 cycles.
All metrics are presented for two different abdominal muscle groups: lateral muscles (named LM, including transverse abdominis, internal and external obliques, in red in Figure B.1 below) and rectus abdominis (named RA, in blue in Figure B.1 below).

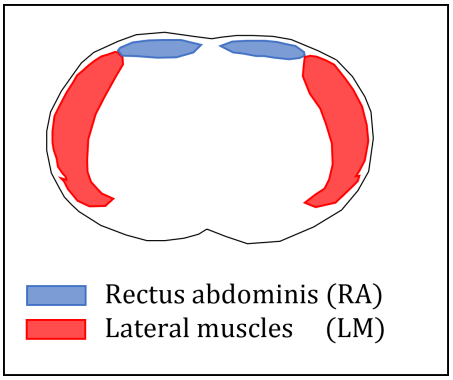

Figure B.1.: Illustration of abdominal muscles segmented

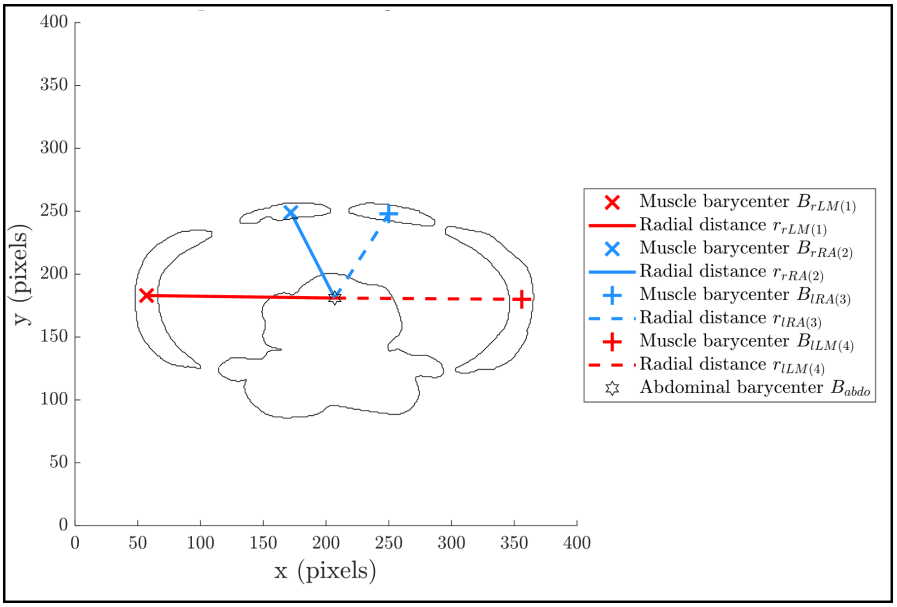

Figure B.2.: Illustration of radial distances and abdominal muscle barycenters

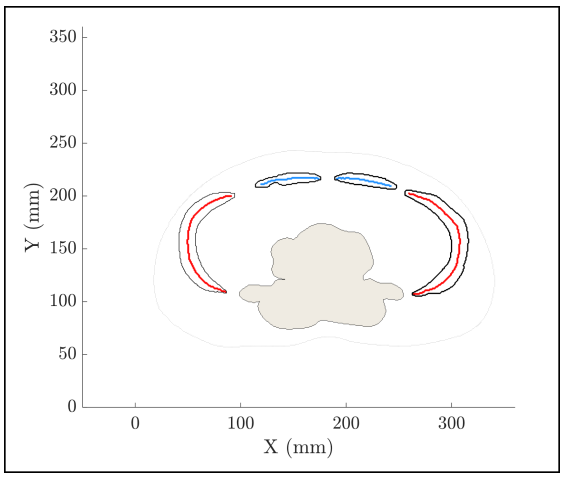

Figure B.3.: Illustration of abdominal muscles length

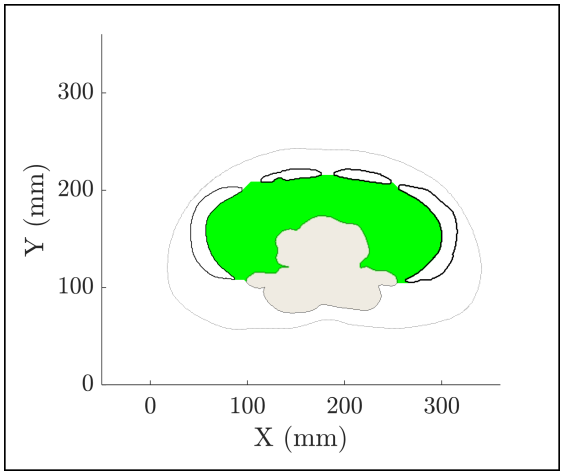

Figure B.4.: Illustration of visceral area

The different metrics are:

- radial displacement of the LM and RA, expressed in mm
- circumferential strain of the LM and RA, expressed in % (presented in the study by Jourdan *et al.*, on Figs. 2 and 4)
- radial strain of the LM and RA, expressed in % (presented in the study by Jourdan *et al.* (Jourdan, Rapacchi, et al. 2022), on Figs. 2 and 4)
- thickness of the LM and RA, expressed in mm (presented in the study by Jourdan *et al.* (Jourdan, Rapacchi, et al. 2022), on Fig. 5)
- length of the medial axis of the LM and RA, expressed in mm (presented in the study by Jourdan *et al.* (Jourdan, Rapacchi, et al. 2022), on Fig. 5) and illustrated by the blue and red lines on Figure B.3
- variation of radial displacement of the LM and RA, expressed as a percentage of the abdominal distance at rest
- radial distance at rest of the LM and RA, expressed in mm, illustrated by the blue and red lines on Figure B.2
- visceral area, which corresponds to the inner surface surrounded by the abdominal muscles and the dorsal zone, independent of the muscle group considered. The visceral area is expressed in cm^2 . This area is illustrated by the green zone on Figure B.4

- variation of the visceral area, expressed as a percentage of its resting value

Dataset structure

This section details the file naming convention and variable/column list of this dataset. The dataset is sorted by folder for each exercice. The data are organized into the following files:

- The files named "Metric_name_" + exercise + ".csv" are the data of each participant (P+number of participant) of the metric considered for the exercise considered.
- The files named "Inter_participants_" + metric_name_ + exercise + ".csv" represent the average of the data for all participants.
- The file "Radial_distance_at_rest.csv" is the radial distance at rest of each participant
- The file named "Visceral_area_at_rest_" + exercise + ".csv" is the visceral area during each exercise session where the participant was at rest.

1. Data for each participant

This section describe the content of the files named: "Metric_name_" + exercise + ".csv". The "Circumferential_strain_breathing.csv" file is taken as an example. This file contains the circumferential strain evolving along time during the breathing exercice of both RA (rectus abdominis) and LM (lateral muscles) of all participants. The columns must be interpreted as follows:

- Column J corresponds to the time vector expressed in seconds, of the 4-th participant
- Columns K and L, named "Circumferential strain (%) LM, P4" and "Circumferential strain (%) RA, P4" are the corresponding circumferential strain values for LM and RA respectively, expressed in percentage.

NB: Data for the breathing exercise are presented for 19 participants (participants 1-8 and 10-20, excluding participant 9 who had no data). Data for the cough and Valsalva exercises are presented for all 20 participants.

2. Data averaged across all participants

This section describe the content of the files named: "Inter_participants_" + metric_-name_ + exercise + ".csv". The "Inter_participants_circumferential_strain_breathing.csv" file is taken as an example. The columns must be interpreted as follows:

- The first column is the average time
- The next column is the MRI metric average across the participants
- The following column is the corresponding standard deviation

NB: Data for the breathing exercise are presented for 19 participants (participants 1-8 and 10-20, excluding participant 9 who had no data). Data for the cough and Valsalva exercises are presented for all 20 participants.

3. Radial distance at rest

The file "Radial_distance_at_rest.csv" is the radial distance at rest of each participant (P+number of participant) of both LM and RA groups, expressed in mm. These morphometric data are independent of the exercise performed.

4. Visceral area at rest

The file named "Visceral_area_at_rest + exercise + ".csv‘ is the visceral area during each exercise session where the participant was at rest. The data are presented for each participant (P+number of participant), expressed in cm^2. These data are very similar throughout the different exercises, depending on the relaxed state of the participant at the beginning of each exercise.

—

Ethical considerations

The data were obtained during a study approved by the French ethics committee (IDRCB: 2019-A00806–51) and was conducted in accordance with national legislation related to interventional research and the declaration of Helsinki.

Anonymization Process

The data has been **fully anonymized** to remove any identifiable information. This dataset was prepared with the utmost care to anonymize all participant-related information while preserving its utility for research. Below are the steps undertaken:

1. **Metadata Review:** The metadata in the resulting files was inspected to confirm the absence of private tags, dates, or any fields containing identifiable information.

2. **Participant ID De-Linking:** A table linking participant names to IDs was permanently deleted. The provided IDs are arbitrary and do not correlate with any real-world identifiers.

3. **Data Review:** Released data was reviewed by expert and has no potential identifying features.

Citation

If you use this dataset in your research, please refer to the "Cite dataset" note to export your bibliography file.

Contact

For further information or questions regarding this dataset, please do not hesitate to contact Victoria JOPPIN at victoria.joppin@proton.me. Any suggestions/comments are also welcome.

C. Appendix: README file of dataset "In vivo intra-abdominal pressure of healthy participants"

The dataset on intra-abdominal pressure on healthy participants, used in chapter 1 and chapter 2, has been archived in a Recherche Data Gouv repository and can be accessed by contacting the research team. This is the corresponding README file containing detailed metadata and instructions for interpreting the data.

This README was generated on 2024-01-23 by Victoria Joppin.
Last updated on 2025-01-16
DOI: https://doi.org/10.57745/BLKGI0

Dataset description

This datasets is related to the data presented in different scientific studies:

- 1st study, "A better understanding of daily life abdominal wall mechanical solicitation: Investigation of intra-abdominal pressure variations by intragastric wireless sensor in humans" published in 2022 by Soucasse *et al.* (Soucasse, Jourdan, Edin, J. F. Gillion, et al. 2022)
- 2nd study, "Towards a better understanding of abdominal wall biomechanics: In vivo relationship between dynamic intra-abdominal pressure and magnetic resonance imaging measurements" published in 2024 by Joppin *et al.* (Victoria Joppin, Jourdan, et al. 2025)

This dataset contains anonymized intra-abdominal pressure (IAP) dat of twenty healthy in vivo participants, providing insights into IAP under different exercise conditions.

- IAP data from **20 healthy participants**
- Each participant performed **3 exercises**
- Data is stored in .csv format with comma delimiters.

Dataset acquisition

The article by Soucasse *et al.* (Soucasse, Jourdan, Edin, J. F. Gillion, et al. 2022) available here presents and explains the intra-abdominal pressure acquisition parameters. Briefly, the objective of the study was to propose a comprehensive evaluation of IAP based on a limited risk and discomfort method. The intra-abdominal pressure was assessed by an ingestible pressure sensor while volunteers realized different exercises: breathing, coughing and the Valsalva maneuver.

Dataset processing

The article by Joppin *et al.* (Victoria Joppin, Jourdan, et al. 2025) available here explains the intra-abdominal pressure data processing. The pressure data was averaged across the different repetitions of each exercise. For instance, if a participant realized three breathing motions (inhale-exhale three times), this data relates to the average of the 3 cycles.

Dataset structure

This section details the file naming convention and variable/column list of this dataset. The dataset is organized into the following files:

- The files named "IAP_" + exercise + ".csv" are the data of each participant (P+number of participant) of the IAP for the exercise considered.
- The files named "Inter_participants_IAP_" + exercise + ".csv" represent the average of the data for all participants.

1. Data for each participant

This section describe the content of the files named: "IAP_" + exercise + ".csv". The "IAP_breathing.csv" file is taken as an example. This file contains the intra-abdominal

pressure evolving along time during the breathing exercice of all participants. The columns must be interpreted as follows:

- Column K corresponds to the time vector, expressed in seconds, of the 6-th participant.
- Column L is the corresponding intra-abdominal pressure values in mmHg.

NB: The IAP is presented for 18 participants, i.e. participants from 1 to 20 excluding the 14-th and 17-th participants who had no data.

2. Data averaged across all participants

This section describe the content of the files named: "Inter_participants_IAP_" + exercise + ".csv". The "Inter_participants_IAP_breathing.csv" file is taken as an example. This file contains the intra-abdominal pressure evolving along time during the breathing exercice averaged accross all participants. The columns must be interpreted as follows:

- The first column is the average time
- The next column is the IAP average across the participants
- The following column is the corresponding standard deviation

NB: The IAP was averaged over the 18 participants presented in the files "IAP_" + exercise + ".csv", i.e. participants from 1 to 20 excluding the 14-th and 17-th participants who had no data.

—

Ethical considerations

The data were obtained during a study approved by the French ethics committee (IDRCB: 2019-A00806–51) and was conducted in accordance with national legislation related to interventional research and the declaration of Helsinki.

Anonymization Process

The data has been **fully anonymized** to remove any identifiable information. This dataset was prepared with the utmost care to anonymize all participant-related information while preserving its utility for research. Below are the steps undertaken:

1. **Metadata Review:** The metadata in the resulting files was inspected to confirm the absence of private tags, dates, or any fields containing identifiable information.

2. **Participant ID De-Linking:** A table linking participant names to IDs was permanently deleted. The provided IDs are arbitrary and do not correlate with any real-world identifiers.

3. **Data Review:** Released data was reviewed by expert and has no potential identifying features.

Citation

If you use this dataset in your research, please refer to the "Cite dataset" note to export your bibliography file.

Contact

For further information or questions regarding this dataset, please do not hesitate to contact Victoria JOPPIN at victoria.joppin@proton.me. Any suggestions/comments are also welcome.